FINAL REPORT

Aquatic Animal Health Subprogram: Identification and Distribution of an Intracellular Ciliate in Pearl Oysters

Shane Raidal, Zoe Spiers, Amanda O'Hara, Frances Stephens, John Creeper, Brian Jones, Robert Adlard, Brett McCullum

February 2009

FRDC Project 2004/086

Author Shane Raidal, Zoe Spiers, Amanda O'Hara, Frances Stephens, John Creeper, Brian Jones, Robert Adlard, Brett McCullum

Title Aquatic Animal Health Subprogram: Identification and Distribution of an Intracellular Ciliate in Pearl Oysters

February 2009

ISBN:978-0-8609-909-8

Printed by MurdochPrint

Aquatic Animal Health Subprogram: Identification and Distribution of an Intracellular Ciliate in Pearl Oysters

Drs Shane Raidal, Zoe Spiers, Amanda O'Hara, Frances Stephens, John Creeper, Brian Jones, Robert Adlard, Brett McCullum

FRDC Project 2004/086

Australian Government

Fisheries Research and Development Corporation

aquatic animal health subprogram

Government of Western Australia

Department of Fisheries

Fish for the future

MURDOCH UNIVERSITY

PERTH, WESTERN AUSTRALIA

February 2009

Table of Contents

List of Tables

List of Figures

FRDC Project 2004/086 Aquatic Animal Health Subprogram: Identification and distribution of an intracellular ciliate in pearl oysters

Principal Investigator: Dr Shane Raidal
Address: Division of Veterinary and Biomedical Sciences
Murdoch University
Murdoch Drive
Murdoch
W.A. 6051

Telephone: (08) 9360 2418
Fax: (08) 9310 4144
email: shraidal@csu.edu.au

Objectives

1. Train a postgraduate in molluscan and aquatic animal health pathology
2. Describe what the parasite is doing to the cells in the oyster including host-ciliate interactions and host specificity.
3. Survey other species of bivalves occurring within an affected farm, i.e. determine the site of the"index case".
4. Survey piggyback spat collected from Zone 1 during the Department of Fisheries piggyback spat research project, for the parasite.
5. Formally describing the intracellular ciliate parasite, its ultrastructure, life cycle and giving it a scientific name.

Non-technical summary

OUTCOMES ACHIEVED:

A significant outcome of the project was the postgraduate training of a veterinary scientist in molluscan pathology thus addressing the international shortage of specialist pathologists in this field. Zone 1 pearling industry stakeholders also benefit directly from the outcome of this project by better understanding the ciliate parasite as a disease threat. This information is required by pearling companies in assessing their level of risk of getting or transmitting the parasite, given that, for environmental reasons, translocation of infected oysters out of Zone 1 is currently not permitted and this impacts on the operation of several companies.

In October 2001 a new parasite was detected in Western Australian pearl oysters which had the effect of severely impeding the movement of stock between fishing zones as well as the biosecurity of hatchery stock. This parasite had not previously been seen in the area despite ongoing surveillance over preceding years. In this project a study was performed to identify the characteristics of the organism, the source and distribution of the infection. The historical distribution of the ciliate was examined using archival records, indicating the highest prevalences occurred in the

warmer months of October to February from 2001 to 2006. This also corresponded to the months of reduced rainfall.

Microscopically the structure and morphology of the parasite was confirmed to be a ciliate organism infecting the cytoplasm of digestive gland cells. These findings were almost identical to a similar parasitic infection that has been found in Canadian mussels. Accordingly, preserved samples of Canadian mussels infected with their intracellular ciliate were obtained and analysed microscopically. This identified almost identical morphological characteristics to the Western Australian ciliate of pearl oysters, with only a slight difference in size that could be attributed to fixation and processing.

An investigation into the pathology associated with the presence of the ciliate in the pearl oysters was performed. A positive correlation between the presence of the ciliate and an inflammatory response of the digestive gland was displayed using statistical techniques. Pathological changes to the infected cells were also demonstrated using electron microscopy. The sensitivity of histology to detect ciliates was also examined, revealing its sensitivity as a diagnostic tool in at risk populations was low (38%) to moderate (50%).

Attempts were made to culture the pearl oyster ciliate in laboratory cell cultures. In order to do this, new methods for culturing pearl oyster cells were developed. The successful culture of adductor muscle, mantle tissue and digestive gland derived cells from pearl oysters was developed and maintained in the laboratory for up to 75 days, using a variety of cell culture media.

Field trials placing naïve spat in pearl farm leases that had prior ciliate infections were performed. No intracellular ciliates were detected in *P. maxima*. Other bivalve species from the same regions were examined histologically for health and parasites. With a total of 345 bivalves surveyed during 2005 to 2007, from 8 geographical locations and over 11 species of bivalve included, only one oyster contained the intracellular parasite. This oyster was a 200 mm male bastard shell (*Pinctada* sp.) from Gales Bay, sampled in October 2006. One protozoal parasite was identified in a novel host bivalve species, and a previously undescribed single celled organism was also discovered. An experimental design for a cross infection trial using oysters housed in aquarium tanks in a biosecure room at Murdoch University, should the ciliate become available, was completed.

Attempts at designing DNA-based tests to detect the infection were performed. However isolation of high quality ciliate DNA from preserved tissue remained elusive due to the low number of parasites within the available infected material and its method of preservation. However a DNA probe using the Ciliophora 16s ssu gene was successfully developed.

List of Abbreviations and definitions

FBS	Foetal Bovine Serum
FCS	Foetal Calf Serum
FHU	Fish Health Unit at Murdoch University
H&E	Haematoxylin and eosin
HPF	High Power Fields (40 x magnification)
Inflammation	The infiltration of haemocytes in oyster tissues
ISH	In situ Hybridisation
NBCS	New Born Calf Serum
NPV	Negative predictive value = number of negative test results for truly disease-free animals divided by the total number of negative test results
PCR	Polymerase Chain Reaction
PPV	Positive predictive value = number positive test results for truly diseased animals divided by the total number of positive test results
SEM	Scanning Electron Microscopy
Sensitivity	The number of diseased animals that test positive divided by the number of truly diseased animals
Spat	juvenile pearl oysters
Specificity	The number of disease-free animals that test negative divided by the number of truly disease-free animals
TEM	Transmission Electron Micrsocopy

Keywords

Pearl oyster, *Pinctata maxima*, mollusc pathology, intracellular ciliate, epidemiology, cell culture, molecular diagnostics, aquatic animal health.

Acknowledgements

The Fisheries Research and Development Corporation (FRDC), the Pearl Producers Association and Murdoch University funded this project.

This project was a collaborative effort and would not have been possible without the contributions of many people around Australia and the world, and we appreciate all the help given during the project. We would like to thank Douglas Bearham, Philip Nicholls, Peter Fallon, Gerard Spoelstra, Michael Slaven, Ian Robertson and Alan Lymbery all from Murdoch University, Dave Mills (Paspaley), Sam Buchanan (Blue Seas), Patrick Moase (MG Kailis), Michael Hood and Mark Longhurst (Morgan & Co.), Leigh Taylor (WA Dept. Fisheries) Donna Cahill (Maxima), Roger Barnard (MG Kailis) and all the members of the Ciliate Project Steering Committee, for their support and assistance over the course of this project. Without their immense investment of time, technical support, financial aid and knowledge, this project would not have been possible.

We would specifically like to thank Shirley Slack-Smith at the Western Australian Museum for her help with the correct identification of bivalves, and Katherine Heel-Miller from the University of Western Australia, for her assistance with the Laser Dissection Microscope. We are indebted to Susan Bower and Gary Meyer at Fisheries and Oceans Canada, and Antonio Figueras at the Instituto Investigaciones Marinas, CSIC, for their enthusiasm to provide an international perspective on the parasite.

Chapter 1: Introduction

1.1 The Pearling Industry in Western Australia

Aquaculture in Australia is the fastest growing primary industry, and since 1990 it has been increasing at an average rate of 13% per year, (Invest Australia, 2004). The Pearling industry is economically important to Western Australia, contributing 96% of the state's total aquaculture production in 2001-02 (ABARE 2003). Pearl exports were worth A$200.8 million in 2002/03 (Dept. Agriculture 2004).

Western Australia's pearling industry began in the 1850's, where natural pearls were found in the *Pinctada albina* oyster at Shark Bay (Government of WA 1994). Later, the silverlip *Pinctada maxima* (Jameson) was discovered further north and by the mid-1860's the industry began to thrive. The *P. maxima* are the largest member of the Pteriidae family used for pearl production (Hancock 1993), and are known for their top quality 'South Sea' pearls and mother of pearl shell (Government of WA 1994).

The industry was devastated by the advent of plastic buttons following World War II, which all but negated the world demand for mother of pearl. However, the pearling business was later revived in 1955 with the establishment of pearl culture farms. Due to their rarity in nature, the seeding of oysters has meant pearls can be produced reliably and efficiently for greater profitability. 1957 was the year of the first harvest of cultured pearls by a joint Japanese-Australian firm, Pearls Pty Ltd (PPL) from their Kuri Bay lease site (Dybdahl and Pass 1985) in Western Australia. Since then, the culture of South Sea pearls has continued to prosper.

The pearl oysters enter the pearl farms either by hatchery growth or wild caught. The reproductive season for the *P. maxima* is October to February, when the temperature rises above 27°C (Hancock 1993). Adult oysters are selected for breeding soundness and, with the help of water changes, spawn in the hatchery environment. The resulting larvae are grown in the hatchery for about two months. The spat (juvenile oysters) are then around 4-8mm in size and are transported to nursery sites on the pearl farms. After a few weeks in the nursery site, spat are then placed out on the pearl leases. The most commonly used system are 'long lines', which consist of panels of oysters hanging from lines strung a few inches below the surface of the water. Other systems include hanging the oysters from pickets on the bottom of the sea and others on surface attachments. The hatchery oysters are ready to be seeded after around two years of age and most are seeded again at least twice more during their productive life, producing a pearl every two years (National Aquaculture Council 2006).

The capture of wild oysters is strictly regulated by the Department of Fisheries. Eighty Mile Beach is the largest fishing ground for *P. maxima*. Other fishing areas

include Exmouth Gulf, Lacepede Is. and Port Hedland. Oysters larger than 120 mm are collected off the bottom by drift divers using a surface supplied breathing system. The oysters are placed in holding tanks in the boats where fresh sea water is pumped over them. After the fishing is completed, usually around September, the catch is transported back to the farm leases and placed on the bottom for a few weeks of acclimatization. After this period, the oysters are selected for the seeding operation. This operation is performed by highly trained technicians.

1.1.1 Australian pearls on the world market

Pearls produced in Australia are exported to over thirty countries, including Hong Kong, the United Kingdom, Switzerland, Japan and the United States, the US being the world's largest market for pearls. In 2001-02 Australian pearl exports were valued at $417.6 million (National Aquaculture Council 2006). Western Australian pearls and the name 'Australian South Sea Pearls' are renowned for their high grade and certified quality.

1.2 Disease threats to Western Australia's the pearling industry

1.2.1 Protective Regulation

The Pearling Industry is highly regulated through the Pearling Act 1990, in order to to minimize the impact of wild shell harvest on the sustainability of the fishery and of other adverse events. Protocols are set in place to protect the industry against communicable diseases.

1.2.2 Pathogens relevant to WA Pearling

There are a number of known infectious diseases that would affect the industry adversely if they were to cause an outbreak in Western Australia. Some of these organisms are endemic in the environment, which highlights the importance of sensitive management practices to reduce outbreaks occurring, or in the event of one, to limit its devastation.

Vibrio bacteria species, particularly *Vibrio harveyi*, have been found to be a significant factor in post-transport mortalities of silverlip pearl oysters, in some cases causing over 80% mortality (Dybdahl and Pass 1985). During transport, oysters were kept at very high densities in the ships for up to five days with inadequate water circulation. These conditions lead to a build up in bacteria and the resultant mortalities. Since the 1980s, improved management practices and translocation protocols have all but eliminated the problem (Dept. of Fisheries 2004).

Haplosporidians are major pathogens of molluscs, among which *Haplosporidium nelsoni* is listed by the OIE and is an exotic protozoan disease of Australia. It is more commonly known as a disease of the American oyster, *Crassostrea virginica*,

however silverlip pearl oysters have been shown to be susceptible experimentally (Herfort 2004). An infection of *H. nelsoni* is known as haplosporidiosis or MSX disease. A species of *Haplosporidium* has been reported in silverlip pearl oysters in north Western Australia (Hine and Thorne 1998) and is currently being investigated (Bearham, Spiers et al 2007).

Bonamia are intrahaemocytic protozoa of the phylum Haplosporidia, which can cause high mortalities in commercially exploited molluscs. *Bonamia ostreae* and *B. exitiosa* are on the list of diseases notifiable to the World Organisation for Animal Health (OIE 2006). *Bonamia* have been officially reported in Western Australia, New South Wales, Tasmania and Victoria, with a closely related species, *Bonamia roughleyi* (syn *Mikrocytos roughleyi*) causing mortalities in the Sydney rock oyster, *Saccostrea glomerata* in New South Wales (Herfort 2004).

Perkinsus olseni/atlanticus causes the disease perkinsosis in Australian abalone, clams and pearl oyster, and has been officially reported in NSW, SA and WA. This protist is suspected of causing up to 40% mortality in greenlip abalone *Haliotis laevigata*, however infection with the disease also affects the hosts marketability (Herfort 2004). *P. olseni/atlanticus* and *P. marinus* are listed as notifiable diseases (OIE 2006), however only *P. olseni/atlanticus* is endemic to Australia (ACT Parliamentary Council 2005).

Bivalves are known to bioaccumulate viruses in their tissues. However, some viruses have been reported to infect molluscs. The difficulty in maintaining continuous bivalve cell lines has meant the study of bivalve viruses is mostly limited to morphological studies (Elston 1997). Papovavirus-like intranuclear inclusion bodies have been recorded to infect Australian silverlip pearl oysters (Norton, Shepherd et al. 1993).

Excavating sponges from the family Clionaidae (Porifera: Demospongiae) have a devastating affect on the adult silver lipped pearl oysters in north Western and Northern Australia. Known commonly as ‘red bum’ it excavates the calcium carbonate of the mollusc shell and damages it to the point where it cannot be marketed, or even to the death of the oyster (Fromont, Craig et al. 2005). Fromont’s study (2005) into excavating sponges in the Northern Territory and Western Australia revealed two species that effected silverlip pearl shell, *Cliona dissimilis* and *Pione velans*.

1.3 Other ciliates found in bivalves

A new species of ciliate named *Stegotricha enterikos* gen. nov. sp. nov. was found in the digestive gland tubules of the Pacific oyster, *Crassostrea gigas* (Bower and Meyer 1993). It was reported to multiply by transverse binary fission. Non-dividing stages have an elongated ovoid body covered by about 16 evenly spaced, slightly oblique kineties (ciliary rows) except for a small naked area on one side of the

posterior end. It is larger than the ciliate affecting mussels, averaging 49.8 µm wide and 18.1 µm long. No inflammation or pathology was associated with infections of this organism (Bower and Meyer 1993).

An *Ancistrocoma*-like ciliated protozoa has been reported in Western Australian silverlip pearl oysters, within the intestine of mature oysters and the gills of spat. These also illicit no host response, so are considered non-pathogenic. It should also be noted that saprophytic ciliated protozoa can be found invading dead or dying oysters (Humphrey and Norton 2005).

In Canada, an intracellular ciliate has been found in mussels, with the host species identified as *Mytilus edulis, Mytilus trossulus* and *Mytilus galloprovincialis* (McGladdery and Bower 2002). Their taxonomic affiliation has been identified as Rhynchodid-like Phyllopharyngea ciliates. The organisms are spindle-shaped 9-16 µm x 4.5-6 µm occurring inside the digestive tubule epithelial cells (McGladdery and Bower 2002). They illicit no obvious host response, despite their intracellular location (Figueras, Jardon et al. 1991). They are said to be found in mussels in northwest Spain and the west and east coasts of North America, including Canada and are considered of Negligible Regulatory Significance in Canada (McGladdery and Bower 2002). On histological examination, these ciliates are similar to the new ciliate under investigation.

1.4 Background

In October 2001, batches of mixed size silverlip (or gold lipped) pearl oysters, *Pinctada maxima*, from farms in the Zone I Fishery, Exmouth Gulf to Port Hedland, were found to be infected with an intracellular ciliate. The ciliate had not previously been seen, despite extensive testing of oysters over at least 7 years. Transmission electron microscopy has revealed elliptical organisms with an average width of 5.53 µm (range of 2.73 to 7.47 µm) and an average length of 11.15 µm (range of 9.02 to 16.2 µm) with 9 ciliates measured. The cells are encircled with cilia whether they are in the lumen of the digestive gland or intracellular.

The presence of the parasite appeared to be associated with inflammation of the gut lining and was found in 3-4% of the samples. At the time the samples that were infected contained high numbers of the parasite, and all infected oysters were under 70 mm diameter. The parasite may not be a major risk to the industry per se, as it did not seem to affect adult shell and consequently it was considered to not be a major risk to production. However, it had occurred in several farm sites, may have been transmitted with shell movements, and it probably contributed to mortalities in shell under 70 mm.

1.5 Need

Similar intracellular ciliates (all undescribed) have been reported from mussels in Spain and Canada, but apparently without inducing the inflammation seen in pearl oysters (McGladdery and Bower 2002). There is therefore a possibility that the pearl oyster parasite has been introduced from overseas. Translocation of infected oysters out of Zone 1 is currently prohibited in an effort to contain the infection, which impacts on the operation of several pearling companies.

The WA Dept of Fisheries Business Plan has a key objective to ensure ecological and environmental sustainability of the pearling industry. This project is of direct benefit to the Western Australian pearling industry by documenting the existence of the new intracellular ciliate and its effect on an economically valuable oyster species. It was designed to establish whether the parasite is in the wild stock oysters in Zone 1 and whether it has a reservoir host. This is required information of pearling companies to correctly assess their level of risk of getting or transmitting the parasite given that, for environmental reasons, translocation of infected oysters out of Zone 1 is currently prohibited. This impacts on the operation of several companies. Another significant outcome of this project is the postgraduate training of a veterinary scientist in molluscan pathology, thus addressing the international shortage of specialist pathologists in this field.

Chapter 2: Methods

2.1 Materials and Methods for the Morphological Investigation

2.1.1 Samples used for histological examination

Over 70,000 histological samples were available from the Western Australian Department of Fisheries as part of the initial survey of farms in Zone 1 and elsewhere, including the index case. These were formalin fixed, paraffin embedded oysters dating from 2001 and formed the basis of the histopathology survey.

Fresh samples of silverlip pearl oysters and other bivalve species where also collected through the duration of this project on field trips to pearl leases and surrounding areas. These included farms in the Montebello Islands and Exmouth Gulf, with the help and support of pearling companies. Live oysters where transported by air to Perth in foam eskys, accompanied with ice packs and moist newspaper. They where then maintained alive at Murdoch University's Fish Health Unit until needed.

2.1.2 Preparation of fresh tissues for Histology

Samples were prepared on site at the pearl leases, where the oysters are removed from the shell and placed into 10% sea water buffered formalin. If the oysters were too small for this process, the whole oyster, including the shell, was placed into the formalin. 24 hours later, the samples were then drained of formalin, washed with water, wrapped in swabs then in sealed plastic bags and transported back to Perth by airplane and processed at either Murdoch University or WA Department of Fisheries.

Some formalin fixed tissues were set aside for electron microscopy, these were placed in 5% sea-water buffered glutaraldehyde and processed as described below. The remaining formalin fixed oysters were decalcified and mounted in paraffin blocks.

2.1.3 Preparation of fresh tissues for Transmission Electron Microscopy

In a fume hood, the adductor muscle was severed to open the oyster and the organs of interest were identified. Sections of the organs, $1mm^3$ in size, where dissected in a puddle of 5% Sorensen's phosphate buffered gluteraldehyde. These sections where then placed in labelled bottles containing 5% glutaraldehyde and kept at 4^oC for 2 hours to overnight. The samples where then washed 3-4 times in 0.07M Sorensen's phosphate buffer. The tissues where then immersed in Dalton's Chrome Osmic Acid for 60-90 minutes at 4^oC. Afterwards, the samples where washed several times with 70% alcohol solution for a minimum 5 minutes duration. This process was repeated

with 90% and 95% ethanol. The samples where then immersed in 100% absolute alcohol making 3 changes over a minimum of 10 minutes. Following this, the tissue was immersed in Propylene Oxide with 2 changes over a minimum of 10 minutes. Then the tissue was emersed into a 60:40 Propylene oxide/Epon mixture for 1 hour at 4^oC, with the infiltration continued with pure 'Epon' on the rotator, with the vial lids off. This was left at room temperature overnight. Embedding of individual tissue blocks in fresh 'Epon' in embedding capsules was then completed in a fume cupboard at room temperature. Finally, polymerization occurred in a 60^oC oven over 24 hours. Embedded blocks of tissue were then ready for sectioning and EM viewing.

2.1.4 Preparation of tissues for Scanning Electron Microscopy

Fresh tissues, cut in small sections where fixed in 2.5-5% Glutaraldehyde for 2 hours or overnight at $4^\circ C$. The tissues where then washed in Sorenson's buffer, then drained and immersed in enough 1% Dalton's Chrome OsO_4 to cover the tissue. The bottles where shaken to increase tissue exposure then kept at $4^\circ C$ for 60-90 minutes, shaking at intervals. The tissues where then washed in a series of 15 minute alcohol dehydration series, 30%, 50%, 70%, 80%, 90% and 95%. The final wash in 3 changes of absolute alcohol was left for over 30 minutes. The tissues where then washed in two changes of amyl acetate over one hour and placed in a critical point dryer. The tissues where then mounted onto specimen stub with double sided tape, coated with gold and stored in the dessicator.

Note: If samples were formalin-fixed and embedded in paraffin the step containing glutaraldehyde was not used. Instead the tissue wase firstly, immersed in xylene (in a fume cupboard), then washed with 100% ethanol and soaked for 15 minutes. This was followed by hydration with 95%, 90%, 80%, 70%, 50% and then 30% ethanol each of which required 15 minutes.

2.1.5 Culturing other ciliates

A culture of *Paramecium* was grown for two main reasons. Firstly, the culture of this ciliate enabled the researcher to develop skills required should the organism of interest be found alive and need to be cultured. Secondly, the culture provided *Paramecium* DNA that was used as a positive ciliate control in PCRs. The *Paramecium* DNA was extracted using a MasterPure cell sample extraction kit.

The method used for *Paramecium* culture was as follows. A cupful of hay was cut into 6 cm lengths and place in a 2 L conical flask container. Taking care to remove the seed heads first, the hay was immersed in 1 L of pond water. The solution was then brought to the boil and allowed to cool slowly. The conical flask was then left uncovered for 24 hours and the inoculated with 5mL of a rich culture of *Paramecium*. The *Paramecium* used in this procedure was supplied by Biological Science and Engineering, Biological Sciences and Biotechnology, Murdoch University.

2.1.6 Bivalve Cell Culture

Establishment of cell cultures from oysters

Sterile seawater containing penicillin and streptomycin was placed in a clean container and aerated. Pearl oysters chosen as donor animals were placed in this container and kept for 48 hours, without food. The container was cleaned daily to remove pseudofaeces and sterile seawater with antibiotics was replenished. Surface contaminants were removed from their shells using a clean knife, then oysters were rinsed in clean seawater, and placed in a clean container and immersed in 1 L sterile seawater with antibiotics. The sterile seawater was changed at 20 minute intervals 3 times. The oysters were then immersed in 70% ethanol for 30 seconds for surface sterilization and air-dried in a laminar flow cabinet. Once dry, the oysters were opened by severing the adductor muscle and removed using a sterile scalpel. The oyster bodies were then immersed in 70% ethanol for 30 seconds and then placed back in the seawater with antibiotics. The antibiotic solution was changed at 15 minute intervals 4 times. The mantle tissue, adductor muscle and digestive gland were identified and removed aseptically from the oysters. The tissues were bathed in Phosphate Buffered Saline, then vigorously washed in Leibovitz L-15 media. This was repeated twice. The tissues were then chopped into fine fragments using sterile scissors and cultured at 28^{o}C.

Growth media and supplements

The growth media used is described fully in section 3.3. The media consisted of varying proportions of Leibovitz L-15 media (Sigma-Aldrich), New Born Calf Serum, pearl oyster haemolymph and antibiotics.

2.2 Materials and Methods for the Pathological Investigation of Organism

2.2.1 Maintaining Bivalves at the Fish Health Unit

The Fish Health Unit was set up for maintaining bivalves for two main reasons. The first reason was to provide expertise and a suitable environment should the organism be found and transmission studies could be started. The second reason was to keep bivalves alive to provide donor tissue for use in the culture of bivalve cell lines.

2.2.2 Source of Bivalves kept at the Fish Health Unit

Wild caught mussels were introduced to the aquariums at the beginning to ensure that the water quality was of a standard suitable for the pearl oysters. Once the salinity, pH, ammonia and other water quality measures where stable, young *P. maxima* were collected from pearl leases and transported back to Perth. Other bivalves were also kept at the FHU, including rock oysters (*Saccostrea cucullata*) from the Montebello Islands.

The following algal cultures where kept at Murdoch University to provide nutrition for the bivalves kept at the Fish Health Unit; Tahitian *Isochrysis galbana* (T-iso) and C*haetoceros muelleri* (Ch.m). The cultures where obtained from Challenger TAFE, Fremantle WA, and where maintained at Murdoch University using sterile Guillards F2 growth media (1 mL/L) in 35 ppm $NaCl_2$ solution.

2.2.3 Transfer of Algae

A solution of Guillard's F2 media (diluted 1 mL in 1 L) in a salt solution (35 ppm) was autoclaved in a suitable glass container for algal growth and allowed to cool. The inside of an operating laminar flow cabinet was sprayed with 70% alcohol and left until evaporated. A Bunsen burner was ignited, before the F2 flask and the Stock culture flask containing the algae were placed in the laminar flow cabinet. The lid was removed from the Stock culture and the neck of flask was flamed. This procedure was repeated with the F2 flask. A small amount of stock culture was poured into the F2 flask until a colour change occurred, while holding flasks above or near the flame. The lids where then reapplied and the bottle labeled correctly with the name of the culture and date of transfer. This procedure was modified from Lewis and Garland et al (1986).

2.2.4 Algal Growth

Algae was grown in 4 L conical flasks in front of a double fluorescent 'Grolux' light (Figure 2.2.1). The tops of the flasks were covered in alfoil flamed on a Bunsen burner prior to application. Aeration from an air pump was provided through a 0.2 µm filter and a syringe with cotton bud also penetrates the lid to allowed excess air to escape. The details of the preparation of Guillard's F2 Medium are included in section 8.1.

2.2.5 Determining cell densities of microalgae using a hemocytometer

Algal cells were counted in a hemocytometer counting chamber. This was important to ascertain the health and viability of the algal culture. The hemocytometer chamber contained two etched grids, separated and surrounded by channels. The central area of the grids has 25 etched squares, each of which was further divided into 16 smaller squares. Motile algal cells such as *T-iso* need to be killed prior to an effective count. This can be achieved by adding a few drops of formalin to a 10mL sample beaker a few minutes prior to counting. It was important to mix the sample to ensure the algal cells were evenly distributed in the solution.

Figure 2.2.1A: The algae was grown in 4 L conical flasks. The tops of the flasks were covered in alfoil and aerated from an air pump through a 0.2 µm filter. A syringe with cotton bud also penetrates the lid to allowed excess air to escape. Labelled on the diagram are the air tube from airpump(A), 0.2 µm filter(B), syringe with cotton bud to allow air to escape (C), and the 4 L flask with orange-coloured algal culture (D). **B:** A photograph of the algal growth setup, including cultures at various stages of maturity.

A

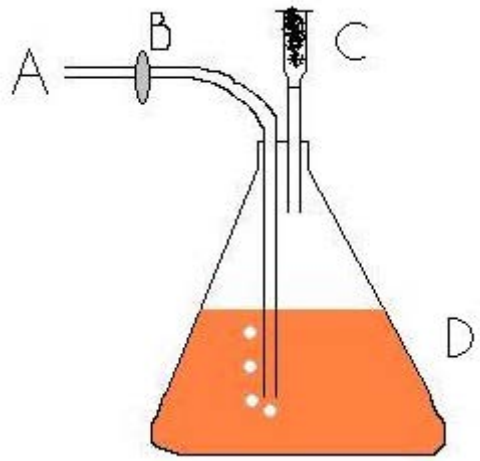

B

2.2.6 Feeding the bivalves

Bivalves were fed twice a week on Mondays and Thursdays with as much algal culture solution as available at the time. This was typically approximately 4-5 L of a dense brown algal culture of both *T-iso* and *Ch.m*. This technique maintained 66 pearl shell and 200 rock oysters in a bank of 8 tanks from mid-July 2005 to mid-November 2005. The tanks had a recirculating filtration system. Young spat were fed daily as described in section 5.3.

2.2.7 The recirculation system

Assorted bivalves were kept at FHU for many months, including mussels, pearl shell and rock oysters. They were maintained in two banks, each consisting of eight aquariums. Each aquarium held 126 L and each filter held 116 L. The water pump was an Onga 413. Each aquarium was aerated with an air stone from a communal air pump and heated to 28^{o}C using individual heaters in each aquarium. Figure 2.2.2 is a photograph of the recirculation system at the FHU.

Figure 2.2.2: The recirculation system at the FHU, each bank consisting of eight aquariums, a filter, water pump and an aeration system.

2.3 Materials and Methods for the Molecular Investigation of Organism

2.3.1 Samples used for the Molecular Investigation

The formalin-fixed, paraffin embedded tissues available from Department of Fisheries where analysed histologically and two oysters where identified as the most highly infected with the organism. Oyster number 3 on Slide 01-4281-09 was found to have an average of 69.7 organisms per high power field, and the third oyster on Slide 01-4281-15 had an average of 8.6 organisms per high power field. The

individual oysters were taken out of their original block (containing less infected oysters) by melting the paraffin and remounted on an individual paraffin block. This was so that slices could be made to use for the extractions. Haematoxylin and eosin (H&E) stained slides of both the blocks where made to confirm the correct oyster had been mounted. Some fresh oyster tissue was also used as a positive control for uninfected oyster DNA. These where collected during field trips and placed in ethanol until DNA extractions where performed.

2.3.2 Extractions from formalin fixed, paraffin embedded tissues

The most effective extraction technique for formalin-fixed, paraffin embedded tissue was found to be the 'Freeze Boil' Extraction technique, from 'Lab 9.25 Johne's Disease Laboratory Manual – EMAI' entitled: 'Preparation of paraffin-embedded tissues for PCR for *Mycobacterium paratuberculosis'* modified from Miller, Jenny et al. 1997.

This extraction technique requires 3 x 12 µm sections in PCR tubes from the paraffin blocks of interest. Firstly, the tube was centrifuged with a Centrifuge 5415D (Eppendorf) at 16,000 g for 60 seconds to pellet the tissue. Then to the tube was added 200 µl water with 0.5% v/v Tween 20. It was then boiled for 10 minutes and afterwards snap frozen in liquid nitrogen for another 10 minutes. This process was repeated and a final boil of 10 minutes is performed. The tube was then centrifuged at 3,000 g for 20 minutes. The supernatant was transferred to a fresh tube. This may contain milky strands. A second tube was prepared with a 1:10 dilution with MilliQ water. The samples may be stored at -20^{o}C. It was recommended to use 5 µl of each sample in the PCR reactions, using both the diluted and undiluted samples.

Another extraction technique used during this investigation was the MasterPure (Epicentre) extraction kit for formalin fixed paraffin embedded tissues, prepared according to manufacturer's instructions.

2.3.3 Extractions from fresh tissue

Fresh tissue or tissue kept in ethanol was extracted using the MasterPure DNA Purification kit (Epicentre) according to manufacturer's instructions.

Chapter 3: Investigations into the morphology of the intracellular ciliate

Photo: Sampling boat used to collect and process oysters in the Montebello Is., 2005

In this Chapter the morphological characteristics of the ciliate parasite were studied in detail. There are three main sections to this Chapter. The first will outline the major morphological characteristics of the parasite. The second is a morphological comparison between the intracellular ciliate of pearl oysters and the intracellular ciliate of mussels. The final part is an attempt to culture cell lines of bivalves so if the intracellular ciliate occurred in the wild, it could be maintained in an oyster cell culture for further study.

3.1 Morphology of the intracellular ciliate of pearl oysters

3.1.1 Introduction: The classification of ciliates

Modern taxonomic classification began in 1758 by Carl Linne (later Latinized to Carolus Linnaeus), who gave species two names, genera and species, and then grouped them further into families, orders, classes, phyla and kingdoms. He devised a scheme of two Kingdoms, Plantae and Animalia. A century later, with the release of Charles Darwin's 'The Origin of Species', biologists began to accept the concept of evolution, and this impacted on their understanding of classification. In 1969, Thomas Whittaker proposed the popular Five Kingdom system. He added three more Kingdoms, Monera, Protista and Fungi. Monera contained the prokaryotic organisms, with Protista incorporating the unicellular eukaryotic organisms, with a few exceptions. Fungi contained the heterotrophic organisms that secreted enzymes to digest their food source in the environment. Animalia contained heterotrophs that ingested other plants and animals before digesting them and Plantae contained the photosynthetic autotrophs.

With the discovery of new organisms that did not fit neatly into the Five Kingdom system, Carl Woese proposed reorganization in the 1980's. The Five Kingdoms where placed into three domains, Eukarya containing Animalia, Protista, Fungi and Plantae, Eubacteria containing the bacteria and Archaea containing all the unusual prokaryotes which did not fit well in the other kingdoms. This restructure attempted to organize biodiversity by evolutionary relationships. A modified five kingdom system is used by Margulis (1990), including Monera (Prokaryotae), Fungi, Animalia, Plantae and Protoctista.

Organisms included in the Kingdom Protoctista are non-plant, non-animal and non-fungal. Protists are the microscopic members of this enormous group of organisms, consisting of a single or a few cells. The antiquated two kingdom system, a relic from Linnaeus, still seems to frustrate biologists. Margulis, (1990), stresses that these organisms are 'no more "one celled animals and one celled plants", than people are shell-less multicellular amoebas.'

Within Kingdom Protoctista is the Phylum Ciliophora. They contain three general features that are found together in no other protoctist; 1. kineties: files of cilia, 2. cytostome: cell mouth around which specialized oral cilia are arranged, and 3. nuclear dualism (dikaryotic): a larger macronucleus and a smaller diploid micronucleus (germ nucleus whose meiotic products are exchanged during conjugation) (Lynn and Small 1990). They are a diverse group of organisms, inhabiting diverse environments worldwide.

Members of the Phylum Ciliophora have cilia at some stage in their life cycle, with rare exceptions. Most of them are phagotrophic, ingesting particulate matter into

food vacuoles at the cytostome, and after the digestive process has completed, they are excreted through the cell anus. This structure can either be a well defined cytoproct or a less organized cytopyge (Lynn and Small 1990). The reproduction of ciliates can be either through sexual conjugation or binary fission. The type and distribution of other cellular structures, such as contractile vesicles, extrusomes, stalks, and loricae can help distinguish between different groups of ciliates.

The outer 1-2 um of the cell is known as the cortex, and is divided into the somatic and oral regions. The somatic region is responsible for locomotion, sensing the environment, surface attachment and the secretion of protective coverings. The oral region however, has the function of sensing and the ingestion of nutrients (Lynn and Small 1990). Beneath the cortex is the infraciliature. This is considered the most striking morphological feature of ciliates (Pitelka 1963). It consists of kinetosomes arranged into longitudinal rows called kineties. The kinetosomes can either be in twos, (dikinetids) with their associated cilia, or single (monokinetids) with their associated cilia. These are termed the locomotor units known as kinetids. In many species there is a long cilia located on the posterior end, know as the caudal cilium.

The reason this parasite is being investigated is due to its sudden occurrence during routine health monitoring of Western Australia's pearling industry. Its distinct histological appearance sets it apart from any normal findings in pearl oyster spat up to that time. The histological similarities between this organism and ones found in mussels in Canada make it an obvious exercise to compare these protists. A similarity between the two may support the theory that this parasite has been transported to Western Australia.

3.1.2 Materials and Methods

The fixation and processing of samples for histology, SEM and TEM was described in more detail in *Chapter 2: Materials and Methods.*

Oyster samples

An archive of more than 70,000 formalin-fixed, paraffin embedded oyster tissues held by the Western Australian Department of Fisheries was made available for examination. These samples were obtained as part of ongoing surveillance health monitoring of the Western Australian pearl oyster industry. All the oysters had been sectioned and embedded according to normal procedures for health testing of pearl oysters, which permitted examination of most organs of the oyster including the digestive gland.

Histopathology

300 archived oyster samples were randomly selected from approximately 2000 samples. All oysters were less than 70 mm in size and of the 300 oysters 136 were from the Montebello Islands in December 2001, 151 were from Exmouth Gulf collected in October 2001 and 13 were from Exmouth Gulf collected in November

2002. Paraffin embedded blocks were sectioned at 4 µm thick, stained with H&E and Feulgen stain, based on routine procedures (Bancroft and Gamble 2002). Some oysters were sectioned at 8 microns for the silver peripheral nervous system (PNS) stain. The 300 H&E stained tissue sections were examined using an Olympus BH-2 microscope (Olympus Optical Co. Ltd.). Immunohistochemical staining was used, including Tubulin alpha (Epitope Specific Rabbit Antibody, Lab Vision Corporation) to stain for cilia. This was performed based on protocol from the manufacturer (Lab Vision Corporation).

Transmission Electron Microscopy (TEM)
Sections of formalin fixed paraffin embedded oysters confirmed to be positive for the ciliate on histology were re-embedded for TEM using standard methods, blocks were sectioned with an Om U3 (C.Reichert, Austria) ultramicrotome, stained with uranyl acetate and lead citrate and viewed with a Philips CM100 BIO TEM.

Scanning Electron Microscopy (SEM)
Sections of formalin fixed paraffin embedded oysters, confirmed to be positive for the ciliate on histology were reprocessed for SEM using standard methods. The specimen was viewed using a Philips XL20 SEM.

3.1.3 Results

Summary of findings:
The spindle shaped body of the cell had an average width of 5.53 µm (range of 2.73 to 7.47 µm) and an average length of 11.15 µm (range of 9.02 to 16.2 µm) with 9 ciliates measured (Figure 3.1.1). It had 9 evenly spaced rows of cilia running obliquely along the length of cell, converging on the anterior and posterior ends. The cilia were long and measure greater than 10µm in length. There was a consistently large nucleus to cytoplasmic ratio, with the ovoid globular nucleus maintaining central positioning. A centrally placed nucleolus was visible in some sections. On TEM, numerous round to slightly ovoid mitochondria were visible, approximately 0.7 µm in size.

Microscopy:
Using 300 archival formalin fixed, paraffin embedded oysters, the initial histological examination was made on over 10,000 ciliates. On histological examination, the organism was observed to be tear-drop shaped with a prominent basophilic lobulated nucleus, surrounded by a halo of faint eosinophilic cilia. The cells appeared to be situated within the cytoplasm of the digestive cells of the oysters digestive gland. Figure 3.1.2 is a photo micrograph of a digestive tubule at high magnification. Several ciliates are infecting the cells of this tubule, each situated within the apical portion of the lightly eosinophilic vacuolated cytoplasm of the digestive cells. No ciliates were observed in any other organs of the oyster, or in any other part of the digestive tract. With approximately 10,000 sections containing ciliates viewed, no

Figure 3.1.1: A representative diagram of the main features of the intracellular ciliate, with the cilia removed. The 9 kineties run obliquely the length of the cell (numbered). Approximately two thirds of the cytopharyngeal structure (C) is beneath the surface of the cell, and is situated on the anterior end. The multi-lobulated macronucleus (N) is located in the centre of the cell, with varying numbers of lobules of varying sizes. The less electron dense nucleolus (L) is positioned in the centre of the nucleus. The scale bar represents 10 µm.

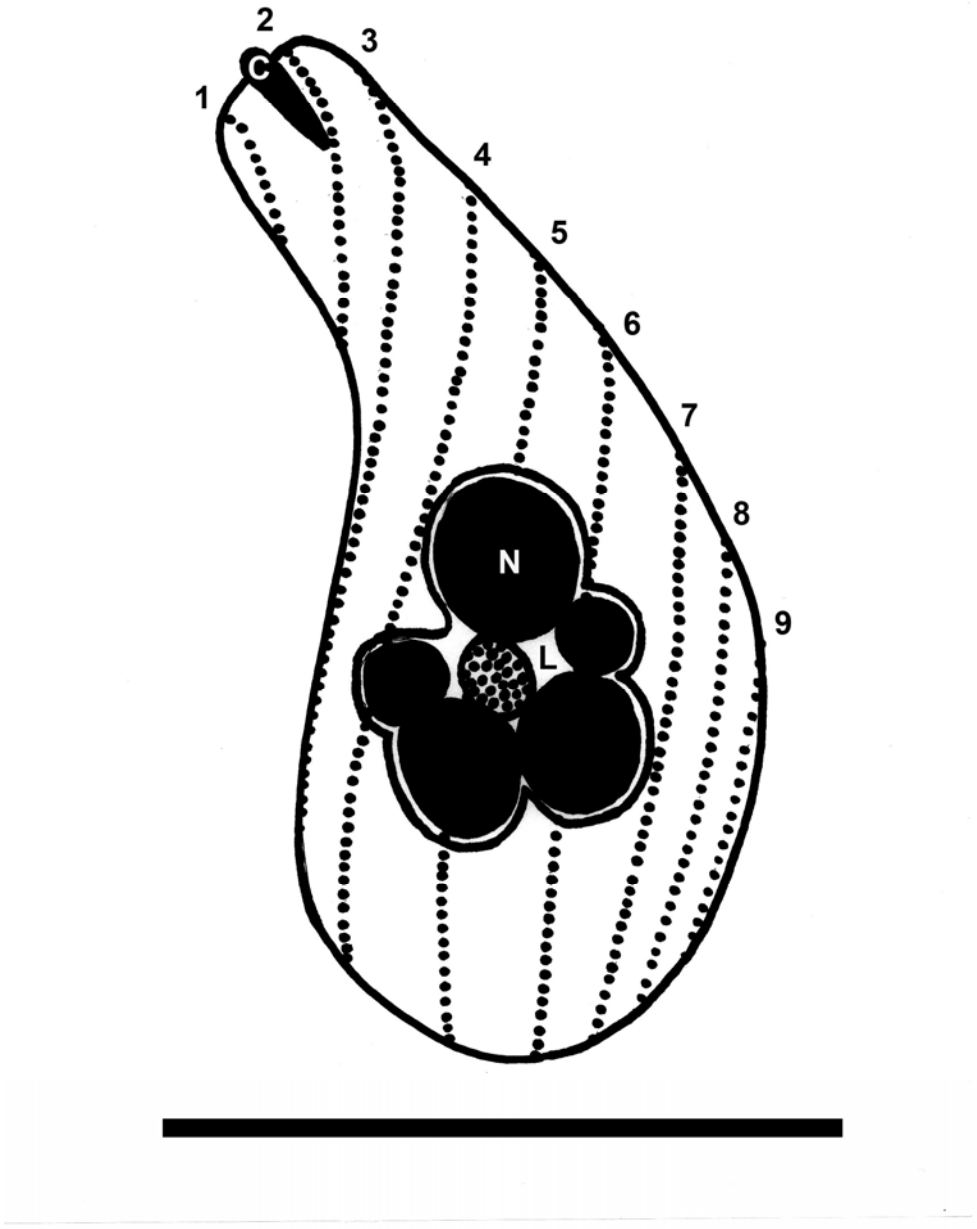

conjugation or dividing cells were observed. On transverse section, the ciliates appeared round with no dorso-ventral flattening.

Examination of histological sections stained with the silver PNS stain highlighted distinct rows of cilia (kineties) running obliquely the length of the cell, converging at the apex and at the caudal end. The visible cilia were of considerable length. The nucleus appeared spherically lobular and centrally positioned. Figure 3.1.3 is a collection of four photos depicting the silver stained ciliates with high magnification. Figure 3.1.3 A to C are the same three ciliates at varying focus, displaying the oblique kineties running the length of the cell. Figure 3.1.3 D is a single silver stained ciliate at transverse section, clearly demonstrating the nine rows of cilia encircling the cell. On the anterior tip, a densely staining rod approximately 2-3 microns in length extends into the cytoplasm, possibly composing part of the cytopharyngeal structure. Figure 3.1.4 is four photos of the silver stained ciliates depicting the rod structure on the anterior tip of the cell. Figure 3.1.4 D shows a ciliate in transverse section, with the rod clearly visible in the centre of the anterior end, indicating the rod extends into the cell.

The shape of the nucleus in routine H&E sections was unusual and to confirm that the lobules were nucleic material a Feulgen stain which preferentially stains chromosomal material or DNA was used. Figure 3.1.5 B depicts the ciliate in this stain, where the dense lobular bodies in the centre of the cell stained intensely for DNA.

The Giemsa stain is usually used for the detection of blood parasites, and is a mixture of methylene blue and eosin. In Figure 3.1.5 C, the nuclei of the Giemsa stained ciliates stained dark blue with the cytoplasm exhibiting a granular appearance. Similarly, the methyl green pyronine stained the nucleus dark purple with a finely granular cytoplasm. This is depicted in Figure 3.1.5 D.

The immunohistochemical stain for Tubulin alpha revealed a positive staining of the cilia of the parasite. Figure 3.1.6 are photo micrographs of the Immunohistochemical staining using antibody for Tubulin alpha. Figure 3.1.6 A is a photo micrograph of two ciliates within the digestive gland of an oyster. A positive orange-staining halo of cilia encircle the body of the parasites, indicating these are cilia. Figure 3.1.6 B is the positive control slide of ciliated epithelium in the lung of a mammal.

Figure 3.1.2: A digestive gland of *P. maxima* with numerous intracellular parasites (100x objective lens). Scale bar 15 µm.

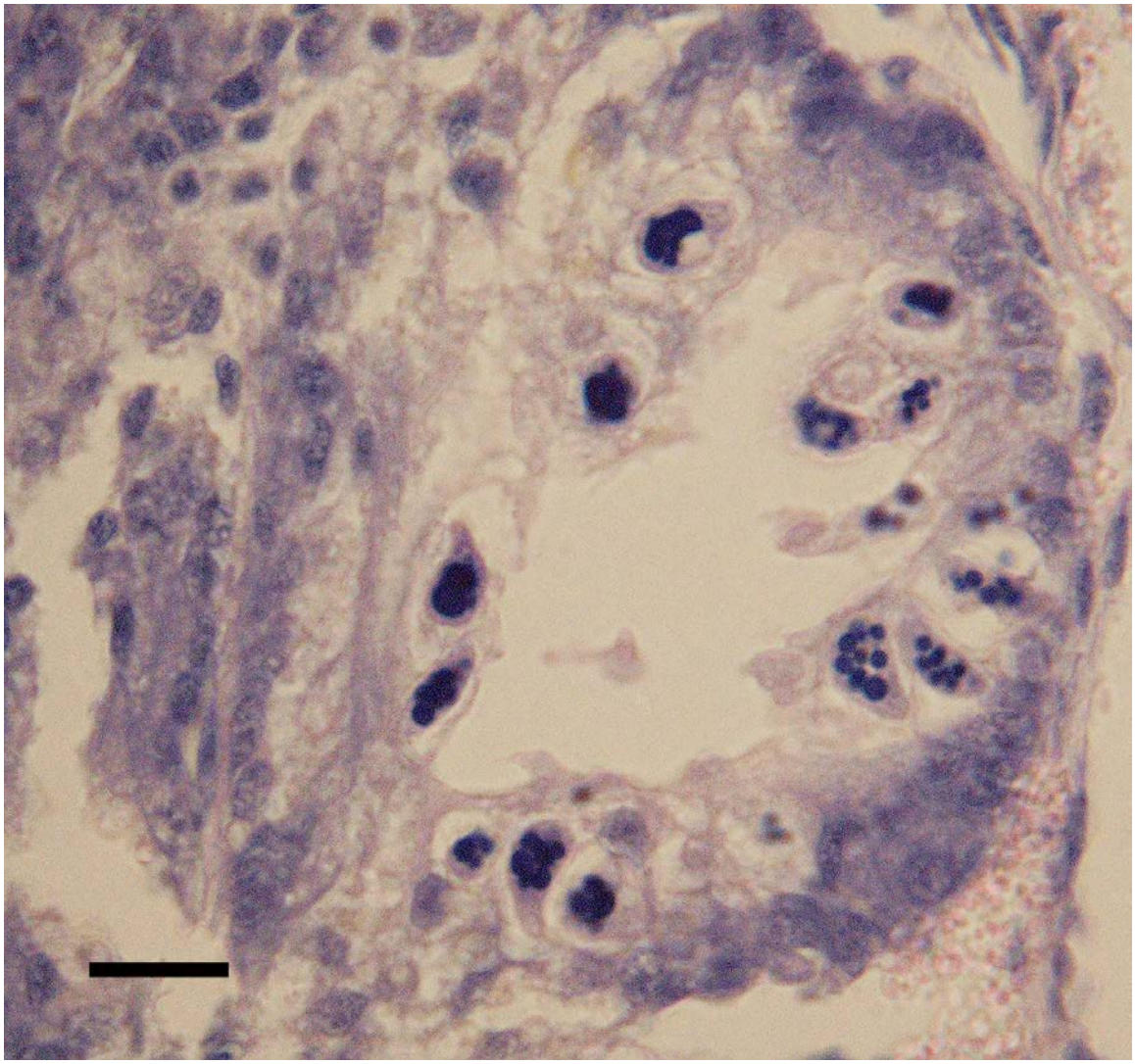

Figure 3.1.3: Three photomicrographs of the same ciliates (A-C) at varying focus using the silver impregnation stain (100x objective lens). The nine oblique kineties are visible along the length of the cells. D: A transverse section of a ciliate depicting the 9 kineties with silver PNS stain. Scale bar is 10 µm.

A

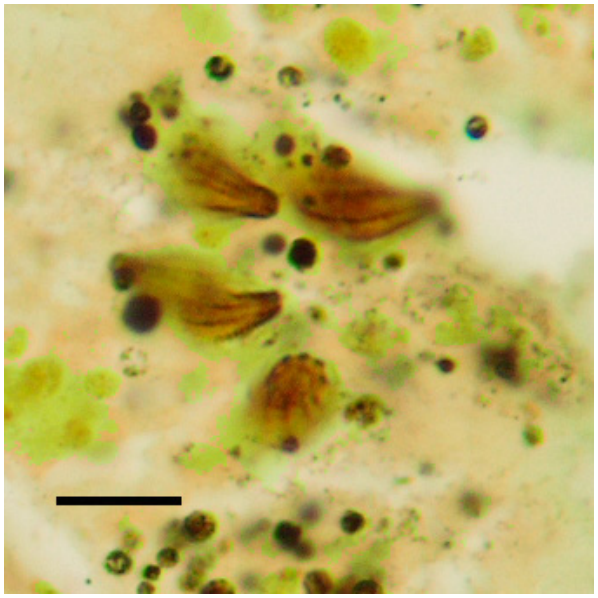

B

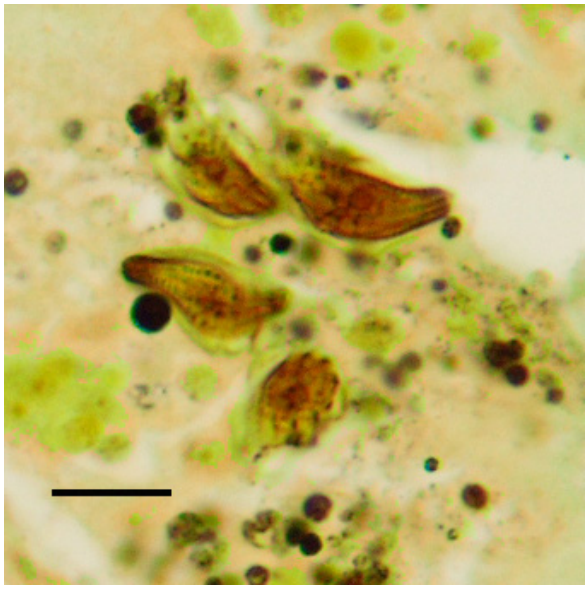

C

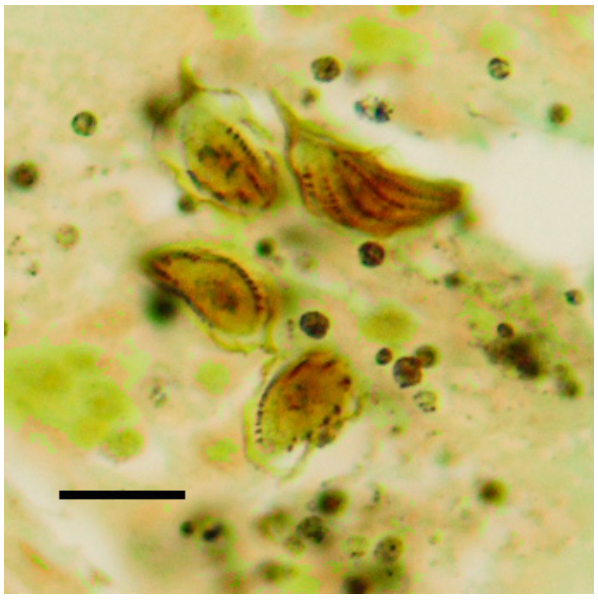

D

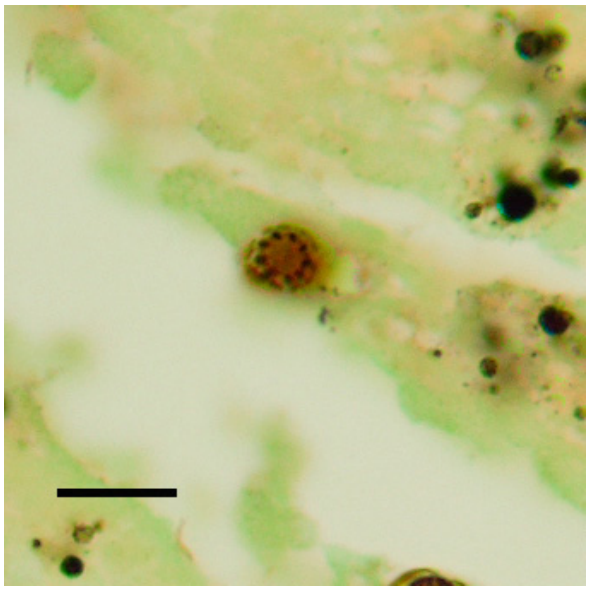

Figure 3.1.4: Four photomicrographs of the intracellular ciliate stain with the silver PNS stain at 100x optical lens. All show the densely staining rod on the anterior tip, approximately 2-3 microns in length, evident in (A) and (C). Approximately two thirds of the structure extends into the cytoplasm of the cell, particularly evident in longitudinal section (B) and transverse section (D). Scale bar is 10µm.

A

B

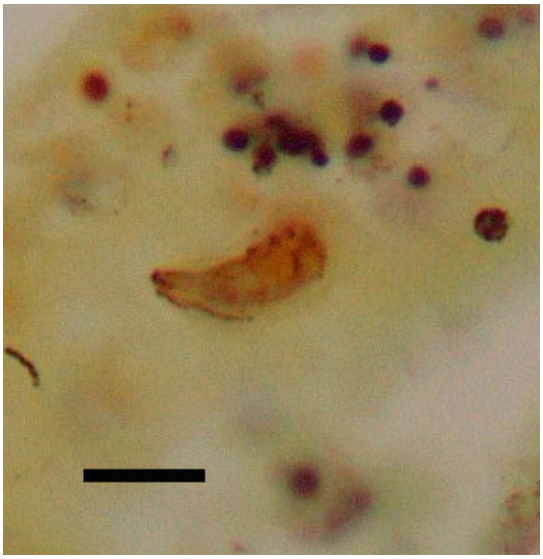

C

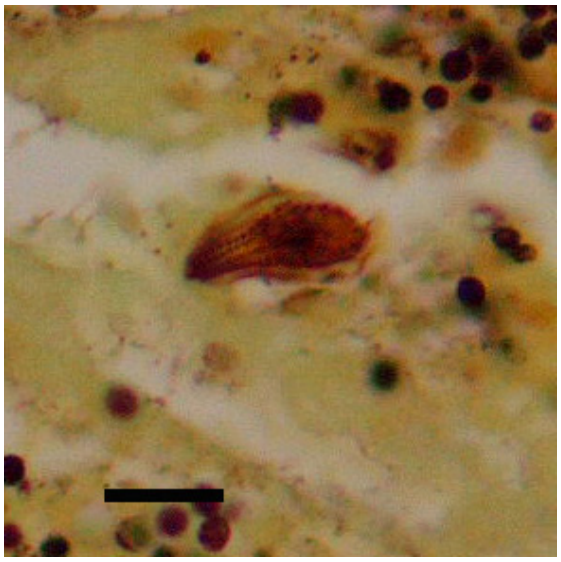

D

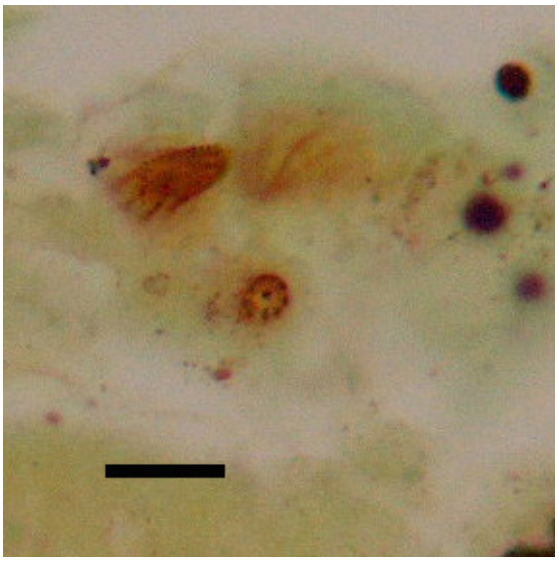

Figure 3.1.5: Four photo micrographs of the intracellular ciliate at 100x optical lens. A: This is the ciliate with the PNS silver stain for comparison. B: The ciliate with the Feulgen stain with the lobular bodies in the centre of the parasite staining intensely for DNA. C: The Giemsa stain highlighted the granular cytoplasm of the ciliate. D: The ciliate stained with methyl green pyronine, indicating a densely stained nucleus and finely granular cytoplasm. Scale bars are 10 µm.

A

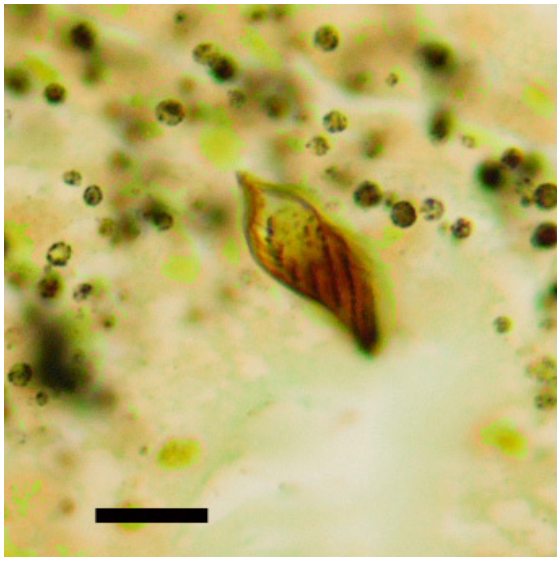

B

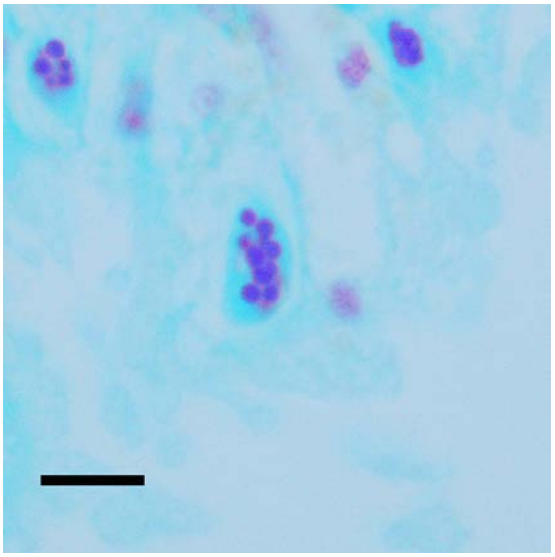

C

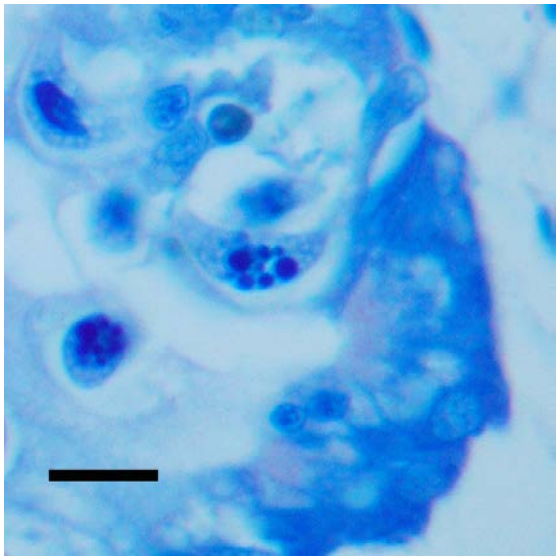

D

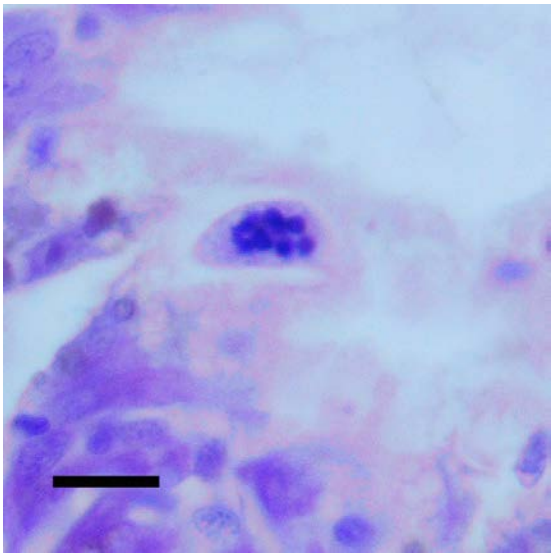

Figure 3.1.6: Immunohistochemical staining using antibody for Tubulin alpha. **A:** a photo micrograph of two ciliates within the digestive gland of an oyster. A positive orange-staining halo of cilia encircle the body of the parasites, indicating these are cilia. **B:** The positive control slide of ciliated epithelium in the lung of a mammal.

A

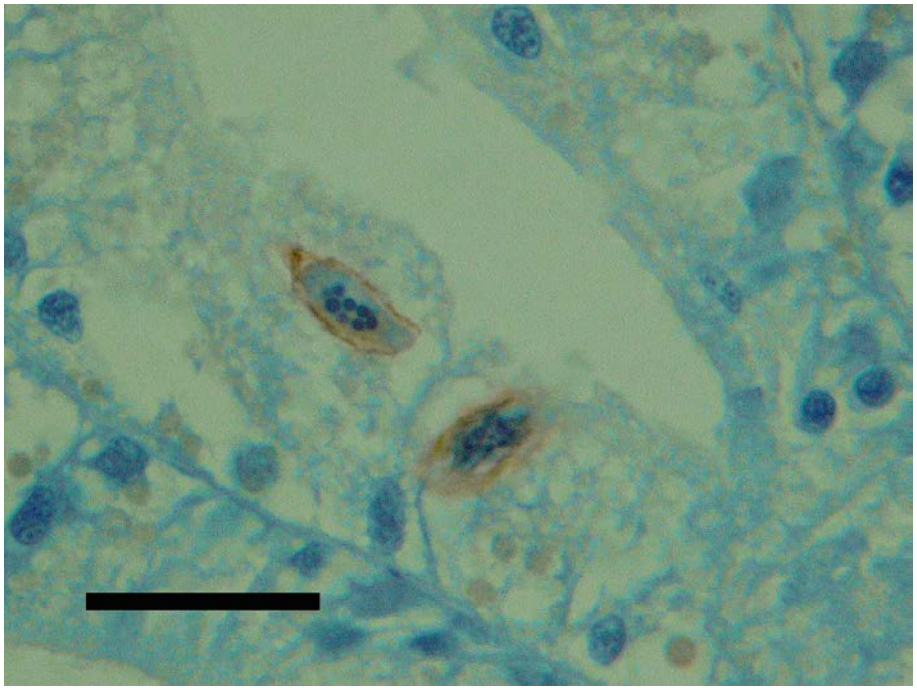

B

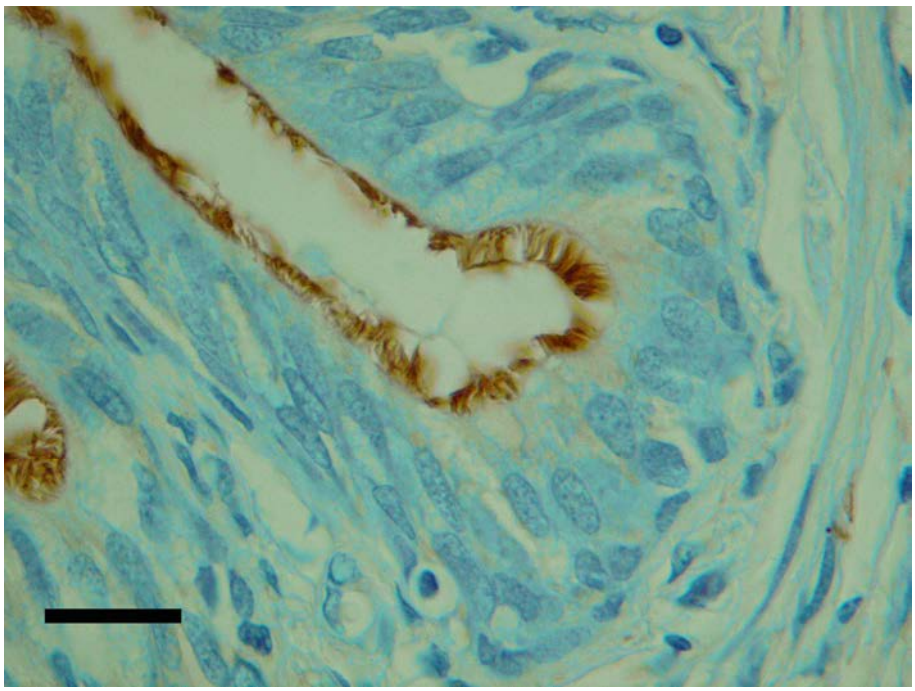

Transmission Electron Microscopy

The quality of the re-embedded TEM sections was not sufficient to reveal fine details of cell architecture. The tear-drop shaped body of the cell had an average width of 5.53 µm (range of 2.73 to 7.47 µm, n= 9) and an average length of 11.15 µm (range of 9.02 to 16.2 µm). It had 9 evenly spaced rows of cilia (monokinetids) running obliquely along the length of cell, converging on the pointed end. Figure 3.1.7 is an electron micrograph of an intracellular ciliate in transverse section, sectioned through the centre portion of the cell indicated by the large cytoplasmic area taken up by the lobulated nucleus. The nine rows of cilia extending evenly from the cell are visible and are numbered. The cilia measure greater than 10µm in length, depicted in Figure 3.1.8, an electron micrograph of two intracellular ciliates, one with its cilia measurable in longitudinal section.

There was a consistently large nucleus to cytoplasmic ratio, with the globular nucleus maintaining central positioning. A centrally placed nucleolus was visible in some sections. This is visible in the transverse sectioned ciliate in Figure 3.1.9 as the less electron dense area within the more electron dense lobules of the nucleus. The nucleus was composed of between 1 and 13 irregularly sized, ovoid lobules, some sections with fusion of the lobules. Many round to slightly ovoid mitochondria were visible, approximately 0.7 µm in size. The cytoplasm had a dense granular appearance and contained numerous round electron dense bodies in cytoplasm approximately 0.2 µm in diameter and fine rows of tubulin-like structures. Each cilia had the 9x2 arrangement, and was greater than 10µm in length. The cytopharyngeal structure was not recognisable on any of the TEM sections.

Ciliates were only observed inhabiting the digestive cells of the pearl oysters' digestive gland. The basophil cells, with their abundant rough endoplasmic reticulum, directly adjacent to infected digestive cells, were apparently unaffected. In cases where up to three ciliates inhabited a single cell, each were separated by host cytoplasmic material.

Scanning Electron Microscopy

Unfortunately no ciliates were observed in the samples processed for SEM. However, the digestive tubules were identified on the specimen. Figure 3.1.10 is a digestive tubule within a pearl oysters digestive gland. The lumen of the tubule is surrounded by epithelial cells of varying height.

Figure 3.1.7: An electron micrograph of the intracellular ciliate in transverse section. 9 rows of cilia (kineties) are visible (numbered). There is a large nucleus (N) to cytoplasmic ratio, and numerous mitochondria (M). Scale bar represents 2 µm.

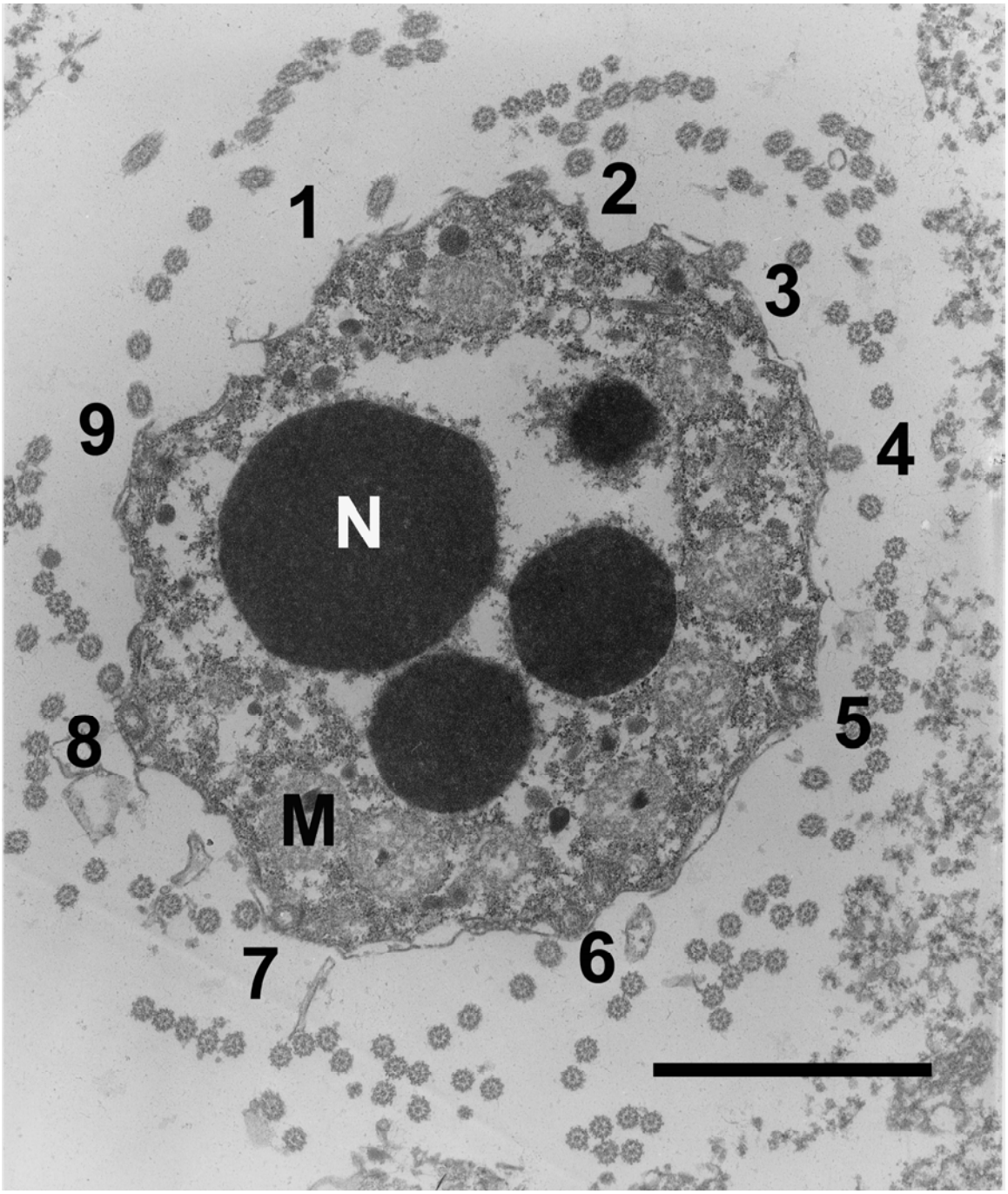

Figure 3.1.8: An electron micrograph of two intracellular ciliates. The cilia (C) of the ciliate (B) are greater than 10 µm in length. A second ciliate (2) is also displaying lengthy cilia. Scale bar = 5 µm.

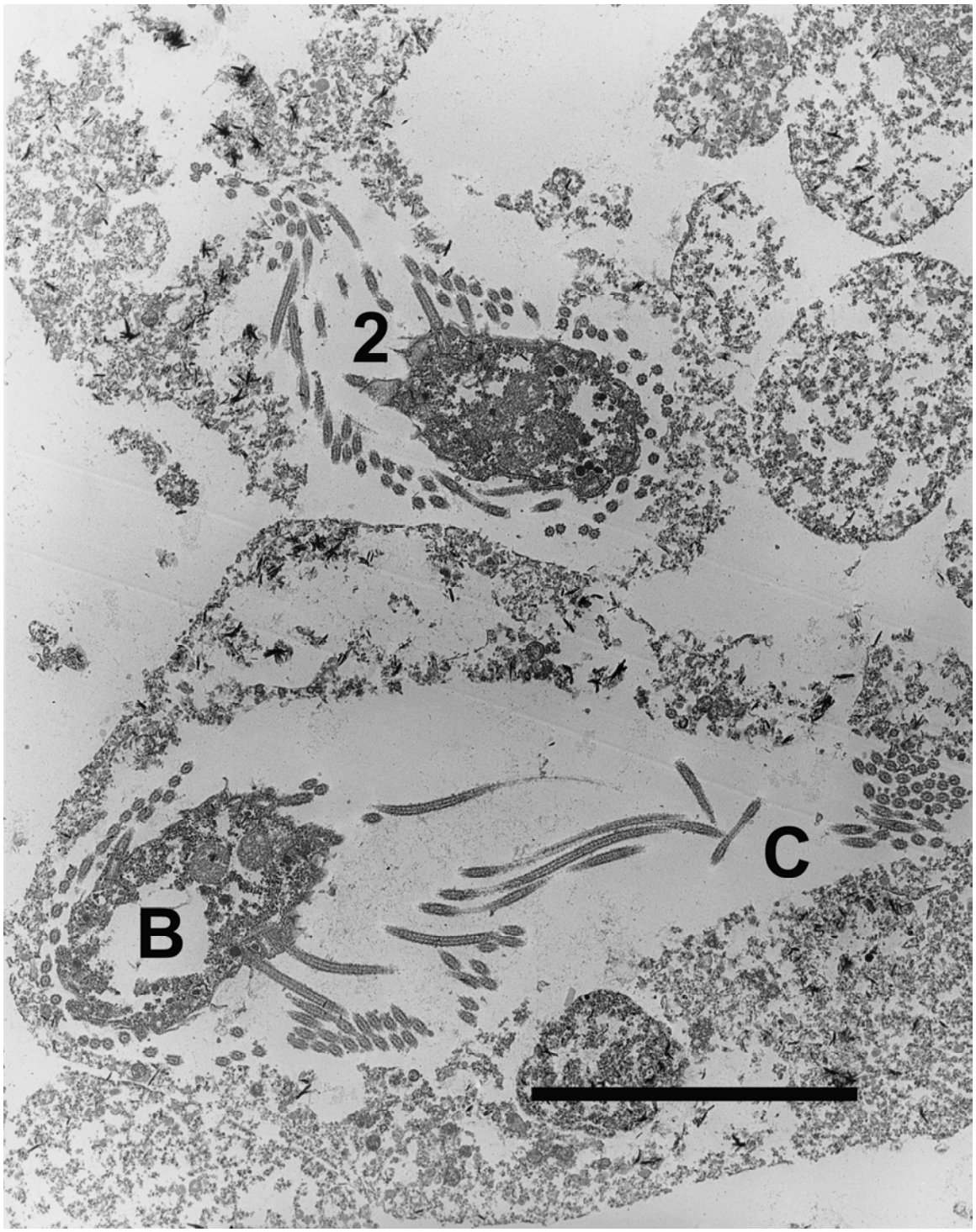

Figure 3.1.9: An electron micrograph of the intracellular ciliate in transverse section. The nuclear lobules are labelled (N) and in their centre is the less electron dense nucleolus (L). Scale bar represents 2 µm.

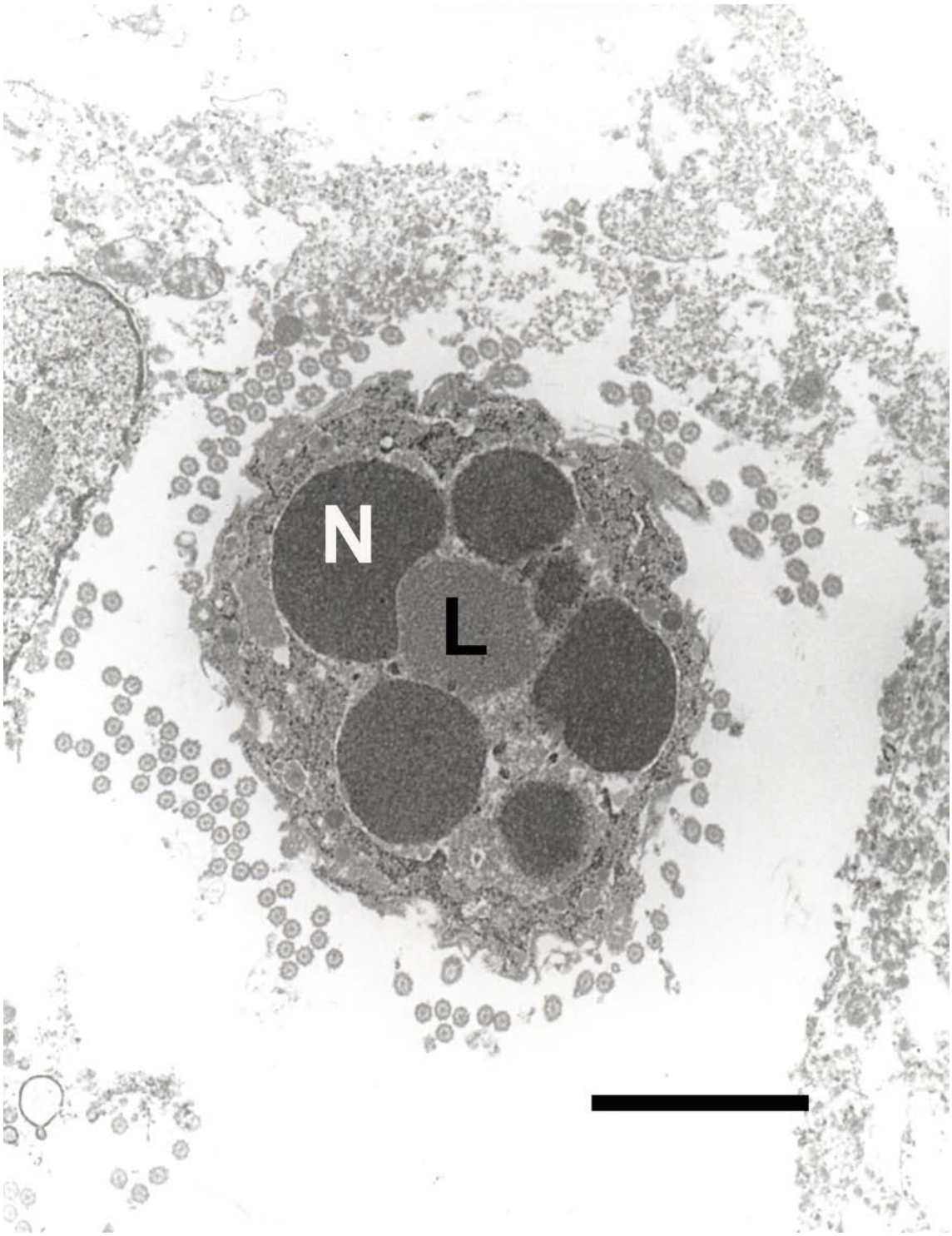

3.1.4 Discussion

In this section of the study, the organism was viewed using histology and transmission electron microscopy using a variety of stains to discover its morphological characteristics. Ideally, the identification of ciliated protists involves using a combination of techniques including live observations, scanning electron microscopy, transmission electron microscopy, silver impregnation and histology (Foissner 1991). Live observations are considered essential in order to discover movement, behaviour and reproduction. Being an intracellular organism limits the ability for live observations, scanning electron microscopy and silver impregnation methods. More recently, molecular techniques have been used for phylogenetic identification. Using 300 archival formalin fixed, paraffin embedded oysters, the initial histological examinations were made on over 10,000 ciliates. Histology is not recommended for the identification of ciliates since key features used for taxonomic characterisation are usually not visible (Laruelle, Molloy et al. 1999); however in this instance it was unavoidable.

Other ciliates that share characteristics

Despite the ultrastructure being obscured due to the processing of the tissues, some characteristics of the intracellular ciliate were visible. In order to identify its taxonomic affiliates, ciliates that shared some of these characteristics were compared with the intracellular ciliate of pearl oysters (Table 3.1.1).

Sphrenophrya dreissenae (Rhynchodida: Sphenophrydae), within the class Phyllopharyngea, are host-specific parasites to the zebra mussel *Dreissena polymorpha* (Laruelle, Molloy et al. 1999). These ciliates parasitise the gill epithelium, and have been reported within the gill water tubes and suprabranchial cavities. High numbers are associated with epithelial hyperplasia, hypertrophy and vacuolisation. Similar to the intracellular ciliate of pearl oysters, *S. dreissenae* has a high macronucleus to cytoplasm ratio with a distinctive large, densely basophilic, globular to banana shaped macronucleus. Distinguishing features from the pearl oyster ciliate is their adult stages lack cilia, and attach to host epithelial cells with a specialised flat sole (Laruelle, Molloy et al. 1999).

Other *Sphenophrya*-like ciliates have been reported from a range of bivalve species in eastern and western U.S., Canada, Europe and Scandinavia. Large numbers can occur in host shellfish with no apparent host-response. In less than 1% of cases the ciliates are intracellular and may cause a xenoma (Bower and McGladdery 2003).

Stegotricha enterikos (Rhynchodida: Ancistrocomidae) parasitizes the digestive gland of Pacific oysters, *Crassostrea gigas* in Canada (Bower and Meyer 1993). This relatively large organism has an approximately 50 x 18 µm ovoid body covered with 16 oblique kineties. A distinctive cytopharyngeal structure was identified, consisting of radially arrayed overlapping microtubules. On light microscopy, this structure

Figure 3.1.10: A scanning electron micrograph of the digestive tubules of a pearl oyster at 859x magnification. The acinar structure of the tubules with variable sized epithelial cells are visible. Scale bar represents 20 µm.

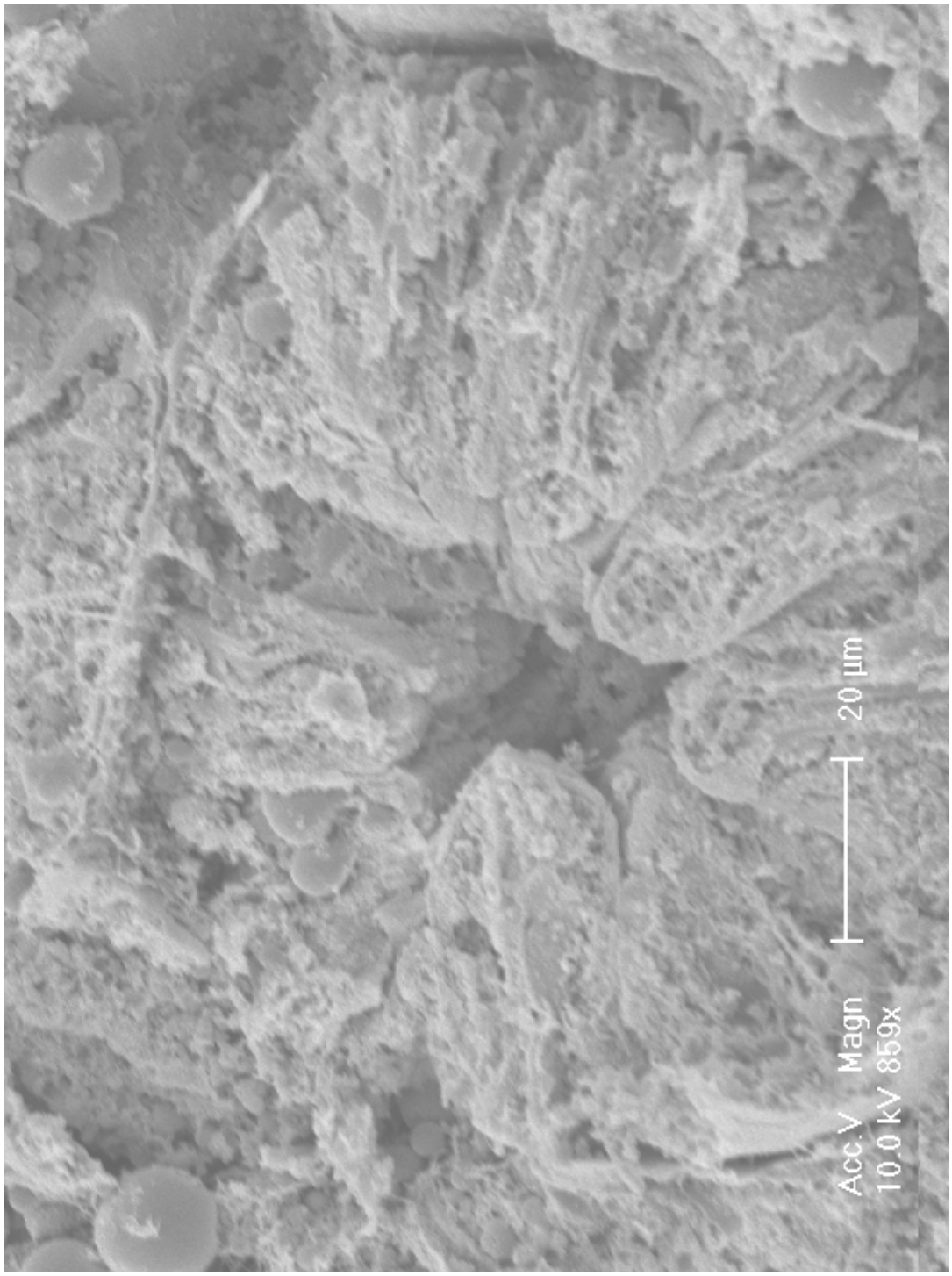

Table 3.1.1: Features of ciliates that share similar characteristics to the intracellular ciliate of pearl oysters and their taxonomic affiliations.

Species	**Cell Size (µm)**	**Cell shape**	**Nuclear features**	**Cilia**	**Cytoplasm**	**Where found**	**Other features**	**Taxonomy**
Intracellular ciliate of pearl oysters	11x5.5	Tear drop	Macronucleus multilobular	9 oblique kineties	Heterogenous	Intracellular in digestive gland cells of *P. maxima*	High macronucleus to cytoplasm ratio Causes host reaction	Yet unspecified
Sphenophrya dreissena (Laruelle, Molloy et al. 1999)	27-37	Helmet	Macronucleus highly irregular (globular to banana shaped)	Lack cilia in adult stage	Pink-purple homogenous without prominent inclusions and vacuoles	Gill epithelium, within gill water tubes of zebra mussels	High macronucleus to cytoplasm ratio Causes tissue reaction at site	Ciliophora Phyllopharyngea Rhynchodida Sphenophryidae
Hypocomagalma dreissenae (Laruelle, Molloy et al. 1999)	32-50	Ovoid	Macronucleus ovoid to spindle	Cilia visible on histology	Heterogenous with prominent inclusions and vacuoles	Gill, mantle cavity and labial palps of zebra mussels	Inserts tentacle into epithelial cell cytoplasm of host	Ciliophora Phyllopharyngea Rhynchodida Ancistrocomidae
Ancistrocoma-like protozoa (Humphrey and Norton 2005)	25-30	Elongate ovoid	Macronucleus ovoid	Cilia visible on histology surrounding cell	Heterogenous	Intestinal lumen of *Pinctada maxima*	Non-pathogenic	Ciliophora Phyllopharyngea Rhynchodida Ancistrocomidae
Stegotricha enterikos (Bowers and Meyer, 1993)	50x18	Elongated ovoid	Spherical macronucleus	16 oblique kineties, 1 sparsely ciliated row	Unspecified	Lumen of digestive gland tubules of pacific oysters *C. gigas*	Light infections, no pathology associated	Ciliophora Phyllopharyngea, order Rhynchodida Ancistrocomidae

bears a resemblance to the cytopharyngeal knob on the anterior end of the pearl oyster ciliate (pers comm., Bower). *S. enterikos* has not been associated with and host pathology, even in heavy infections, greater than 25 ciliates per wet mount (Bower and Meyer 1993).

Another Ancistrocomid worth mentioning is *Hypocomagalma dreissenae* (Rhynchodida: Ancistrocomidae), which parasitises the gills of the zebra mussel *Dreissena polymorpha* (Laruelle, Molloy et al. 1999). Although larger than the pearl oyster ciliate at 32-50 µm, this organism keeps its cilia as an adult and is found attached to various epithelial surfaces on the mussel by means of a tentacle inserted in the host cell cytoplasm. Despite this seemingly brutal attachment method, only a few organisms are seen in any one mussel and have not been associated with any pathology.

An *Ancistrocoma*-like ciliated protozoa has been reported in Western Australian silverlip pearl oysters, within the intestine of mature oysters and the gills of juveniles. These cause no host response, so are generally considered non-pathogenic (Humphrey and Norton 2005). These are many times larger than the intracellular ciliate and have been found parasitizing the same individual.

Future research recommendations
In order to correctly identify the taxonomic affiliations of this parasite, the cortical ultrastructure must be clearly visualised. The somatic kinetid is a highly conserved region of the ciliate and therefore forms the basis of the taxonomic characterisation, reviewed by Lynn and Small (1990). Foissner (1991), highlighted the importance of using a variety of visualisation techniques, such as TEM, SEM, silver impregnation and live observation, to acquire a complete understanding of the ciliates structure and characteristics, before one attempts to describe a new organism.

3.2 Comparative morphology of Canadian mussel ciliate

3.2.1 Introduction

Intracellular parasitic Rhynchodid-like Phyllopharyngea ciliate infections have been reported in mussels *Mytilus edulis*, *Mytilus trossulus* and *Mytilus galloprovincialis* in Canada (McGladdery and Bower 2002), America (Figueras et al. 1991) Spain (Villalba et al. 1997), and Germany. In mussels, the parasite has not been found to be associated with any pathological changes (Figueras et al. 1991) and are considered Negligible Significance in Canada (McGladdery and Bower, 2002). Due to its sudden appearance in pearl oysters in Western Australia and its associated pathology, the origin of the Australian intracellular ciliate needed to be investigated. To discover whether the ciliates from Australia and Canada were related, or in fact were the same organism, a morphological comparison was made between the intracellular ciliate of

Australian pearl oysters and the intracellular ciliate of Canadian mussels, with the aid of Fisheries and Oceans Canada.

3.2.2 Methods

The fixation and processing of samples for histology and TEM was described in more detail in *Chapter 2: Materials and Methods*.

Mussel samples
Mussel tissue (*Mytilus sp*.) infected with the intracellular ciliate were made available from Oceans and Fisheries Canada. The sample was collected from Sooke, British Columbia, Canada in August 1989 and was preserved in Davidson's fixative and embedded in paraffin according to standard procedures.

Histopathology
Paraffin embedded blocks were sectioned at 4 microns, stained with haematoxylin and eosin (H&E) based on routine procedures (Bancroft and Gamble 2002). Some oysters were sectioned at 8 microns for the silver peripheral nervous system (PNS) stain. The stained tissue sections were examined using an Olympus BH-2 microscope (Olympus Optical Co. Ltd.).

Transmission Electron Microscopy (TEM)
Sections of formalin fixed paraffin embedded oysters confirmed to be positive for the ciliate on histology were re-embedded for TEM using standard methods, blocks were sectioned with an Om U3 (C.Reichert, Austria) ultramicrotome, stained with uranyl acetate and lead citrate and viewed with a Philips CM100 BIO TEM.

3.2.3 Results

Light Microscopy
H&E stained sections showed a tear-drop shaped ciliated organism approximately 10-15 µm x 5 µm in size. All organisms were situated within the cytoplasm of digestive epithelial cells. They had a multilobulated nucleus, with varying numbers of round lobules of varying sizes and a large nucleus to cytoplasmic ratio. The ciliates exhibited a basophilic and finely granular cytoplasm and the entire cell was surrounded by a halo of cilia, within an area free of host cytoplasmic material. Figure 3.2.1 is a photo micrograph at high magnification, depicting several ciliates inhabiting the cells of a tubule, each situated within the apical portion of the vacuolated cytoplasm of the digestive cells. Some cells are infected with more than one ciliate.

The samples stained with the silver PNS stain displayed oblique rows of cilia (kineties) running the length of the cell, converging on either end of the organism. Figure 3.2.2 depicts four photomicrographs of silver stained intracellular ciliates of mussels at high magnification. Figure 3.2.2 A is a longitudinal section of a ciliate, displaying the rows of cilia running obliquely along the length of the cell, converging

at the ends. Figure 3.2.2 B depicts a transverse section of the ciliate, with the nine oblique kineties visible encircling the cell. A densely staining rod, similar to the cytopharyngeal structure described on the intracellular ciliate of pearl oysters was also visible on some sections. Figure 3.2.2 C and D are photographs of this structure on ciliates in a mussels digestive gland.

Transmission Electron Microscopy

Similarly to the pearl oyster samples, the quality of the re-embedded TEM sections was not sufficient to reveal fine details of cell architecture. The tear-drop shaped cell of the organism had an average width of 5.05 µm (range of 4.0-6.13 µm, n= 6) and an average length of 16.27 µm (range of 19.89-12.66 µm). It had 9 evenly spaced rows of cilia (monokinetids) running obliquely along the length of cell, converging on either end. There was a consistently large nucleus to cytoplasmic ratio, with the globular nucleus maintaining central positioning. The nucleus was composed of between 1 and 11 irregularly sized, ovoid lobules, some sections with almost complete fusion of the lobules. Many round to slightly ovoid mitochondria were visible, approximately 0.66 µm in size. The cytoplasm had a dense granular appearance and contained fine rows of tubulin-like structures. Ciliates were inhabiting the cytoplasm of the digestive cells. In cases where more than one ciliate inhabited a single host cell, each were separated by host cytoplasmic material.

Figure 3.2.1: The digestive gland of a mussel, *Mytilus sp*. with numerous intracellular parasites (100x objective lens). Scale bar 15 µm.

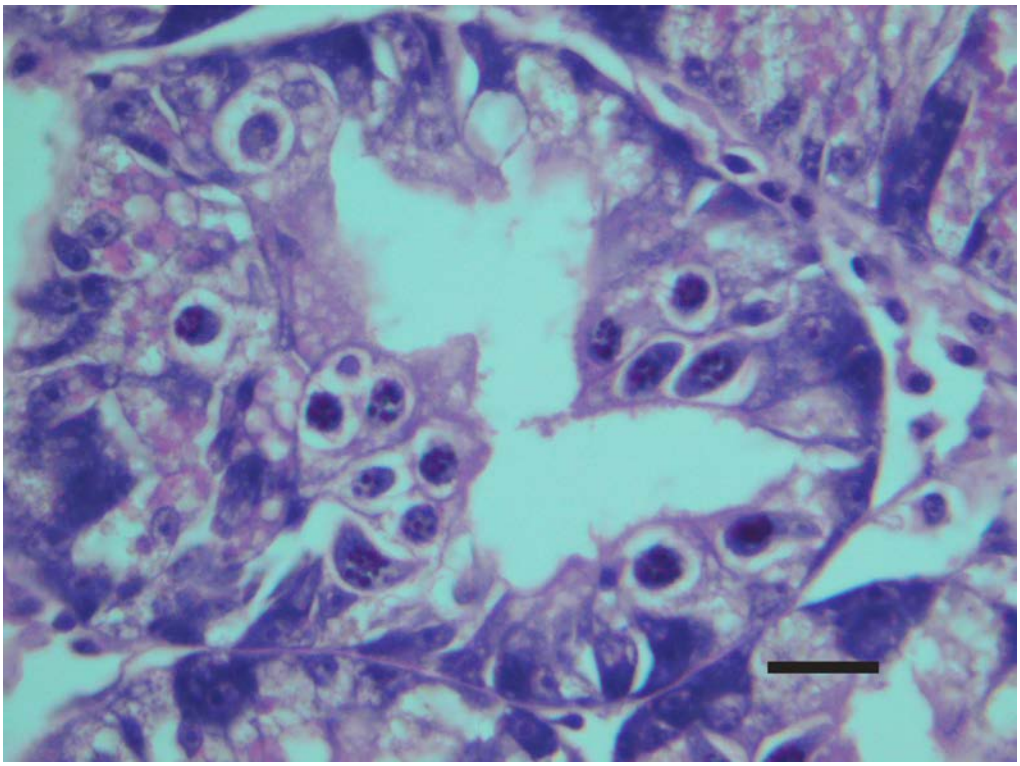

Figure 3.2.2: Four photomicrographs of silver stained intracellular ciliates of mussels (100x objective lens). A: A longitudinal section of a ciliate, displaying the rows of cilia running obliquely along the length of the cell, converging at the ends. B: A transverse section of the ciliate, with the nine oblique kineties visible encircling the cell. C and D: The densely staining rod cytopharyngeal structure is visible at the apex of the cell. Scale bar is 10 µm.

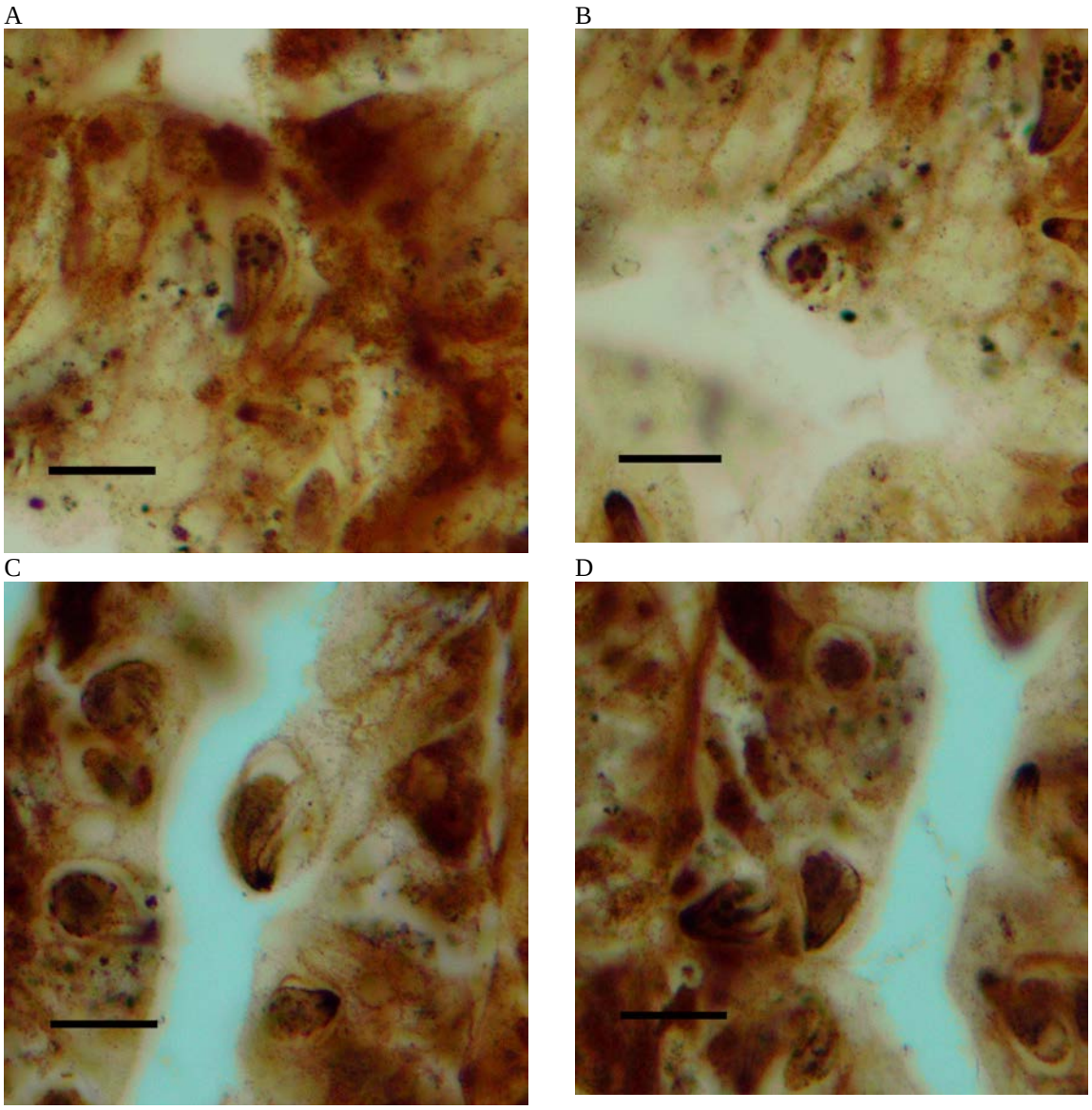

Figure 3.2.3 is an electron micrograph of an intracellular ciliate of mussels in oblique section. The multi-lobulated nucleus in the centre of the cell contains a less electron dense nucleolus. The cilia encircle the cell and are within an area void of host cytoplasmic contents. Numerous mitochondria are visible, contained within the ciliates cytoplasm. Figure 3.2.4 is an electron micrograph of the intracellular ciliate in midline transverse section. Nine rows of cilia (kineties) are evenly spaced around the cell. There is a large nucleus to cytoplasmic ratio, with many of the nuclear lobules fused in this specimen. Figure 3.2.5 is photo micrograph of two intracellular ciliates inhabiting digestive cells of a mussels digestive tubule. The brush border of the digestive cell is visible, indicating the ciliates are situated within the host cell, inside an area void of cytoplasmic material. The lumen of the tubule is also distinguishable, as are the lysosomal bodies of the digestive cells.

3.2.4 Discussion

Intracellular parasitic ciliate infections have been reported in mussels in Spain (Villalba et al. 1997), the east and west coasts of America (Figueras et al. 1991) including Canada (McGladdery and Bower 2002) and the German East-Frisian coast. The host species include *Mytilus edulis, Mytilus trossulus* and *Mytilus galloprovincialis* and the taxonomic affiliation of the parasite has been identified as Rhynchodid-like Phyllopharyngea ciliates. In infected mussels the organisms infect the digestive tubule epithelial cells (McGladdery and Bower 2002) but do not elicit any significant host response despite their intracellular location (Figueras, Jardon et al. 1991) and because of this are considered of negligible regulatory significance in Canada, (McGladdery and Bower 2002). They have been reported with a prevalence of up to 40% in Spain, however elsewhere are usually found at less than 1%.

The similarities between the intracellular ciliate found in Canadian mussels and the Australian intracellular ciliate of pearl oysters is alarming. On histological examination, Jones and Creeper 2006 noted the close morphological similarities between the two ciliates, and the TEM sections analysed here have supported this statement. The ciliates of mussels were found to be tear-drop shaped cells with an average width of 5.05 µm (range of 4.0-6.13 µm) and an average length of 16.27 µm (range of 19.89-12.66 µm) with 6 ciliates measured. Similarly, the intracellular ciliates of pearl oysters were found to be tear-drop shaped organisms with an average width of 5.53 µm (range of 2.73 to 7.47 µm) and an average length of 11.15 µm (range of 9.02 to 16.2 µm) with 9 ciliates measured (Figure 3.2.6). Given the differences in processing, ie. the pearl oyster ciliates were fixed in formaldehyde solution, while the mussel ciliates were fixed in Davidson’s, and the limitations of measuring pleomorphic structures on TEM sections, these measurements are similar.

Figure 3.2.3: An electron micrograph of the intracellular ciliate of mussels in oblique section. The lobulated nucleus (N) in the centre of the cell contains a less electron dense nucleolus (L). The cilia encircle the cell (C) and are within an area void of host cytoplasmic contents (V). Numerous mitochondria are contained within the ciliates cytoplasm (M). Scale bar depicts 5 µm.

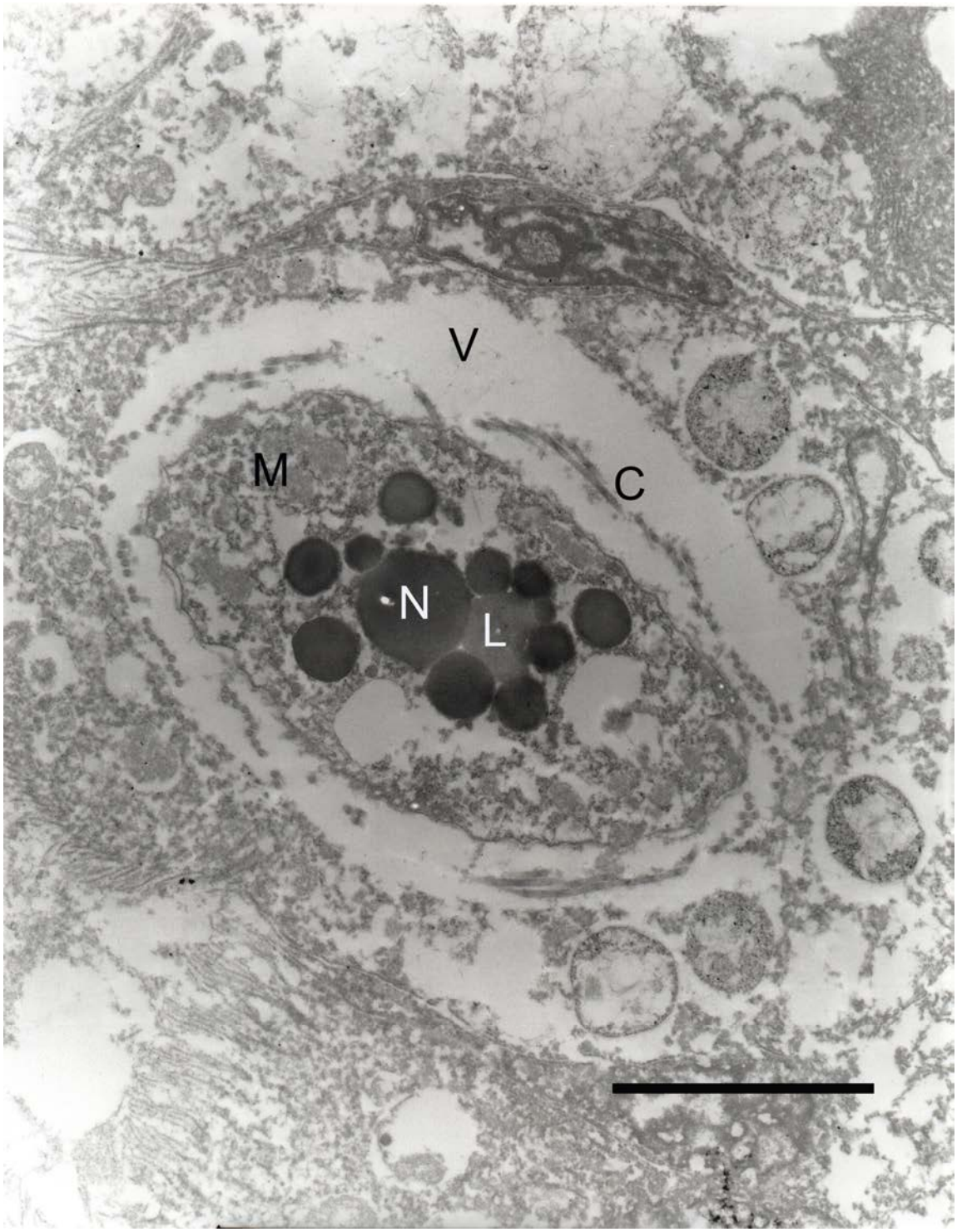

Figure 3.2.4: An electron micrograph of the intracellular ciliate in transverse section. 9 rows of cilia (kineties) are visible (numbered). There is a large nucleus (N) to cytoplasmic ratio. Scale bar represents 2 µm.

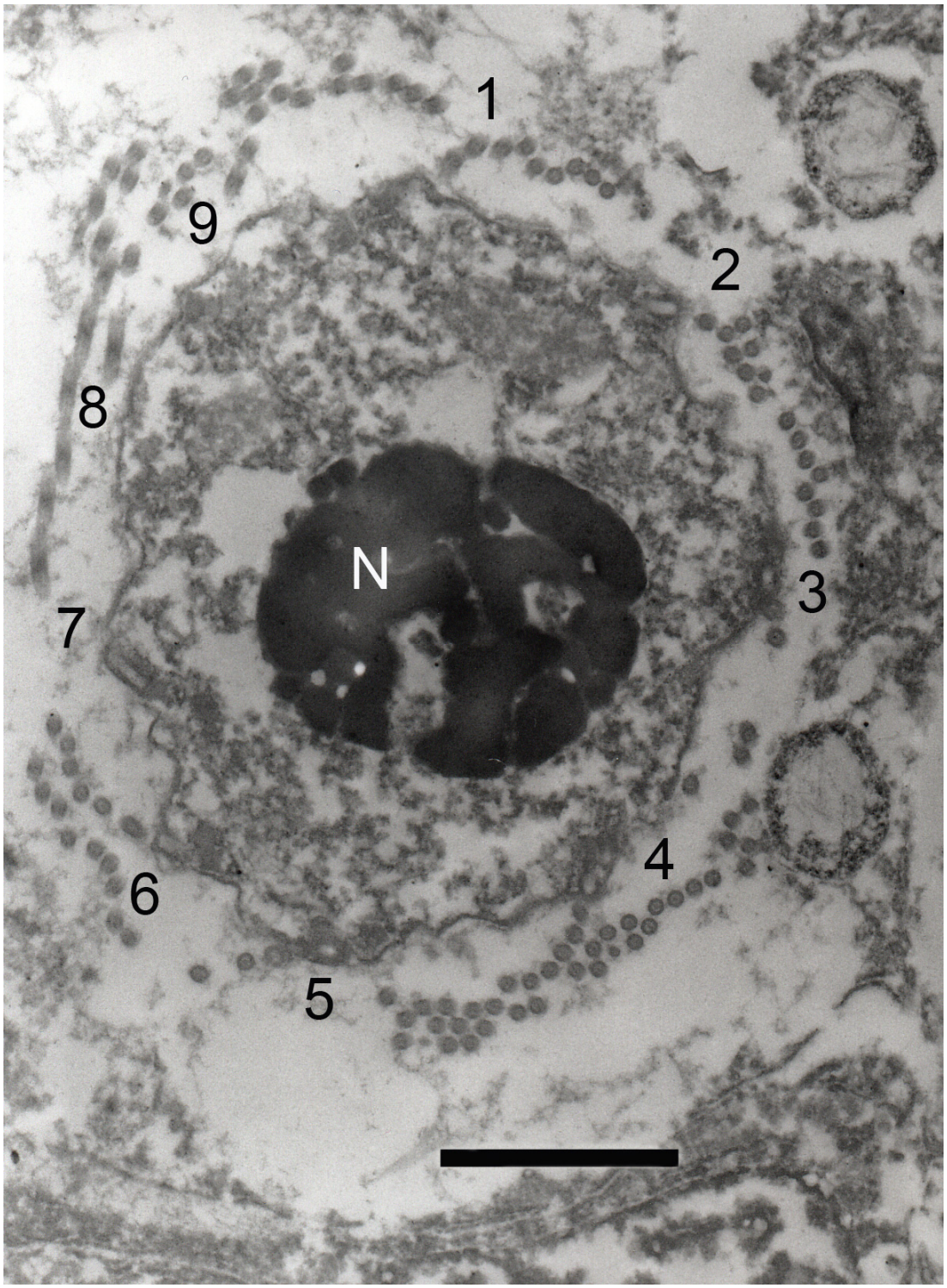

Figure 3.2.5: A photo micrograph of two intracellular ciliates (C1 and C2) inhabiting digestive cells of a mussels digestive tubule. The brush border (B) of the digestive cell is visible, indicating the ciliates are situated within the host cell, inside an area void of cytoplasmic material (V). The lumen of the tubule is also distinguishable (T), as are the lysosomal bodies of the digestive cells (L). Scale bar represents 10 µm.

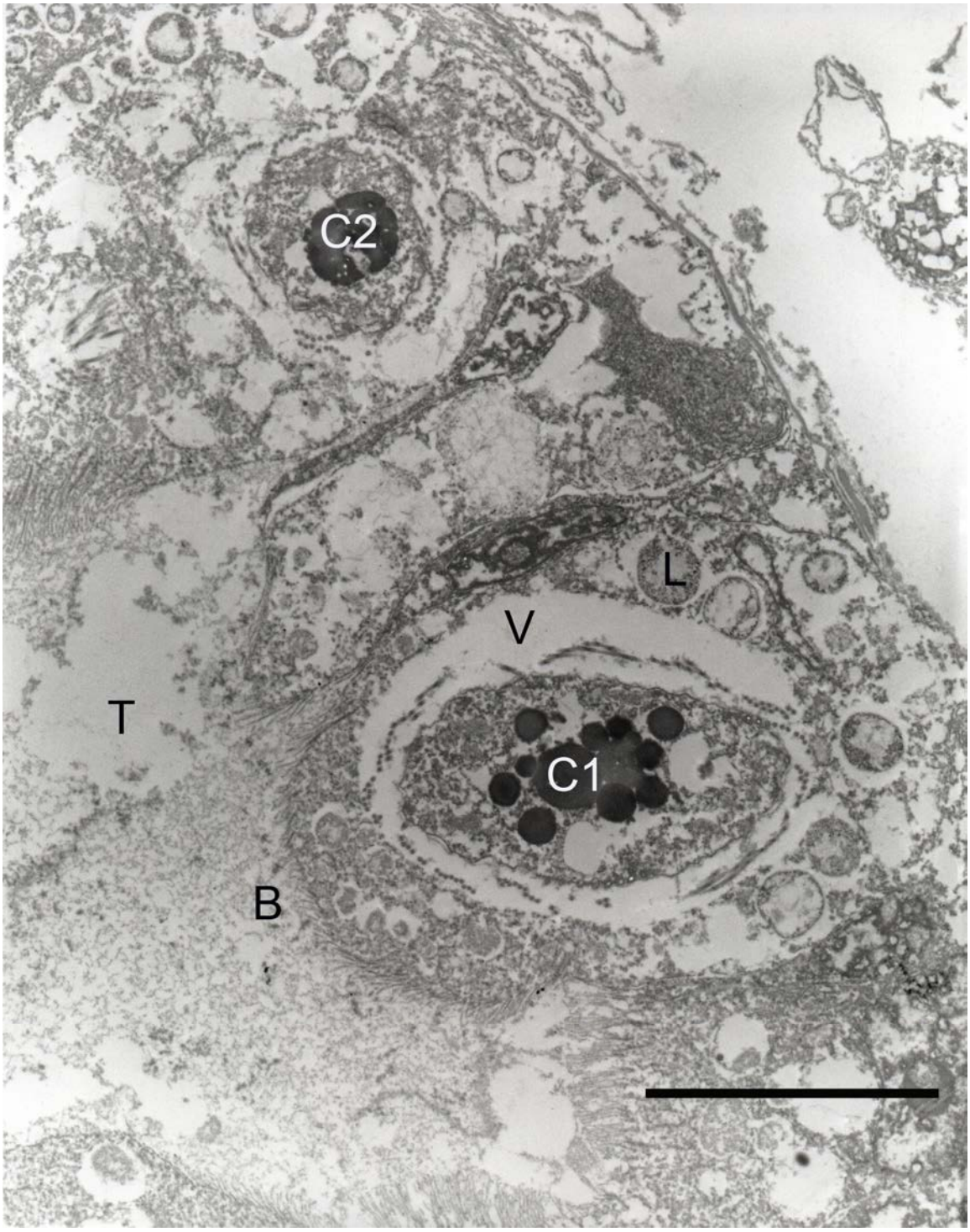

Figure 3.2.6: A: A box plot comparing the width of the mussel and pearl oyster ciliates in µm. The mean width of the pearl oyster ciliate was 5.53 µm and the mean width of the mussel ciliate was 5.05 µm. B: A box plot comparing the length of the pearl oyster and mussel ciliates in µm. The mean length of the mussel ciliate was 16.27 µm and the mean length of the pearl oyster ciliate was 11.15 µm.

A

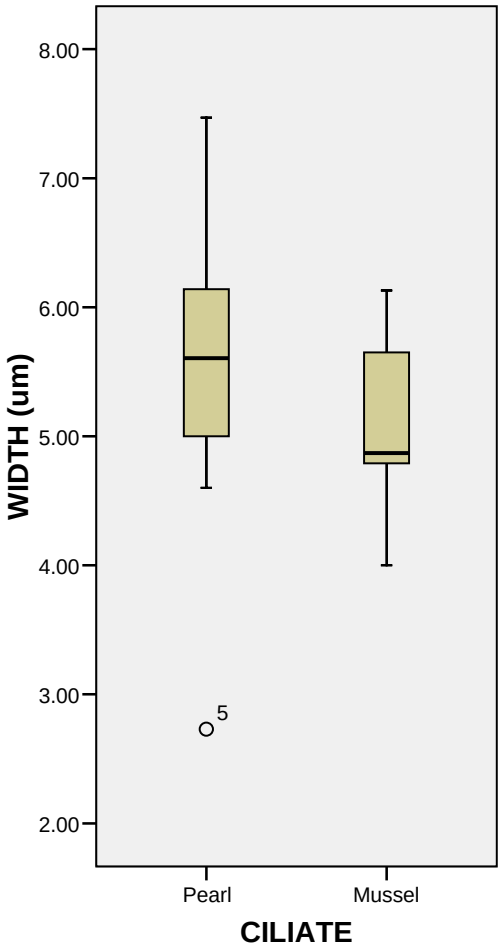

B

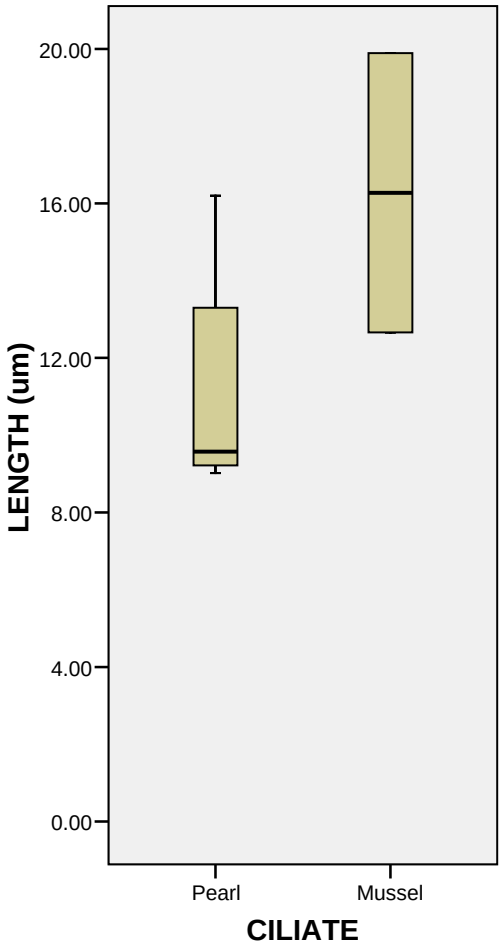

All other ciliates have been recorded in mussels. This gives rise to questions as to the origin of the intracellular ciliate of pearl oysters. Is this ciliate the same species found in Northern Hemisphere mussels? If this were the case, the ciliate could have been inadvertently transported to Australia by ocean going vessels, or imported to Australian waters with the international transfer of aquatic animals. This would not be the first time organisms have accidentally been transported around the world. In 1999, the Northern Territory's Cullen Bay Marina was found to be infested with the exotic Black Striped Mussel, *Mytilopsis* sp. during routine harbour surveys by CSIRO Centre for Research on Introduced Marine Pests. This mussel is a native of Central and South America, and its ability to efficiently colonise and reproduce has made it a pest in Fiji, Hong Kong, Japan, Taiwan and India. It is generally believed the transport of the mussel to new areas can be linked to vessel hull fouling, or as larvae in ballast water (Fisheries 2005).

A recent study into the phylogeny of a *Bonamia* sp. in Morehead City port revealed an affinity to Australasian *Bonamia* spp. (Bishop and Carnegie et al 2006). Surveillance of areas outside the port failed to detect the parasite, which supports the theory that the bivalve parasite was an introduction into the port from the southern hemisphere through shipping activity, perhaps in ballast water. A review by Ruiz and Fofonoff et al 2000 into the invasion of non-indigenous species of invertebrates and algae in North America found a link between trade patterns and the introduction of these species. Although they conceded a bias in their data, they reported that most invasions over the last 200 years have resulted from shipping.

Another option is if the ciliate is endemic to Australia. It could be an endemic parasite to mussels in the Exmouth area, and has for some reason, jumped bivalve hosts and infected the pearl oysters. A comprehensive survey of the bivalves in the area of the ciliate infections could provide the origin of the parasite, perhaps another mussel species in the area.

The increased pathogenicity of the ciliate in pearl oysters compared with other bivalve species may be due to a number of factors. An increase in virulence has been reported when a pathogen is introduced to a naïve host, such as *Haplosporidium nelsoni* infections in Eastern oysters, *Crassostrea virginica*, compared with its natural host *C. gigas* (Burreson and Stokes 2000), that result in higher prevalence of disease and mortality. Other factors contributing to increased virulence could be anthropogenic, including the increased stress animals within aquaculture farm experience, thereby increasing their susceptibility to infection and disease (Murray and Peeler 2005).

3.3 Bivalve Cell Culture

3.3.1 Introduction: The culture of bivalve cell lines

Cell culture is an important tool in the research of diseases, particularly rickettsial and viral diseases. The lack of continuous marine bivalve cell lines has meant the study of obligate intracellular parasites is limited to morphological investigation and in vivo experiments (Elston 1997). The understanding of bivalve cell biology would also be greatly improved with the discovery of reliable culture methods (Chen and Wen 2000). An economic potential also exists in the pearling industry should the reliable culture of mantle tissue be accomplished, which is necessary for pearl seeding.

Cell culture is the maintenance of cells outside the body of the donor organism. There are three broad categories of cell cultures, namely primary, secondary and continuous (Jimenez 2005). Primary cell cultures are cells taken directly from the donor organism and may divide once or twice, but eventually die within a short amount of time. Secondary cell cultures are able to divide, sometimes up to 50-100 times, before eventually dying. And finally, immortalized (or continuous or permanent) cell lines can keep alive and proliferating continually as long as culture conditions are kept optimal (Jimenez 2005).

Various cell types have been used in attempts to produce continuous cell lines, including heart, mantle, hemocyte, larvae, embryo, gonad, palp and digestive gland cells. Heart cells have been most frequently used, due to the relative ease of obtaining an aseptic sample (Chen and Wen 2000). Faucet et al (2004) combated this problem of contamination in the culture of digestive gland cells by maintaining the mussels *Mytilus edulis* in clean, oxygenated sea water for 48 hours prior to processing. Embryonic cell lines have a great potential for establishing continuous cell lines, however none have yet been achieved.

An investigation into the success of various growth media for harm clam, *Meretrix lusoria*, heart cell cultures concluded L-15 (Leibovitz) media gave best results (Wen, Kou et al. 1993). This media has been used by several researchers on other bivalve species with encouraging outcomes (Le Deuff, Lipart et al. 1994; Renault, Flaujac et al. 1995; Faucet, Maurice et al. 2004). In one study, however, it was noted that L-15 media contained no proline or taurine, amino acids found at high concentrations in oyster fluid and tissues (Chen and Wen 2000). Therefore, it was considered that the addition of these substances may improve culture results. Natural products such as hemolymph can be used to supplement the growth media (Le Deuff, Lipart et al. 1994), and the addition of extract from the oysters' reproductive gland was also found to improve the life of cells in vitro (Chen and Wen 2000). A table representing some of the most useful cell culture media for bivalves is presented in Table 3.3.1.

For the establishment of a permanent cell line, effective cell proliferation must be achieved. Attempts have been made in the past using carcinogens and the oncogenes,

ras and myc (reviewed by Chen and Wen 2000) with disappointing results. Wen et al. (1993) maintained hard clam heart cells for six subcultures with the addition of pronase and collagenase to promote proliferation. In the same study, it was found that the addition of insulin, fibroblast growth factor and epidermal growth factor had no effect (Wen, Kou et al. 1993). Later, various coated and uncoated culture flasks were tested to discover whether they could assist in cell adhesion and proliferation, with poly-d-lysin coated flasks showing the most promising results (Renault, Flaujac et al. 1995).

Morphological studies give limited information about the disease organisms and pathological interactions. Cell culture is a required tool to properly investigate pathogens which replicate intracellularly. So far, the culture of silverlip pearl oyster cells has not previously been attempted, and is an area in need of further research.

3.3.2 Materials and Methods

Bivalves where kept at the Murdoch University Fish Health Unit to act as tissue donors. These were maintained using techniques described in section 2.3.1. The tissue culture technique was also described in section 2.1.6. The haemolymph was collected by cooperating members of the pearling industry, based on procedures outlined in section 8.5. The donor oysters were kindly provided by members of the pearling industry.

A variety of cell culture media were used during this experiment. Due to the success of using L-15 Leibovitz culture media as the primary medium with the culture of other bivalve species, this was used during this study. New Born Calf Serum (NBCS) was also added at 10% to provide essential factors for cell proliferation, as a similar product, Foetal Calf Serum (FCS) or Foetal Bovine Serum (FBS) has been helpful to other researchers.

Media M1 contained 90% L-15 media, 10% NBCS and antibiotics penicillin and streptomycin. Its osmolarity was 324 mmol/kg with a pH of 7.59. Media M2 contained 70% L-15, 10% NBCS and 20% pearl oyster haemolymph, plus antibiotics. It had an osmolarity of 615 mmol/kg. Media M3 contained no L-15, instead had 90% haemolymph and 10% NBCS, with antibiotics. This had an osmolarity of 1507 mmol/kg. Media M8 contained 80% L-15, 10% NBCS and 10% haemolymph, plus antibiotics. It had an osmolarity of 366 mmol/kg and a pH of 7.54. Media M9 was developed after there were contamination issues with Media M2, so M9 contains the

Table 3.3.1: A table representing the culture media and conditions that were found to be beneficial to cell growth by several researchers. Many researchers found L-15 media the most rewarding, with various additives including haemolymph, foetal bovine serum (FBS) and collagenase. Flasks coated in poly-d-lysin were also found to be beneficial.

Reference	Bivalve species	Tissue	Media	Beneficial additives	Time	Temperature
Wen, Kou et al 1993	Hard clam *Meretrix lusoria*	heart	2xL-15, 10% FBS	pronase, collagenase at 100µg/ml	subcultured 6 times	28°C
Domart-Coulon, Doumenc et al 1994	Pacific oyster *Crassostrea gigas*	heart	modified L-15, 10% FBS	hormones, protective agents, lipidic mediators	3 months	20°C
Renault, Flaujac et al 1995	European flat oyster *Ostrea edulis*	heart	3% L-15, sterile sea water, Japanese oyster haemolymph (1:1), 10% FBS	poly-d-lysin flask	3 weeks	20°C
Buchanan, La Peyre et al 1999	Eastern oyster Crassostrea virginica	heart	JL-ODRP-4	poly-d-lysin flask	5 days	25°C
Chen and Wen 1999	Pacific oyster *C. gigas* , Hard clam *M. lusoria*	heart	2xL-15, 10% FBS	collagenase 100µg/ml	5 months	28°C
Le Marrec-Croq, Glaise et al 1999	Scallop *Pecten maximus*	heart	sterile sea water, 10% L-15, 10% FBS	no additives	1 month	15°C
Faucet, Maurice et al 2004	Common mussel *Mytilus edulis*	digestive gland, gill	L-15, 10% FBS	no additives	72 hours	18°C

same proportions of additives however the haemolymph was filtered using a smaller filter of 0.2 µm filter. With this change, the osmolarity was now 436 mmol/kg with a pH of 7.45.

Media MN1 was developed with a double concentration of L-15, as Wen, Kou et al 1993 had had some success with this method. The Media MN1 contained 90% double strength L-15, 10% FBCS and antibiotics. The osmolarity of the solution was >2000 mmol/kg with a pH of 6.99. Media MN8 contained 80% double strength L-15, 10% haemolymph and 10% NBCS, with antibiotics. Its osmolarity was >2000 mmol/kg with a pH of 7.00. MN9 contained 70% double L-15, 20% haemolymph and 10% FBCS, with antibiotics. Its osmolarity was also >2000 mmol/kg and had a pH of 6.98. These are summarised in Table 3.3.2.

Table 3.3.2: A table representing the ingredients and their proportions of the various cell culture media used during the cell culture study, their osmolarity and pH.

MEDIA	**M1**	**M2**	**M3**	**M8**	**M9**	**MN1**	**MN8**	**MN9**
L-15	90%	70%	0%	80%	70%	2x 90%	2x 80%	2x 70%
NBCS	10%	10%	10%	10%	10%	10%	10%	10%
Haemolymph	0%	20%	90%	10%	20%	0%	10%	20%
P&S	present	present	present	present	present	present	present	present
Osmolarity (mmol/kg)	324	615	1507	366	436	>2000	>2000	>2000
pH	7.59			7.54	7.45	6.99	7.00	6.98

Cells from the oysters digestive gland, mantle tissue and adductor muscle were cultured during the study. They were cultured using the different medias and using either uncoated flasks or poly-d-lysin coated flasks. Measurements and photographs of cultures were taken using Motic Images Plus 2.0 camera and software. The growth of the cells and their covering of the flask was subjectively graded. Cultures were considered no longer viable when the cells stopped replicating.

3.3.3 Results

The cell culture of adductor muscle derived cells

The cells derived aseptically from the adductor muscle of pearl oysters were cultured in media M1, M2, M3, M8, M9, MN1, MN8 and MN9. No cell growth was observed with media M2 and M3, so they were no longer included in future cultures. Uncoated

flasks and flasks coated with poly-d-lysin were used. Cell growth occurred using M8, M9, MN1, MN8 and MN9 with uncoated flasks, and using M1, M9, MN1 and MN8 with the poly-d-lysin coated flasks. The growth of the adductor muscle derived cells was tabulated in Table 3.3.3.

Due to the successful growth covering the uncoated flasks of cells in media M8 and M9, the cultures were sub-cultured on day eleven. Photographs of these cells one day prior to splitting are included in Figure 3.3.1. The original flask failed to grow after splitting, however the sub-cultured cells grew very well, and were confluent by day 57 and were again split and sub-cultured. After the second split, neither of the new sub-cultures replicated further, and the split cells in media M9 failed to grow as well. The split cells in media M8 continued to grow, however, and were again reaching confluence by the closure of the experiment on day 75.

There was a small to moderate growth recorded for the cells cultured in media MN1, MN8 and MN9 in the uncoated flasks and M1, MN1 and MN8 of the poly-d-lysin coated flasks. This only continued for approximately 2 weeks before the cells ceased replicating and the cultures stagnated. There was a small amount of growth in media M9, however the cells were out-competed by a concurrent fungal contamination.

The cell culture of mantle derived cells

The cells derived aseptically from the mantle of pearl oysters were cultured in media M1, M2, M3, M8, M9, MN1, MN8 and MN9. No cell growth was observed with media M2 and M3, so they were no longer included in future cultures. Uncoated flasks and flasks coated with poly-d-lysin were used. Cell growth occurred using M1, M8, M9, MN1, MN8 and MN9 with uncoated flasks, and using M1, M8, MN1 and MN9 with the poly-d-lysin coated flasks. The growth of the mantle derived cells was tabulated in Table 3.3.4.

Table 3.3.3: The cell culture results for the adductor muscle derived cells

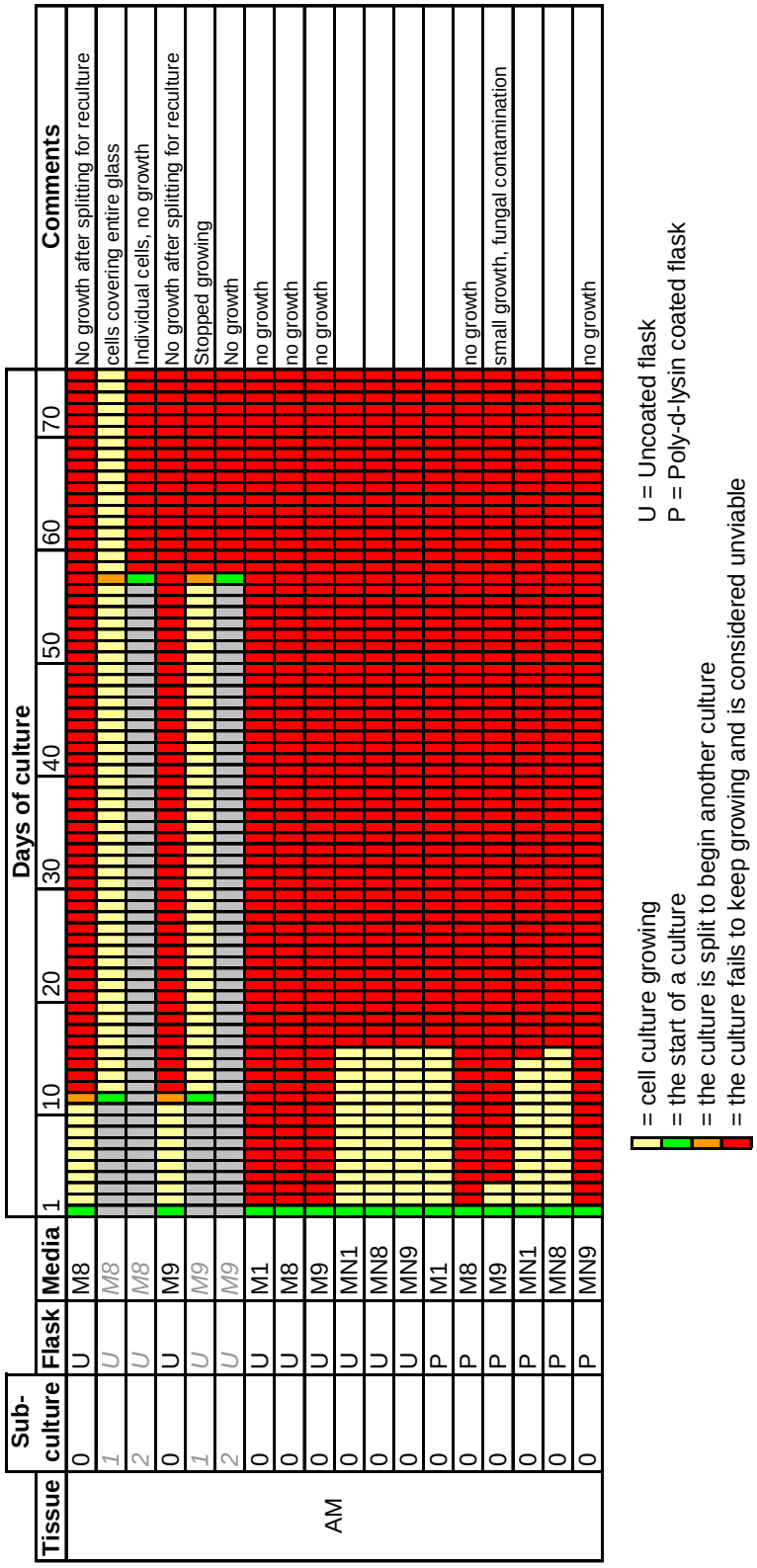

Figure 3.3.1: The culture of adductor muscle derived cells. Individual cells were measured as approximately 11µm in size. **A:** Adductor muscle cells in media M8 at 10 days.
B: Adductor muscle cells in media M9 at 10 days. This was one day prior to splitting for the first sub-culture, when cells were confluent.

A

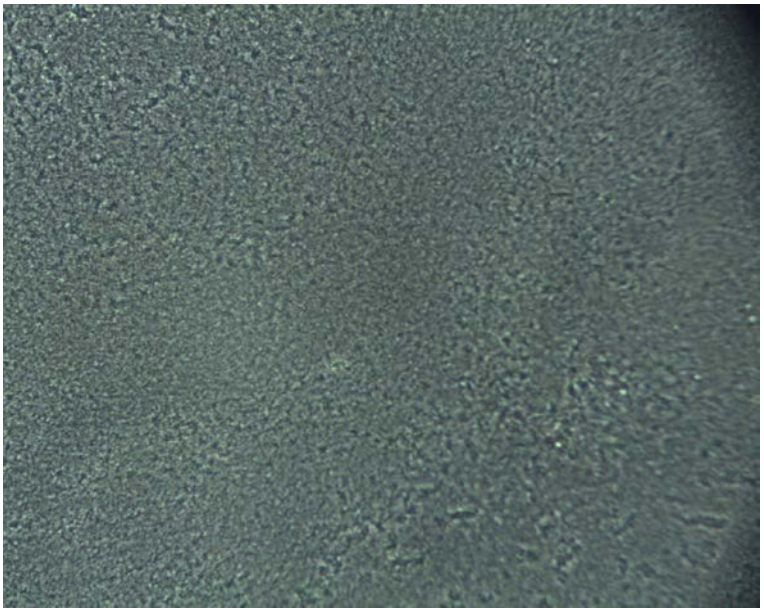

B

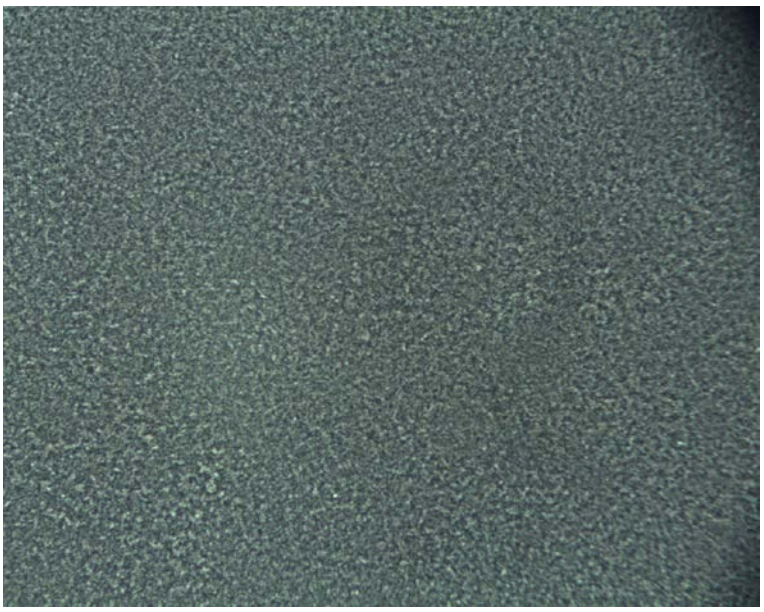

The cells grew very well with the uncoated flasks in media M1, M8 and M9. With media M9, the cells reached confluence by day 11 and were split and sub-cultured. Figure 3.3.2 A is a photomicrograph of mantle cells in media M9 at 10 days, one day prior to splitting for the first sub-culture, when cells were confluent. Both the split cells of the original culture and the new sub-culture grew slowly and were confluent by day 57, when the sub-cultured ones were split and further sub-cultured. Both attached well and grew until the completion of the experiment on day 75. At day 75, the original culture was confluent, the first sub-culture was covering approximately 25% of the flask, and there was growth in the third sub-culture, limited only by the drying media. The cells cultured in media M1 grew slowly but continuously until day 54 when they ceased and were considered no longer viable. Figure 3.3.2 B is a photomicrograph of the explant culture of mantle cells in media M1 at 22 days. The cells appeared to have fibroblastic-like morphology. The cells cultured in media M8 grew continuously, albeit slowly until the completion of the experiment on day 75.

There was a small to moderate growth recorded for the cells cultured in media MN1, and MN8 in the uncoated flasks and M8, MN1 and MN9 of the poly-d-lysin coated flasks. These grew for approximately 2 weeks before the cells ceased replicating and the cultures were no longer considered viable. There was a small amount of growth in media M1 uncoated and MN9 and M1 of the poly-d-lysin flasks for approximately 3 days before contamination of fungus and Ancistrocomid-like ciliates limited growth. The cells in the uncoated flask with media M8 grew for approximately 10 days before contamination destroyed the culture.

The cell culture of digestive gland derived cells

The cells derived aseptically from the digestive gland of pearl oysters were cultured in media M1, M2, M3, M8, M9, MN1, MN8 and MN9. No cell growth was observed with media M2 and M3, so they were no longer included in future cultures. Uncoated flasks and flasks coated with poly-d-lysin were used. Cell growth occurred using M1, M8, M9, MN1, MN8 and MN9 with uncoated flasks, and using M1, M8, MN1 and MN9 with the poly-d-lysin coated flasks. The growth of the digestive gland derived cells was tabulated in Table 3.3.5.

The best growth was obtained using uncoated flasks and media M8 and M9. Digestive gland derived cells in media M9 were confluent by day 11, when the culture was split and sub-cultured. Figure 3.3.3 A is a photomicrograph of the culture of digestive gland derived cells in media M9 at 10 days, one day prior to splitting for the first sub-culture, when cells were confluent. The original culture continued to grow after splitting and was confluent by the end of the experiment on day 75. The sub-cultured cells in media

Table 3.3.4: The cell culture results for the mantle tissue (CT) derived cells

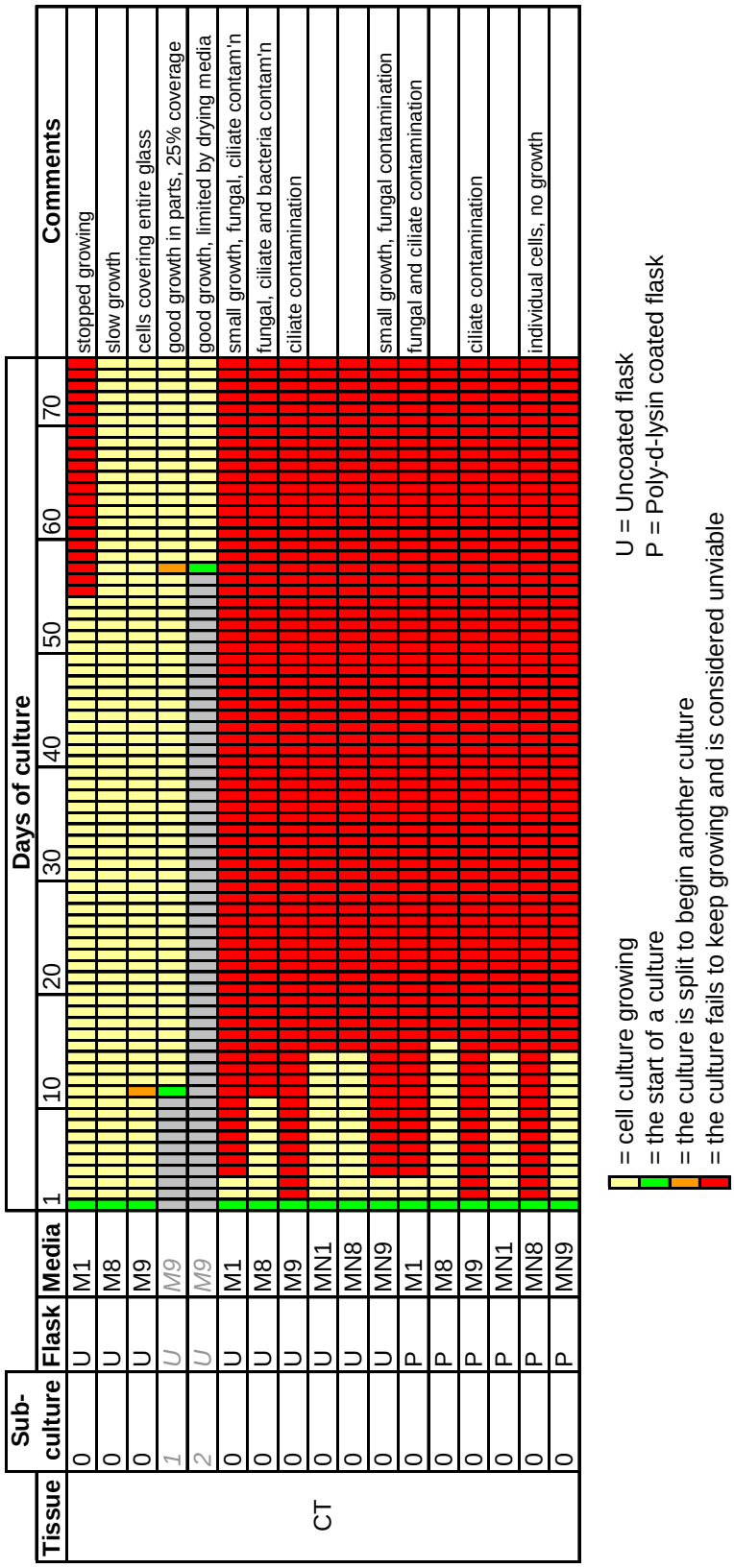

Figure 3.3.2: The culture of mantle derived cells. Individual cells were measured as approximately 10µm in size. **A:** Mantle cells in media M9 at 10 days. This was one day prior to splitting for the first sub-culture, when cells were confluent. **B:** The explant culture of mantle cells in media M1 at 22 days. The explant (E) is the remnant of mantle tissue, and the cells (C) are growing from it into the media (black line). The cells appear to have fibroblastic-like morphology.

A

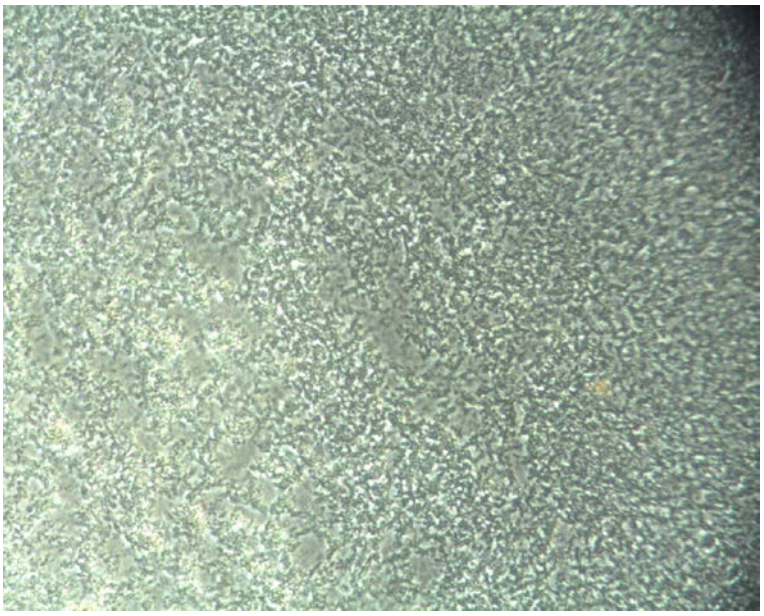

B

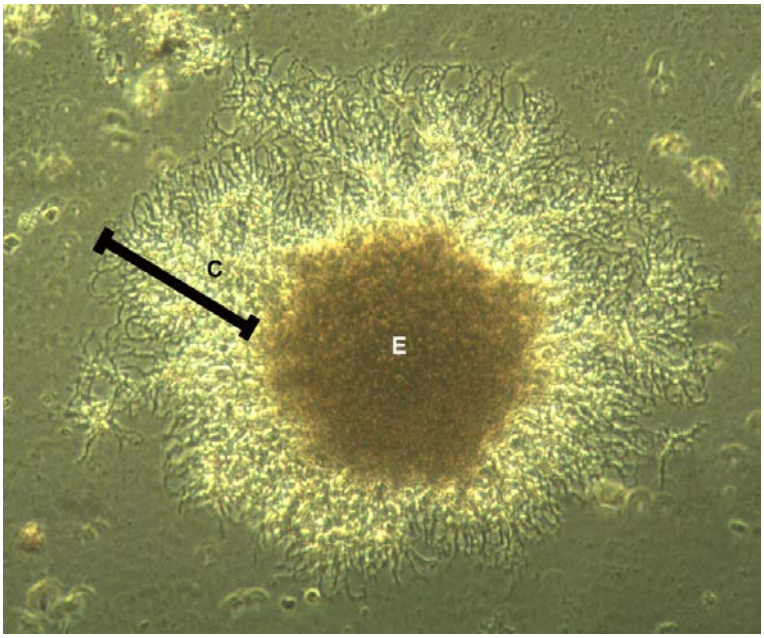

Table 3.3.5: The cell culture results for the cells derived from digestive gland (DG)

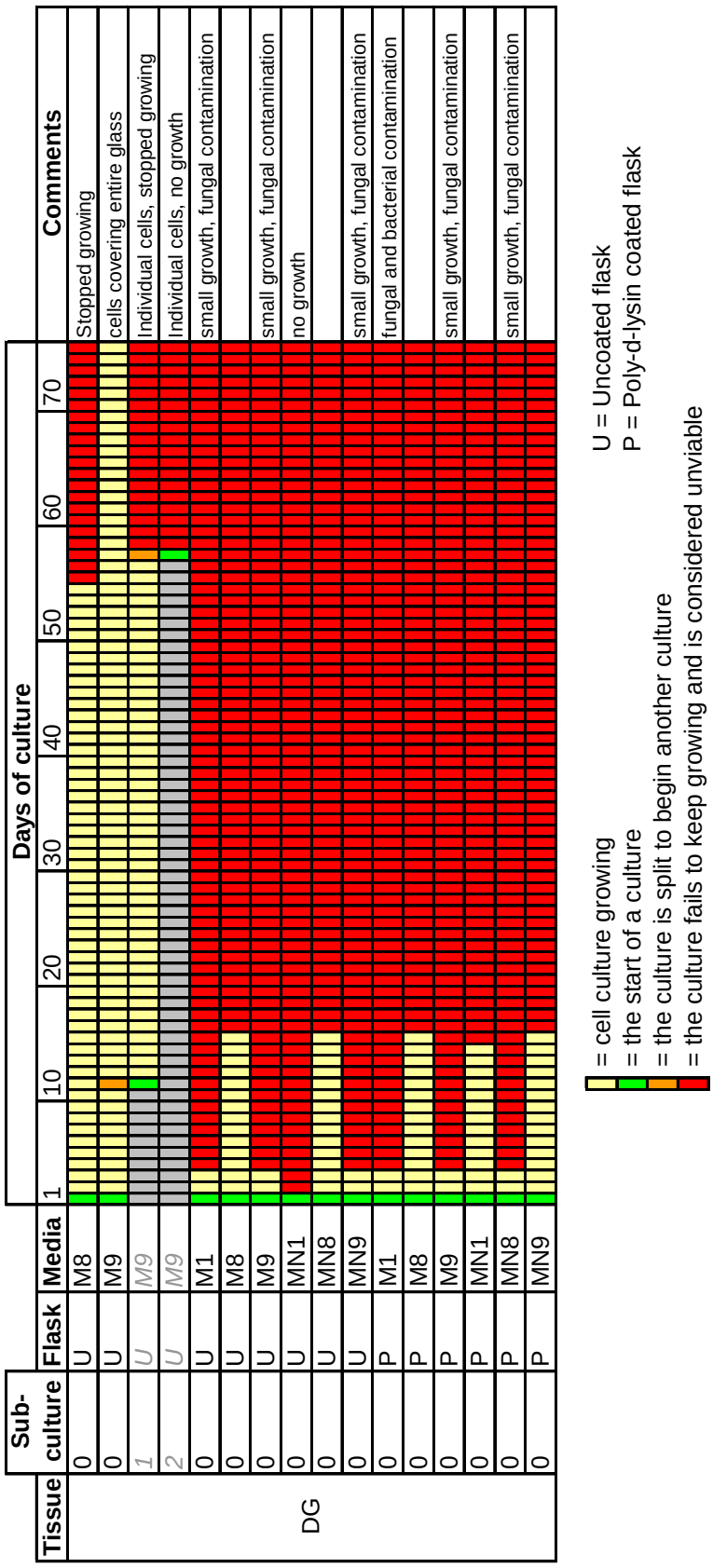

Figure 3.3.3: The culture of digestive gland derived cells. Individual cells were measured as approximately 11µm in size. **A:** Digestive gland cells in media M9 at 10 days. This was one day prior to splitting for the first sub-culture, when cells were confluent. **B:** The explant culture of mantle cells in media M8 at 10 days.

A

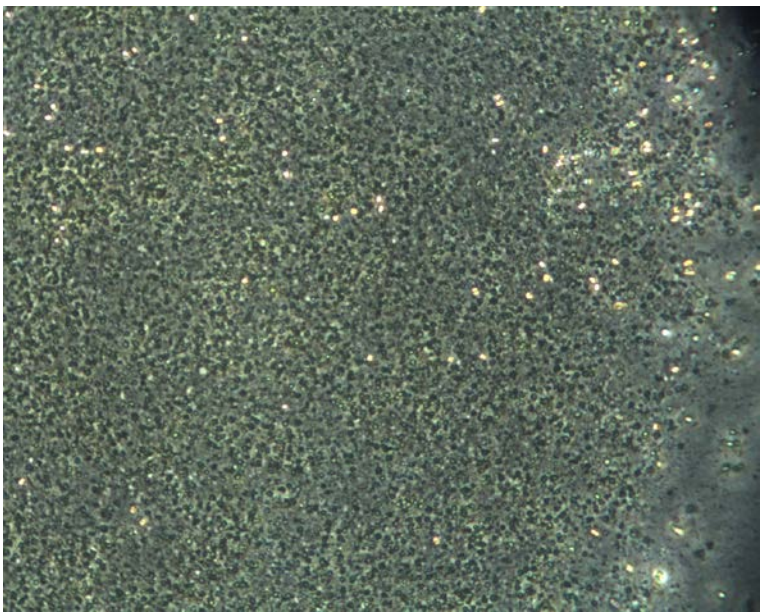

B

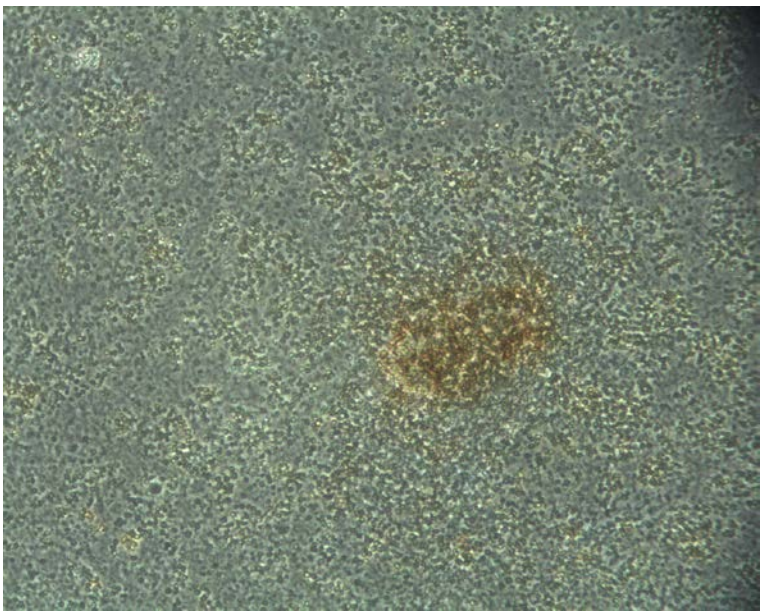

M9 grew until confluence by day 57 when they were split and sub-cultured. Unfortunately neither the split cells or the newly sub-cultured cells continued to grow afterwards. The digestive gland cells in media M8 grew continuously, albeit slowly until day 54 when no more growth was recorded and they were considered non-viable. Figure 3.3.3 B is a photomicrograph of the mantle cells in media M8 at 10 days, growing out from the explant.

Moderate growth was observed of the digestive gland derived cells culture in media M8, MN1 and MN9 using the poly-d-lysin coated flasks and media M8 in the uncoated flasks. These continued to grow for approximately 2 weeks when they stopped growing and were therefore considered unviable. Fungal contamination and in one case bacterial contamination limited growth to 3 days of the cells cultured in media MN8, M9 and M1 of the coated flasks and M1, M9 and MN9 in the uncoated flasks.

3.3.4 Discussion

During this study, pearl oyster cells were successfully grown in vitro for a maximum of 75 days, limited only by the length of the study. Digestive gland-derived cells were grown in media M8 for 54 days, and in media M9 for 75 days with one successful sub-culture. Media M8 contained 80% L-15, 10% FBCS and 10% pearl oyster haemolymph. It had an osmolarity of 366 mmol/kg and was slightly alkaline at pH 7.54. Media M9 was the best at growing digestive gland cells, and contained 70% L-15, 10% NBCS and 20% pearl oyster haemolymph. Its pH was 7.45 with a higher osmolarity of 436 mmol/kg.

Adductor muscle derived cells were grown for a maximum of 65 days, with one successful sub-culture in media M8 and M9. These two media were best for growing mantle derived cells also, with a maximum growth time of 75 days and two successful sub-cultures using M9. Media M1 was also successful at growing mantle derived cells, however this growth was slow and only continued for 54 days, with no sub-cultures. Media M1, when compared with M8 and M9, contained no haemolymph, had a lower osmolarity of 324 mmol/kg and a higher pH of 7.59. This suggests that the oyster haemolymph may contain essential nutrients and growth factors required for cell proliferation in vitro.

The use of different culture flasks was also compared. The best results came from using uncoated flasks, with growth up to 75 days. The longest growth obtained using poly-d-lysin coated flasks was approximately two weeks from an explant culture. The poly-d-lysin coated flasks may be beneficial for use when splitting cells for subculture, as they could assist with cell adhesion, however the study indicated no advantage of using them for the initial explant culture. During the study, after splitting many of the cultures failed to grow. If the study was repeated, poly-d-lysin

coated flasks could be used after splitting to determine their effectiveness at this stage.

Other media was used to determine the best combination of additives. A double strength L-15 solution was used, however the resulting media, MN1, MN8 and MN9, had an osmolarity of >2000 mmol/kg and only sustained growth for a maximum of two weeks. The pH of the media was neutral, 6.98 - 7.00; however, the extremely high osmolarity could have impeded proliferation and survival.

Despite soaking the oysters in sterile seawater containing broad spectrum antibiotics, contamination continued to be a problem throughout this study. Many cultures had promising beginnings, only to be out-competed with either bacteria, fungus or ciliates. An antibiotic sensitisation test could be performed on the contaminating bacteria to determine why the penicillin and streptomycin were not effective in limiting its growth. An anti-protozoal medication, such as metronidazole, could be introduced in future experiments to limit the growth of the Ancistrocomid-like ciliates. This could not be included in the maintenance culture media, however, as it was hoped that these cell lines could be used to grow the intracellular ciliate in future, and these medications would have impaired that experiment. The fungal contaminants could be limited by a broad spectrum antifungal medication, such as amphotericin B, used successfully in many other cell culture media.

This study was a promising beginning for the culture of cells from the mantle, adductor muscle and digestive acini of pearl oysters. Due to the economic potential of such an endeavour, the pearling industry could benefit greatly from future research in this area. A longer study, greater than 75 days, would determine the long term growth potential of these primary cell lines. The use of immunohistochemistry and transmission electron microscopy could better determine the derivation of these cell lines, and could identify the growth of the economically important, pearl-producing mantle epithelial cells.

Chapter 4: Investigations into the pathology associated with intracellular ciliate infections in pearl oysters

Photo: A long line used for sampling at Gales Bay, Exmouth Gulf 2007

In this Chapter the host reaction to ciliate infection was studied in pearl oysters. There are two main sections to this Chapter. The first is a histological study of a group of at-risk oysters, and their host reaction in response to the presence of the ciliate. The second is an investigation into the ultrastructural changes associated with an infection, using transmission electron microscopy.

4.1 Pathology associated with ciliate infections

4.1.1 Introduction: Host response of bivalves

The inflammatory response of a bivalve involves both cellular and humoral elements. Humoral defence factors have been studied in numerous bivalve species, including the eastern oyster and the pacific oyster. A review of these findings by Chu (1988) indicated the humoral defence appeared to be innate and non-specific, with memory yet to be demonstrated.

The cellular defence mechanisms of bivalves consist of cellular infiltration at the affected site, phagocytosis and finally the elimination or encapsulation of the foreign object. Sparks and Morado (1988) explained that the pattern of host response is basically similar, irrespective of species of host bivalve, harmful agent or site of injury. The general outline of events following an injury, whether physical, chemical or biological, included infiltration by hemocytes, formation of an aggregated hemocytic plug, replacement of damaged tissues with elongated hemocytes, deposition of collagen by fibroblasts, removal of necrotic tissue debris by phagocytic granulocytes, and finally, the restoration of the normal architecture of the tissue.

Hemocytes are the ‘blood cells’ of bivalve molluscs. This term was proposed in 1968 by Farley (1968), as a more appropriate name. Prior to this the defensive cells were referred to with descriptive terms such as leucocyte, amoebocyte and phagocyte (Stauber 1950; Pauley and Sparks 1967). Some authors refute the arguments made by Farley (1968) that the term leukocyte is an exclusively vertebrate term, citing that definitions used in making those arguments where not from a reputable scientific glossary and prefer to continue to use it (Cheng and Rifkin 1970). If only for the sake of continuity and ease of reading, bivalve blood cells will be referred to as hemocytes for the remainder of the text.

There has been much debate over the classification of the various hemocytes, with some authors classifying on the basis of cytoplasmic organelles, morphology of the nucleus, or cytogenesis and cell function (reviewed by Auffret, 1988). The presently accepted scheme, proposed by Cheng (1981), is generally based on morphology, where there are two main types of hemocytes, granular hemocytes, known as granulocytes, and nongranular hemocytes, named hyalinocytes (Auffret 1988). Granulocytes are more easily observed and it has been suggested they are more important in the inflammatory reaction due to their phagocytic activity (Pauley 1966). It might also be noted that ‘agranular hemocytes’ contain no visible granules, however are thought to derive from the same hemopoietic line as granulocytes. Hemocytogenesis of bivalve cells is still under investigation, with preliminary results indicating a separate hemopoietic line for granulocytes and hyalinocytes (Auffret 1988).

The inflammatory response of the eastern oyster, *Ostrea virginica* was observed after an intravascular injection of India ink (Stauber 1950). Within 2-4 hours of the injection, particles of ink where observed in the accumulating hemocytes, indicating active phagocytosis. These ink laden hemocytes then travel throughout the oyster and are eventually eliminated. The process by which the phagocytes migrate through the epithelial surfaces is known as diapedesis, and was observed from 8 days post-injection. This was the first report of such a process occurring.

Another observation was made when talc powder was injected into the adductor muscle and the Leydig cells of the oyster *Crassostrea gigas* (Pauley and Sparks 1967). In this study, hemocytic infiltration, accompanied by oedema, was observed at 16 hours post-injection. The response after this stage differed from that observed by Stauber (1950). After 24 hours, elongated cells with round nuclei began forming granulomatous tissue around the talc. Between 40 and 56 hours, the peripheral hemocytes became arranged parallel to each other. The central cells became necrotic after 88 hours and nuclei of the peripheral cells started elongating after 128 hours. By 328 hours post-injection, well formed granulomas were observed, consisting of a scattering of elongated hemocytes throughout the lesion and a peripheral band of hemocytes approximately 25-100 cells thick (Pauley and Sparks 1967). Brown pigmented cells of questionable function were observed in these lesions from 56 hours. A similar host response was observed after turpentine injection; however this was complicated by the irritant affect of the injected agent (Pauley 1966).

It was suggested during the study performed by Stauber (1950) that ambient temperature may play a role in the activity of hemocytes. Due to the fact that bivalves are poikilothermic and osmoconforming, it is not surprising that their environment can impact the internal functions of the oyster. Fisher (1988) reviewed the environmental influence on bivalve hemocyte function, with particular interest in both salinity and temperature. It was found that high salinity and very low salinity limited hemocyte spreading and locomotion. This could be a factor in MSX disease, caused by *Haplosporidium nelsoni*, which seems to occur in high salinity regions. It was also noted that increased temperatures enhanced hemocyte function, whereas extremely high temperatures may impair their function. *Perkinsus marinus* is a parasite which infections are most severe in warmer weather (Fisher 1988).

4.1.2 Materials and Methods

Oyster samples

An archive of more than 70,000 formalin-fixed, paraffin embedded oyster tissues held by the Western Australian Department of Fisheries was made available for examination. These samples were obtained as part of ongoing surveillance health monitoring of the Western Australian pearl oyster industry. All the oysters had been sectioned and embedded according to normal procedures for health testing of pearl oysters, which permitted examination of most organs of the oyster including the digestive gland.

Histopathology

300 archived oyster samples were randomly selected from approximately 2000 samples using a stratified random design. Known at-risk populations (strata) were randomly at the level of histology blocks, which contained a variable number of oysters. Blocks contained a variable number of oysters. All oysters were less than 70 mm in size and of the 300 oysters 136 were from the Montebello Islands in December 2001, 151 were from Exmouth Gulf collected in October 2001 and 13 were from Exmouth Gulf collected in November 2002. Paraffin embedded blocks were sectioned at 4 µm, stained with H&E stain based on routine procedures (Bancroft and Gamble 2002).

To assess any correlation between the presence of infection with any host inflammatory response the 300 H&E stained tissue sections were examined using an Olympus BH-2 microscope (Olympus Optical Co. Ltd.). On low magnification the digestive gland was subjectively graded for its inflammatory response (Figure 4.1.1). A score of between 0 and 40 was given; normal oysters were given the score of zero, oysters with a mild inflammatory reaction in the digestive gland were given a score from zero to 5, a moderate inflammatory response was given a score between 5 and 10 and a severe reaction was graded between 10 and 40. The numerical grade roughly correlated to the percentage of digestive gland that consisted of the haemocyte infiltrate.

Photographs where taken using an Olympus DP21 camera (Olympus Optical Co. Ltd.). Each oyster was given an individual number for identification and the cut section on the slide was measured in millimeters.

The digestive gland was then viewed under 40x magnification and using an electronic stage (MS316, Lang GMBH & Co.) and 20 High Power Fields (HPF) were examined. The ciliates were counted in the 20 HPFs and then divided by 20 to give an average burden per HPF. The 20 HPFs were selected randomly using the motorised microscope stage, programmed with a step length that ensured that each horizontal and vertical step did not overlap the previous field of view, ensuring no area of digestive gland was counted twice. Where the digestive gland was not large enough for 20 independent HPFs to be counted, the total number of ciliates was divided by the number of HPFs examined, to obtain the average parasite burden per HPF.

Figure 4.1.1: An infected pearl oyster digestive gland with numerous intracellular ciliates (black arrows) and a hemocytic infiltrate (red arrows). Scale bar: 50 µm.

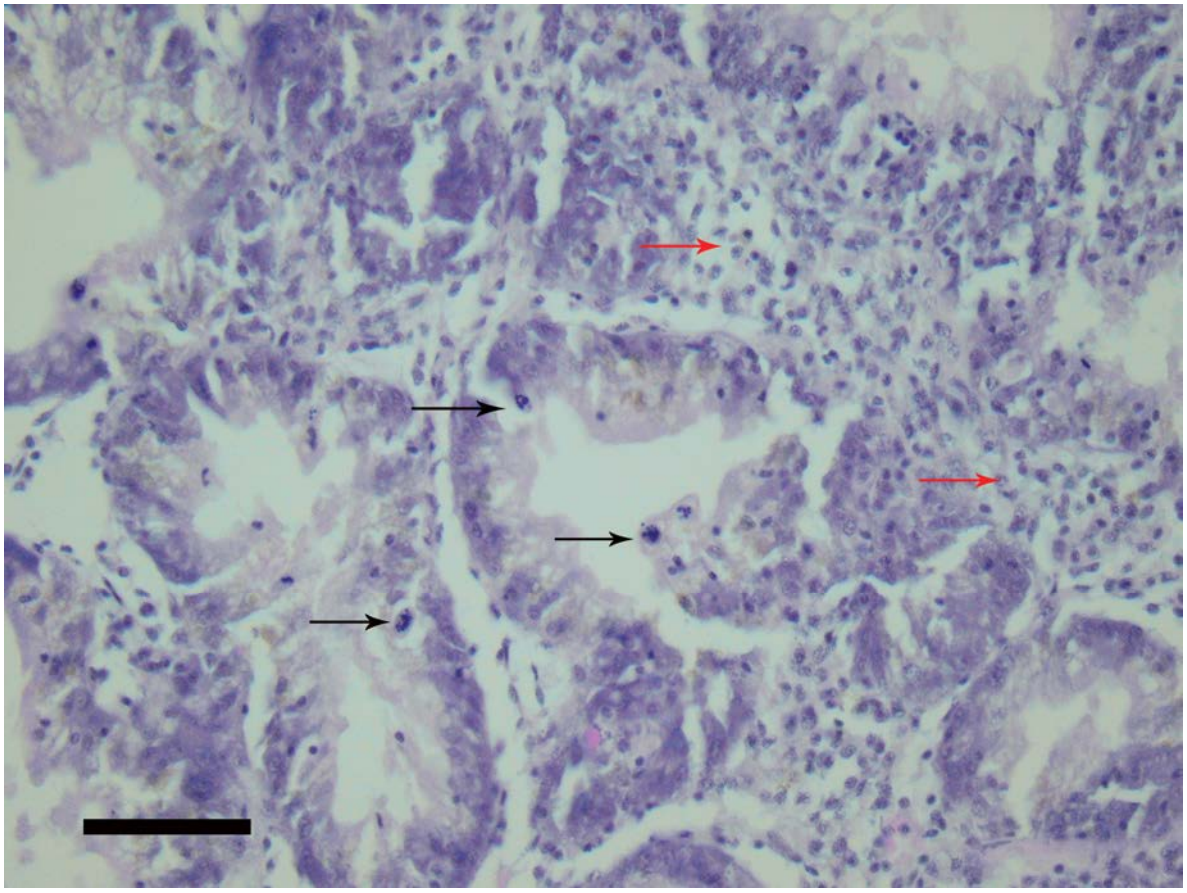

4.1.3 Results

Of the 300 selected oysters examined, 157 were found to be positive for the intracellular ciliate. All the parasite average burden per HPF values were between 0 and 16, except three oysters whose parasite burden was 65, 69 and 52. For these particular oysters, their value of parasite burdens were placed in a category of greater than 20 so it no longer interfered with statistical calculations. The importance of these outliers is discussed later. The oysters that were negative for the parasite were placed in the group named 'Negative'. Oysters containing the parasite were grouped into three roughly equal categories, so oysters with an average parasite burden per HPF between 0 and 0.35 were considered to have 'Low' burdens, the oysters between 0.35 and 1.29 were 'Moderately' infected and those over 1.29 were considered 'Highly' infected.

The individual counts of burden per HPF produced a negative binomial distribution. A Pearson Correlation test performed on the data of inflammation and burden per HPF produced a positive correlation of 0.315, significant to the 0.01 level (Table 4.1.1). This suggests there is a positive relationship between the host inflammatory response and the presence of the ciliated parasite. A Kruskal-Wallis test performed on all the groups also supported this finding, indicating a highly significant difference between the groups.

Table 4.1.1: Pearson Correlation between average inflammation and average parasite burden per High Power Field (SPSS output).

		Average Inflammation	Average parasite burden per HPF
Average Inflammation	Pearson Correlation Sig. (2-tailed) N	1 300	.315(**) .000 300
Average parasite burden per HPF	Pearson Correlation Sig. (2-tailed) N	.315(**) .000 300	1 300

**Correlation is significant at the 0.01 level (2-tailed).

The raw values from the inflammation grade and the grouped parasite burden values were plotted on a box plot, where a marked increase in mean inflammation was observed in oysters with a high parasite burden (Figure 4.1.2). This box plot displayed the mean inflammation into Negative, Low and Moderate groups. To determine whether the group with a high parasite burden was considerably different than the other groups, a Kruskal-Wallis test was performed. The Negative, Low and Moderate groups were merged, and compared to the High group, with the results

being a Kruskal-Wallis chi squared of 11.5831, with df of 1 and p-value of 0.0006655. This indicates a highly significant difference.

A scattergram was produced to plot the average inflammation and the average parasite burden per HPF against the size of oyster in millimetres (Figure 4.1.3). Both the inflammation and burden displayed a normal distribution against size, with a peak just over 15 mm. The three individual 'outliers' display a high parasite burden with a relatively low inflammatory response. In the case of the majority of oysters, the curve of parasite burden closely matches that of the inflammatory response, indicating the two may be linked.

4.1.4 Discussion

The results of this histopathological study has shown a significant positive relationship between the intracellular ciliate parasite burden and the severity of the host inflammatory response in an outbreak of infected pearl oysters from a major pearl producing region of Western Australia.

The digestive system of all animals is an interface to the outside environment and therefore is a common place for inflammatory reactions to initiate. In molluscs, inflammation, or the infiltration of haemocytes, is a non-specific response. Sparks and Morado (1988) explained that host response is basically similar, irrespective of species of host bivalve, harmful agent or site of injury. This is consistent with the large number of oysters seen in this study mounting a mild inflammatory reaction without any visible aetiology. However, when the group of oysters with high parasite burden were analysed, these were most likely to have a more severe inflammatory infiltrate when compared with those exhibiting a lesser or negative parasite burden.

As seen on the scattergram of Figure 4.1.3, both the burden and the inflammation of affected oysters peaked at around 15 mm in size, with a normal distribution. This may indicate the oysters are effectively mounting a defensive response and are clearing the infection as they grow towards 35 mm in size. There were a few exceptions to this trend, being the individual oysters that had the highest parasite burden and an insignificant host response. The two most likely explanations for this occurrence is the oysters were unable to mount an effective host response and therefore the ciliates have been able to thrive, or there was an overwhelming burden of ciliates and the individual oysters have exhausted their inflammatory capabilities.

Figure 4.1.2: A box plot depicting the relationship between average parasite burden per HPF and the severity of the average inflammation of the digestive gland.

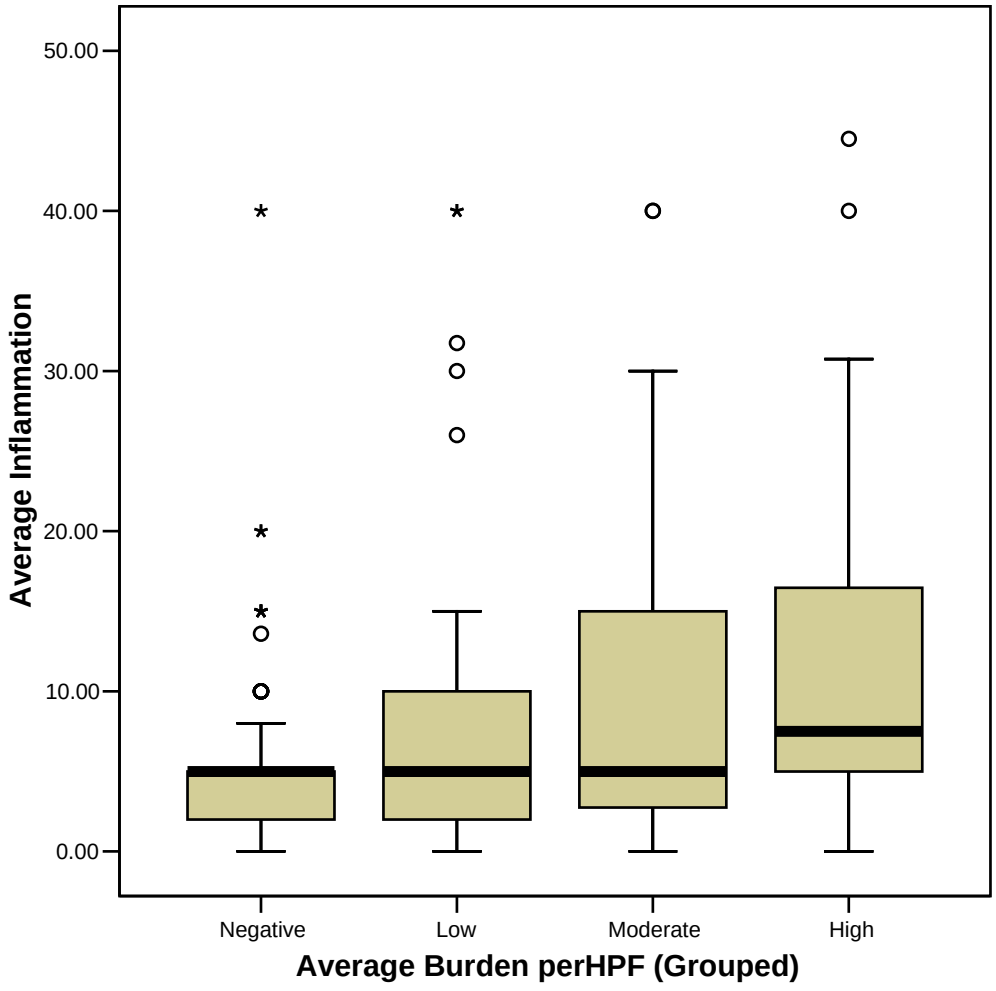

Figure 4.1.3: A scattergram depicting the average inflammation and the average parasite burden per HPF against the size of oyster. Both the inflammation and burden displayed a normal distribution against size, with a peak just over 15 mm.

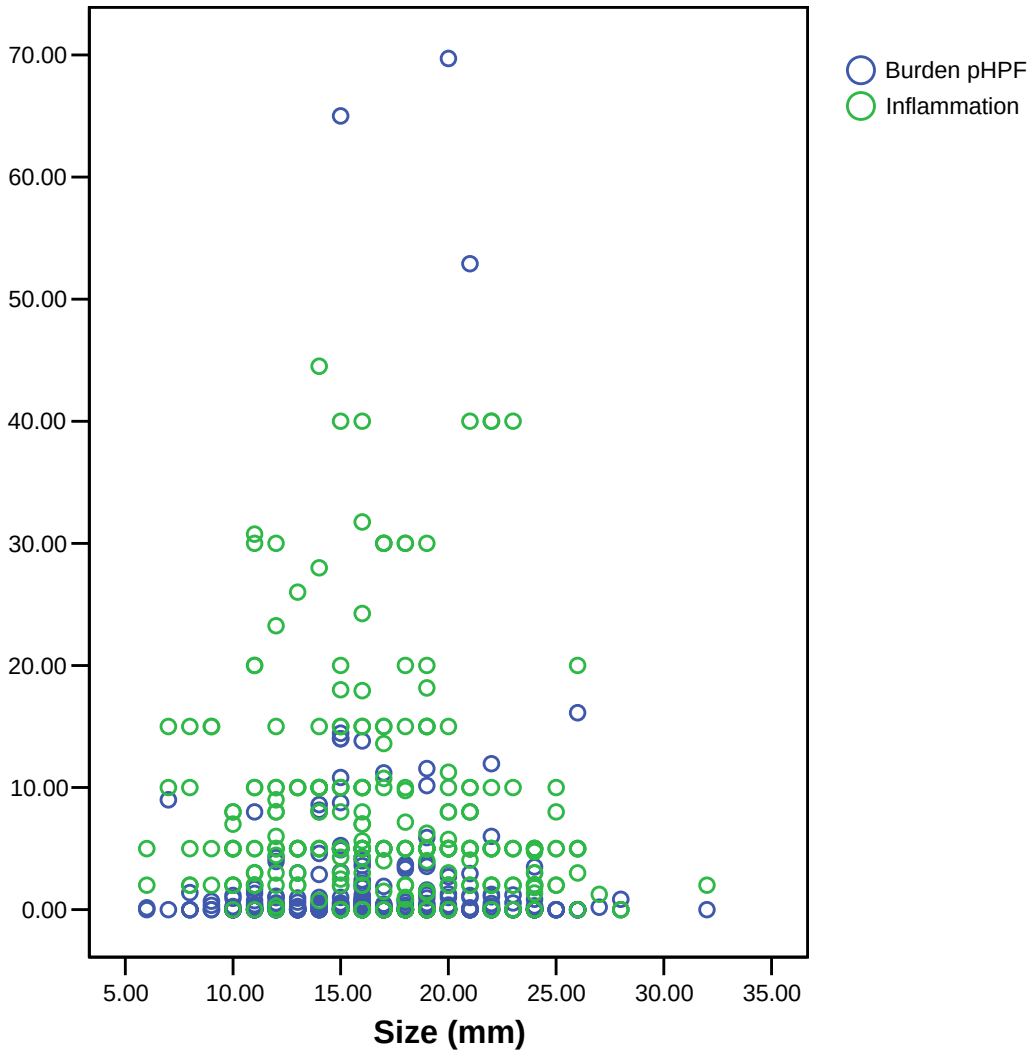

In summary, there was a significant correlation between the burden of intracellular ciliated protozoa in the digestive gland and the severity of the host inflammatory response. This indicates the organism may be pathogenic and not simply a harmless commensal. Certain environmental conditions may be necessary for outbreaks to occur. Further study into the intracellular ciliate is required to further characterise it and determine its biology. A survey of aquatic invertebrates that share habitat with pearl oysters may determine if it is an obligate parasite specific to pearl oysters, or perhaps an opportunistic parasite of bivalves and other aquatic invertebrates.

4.2 Ultrastructural interactions

4.2.1 Introduction

In the previous section it was discovered that there was an association between the presence of the parasite in the digestive gland and an infiltrate of hemocytes. In order to discover the local effect the ciliate was having on the individual cells, transmission electron microscopy was utilised.

4.2.2 Materials and Methods

Oyster samples

An archive of formalin-fixed, paraffin embedded oyster tissues held by the Western Australian Dept of Fisheries was made available for examination.

Transmission electron microscopy

Sections of formalin fixed paraffin embedded oysters confirmed to be positive for the ciliate on histology were re-embedded for TEM using standard methods, blocks were sectioned with an Om U3 (C.Reichert, Austria) ultramicrotome, stained with uranyl acetate and lead citrate and viewed with a Philips CM100 BIO TEM.

4.2.3 Results

Ciliates were observed inhabiting the digestive cells of the pearl oysters' digestive gland. The basophil cells, with their abundant rough endoplasmic reticulum, directly adjacent to infected digestive cells, were apparently unaffected. In contrast, the absorptive digestive cells inhabited by ciliates had disrupted cytoplasm with increased vacuolation. Figure 4.2.1 is an electron micrograph of a digestive cell infected with two intracellular ciliates, displaying vacuolated cytoplasm, disruption of normal cellular components and an area free of cytoplasmic material directly surrounding the intracellular ciliates. The figure also displays two adjacent unaffected basophil cells. The nucleus of the infected cells showed degenerative changes such as fragmented borders with segmental loss of the double membrane. Another consistent change was captured in Figure 4.2.2, an electron micrograph depicting the basal membrane of infected cells appearing segmentally thickened with folded, lamellar changes.

In some sections, segments of a single membrane were observed between the ciliate and the host cell, this with the absence of host cytoplasmic material within this area, indicated that the ciliate may have been surviving within a phagocytic vacuole inside the host cell. Figure 4.2.3 is an electron micrograph of a ciliate within an area free of cytoplasmic material, partially bordered by remnants of a membrane. The nucleus of this cell appears in tact, without the sign of degeneration seen in other infected cells, however the cytoplasm of the cell has vacuolar degenerative changes. In cases where up to three ciliates inhabited a single cell, each were separated by host cytoplasmic material.

4.2.4 Discussion

Relatively few parasites choose to inhabit the intracellular spaces of their host organism. This is probably due partly to the hostile nature of the inside of a host cell, and the many hazards to survival needed to overcome by the parasite for the success of this kind of living. Firstly the parasite must recognise, select and then enter the host cell, all the while evading the host immune response. Once inside the cell the parasite must avoid the intracellular killing mechanisms of the cell and obtain nutrients to survive. Finally, the parasite must exit the cell in order to reinfect another or progress in the extracellular stages of their life cycle. The mechanisms by which the intracellular parasites accomplish this are considerably varied, so generalisations are impossible (Moulder 1985).

Intracellular parasites and their mechanisms of entry

Parasites may enter the body of a host via a range of means, both passive and active. In the case of aquatic bivalves, they may assist the entry of suspended protozoal parasites by the creation of the water current passing over their gills and palps (Cheng 1988). The parasite itself may prepare for this transition by encysting, in the case of many amoebae. Another form of passive entry is with the use of a vector, for example *Perkinsus marinus* and *Boonea impressa*. Active entry is utilised by the parasite *Hartmannella tahitiensis*, reviewed by Cheng, 1988, whereby it secretes penetration enzymes when in contact with stressed *Crassostrea commercialis* oysters. The digestive gland being the target organ of the intracellular ciliate may support the theory that the ciliate gains entry via the passive means of ingestion by the pearl oyster. No other tissues of the oysters were found to be affected by the ciliate, therefore a migration of the parasite from another site of entry is

Figure 4.2.1: An electron micrograph of two intracellular ciliates (C) inhabiting a digestive cell(D) with vacuolar changes and a degenerative nucleus. In contrast the basophil cells (B) adjacent to the infected cell appears unaffected. Scale bar 10 µm.

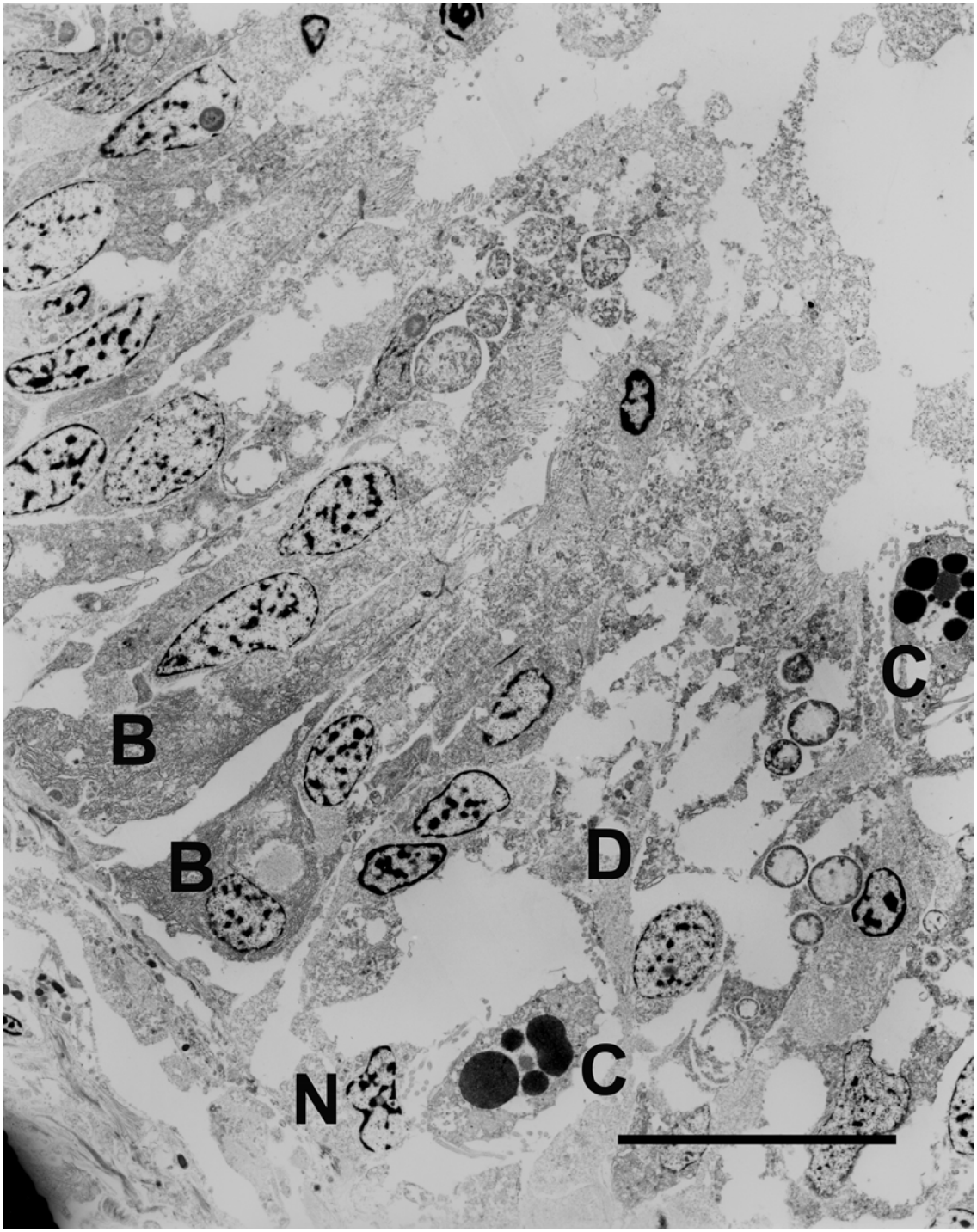

Figure 4.2.2: An electron micrograph of the intracellular ciliate in a digestive cell. The vacuolated cytoplasm surrounding the parasite (V), the degenerative changes in the nucleus of the host cell (N) and the thickened, lamellar changes in the basal membrane adjacent to the infected cell (B) are visible. Scale bar 10 µm.

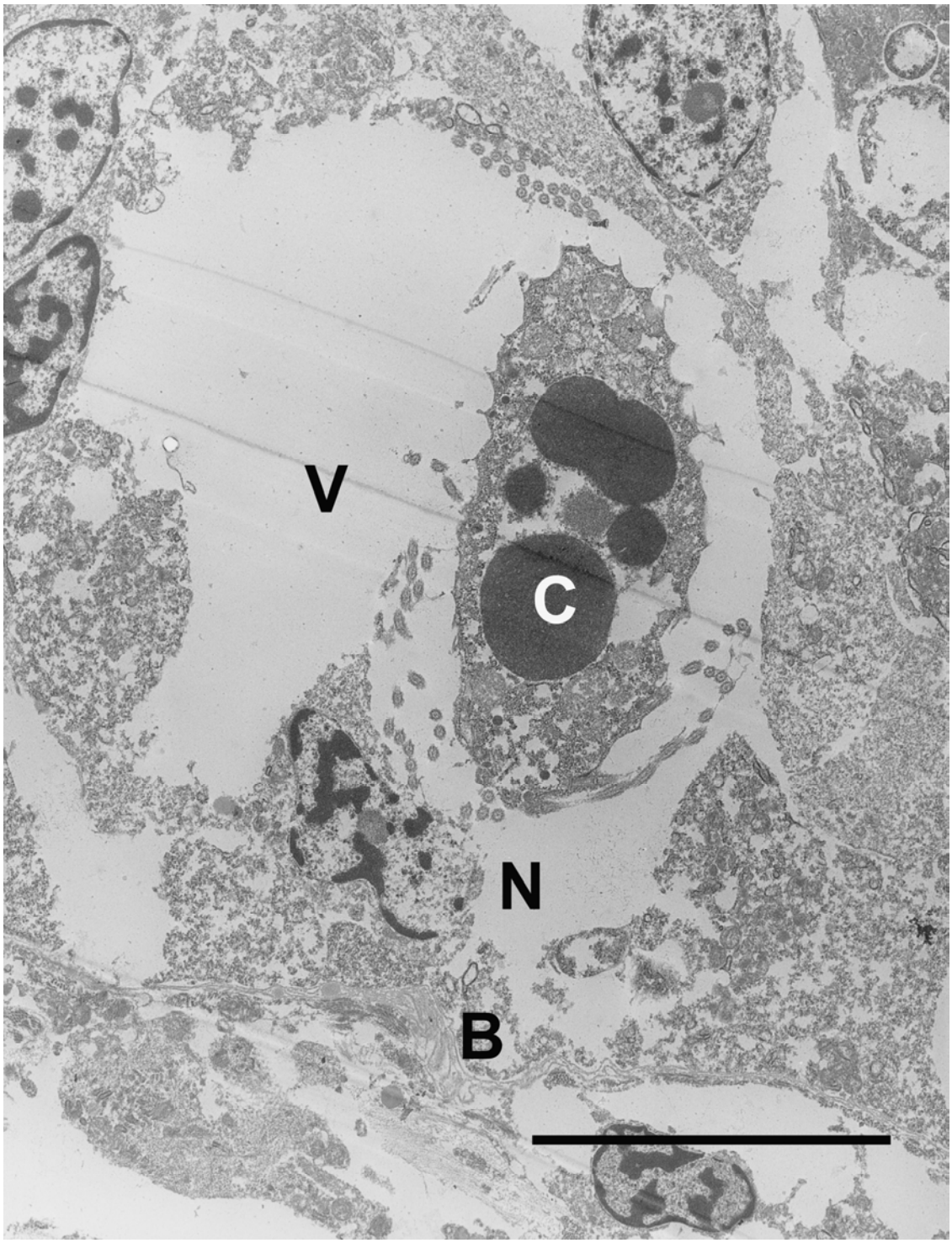

Figure 4.2.3: An electron micrograph of the intracellular ciliate (C), displaying the cilia (A), inside the remnants of a membrane (M) surrounding the structure. Within the cytoplasm of the host cell are lysosomal bodies (L). Scale bar 5 µm.

highly unlikely, as is the case of sporozoite and ookinete stages of Apicomplexan parasites (Leiriao, Rodrigues et al. 2004).

Most intracellular parasites have a specific target cell, for example the Haplosporidia protozoan *Bonamia ostreae* usually infects hemocytes of the European flat oyster *Ostrea edulis*, however others are able to inhabit many types of cells, for example the Apicomplexan *Toxoplasma* spp. that can exploit any nucleated cell. The discovery of the intracellular ciliate exclusively in the digestive cells of the pearl oysters digestive gland suggests the parasite has an affiliation with this particular target cell.

The mechanism by which the parasite enters the selected cell is also widely varied. This is dependant on both parasite factors and host cell factors. The characteristics of the ciliates target, the digestive cell, may assist in the parasites entry into the cell. These cells have a vacuolated appearance, with a brush border and an active lysosomal apparatus (Cockman 1982). Being an absorptive cell, they are capable of such functions as phagocytosis and pinocytosis (Pal 1971b). Some obligate intracellular parasites have been shown to utilise this ability in their target cells as a means of invading the intracellular space.

The intracellular parasite *Leishmania* preferentially invades professional phagocytic cells. This is a relatively passive process for the parasite (Jones 1981; Denkers and Butcher 2005). The *Leishmania* promastigotes are coated with serum opsonins and are internalised via receptor-mediated phagocytosis (Leiriao, Rodrigues et al. 2004).

Another characteristic of a target cell that may assist in the entry of an intracellular ciliate is their membrane repair mechanisms. *Trypanosoma cruzi* is a protozoan parasite capable of invading every nucleated cell in the mammalian host body. It does this by manipulating the cells natural mechanisms of cellular wound repair, namely the Ca^{2+} dependant lysosome exocytosis pathway (Burleigh and Woolsey 2002; Tan and Andrews 2002). The attachment of the *T. cruzi* trypomastigote to the cell surface triggers an elevation in the intracellular free Ca^{2+} concentration, disruption of actin and the subsequent recruitment of lysosomes to the site. The parasite then enters the cell within a parasitopherous vacuole formed by the lysosome-derived membranes (Leiriao, Rodrigues et al. 2004). As a result, this successful parasite is not limited to target cells with the ability of phagocytosis.

Toxoplasma gondii also has the ability to invade not only phagocytic cells, but cells that don't have the phagocytic function as well. In the case of entry into non-phagocytic cells, the host cell plays a passive role during invasion (Morisaki, Heuser et al. 1995), in contrast to the mechanisms by which *T. cruzi* manipulate (Denkers and Butcher 2005). Once in contact with the target cell, the parasite manoeuvres itself so its apical end attaches to the host cell surface, using an active gliding motion similar to that of other Apicomplexans (Wetzel, Schmidt et al. 2005). Once attached, the actin-myosin cytoskeleton allows for active penetration into an invagination of

the host membrane, forming a parasitopherous vacuole (Morisaki, Heuser et al. 1995). The intracellular ciliate of pearl oysters retains its cilia while intracellular, unlike other ciliates such as *Sphenophrya*, therefore this motile ability may play an important role in the invasion of host cells.

Another active process of invasion developed by intracellular parasites is the zippering of *Theileria* sporozoites. *Theileria* differs from other apicomplexans as its invasive stage is non-motile and therefore does not re-orient itself on the host cell to enter apical-end first, using an actin cytoskeleton (Shaw 2003). Instead, the parasite enters the host cell once attached by progressive circumferential 'zippering' of both membranes. This is a passive process for the host cell with no mechanisms activated in the case of phagocytosis, and the resulting parasitopherous vacuole is of host origin.

Once the parasite has gained entry into the host cell, it must avoid the cells defence mechanisms. Again, the ways in which intracellular parasites accomplish this are numerous and vastly different. Depending on the individual needs of the life cycle stages of these parasites, they may either live inside a parasitopherous vacuole, such as *Toxoplasma gondii* (Suss-Toby, Zimmerberg et al. 1996), and *Leishmania* (McConville, de Souza et al. 2007), or free in the cytoplasm. There were parts of a membrane surrounding the intracellular ciliate of pearl oysters visible in some TEM samples, perhaps indicating the presence of a parasitopherous vacuole (Refer to *Morphology Section*). It may however, be the remnants of the entry mechanism of the parasite and has been damaged to allow the ciliate to escape free into the cytoplasm. This method of escaping the vacuole soon after entrance into the cell is used by *Theileria* sporozoites (Shaw 2003) and *Trypanosoma* amastigotes (Cheng 1988) to escape lysosomal degradation. The digestive cell of a bivalves digestive gland is abundant with such lysosomes (refer to *Morphology Section*).

Challenges of the intracellular ciliate

The intracellular ciliate of pearl oysters has utilized a unique habitat, whereby it must overcome numerous challenges for survival. As discussed, each intracellular parasite has customised an entry mechanism into their host cell. Since discovery of this mechanism usually requires in vitro experimentation and the use of video microscopy (Morisaki, Heuser et al. 1995; Suss-Toby, Zimmerberg et al. 1996; Tan and Andrews 2002), this is an avenue for future research. In the mean time, however, the entry mechanism of this interesting ciliate can only be theorised. The fragment of membrane viewed on TEM initiates the argument that the ciliates invasion method may involve vacuole-mediated transport. This could either be through host cell-mediated phagocytosis, which is possible for this cell type, or a parasite-initiated form of entry, perhaps using the lysosomes like *Trypanosoma*. Characterisation of this membrane, similar to the immunohistochemical studies made on the microsporidia *Encephalitozoon cuniculi* by Fasshauer, Gross et al. 2005 would help solve this dilemma.

The fact that the membrane seen on TEM was discontinuous and not present in all sections may be an indication that the ciliate escaped to the cytoplasmic space soon after invasion. The lack of cytoplasmic material surrounding the ciliate may be the result of motile cilia, and not the indication of a membrane. Changes observed in the nucleus of the host cell also support the argument for the intracytoplasmic position of the ciliate. Being a professional absorptive cell, a membrane bound foreign body could quickly become the target for lysosomal digestion and therefore evasive actions would need to be taken.

Another challenge for the intracellular ciliate to overcome is host cell sloughing. Similarly to vertebrate intestinal epithelial cells, there is a general belief that aged digestive cells are sloughed into the lumen of the digestive gland. For the intracellular parasite, this is either a death sentence or a new opportunity of infection. No ciliates were seen in the lumen of the digestive tubules. This could either mean the parasites are moving between adjacent cells or they are unable to survive for long in the lumen environment, and are flushed from the digestive gland or digested. In order to understand this process more thoroughly, a controlled pathogenesis study would need to be performed.

Implications of this study on the pearling industry

This study has confirmed a positive correlation between the presence of the intracellular ciliate and pathology to the pearl oyster. In light of this information, it would seem the ban on translocation of infected oysters out of Zone 1 was justified. This parasite adversely affects the nutrient absorbing organ, the digestive gland, of pearl oysters. Further studies may need to be conducted to ascertain the precise effect that this has on the growth and productivity of the oyster, however it can be assumed that it would be a negative one. As with any production animal, any threat to the health of a pearl oyster in the farm environment must be taken seriously, as it could have a significant financial impact in the long term.

Chapter 5: Epidemiology of the intracellular ciliate

Photo: Sampling for bivalves in the Montebello Islands, 2005 (photo by D. Bearham)

In this Chapter the epidemiology of the intracellular ciliate infection was studied. The first part is a collation of field trials performed between 2005 and 2007 with pearl oysters, by placing naïve spat in areas of previous known infections. These oysters were examined histologically for the presence of the ciliate and other parasitic burdens. The second part of this Chapter is a study into the sensitivity of histology as a screening tool for the detection of ciliate infections. Thirdly, the Fish Health Unit at Murdoch University was set up for cross infection trails and an experiment plan was devised for the event that a ciliate infection was discovered. The fourth section of this Chapter is a survey of bivalves in areas close to previous ciliate infections, to discover whether a bivalve reservoir of infection exists. The last two parts to this Chapter are an historical inspection of the ciliate outbreaks that occurred from 2001 to the present.

5.1 Field Trials for the infection of pearl oysters with the ciliate by placing naïve spat in areas of previous infection

5.1.1 Introduction

Silverlip pearl oysters formed the basis of this investigation since they were the only species found to be infected by the protozoal organism and it is an economically important bivalve. The sampling was focused around the Montebello Islands and Exmouth Gulf where the intracellular organism was most recently found. Figure 5.1.1 and Figure 5.1.2 are maps of the area of Western Australia involved in the study. The sites sampled were the only previously infected sites that were still serviced by pearling companies. A site at Lowendale Is. was also affected but is no longer regularly serviced by a pearl company and therefore it was not financially viable to sample there. One batch of hatchery reared oysters from Whalebone Island were also included in the survey.

5.1.2 Materials and Methods

Four batches of oysters were made available for examination by Morgan & Co. These oysters were collected after inhabiting an area previously known to be infected with the ciliate. One batch of hatchery oysters were provided from Whalebone Island by Kailis Bros., for examination.

Sampling pearl oysters from Montebello Islands, July 2005

Silverlip pearl oysters where collected in July 2005 from long-lines on the pearl lease at Montebello Islands with the co-operation of Morgan & Co (Figure 5.1.3A). Four sites where sampled, including the long-lines at Bluebell Island, (20^{o}23’43”S, 115^{o}31’18”E), Horseshoe Lagoon, (20^{o}23’43”S, 115^{o}34’00”E), Burgundy Bay, (20^{o}24’00”S, 115^{o}34’00”E), and Turtle Bay, (20^{o}26’00”S, 115^{o}31’35”E). All shell sampled at these sites where less than 70 mm in size. Oysters where collected from Bluebell Island (n=20), of which 4 were fixed and 16 transported to Perth live. These numbers were similar for Horseshoe Lagoon, Burgundy Bay and Turtle Bay. The total number of oysters collected was 80; 16 fixed and 64 transported to Perth alive, (Table 5.1.1). They were between 19-42 mm in size.

Figure 5.1.1: A map of Western Australia, noting the region of Exmouth, containing the Montebello Islands and Exmouth Gulf, where the oysters were collected. (WALIS 2002)

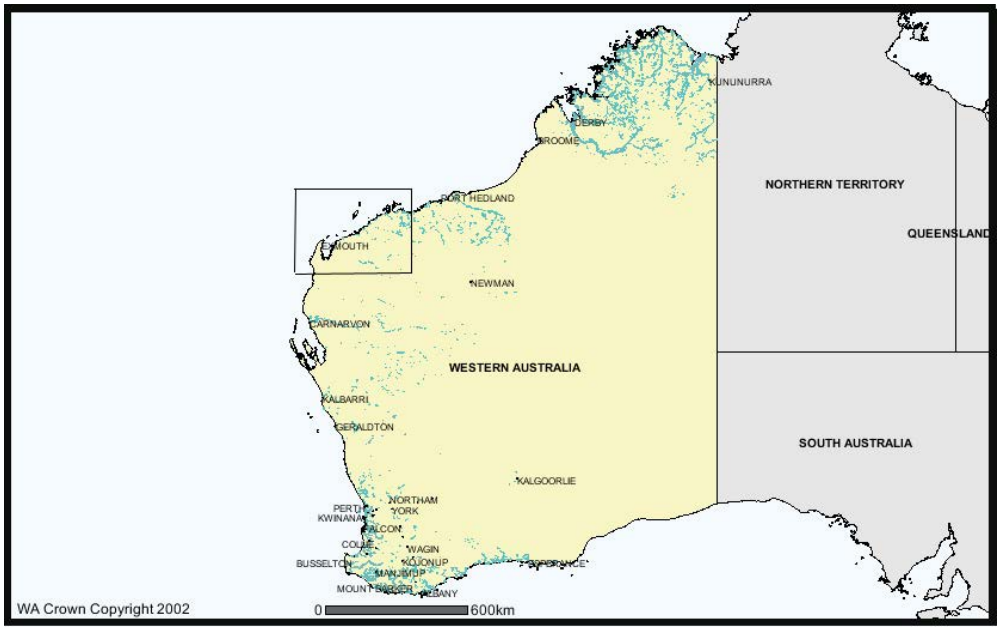

Figure 5.1.2: A map of the two sampling regions off the coast of Western Ausralia and their association with the mainland. (WALIS 2002)

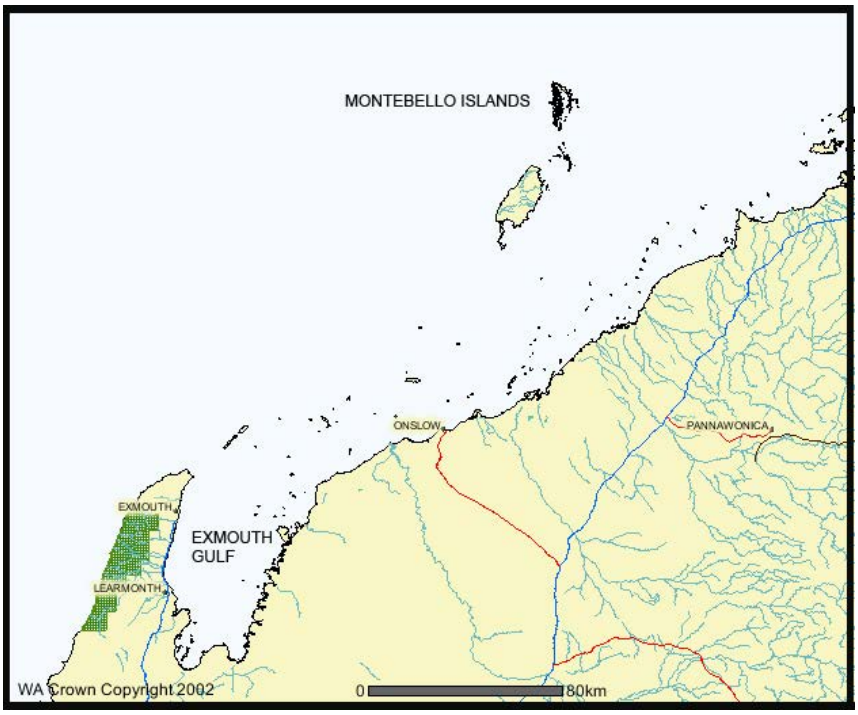

Figure 5.1.3: A: Photo of Montebello Islands, taken from a sea plane July 2005
B: Photos of the long lines at Gales Bay, Exmouth Gulf May 2007, on the left is a photo of a long line, on the right is a view into the water showing a panel of pearl oysters suspended just below the surface, photos by Z. Spiers

A

B

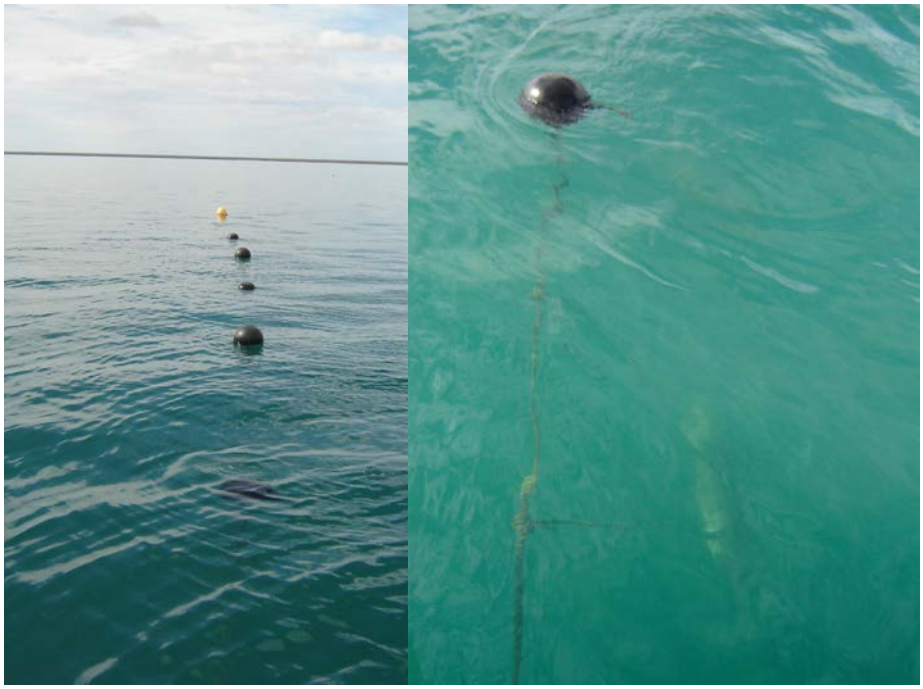

Table 5.1.1: Table of silverlip pearl oysters sampled from the Montebello Islands July 2005

Site \ Samples taken	Fixed	Live	Total
Bluebelle Island	4	16	20
Horseshoe Bay	4	16	20
Burgundy Bay	4	16	20
Turtle Bay	4	16	20
Total sampled	16	64	**80**

The fixed pearl shell were opened with a sharp knife, the digestive gland was identified and the whole oyster was cut in half sagittally with a scalpel. It was ensured that digestive gland was present in both halves. One half was placed in 10% formalin (in seawater) and the other in 100% ethanol. Both sample jars were labelled to identify individual bivalves. The formalin fixed tissue was later processed for histological examination and the ethanol samples where kept for molecular testing.

Field Trial in Giralia Bay, Exmouth Gulf and associated sampling in September 2006

In April 2006, 4000 silverlip pearl oyster spat 10 mm in size where placed in a research trial in Exmouth Gulf, alongside normal farm spat. They were deployed with the help of Morgan & Co. on the settlement medium, being 500 mm long plastic slats. The plan was to sample every 3 months, however the deployment and sampling were delayed due to repeated cyclone activity in the area. The sampling did eventually occur in September 2006 from Giralia Bay (22^{o}26’60”S, 115^{o}34’00”E) Lease A. Pearl oyster spat were collected, halved with one half of the oyster fixed in 10% sea water buffered formalin and the other half placed in 100% ethanol (n=165). These spat were between 14 – 63 mm in size.

Sampling from Whalebone Island, September 2006

In September 2006, a batch of hatchery reared pearl oyster spat were made available for examination by Kailis Bros., to assist in looking for the ciliate. These oysters were between 17 and 29mm in size. The entire oyster was placed in 10% sea water buffered formalin and processed for histology, then stained with H&E.

Field Trial in Exmouth Gulf and associated sampling in May 2007

In May 2007, 20 pearl oyster spat were sampled from Line 1 Gales Bay (22^{o}26’60”S, 114^{o}20’60”E) Lease B, having been transferred from Giralia Bay one week previously to this area, known to have been found to have the intracellular ciliate in October of previous year (Figure 5.1.3B). These oysters were between 12 – 38 mm in size. During the same field trip, 30 pearl oysters between the sizes of 50-100mm were collected from the Bottom line, Gales Bay B, having been transferred from Giralia Bay 6 months previously to this area, which had been found to have ciliate in October of previous year.

Processing samples for histological examination
The samples fixed in formalin were processed into paraffin embedded blocks according to standard procedure and stained with Hematoxylin and Eosin. They were observed using an Olympus BH-2 microscope (Olympus Optical Co. Ltd.).

5.1.3 Results

A total of 231 pearl oyster spat, from pearling leases in the Montebello Islands and Exmouth Gulf, were examined microscopically for the presence of the ciliate. Their sizes ranged from 14 mm to 100 mm. All of these oysters were incorporated into the normal maintenance regime of other pearl oysters on the farms of origin.

Results of sampling from Montebello Islands in July 2005
There were 16 oysters collected from leases in the Montebello Islands in July 2005. A quarter of the 16 were collected from Turtle Bay, four oysters were from Blue Bell, four from Horseshoe Bay and the remaining four were collected from Burgundy Bay. The oysters were between 19-42 mm in size. One of the spat was identified as male on histological examination, by the presence of spermatogenesis in the gonad. The remaining 16 were of unspecified sex, most likely undeveloped juveniles. One oyster contained an infection of Ancistrocomid-like ciliates in gut. Of the 16, three were infected with gregarine bodies in the digestive gland. One oyster exhibited a mild inflammation in digestive gland, and one oyster contained a metazoan parasite in its mantle. One of the oysters contained a segmental exoskeleton of a copepod in the connective tissue adjacent to digestive gland, without any associated host response.

Results of sampling from Giralia Bay A, Exmouth Gulf in September 2006
There were 165 oysters sampled from Giralia Bay Lease A, between 14 – 63 mm in size. The sizes of the oysters had a normal distribution with a mean of 40.24 mm, and a standard deviation of 7.866 (Figure 5.1.4). Only 11 of the spat were identified as male, and the remainder unspecified, presumed immature. Oysters with gregarine bodies in their digestive epithelia numbered 38, with one of these also containing gregarine bodies in the lumen of the gut. Sections of a metazoan parasite were observed in 14 oysters. Four of these infections were in the digestive tubule lumen, one of which was associated with a multifocal to coalescing inflammatory infiltrate of the digestive gland. Five oysters contained the metazoan parasites within the lumen of the gut, one of which was associated with a diffuse moderate inflammatory infiltrate, and focal necrosis and sloughing. Two oysters contained these parasites in the lumen of their stomach. One of which was associated with a diffuse moderate inflammatory infiltrate and both also contained Ancistrocomid ciliates. One metazoan parasite was located in the lumen of the oesophagus, and three oysters contained metazoan parasites within a lesion of degeneration and necrosis of the digestive gland.

Some oysters contained focal areas of chronic necrosis and degeneration, similar to the ones with intralesional metazoan parasites. While other areas of the same digestive gland appeared to be morphologically normal, there were large focal areas of disruption to the normal tubular architecture. The digestive cells appeared swollen and vacuolated with indistinct cell borders and fragmented pyknotic nuclei (Figure 5.1.5). Intralesional metazoan parasites were sometimes discovered, indicating the necrotic foci could be a result of chronic metazoan infections.

Other oysters displayed a more diffuse abnormality of their digestive glands. Figure 5.1.6 is of two oysters' digestive glands displaying signs of starvation, however on first sight they have very different appearances. On further inspection the tubules were dilated in both cases, the lumen contained sloughed epithelial cells, and the digestive cells remaining were vacuolated with disruption to cellular adhesions.

Of the 165 oysters sampled, 35 contained Ancistrocomid-like ciliates within the lumen of the gut. Seven of these infections extended into the lumen of the digestive tubules, ten were described as heavy infections, and 14 also had concurrent infections with either bacteria, metazoans or gregarine bodies. Two oysters displayed oedema of the connective tissue of the mantle, and one of these oysters had concurrent moderate multifocal inflammation in the interstitium of the gill, and mild diffuse inflammation in the digestive gland.

An inflammatory infiltrate was present in 48 of the 165 oysters. Oysters with diffuse inflammation throughout their digestive glands numbered 25; 17 mild and 8 were moderate. Eight spat had a mild infiltrate of haemocytes associated with the interstitium of the gut; four of these were in a diffuse pattern, and four with a multifocal distribution. Four oysters had a moderate inflammatory infiltrate associated with the gut interstitium, two were diffuse and two were multifocal in distribution. One oyster had a moderate metazoan parasites were sometimes discovered, indicating the necrotic foci could be a result of chronic metazoan infections.

Figure 5.1.4: A histogram of the size distribution in the oysters from Exmouth Gulf, sampled in 2006. The sizes have a normal distribution with a mean of 40.24 and a standard deviation of 7.866.

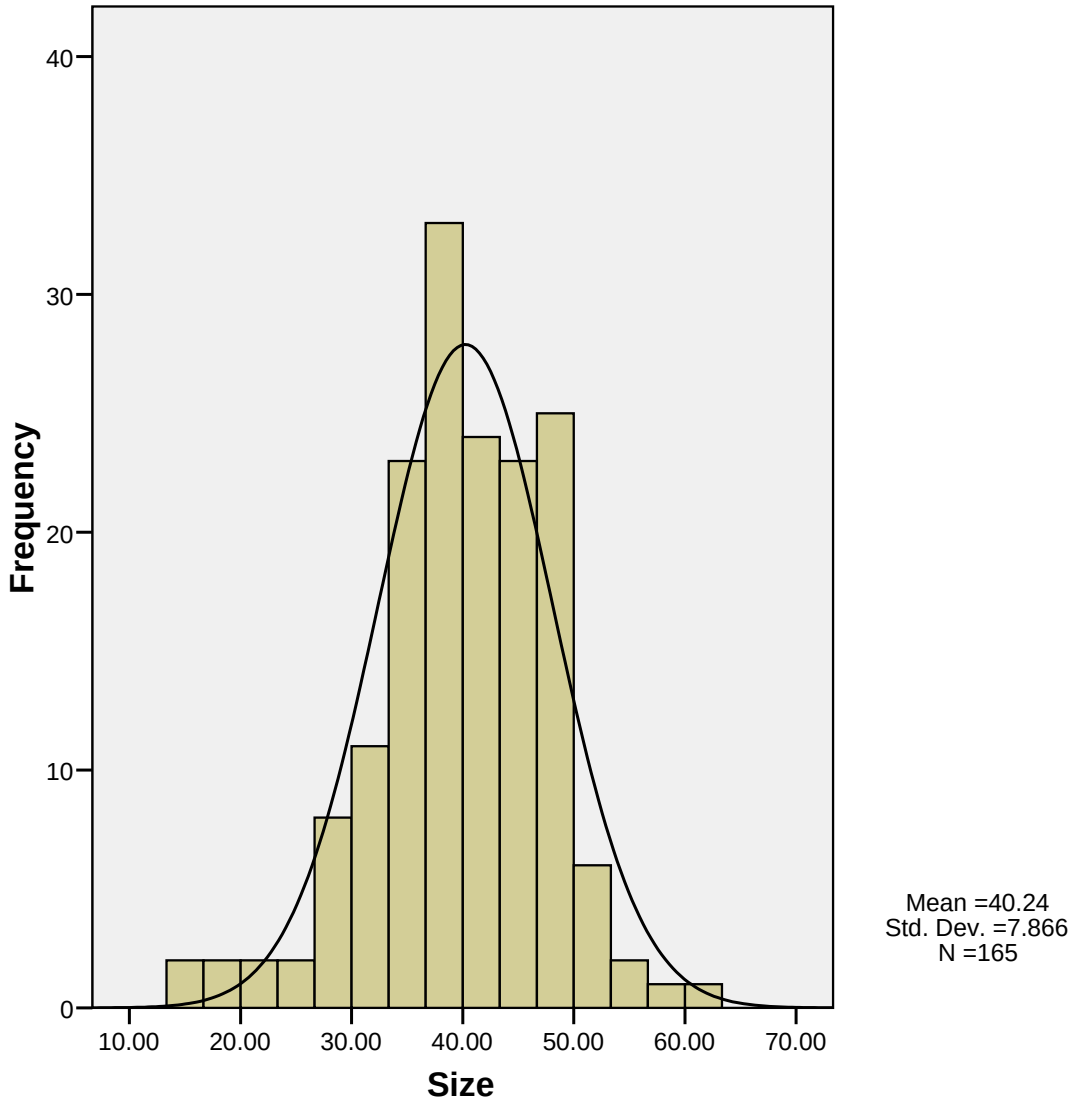

Figure 5.1.5: Two photomicrographs of the digestive glands of pearl oysters from Giralia Bay, sampled September 2006. A: A focal area of chronic necrosis and degeneration with disruption to the normal tubular architecture, swollen and vacuolated digestive cells with indistinct cell borders and fragmented pyknotic nuclei. B: Another digestive gland with a similar pattern of degeneration, with an intralesional metazoan parasite (arrow). Scale bars: 150 µm.

A

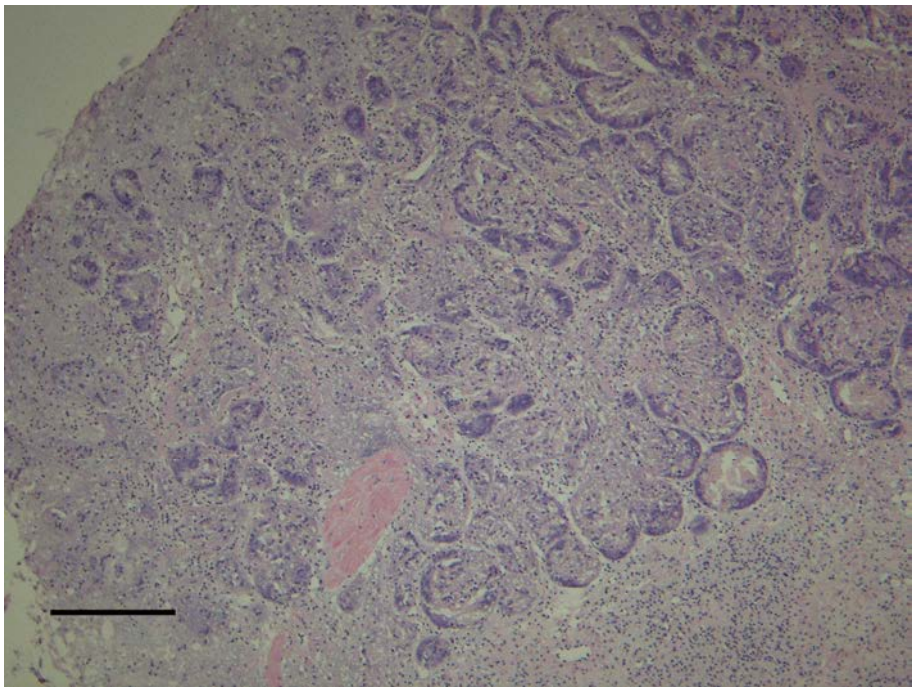

B

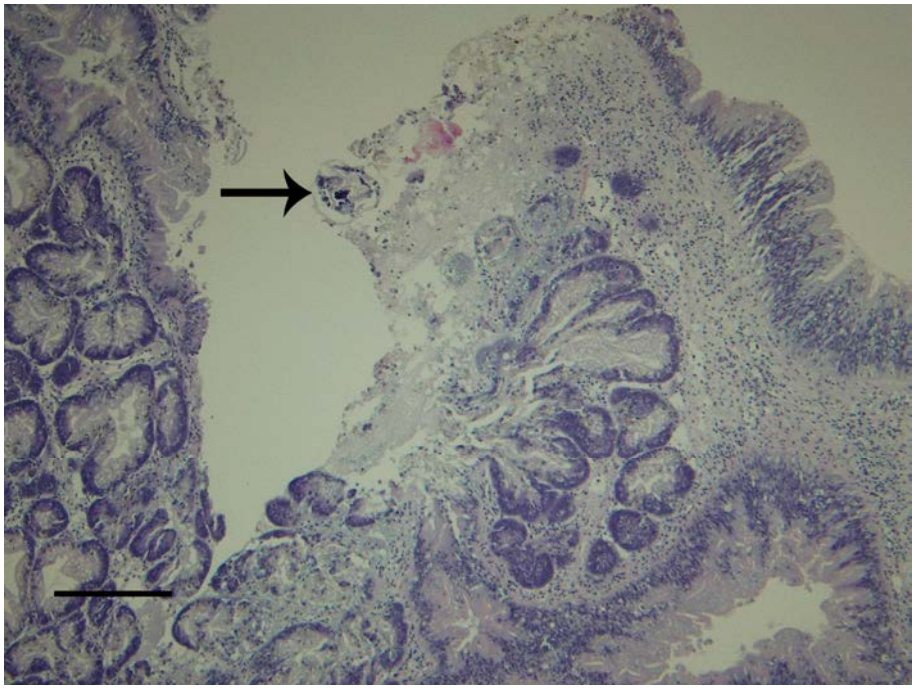

Other oysters displayed a more diffuse abnormality of their digestive glands. Figure 5.1.6 is of two oysters' digestive glands displaying signs of starvation, however on first sight they have very different appearances. On further inspection the tubules were dilated in both cases, the lumen contained sloughed epithelial cells, and the digestive cells remaining were vacuolated with disruption to cellular adhesions.

Of the 165 oysters sampled, 35 contained Ancistrocomid-like ciliates within the lumen of the gut. Seven of these infections extended into the lumen of the digestive tubules, ten were described as heavy infections, and 14 also had concurrent infections with either bacteria, metazoans or gregarine bodies. Two oysters displayed oedema of the connective tissue of the mantle, and one of these oysters had concurrent moderate multifocal inflammation in the interstitium of the gill, and mild diffuse inflammation in the digestive gland.

An inflammatory infiltrate was present in 48 of the 165 oysters. Oysters with diffuse inflammation throughout their digestive glands numbered 25; 17 mild and 8 were moderate. Eight spat had a mild infiltrate of haemocytes associated with the interstitium of the gut; four of these were in a diffuse pattern, and four with a multifocal distribution. Four oysters had a moderate inflammatory infiltrate associated with the gut interstitium, two were diffuse and two were multifocal in distribution. One oyster had a moderate diffuse inflammation of gill interstitium, one had a mild multifocal infiltrate of the digestive gland and one oyster had exhibited a mild multifocal inflammation of interstitium of mantle. Three oysters had a moderate multifocal to coalescing infiltrate of the digestive gland and one had a moderate multifocal inflammation of palps. Six granulomas were identified within various organs of the oysters examined. One granuloma was located in the connective tissue near gut, one in the connective tissue of mantle, one in connective tissue of the palps, two were within the digestive gland and one was located in connective tissue adjacent to adductor muscle. No causative factors were identified in any of these granulomas. Two oysters had digestive glands with focally extensive severe inflammation, one oyster contained moderate focal inflammation of the heart, and one oyster exhibited mild focal inflammation of its digestive gland and gut epithelium.

Figure 5.1.6: Two photomicrographs of the digestive gland of two starving pearl oysters from Giralia Bay, sampled September 2006. The tubules of the digestive glands were dilated, the lumen contained sloughed epithelial cells, and the digestive cells remaining were vacuolated with disruption to cellular adhesions. Scale bars: 80 µm

A

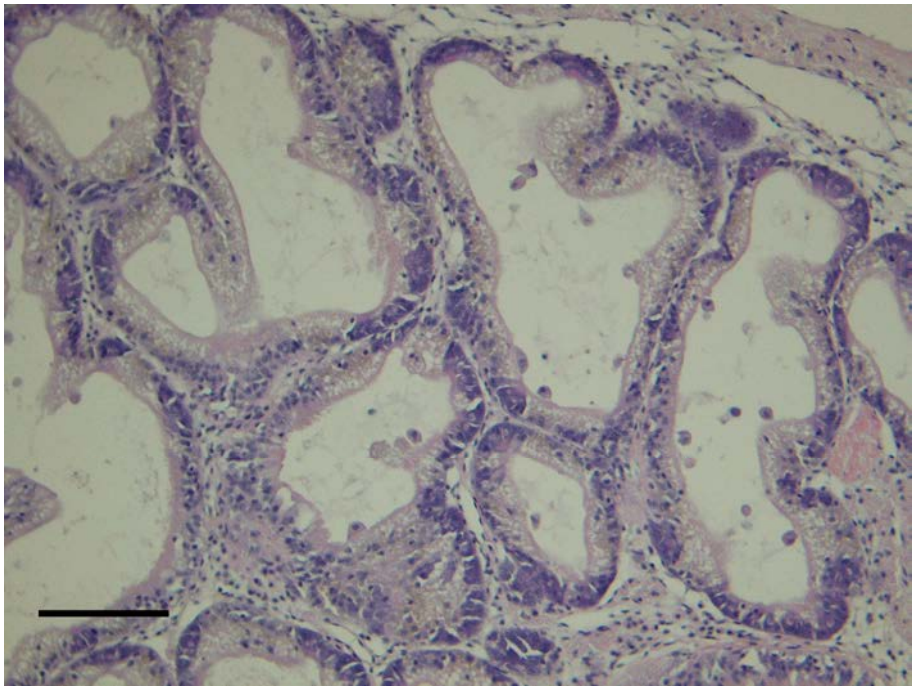

B

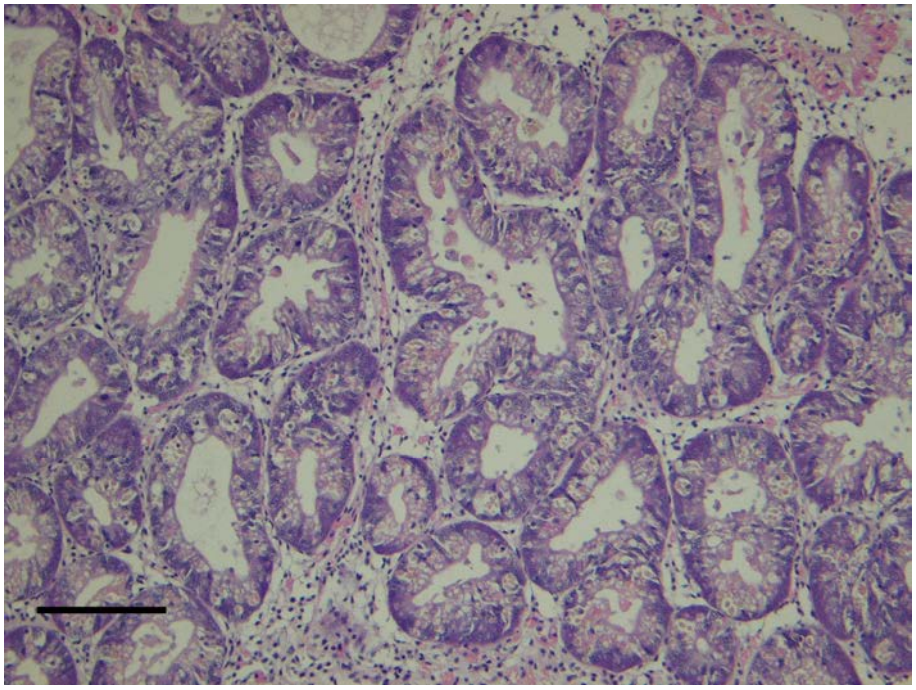

Of the 165 oysters sampled, 12 of these had evidence of a bacterial infection. All 12 were associated with a degenerative necrotic lesion. Seven of these infections were associated with massive degenerative necrosis of the gut and digestive gland, with the bacteria within the gut epithelia and adjacent connective tissue. One of these also had concurrent ancistrocomid and gregarine infections, two with ancistrocomids only. Three were associated with degenerative necrosis of the palp epithelia, with bacteria present in the epithelia and surrounding connective tissue. One of these had a concurrent ancistrocomid infection. Two bacterial infections were associated with degenerative necrosis of the mantle epithelium. Figure 5.1.7 is a photomicrograph of the digestive gland of a pearl oyster with a bacterial infiltrate. There was disruption of the digestive gland architecture, the digestive cells appeared swollen and vacuolated, and the area contained a moderate infiltrate of haemocytes. The gut epithelium was severely ulcerated and the underlying connective tissue contained large colonies of bacteria.

One oyster contained a large accumulation of haemocytes in the tubules of the digestive gland, possibly an accumulation as a result of diapedesis. Haemocytes were observed traversing the wall of the tubule. In the centre of the mass of cells were three eosinophillic crystalline starburst arrangements. One was approximately 40-45 µm at its widest point, and another was approximately 25-30 µm across. A third paler staining starburst was between the two and was approximately 15-20 µm in size (Figure 5.1.8).

Two oysters contained unusual single celled organisms, approximately 5-8 µm in length. These were found in the lumen of the digestive tubule, traversing the epithelial lining of the tubules and the interstitium of the digestive gland. Infected oysters contained large numbers of these organisms, up to 80-100 per 100x high power field. Their presence was associated with a moderate local haemocytic infiltrate. The organisms were ovoid with a densely basophilic ovoid nucleus in the centre of their cell, and a bright eosinophilic cytoplasm (Figure 5.1.9).

The oysters were grouped into those that had abnormalities on histological examination (Abnormalities Detected) and those that were free from abnormalities (No Abnormalities Detected: NAD). These two groups were plotted on a box plot to determine whether there was a significant difference between the size of the oysters in each group. This was to test a hypothesis that the larger animals were healthier and more robust from infection than the smaller ones. The box plot displayed two groups with nearly identical means, disproving this hypothesis (Figure 5.1.10). To test whether the box plot displayed an accurate result, A Mann-Whitney U Test was performed, using SPSS 12.0.2 for Windows (Table 5.1.2). SPSS generated results of a Mann-Whitney U Test on the size of NAD oysters compared with those where

Figure 5.1.7: A photomicrograph of the digestive gland of a pearl oyster from Giralia Bay, sampled September 2006. The digestive gland architecture has been disrupted, the digestive cells appeared swollen and vacuolated, and the area contained a moderate infiltrate of haemocytes. The gut epithelium was severely ulcerated and the underlying connective tissue contained large colonies of bacteria. Scale bar: 80 µm.

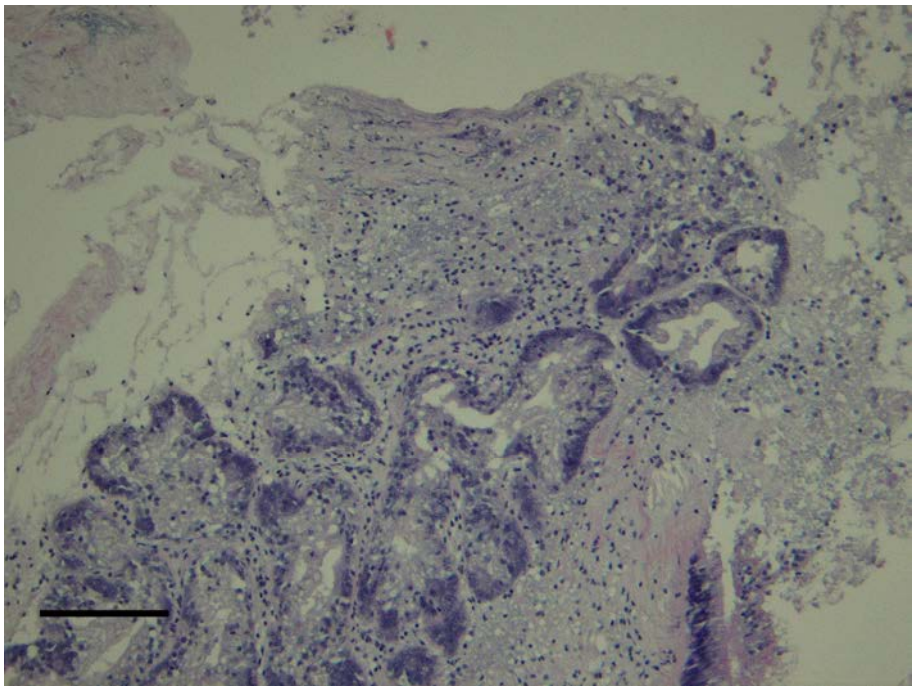

Figure 5.1.8: Two photomicrographs of the digestive gland of a pearl oyster from Giralia Bay, sampled in September 2006. The oyster contained a large inclusion of haemocytes in the tubules of the digestive gland as a result of diapedesis. In the centre of the mass of cells, three eosinophillic starburst arrangements were observed. A: The digestive tubules with a mass of cells within the lumen (20x magnification), Scale bar 80 µm. B: The starburst arrangement in the centre of the cells (40x magnification). Scale bar 40 µm.

A

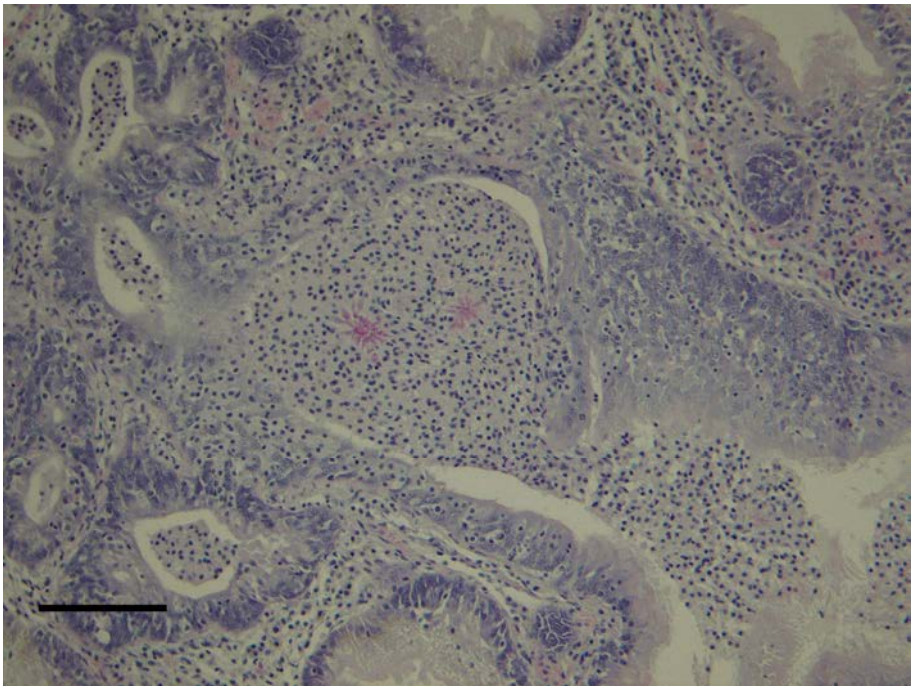

B

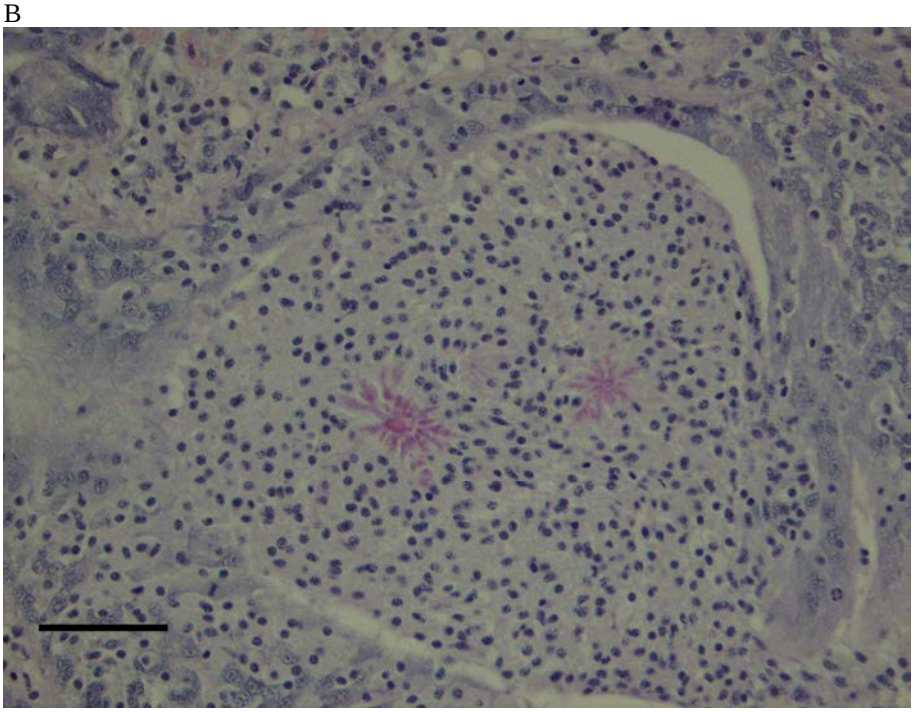

Figure 5.1.9: Two photomicrographs of the digestive gland of a pearl oyster from Giralia Bay, sampled in 2006. They contain unusual single celled organisms, approximately 5-8 µm in length in the lumen of the digestive tubule, traversing the epithelial lining of the tubules and the interstitium of the digestive gland. Their presence was associated with a moderate local haemocytic infiltrate. A: A tubule at 40x magnification, with a heavy infection of this organism, scale bar: 40 µm. B: The same tubule at 100x oil magnification, with many of the organisms, three of which have arrows pointed at them, scale bar: 20 µm.

A

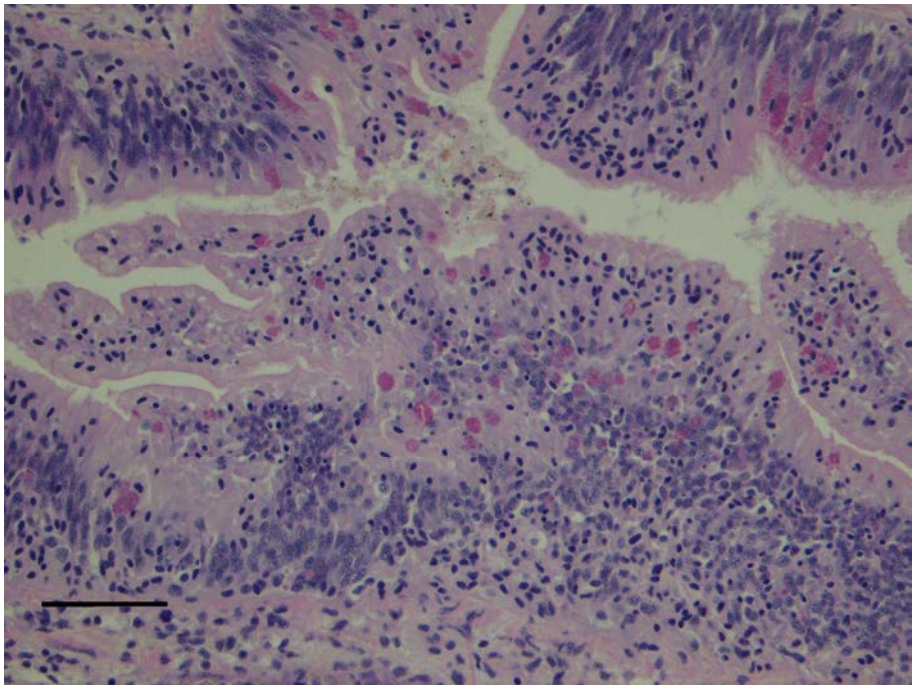

B

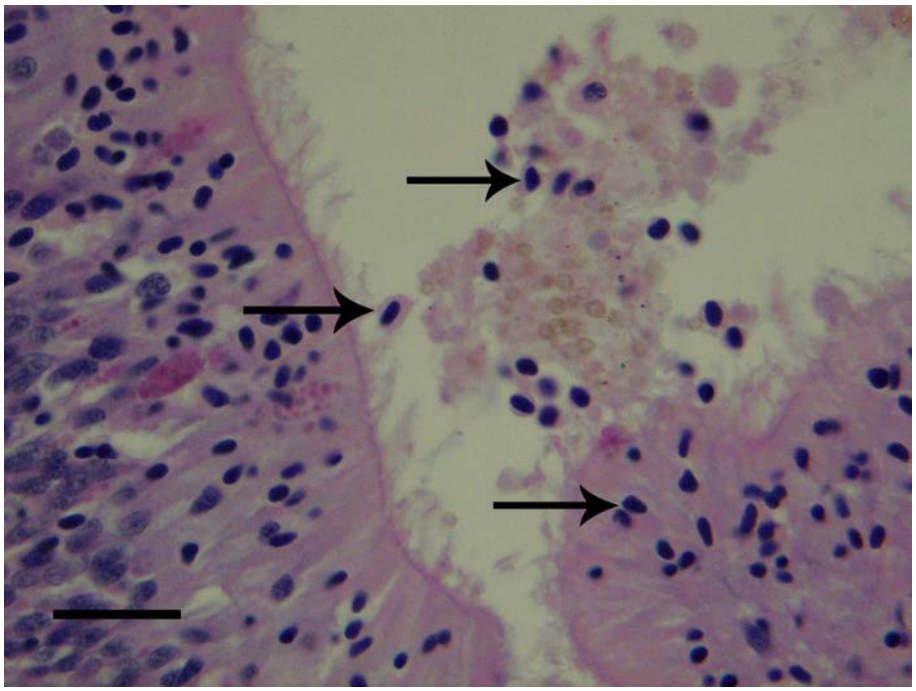

Figure 5.1.10: Box plot comparing the size of the oysters in the two groups, the oysters that were found to have abnormalities in their tissues, and those that did not and were deemed No Abnormalities Detected (NAD), corresponding to good health. The oysters included in this graph were from the September 2006 Exmouth Gulf sampling.

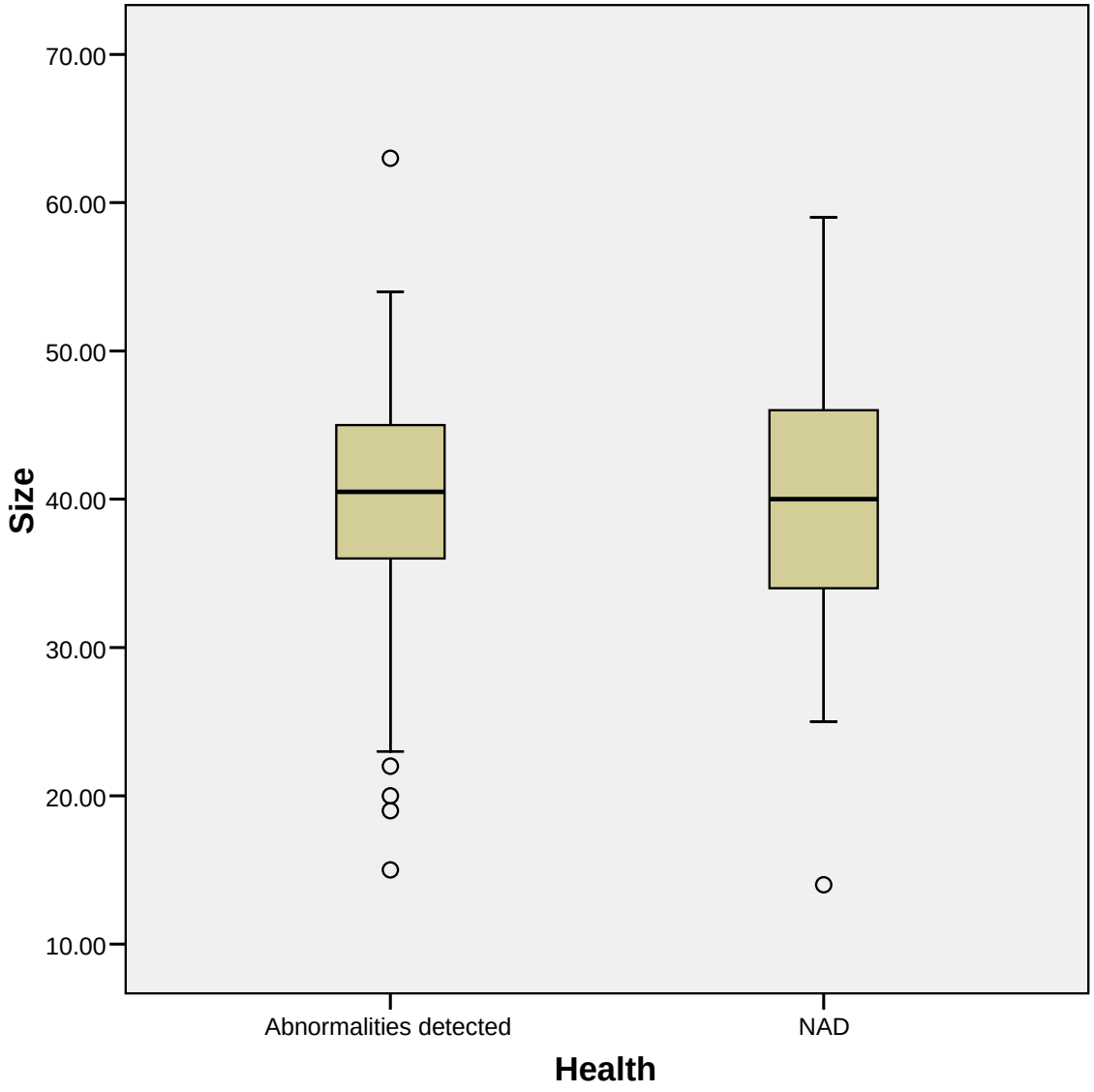

Table 5.1.2: The SPSS generated results of a Mann-Whitney U Test on the size of NAD oysters compared with those where Abnormalities were detected, from the oysters sampled from Exmouth Gulf in 2006. The Z value was -.485, with a Asymp. Sig (2-tailed) of not less than or equal to 0.05, therefore the difference between the groups is not significant.

Test September 2006: NAD oysters vs. Abnormalities Detected

	Size
Mann-Whitney U	2413.500
Wilcoxon W	3274.500
Z	-.485
Asymp. Sig. (2-tailed)	.628

a Grouping Variable: Health

abnormalities were detected, from the oysters sampled from Exmouth Gulf in 2006 produced a Z value of -.485, with an Asymp. Sig (2-tailed) of 0.26.8 Therefore the p value was not less than or equal to 0.05, indicating the difference between the groups is not significant. There was no significant difference between the sizes of the healthy oysters (NAD) and those with abnormalities detected.

Results of sampling hatchery spat from Whalebone Island, September 2006
A total of 53 oysters were viewed using microscopy from Whalebone Island. These spat were between 17 and 29 mm in size, with a mean of 22.28 and a standard deviation of 2.656 (Figure 5.1.11). All 53 were of unspecified sex, most likely immature. Of the oysters viewed, 30 contained Ancistrocomid parasites within their gut lumen. Six of these infections had extended into the digestive gland tubules. One oyster contained a metazoan parasite in the lumen of the gut. The same oyster had a multifocal haemocytic infiltrate in its digestive gland. One oyster had a pea crab in its mantle cavity. Two oysters displayed characteristics of oedema in their connective tissue, including expanded stroma and enlarged haemolymph vessels. Of the 53 oysters examined, seven displayed areas of necrosis. Four of these had focal degenerative necrotic areas, with two described as extensive. Two oysters showed a multifocal pattern of necrosis in their digestive gland, one associated with a multifocal inflammatory response, and both had concurrent Ancistrocomid infections. One oyster had focal necrosis of the epithelium of the stomach.

Figure 5.1.11: A histogram representing the size distribution of the hatchery oysters from Whalebone Island. With N=53, the mean size (in mm) was 22.28, with a standard deviation of 2.656.

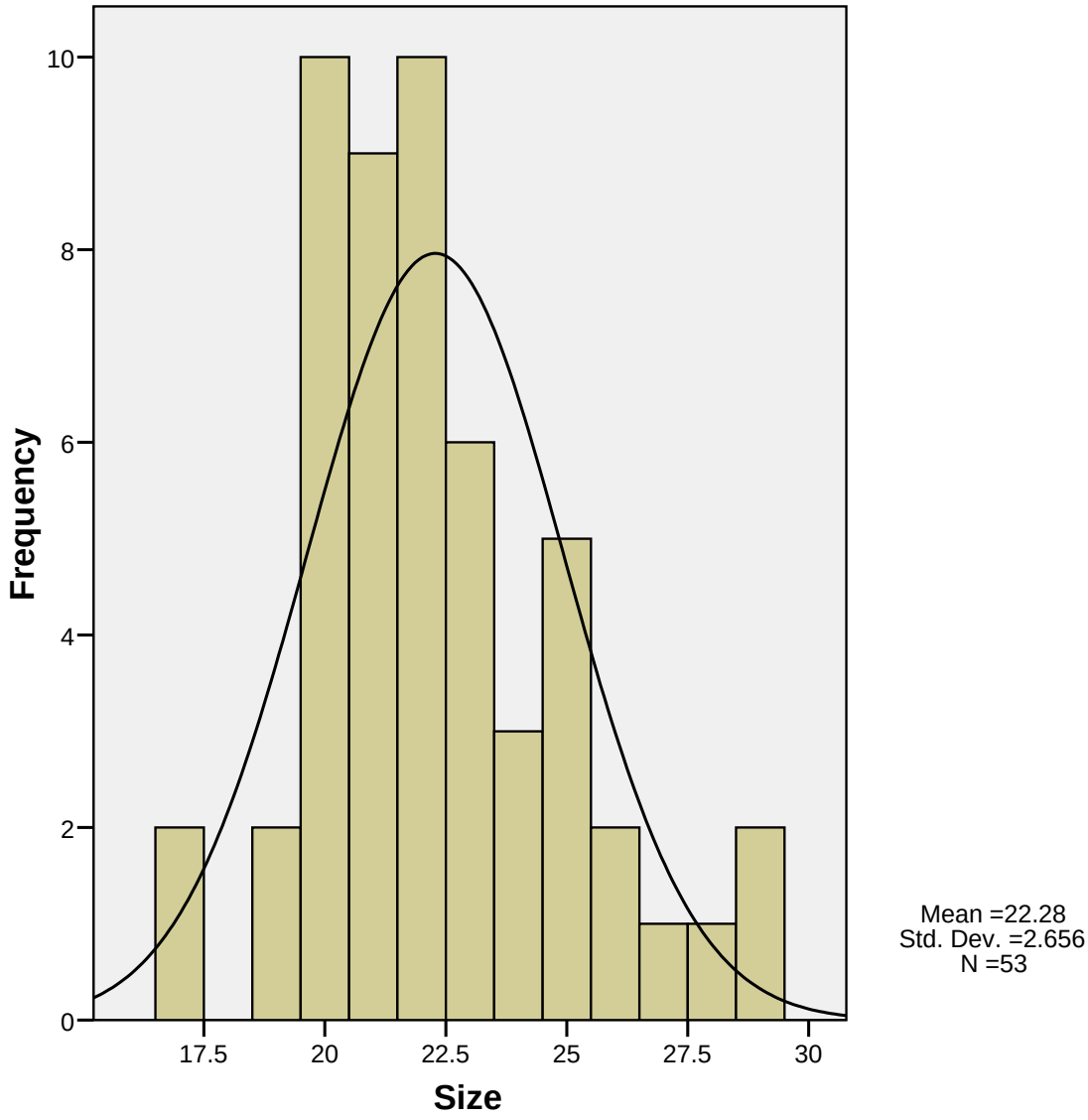

Fourteen of the 53 oysters examined displayed an increased number of haemocytes in their tissues. Three oysters had a diffuse inflammatory infiltrate in their digestive gland, one moderate and two were mild. Three oysters had an inflammatory infiltrate with a multifocal pattern in their digestive gland, two mild and one moderate. Three oysters had a focal area of mild inflammation in their digestive gland. Five oysters had an inflammatory infiltrate affecting the connective tissue surrounding their gut. Three had a mild diffuse pattern of infiltrate, one had a mild multifocal distribution and one was a moderate multifocal pattern. Three of the five oysters with inflammation surrounding their gut had a concurrent Ancistrocomid ciliate infection.

The health of the Whalebone Island spat relative to their size was plotted on a box plot graph, using SPSS. The oysters were divided into those that were found to have parasites, oedema, necrosis or inflammation, named 'Abnormalities detected', and those that no abnormalities were found in, namely 'NAD'. The mean size of oysters, based on the box plot, appear to be larger for the group with NAD, compared with those where abnormalities were detected (Figure 5.1.12). To test this hypothesis, a Mann-Whitney U test was performed, using SPSS. The Asymp. Sig (2-tailed) was 0.034 (less than 0.05), therefore the difference between the groups is significant (Table 5.1.3). It supports the hypothesis that the healthy oysters (with NAD) were significantly larger than the oysters with abnormalities.

Results of sampling from Exmouth Gulf in May 2007, Line 1 Gales Bay B
Pearl oyster spat were sampled from Line 1, Gales Bay B, with sizes ranging between 12 – 38 mm in size (n=20). Figure 5.1.13 is an histogram of the size distribution from Line 1, showing the mean as 27.4 mm, with a standard deviation of 6.369. All 20 were of unspecified sex, or likely immature. One oyster contained the bizarre ovoid single-celled organisms describe previously in Figure 5.1.9. Two of these oysters contained Rickettsial-like bodies in the digestive gland epithelial cells. One of these was associated with a moderate diffuse inflammatory infiltrate of the digestive gland. The bodies were intensely basophilic ovoid bodies, approximately 30 – 50 µm in size, within the cytoplasm of digestive gland cells.

Figure 5.1.12: The health of the Whalebone Island spat relative to their size. The size of the oysters based on the box plot appear to be larger for the group with NAD, compared with those where abnormalities were detected.

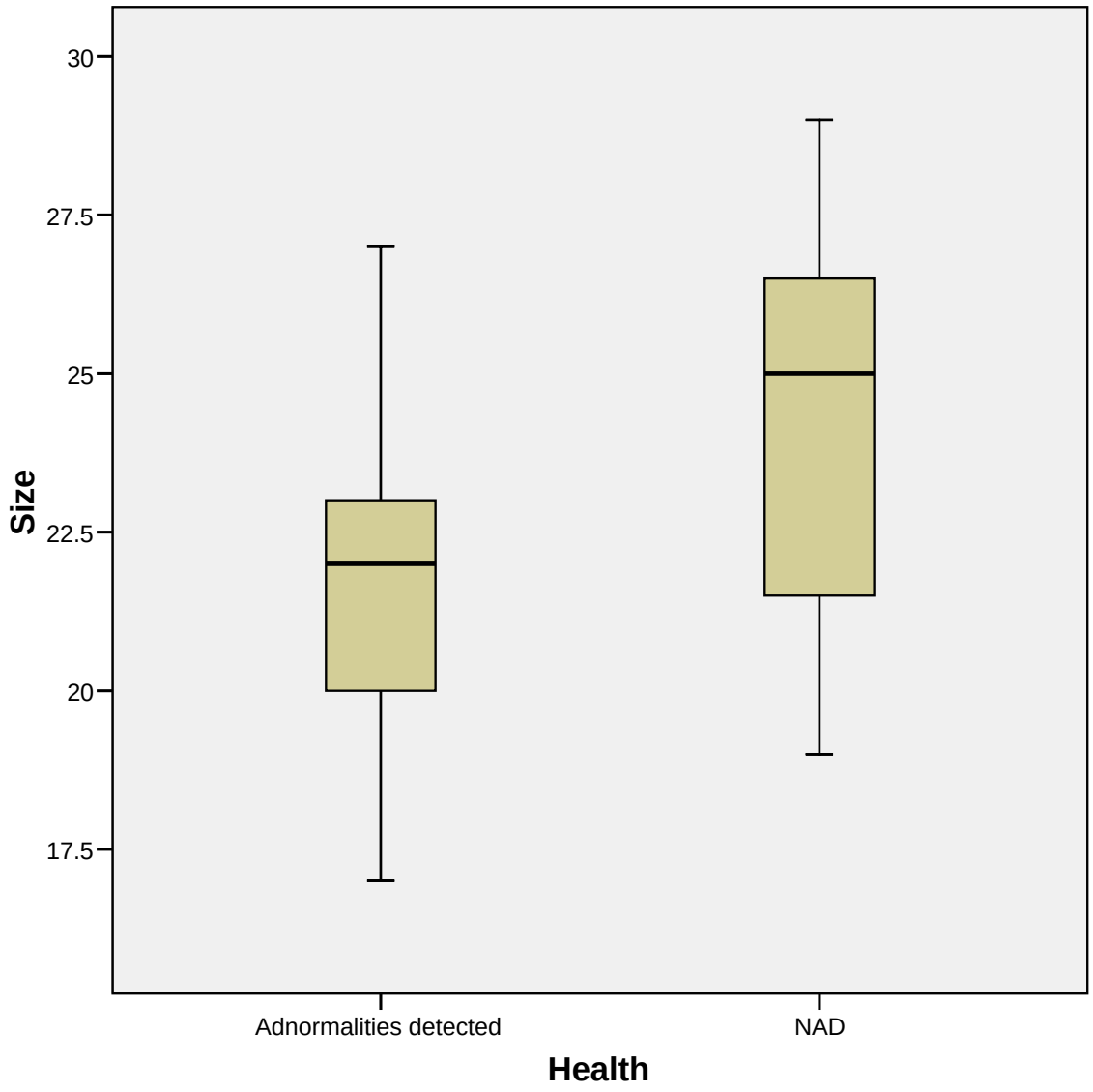

Table 5.1.3: A Mann-Whitney U test using SPSS. The sizes of the oysters that were found to have abnormalities were compared with those that were deemed NAD. The Asymp. Sig (2-tailed) was less than 0.05, therefore the difference between the groups is significant. The healthy oysters (with NAD) were significantly larger than the oysters with abnormalities.

Test Whalebone spat September 2006: NAD oysters vs. Abnormalities Detected

	Size
Mann-Whitney U	135.500
Wilcoxon W	1038.500
Z	-2.116
Asymp. Sig. (2-tailed)	.034

a Grouping Variable: Health

One oyster contained a metazoan parasite in the interstitium of the digestive gland. This was associated with a focal infiltrate of haemocytes. Five oysters had a mild to moderate diffuse infiltrate of haemocytes in the digestive gland. One was associated with digestive cells containing vacuoles of eosinophilic material, approximately 5-10µm in size. One was associated with an infection of Rickettsial-like bodies. One oyster displayed a loss of epithelia on its palps. There was also a concurrent inflammation of the digestive gland of the same animal. One oyster had a thinning and loss of epithelium around adductor muscle. This oyster also had a concurrent moderate diffuse inflammation of the digestive gland. Three of the 20 oysters sampled had focal degenerative necrosis of the digestive gland. One of these had a concurrent diffuse inflammatory infiltrate around the gut.

Results of sampling from Exmouth Gulf in May 2007, Bottom Line, Gales Bay B
In May 2007 30 pearl oysters were sampled from the Bottom line, Gales Bay B. 17 of these were males, the others unspecified sex. They were all between 50mm and 100 mm in size, with a mean of 78.17 and a standard deviation of 12.069 (Figure 5.1.14). Three oysters contained gregarine bodies in their digestive glands. One of these with a moderate diffuse inflammatory infiltrate in the digestive gland. Eight had Ancistrocomid ciliates in their digestive tract, four of which had infiltrated into the digestive gland tubules. Five oysters that contained Ancistrocomid ciliates did not have any concurrent inflammation within their bodies. Two oysters contained metazoan parasites. One of these parasites were located in the mantle connective tissue, encapsulated in a granuloma. Another was located in the lumen of the oesophagus and was not associated with any host response. Of the 30 oysters examined, seven contained focal areas of necrosis in the digestive gland. These were characterised by epithelial sloughing,

Figure 5.1.13: An histogram of the size distribution in millimetres from Line 1. The mean is 27.4 mm, with a standard deviation of 6.369.

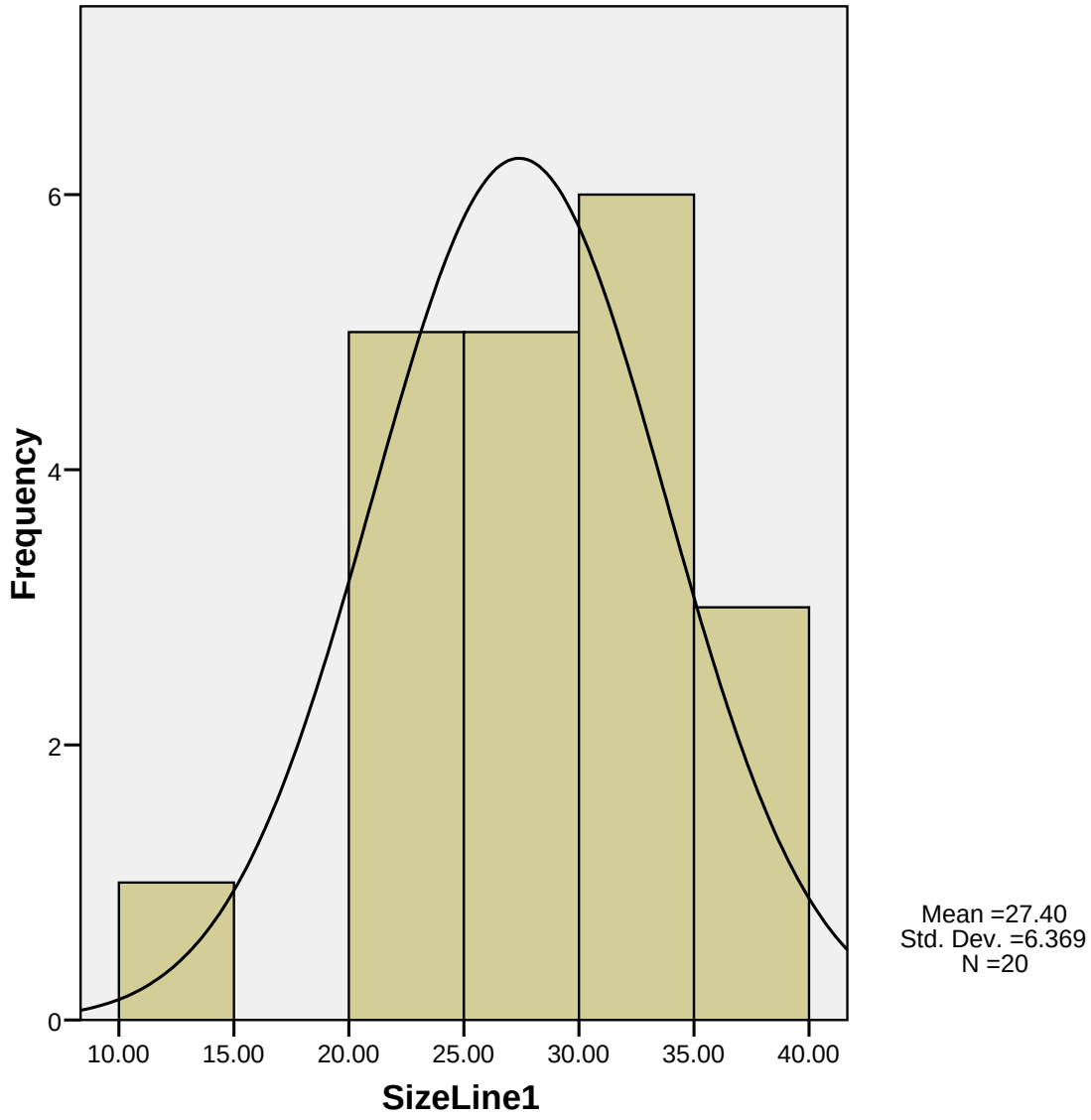

Figure 5.1.14: An histogram of the size distribution from the Bottom Line in millimetres, sampled May 2007. The mean was 78.17 with a standard deviation of 12.069.

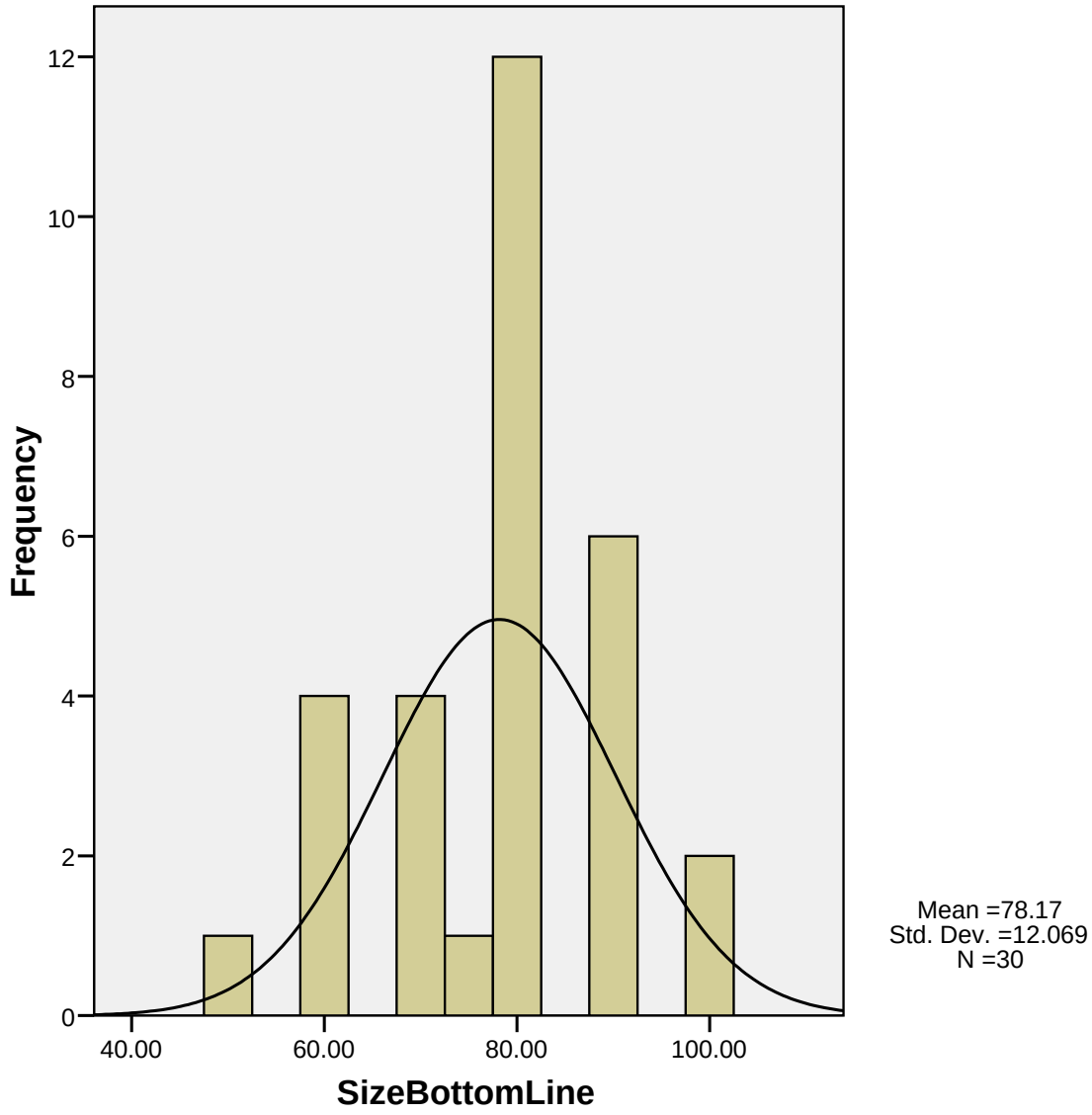

Figure 5.1.15: Two photomicrographs of a pearl oyster from the Bottom Line, sampled May 2007. A: The mantle epithelium of a pearl oyster with expanded haemolymph vessels and connective tissue stroma. The mantle epithelium was disrupted with vacuolation and separation along the basal lamina. B: The gut epithelium of the same animal, also displaying enlarged haemolymph vessels, connective tissue expansion and vacuolar changes in the epithelial cells. Scale bars: 40 µm

A

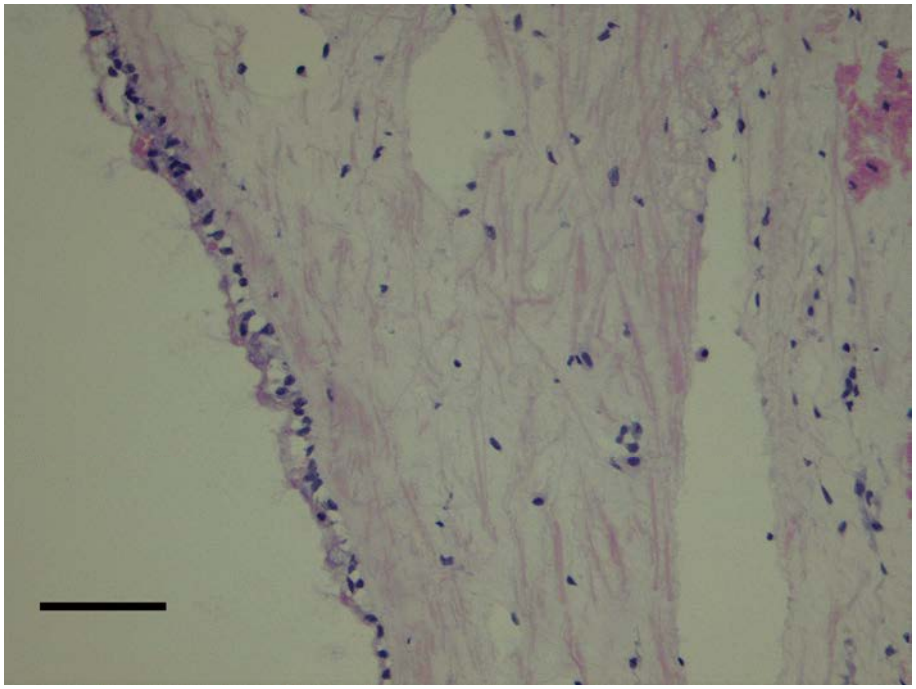

B

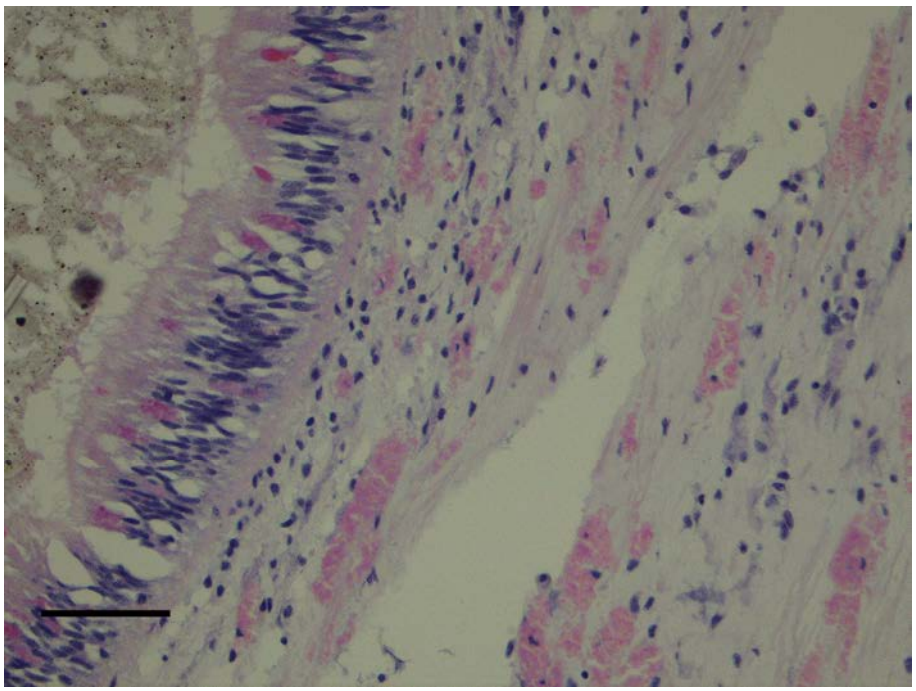

pyknotic nuclei and vacuolated cytoplasm. One also had necrosis of the oesophagus epithelium. Three oysters showed evidence of oedema, with expanded haemolymph vessels and connective tissue stroma. Two also had concurrent loss of epithelia of the mantle. Loss of epithelia in other parts of the oyster was a characteristic found in six other individuals. Figure 5.1.15 A depicts the mantle epithelium of a pearl oyster sampled from the Bottom Line. The haemolymph vessels were markedly expanded, as was the connective tissue stroma of the surrounding area. The mantle epithelium appeared disrupted with vacuolation and separation along the basal lamina. Figure 5.1.15 B is the gut epithelium of the same animal, also displaying enlarged haemolymph vessels, connective tissue expansion and vacuolar changes in the epithelial cells.

The oysters from Line 1 and the Bottom line were combined for statistical analysis. The oysters were then grouped into the parasites that were found in their tissues. These included a group for Gregarine bodies, a group for Ancistrocomids, a group for Rickettsial bodies, a group for other abnormalities (such as inflammation of unknown causes and metazoan parasites), and those that were NAD. Figure 5.1.16 is a box plot comparing the sizes of oysters affected by different parasites. The oysters containing the Ancistrocomid and the Gregarine parasites had a higher mean size, at close to 80mm, compared to the other groups. The oysters found with Rickettsial bodies within their digestive gland have a significantly smaller mean size, at around 25mm. The oysters that contained other abnormalities had an average size around 60mm, and the oysters that contained no abnormalities had a mean of approximately 30mm. This may indicate the smaller oysters are more susceptible to an infection of Rickettsial bodies, compared to larger oysters.

Combined pearl oyster survey for analysis

All oyster from the field trials were combined and analysed. The size distribution of the oysters in all the field trials combined (in mm) was plotted on a histogram. The mean was 39.8mm with a standard deviation of 17.139 (Figure 5.1.17). The sizes of the males and the oysters of unspecified sex were compared using a box plot (Figure 5.1.18). From the box plot, the males appear to have a higher mean than the unspecified sex, indicating the unspecified sex oysters may be sexually immature. To check this hypothesis, a Mann-Whitney test was performed using SPSS, and the output is displayed in Table 5.1.4. The test gave a p value of less than 0.05, and therefore the sizes of the males compared with the oysters of unspecified sex were significantly different. The males are significantly larger than the oysters that did not have mature gonads on histological examination.

Figure 5.1.16: A box plot comparing the sizes of oysters affected by different parasites. The oysters containing the Ancistrocomid and the Gregarine parasites have a higher mean size, at close to 80 mm, compared to the other groups. The oysters found with Rickettsial bodies within their digestive gland have the smallest mean size, at around 25 mm. The oysters that contained other abnormalities had an average size around 60 mm, and the oysters that contained no abnormalities had a mean of approximately 30 mm.

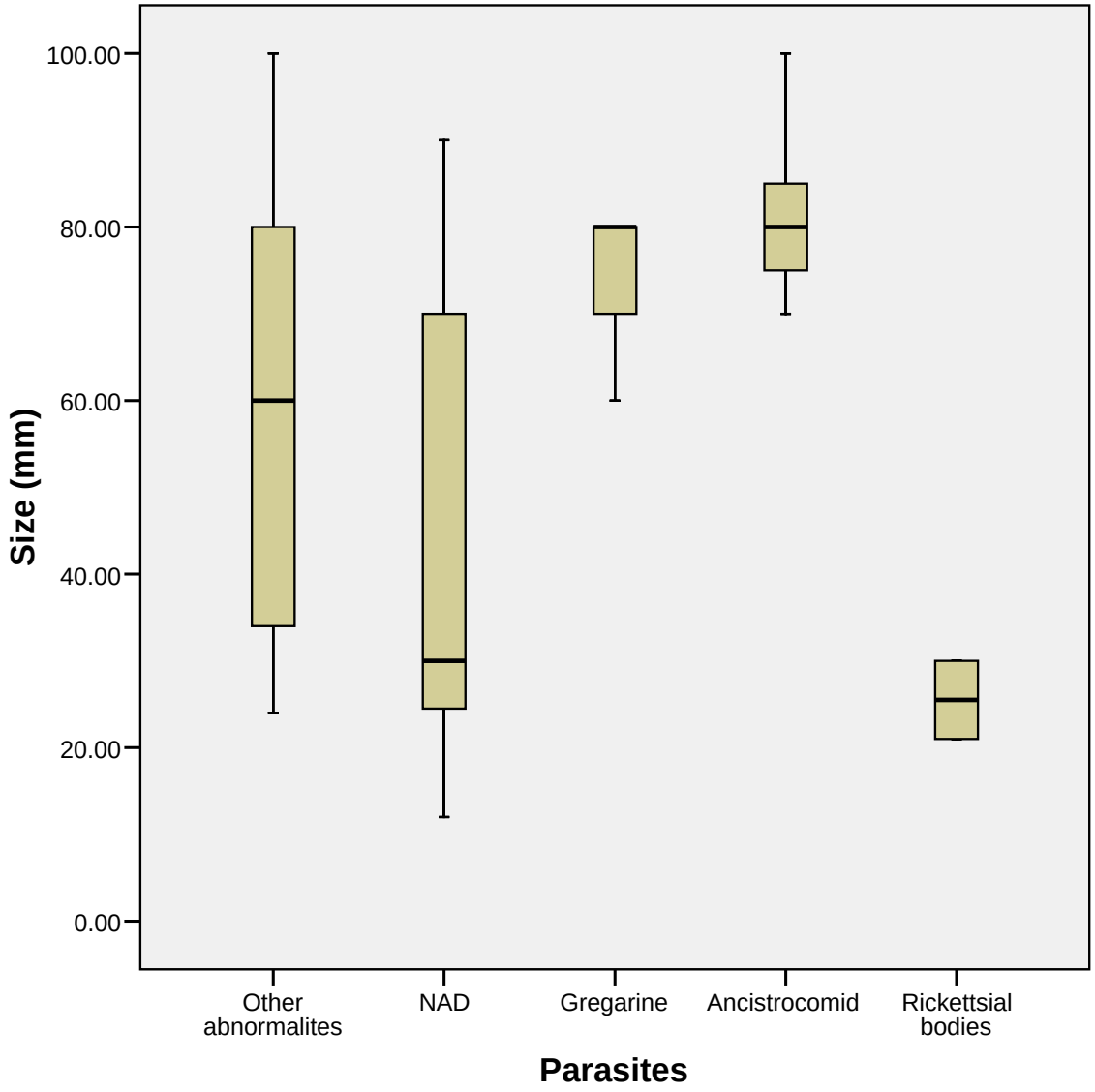

Figure 5.1.17: Size distribution of the oysters in all the field trials combined (in mm). The mean is 39.8mm with a standard deviation of 17.139.

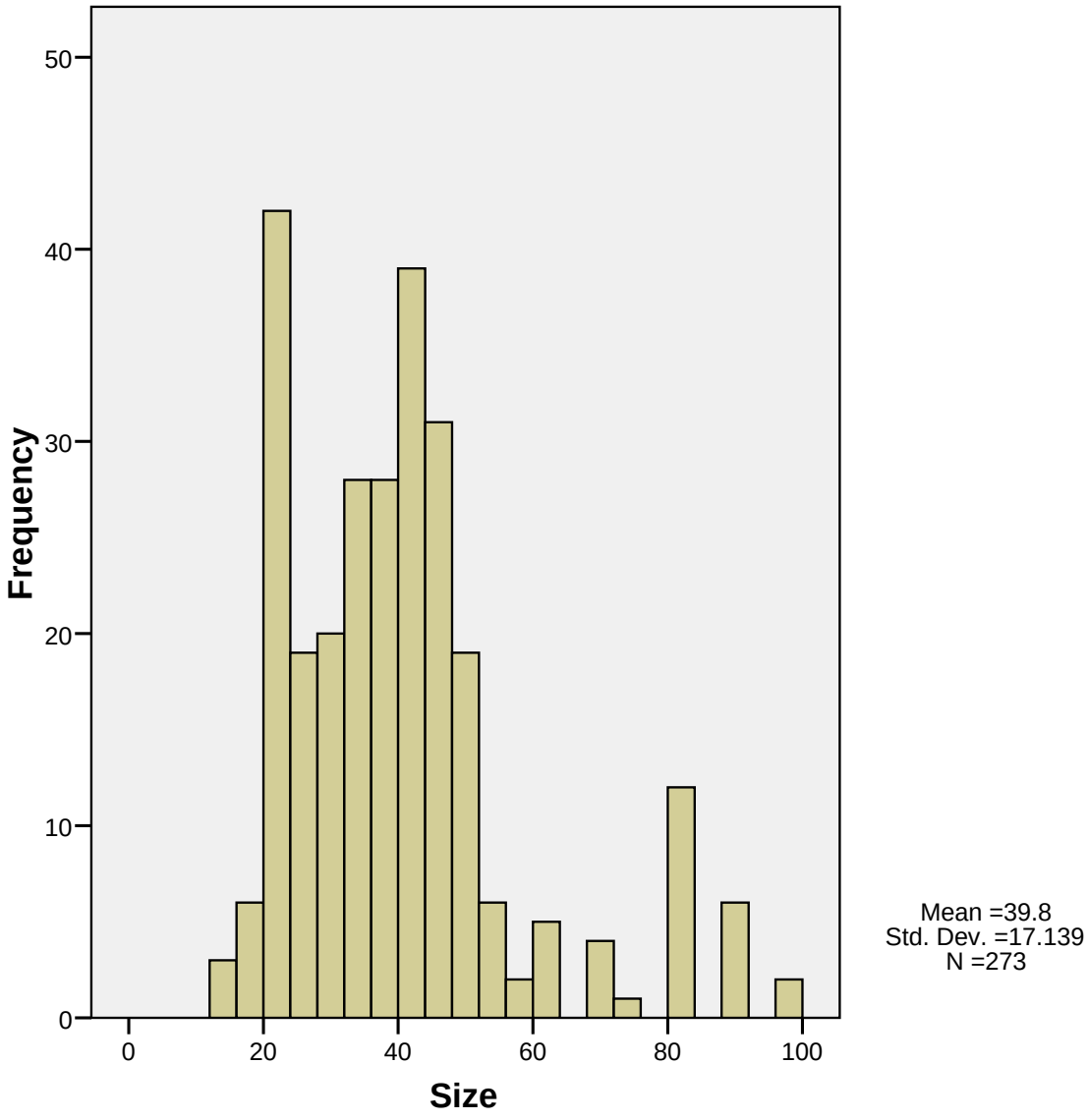

Figure 5.1.18: A box plot comparing the sizes of the males and the oysters of unspecified sex. From the box plot, the males appear to have a higher mean than the unspecified sex, indicating the unspecified sex oysters may be sexually immature.

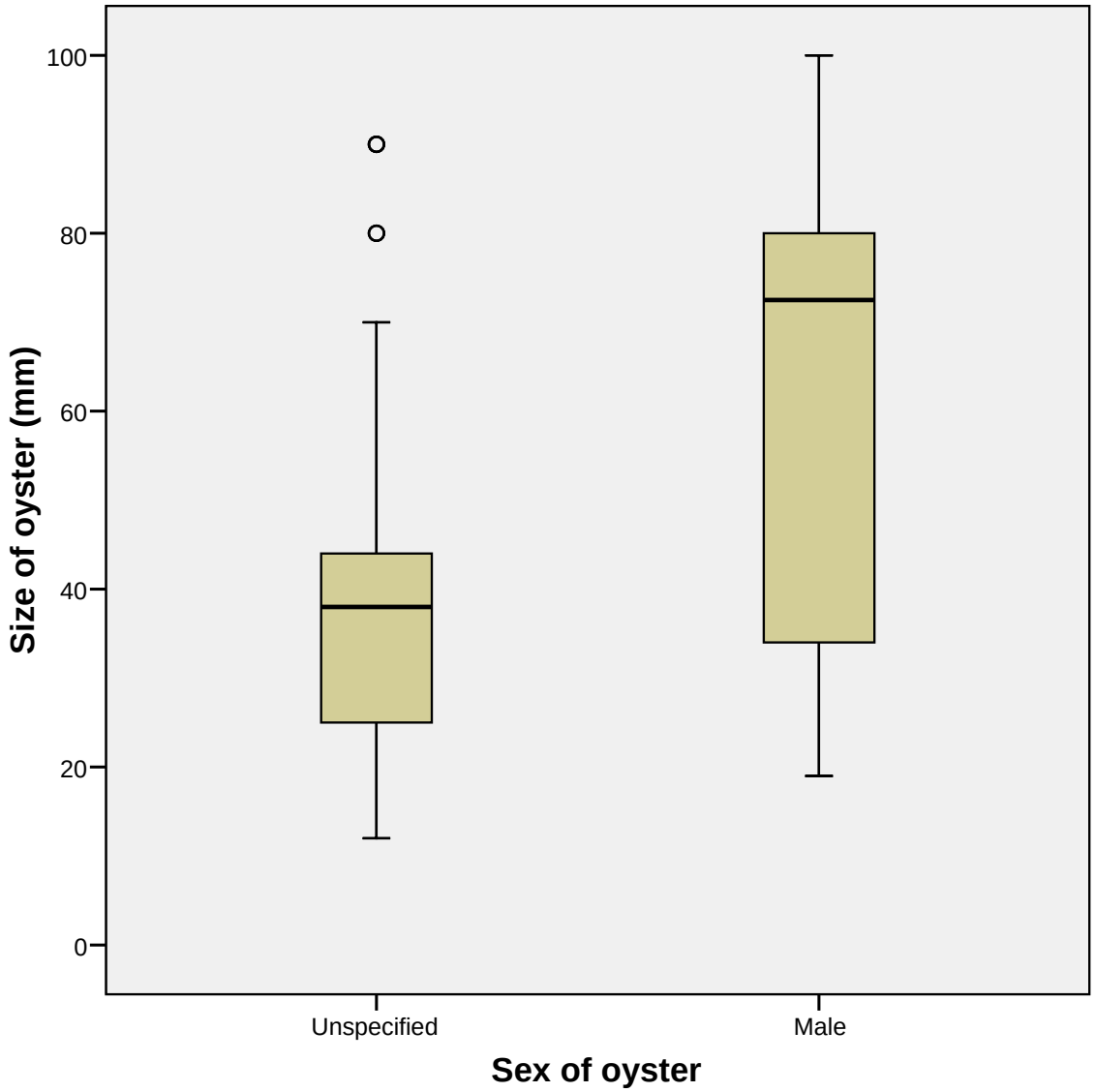

Similarly to what was performed on the oysters from Exmouth Gulf in May 2007, the oysters were grouped into the parasites that were found in their tissues. These included a group for Gregarine bodies, a group for Ancistrocomids, a group for those oysters infected with both Ancistrocomids and Gregarine bodies, a group for Rickettsial bodies, a group for other abnormalities (such as inflammation of unknown causes and metazoan parasites), and those that were NAD. Figure 5.1.19 is a box plot depicting the results of comparing the sizes of the oysters in each of these groups. From the box plot, the oysters with Rickettsial bodies appeared to have a smaller mean than the other groups. The group of oysters affected with Gregarine bodies appeared to have a larger mean size compared with the others. A Kruskal Wallis test was performed, using SPSS, to determine whether there was a significance difference in the sizes of the oysters affected by the different parasite groups (Table 5.1.5). The significance level was valued at 0.002, which is less than 0.05, therefore indicating there was a significant difference between the groups. From the ranking, the mean size of the oysters infected with the Rickettsial bodies was significantly lower, at a rank value of 54.25, than the oysters affected by other parasites. The second smallest sized group were the oysters that were infected with Ancistrocomid ciliates, with a value of 111.78, while the largest oysters were affected by the Gregarine bodies, at 165.43, as the box plot suggested.

Table 5.1.4: The Mann-Whitney test output, as generated by SPSS gave a p value of less than 0.05, and therefore the differences in size between the males and the unspecified sex oysters was significant.

Test comparing relative sizes of Males and those of Unspecified sex

	Size
Mann-Whitney U	1868.500
Wilcoxon W	32003.500
Z	-3.948
Asymp. Sig. (2-tailed)	.000

a Grouping Variable: Sex

Figure 5.1.19: A box plot depicting the sizes of the oysters that were affected by various parasites.

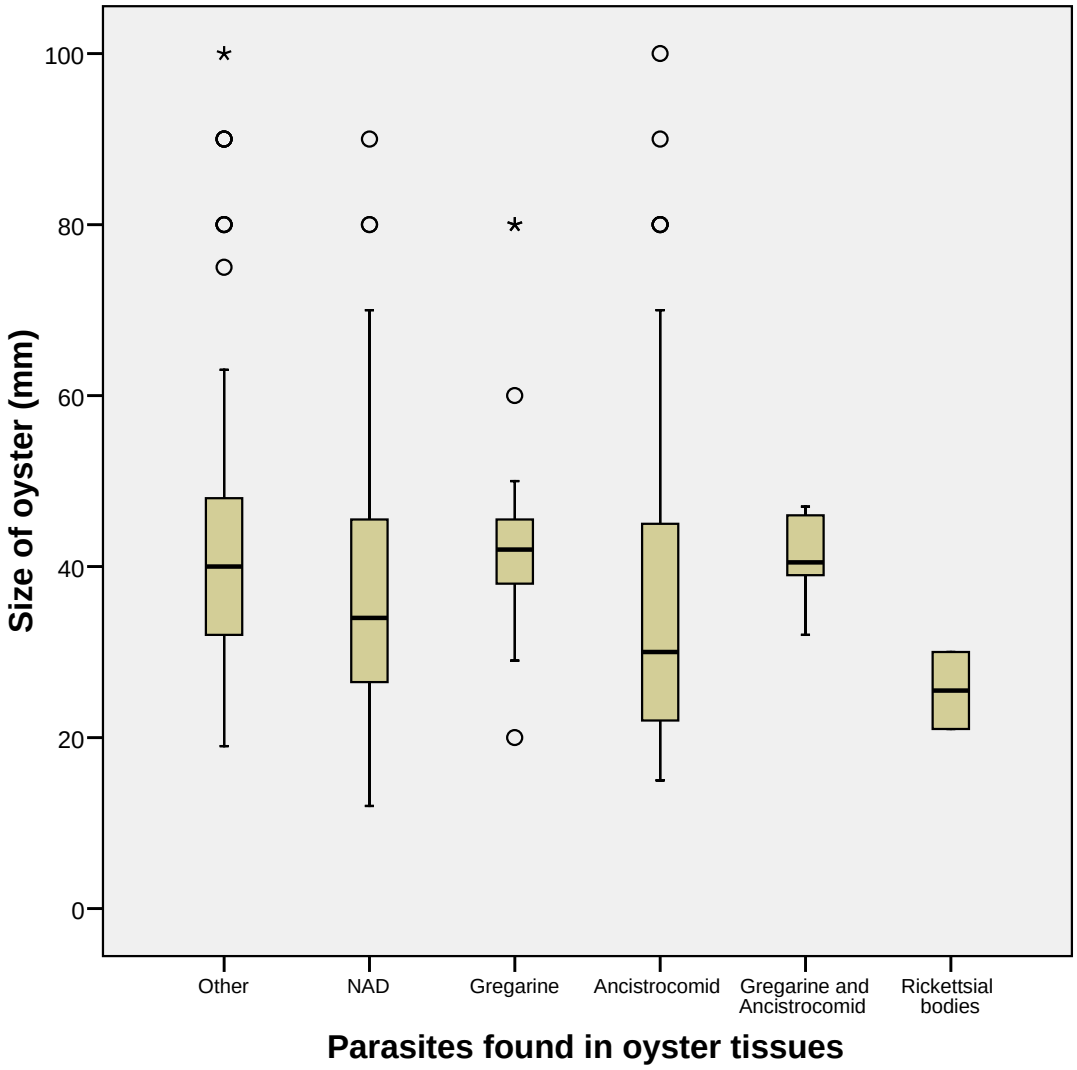

Table 5.1.5: An SPSS output table of a Kruskal Wallis test determining whether there is a significance difference in the sizes of the oysters affected by the different parasite groups. The significance level was valued at 0.002, which is less than 0.05, therefore indicating there is a significant difference between the groups. From the ranking, the mean size of the oysters infected with the Rickettsial bodies is significantly lower than the oysters affected by other parasites. The second smallest sized group were the oysters that were affected by the Ancistrocomids, while the largest were affected by Gregarine bodies.

Test to compare the sizes of oysters affected by various parasites

	Size
Chi-Square	18.801
df	5
Asymp. Sig.	.002

a Kruskal Wallis Test

b Grouping Variable: Parasites

Ranks

	Parasites	N	Mean Rank
Size	Other	93	152.05
	NAD	71	126.21
	Gregarine	36	165.43
	Ancistrocomid	65	111.78
	Gregarine and Ancistrocomid	6	161.58
	Rickettsial bodies	2	54.25
	Total	273	

5.1.4 Discussion

A total of 284 oysters were examined as part of the survey, from previously infected sites in the Montebello Islands and Exmouth Gulf. One new organism was observed inhabiting the digestive gland of two oysters from Giralia Bay, sampled in September 2006 and one oyster sampled from Gales Bay Line 1 in May 2007. This invasive protozoal parasite has not previously been reported in pearl oysters in Western Australia.

The parasite populations of each of the batches of oysters sampled varied considerably. The prevalences of oysters infected with the most common parasites were tabulated in Table 5.1.6. The most common parasite encountered were the Ancistrocomid ciliates. The hatchery spat from Whalebone Island recorded the highest prevalence of this parasite with 57% of the oysters examined displaying this infection. This was in contrast to the oysters from Line 1 Gales Bay, where no Ancistrocomid ciliates were found. This ciliate has not been reported to cause any pathology, so is considered a commensal. It is unknown why the hatchery-reared spat from Whalebone Island had such a considerably higher infection compared with the oysters from Gales Bay.

Rickettsial bodies were only observed in oysters from Line 1 Gales Bay, and invasive bacteria were only observed in oysters from Giralia Bay. No intracellular ciliates were observed during the survey of the pearl oysters. Cyclonic activity in the area limited the ability to sample spat at regular intervals, and this may have contributed to the failure to find the ciliate. It is also possible the number of oysters sampled at some sites, such as Montebello Islands and Gales Bay Line 1, was not sufficient to detect an infection of very low prevalence. Despite the enormous support and assistance provided by members of the pearling industry, financial and logistical constraints sometimes inhibited ideal scientific sampling.

5.2 Reliability of histological examination for the detection of intracellular ciliates in the digestive gland of pearl oysters

5.2.1 Introduction

Histology is widely used in aquaculture as an effective and reliable method of disease surveillance (Diggles, Cochennec-Laureau et al. 2003). During routine health surveillance of the Western Australian pearling industry in 2001, a novel intracellular ciliate was discovered (Jones and Creeper 2006). Since this parasite has not yet been characterised or taxonomically assigned, histopathological examination provides the only method for detecting its presence in pearl oyster stock.

Table 5.1.6: Table of combined results of the pearl oyster field trials, the different locations and a summary of the most common parasites found on examination.

Location (date)	Montebello Is. (Jul 05)	Giralia Bay A (Sept 06)	Whalebone Is. (Sept 06)	Gales Bay Line 1 (May 07)	Gales Bay Bottom Line (May 07)	Total (%)
number of oysters examined	n=16 (%)	n=165 (%)	n=53 (%)	n=20 (%)	n=30 (%)	n=284 (100%)
Ancistrocomid-like ciliates	1 (6%)	35 (21%)	30 (**57%**)	0 (0%)	8 (27%)	74 (26%)
Gregarine bodies	3 (19%)	37 (**22%**)	0 (0%)	0 (0%)	3 (10%)	43 (15%)
Metazoan parasites	2 (**13%)**	14 (8%)	1 (2%)	1 (5%)	2 (7%)	20 (7%)
Rickettsial bodies	0 (0%)	0 (0%)	0 (0%)	2 (**10%**)	0 (0%)	2 (<1%)
Invasive bacteria	0 (0%)	12 (**7%**)	0 (0%)	0 (0%)	0 (0%)	12 (4%)
Oedematous changes	0 (0%)	0 (0%)	2 (4%)	0 (0%)	3 (**10%**)	5 (2%)
Single celled organism	0 (0%)	2 (1%)	0 (0%)	1 (**5%**)	0 (0%)	3 (1%)
Totals	6 (38%)	100 (60%)	33 (62%)	4 (20%)	16 (53%)	159 (56%)

Percentages were rounded to the nearest whole number, the highest percentage for each parasite in bold.

In this investigation, we assessed the limits of detection of histology as a means to detect and diagnose infections of an intracellular ciliate using archival oysters collected during the initial outbreak of the parasite in 2001. The sensitivity and negative predictive value of histological examination were calculated using serial sections through the digestive gland of oysters in an at-risk population. We also discussed the implications of these findings on the reliability of routine health monitoring using histology.

5.2.2 Materials and Methods

1. Source of oysters from an at-risk population

Archived formalin fixed, paraffin embedded tissues where available for histological examination from the Dept of Fisheries as part of ongoing surveillance health monitoring of the Western Australian pearl oyster industry. For the purpose of analysing the sensitivity of histology as a diagnostic tool, a population of oysters with the disease were selected to contribute to the study (Figure 5.2.1). These oysters were part of the initial outbreak of the parasite during 2001. From the oysters collected during the outbreak, 300 were selected at random and analysed for the presence of the ciliate. 143 of the 300 were positive for the ciliate, and of these

oysters, 10 that were negative for the ciliate on histological examination and displayed a diffuse inflammatory infiltrate throughout their digestive gland were randomly selected and included in the study, and named Group A. These oysters were screened to rule out any other obvious aetiology causing the inflammation. Another group of 7 oysters that were negative for the ciliate on histological examination and displayed no inflammatory response were included also. These were named Group B. There were only 7 oysters with these characteristics within the population of 143 oysters positive for the ciliate. Once the 17 oysters were chosen, 5 serial sections were cut, in addition to the original section, and routinely stained with haematoxylin and eosin. These were analysed using an Olympus BH-2 microscope at Murdoch University.

Figure 5.2.1: Outline of the process by which at-risk oysters were selected for the study.

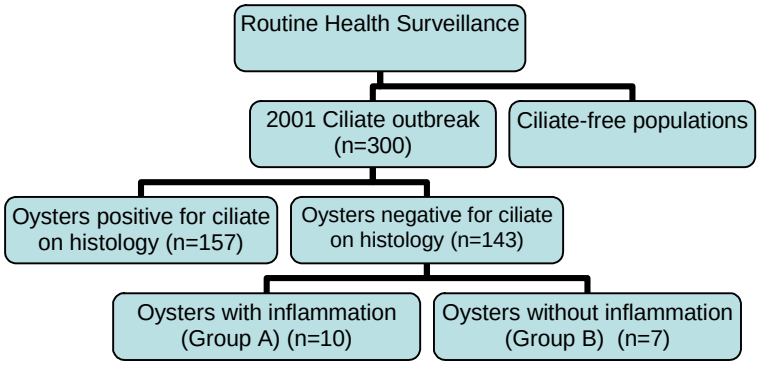

2. Analysis of histological sections for the presence of the ciliate and inflammation
The 5 serial sections and the original section of individual oysters were examined microscopically for inflammatory infiltrate in the digestive gland and the presence of intracellular ciliates. For the purpose of this investigation, oysters that were negative for the ciliate on the original section plus all five serial sections were deemed a 'true negative'. In addition, if a single ciliate was found on any one of the sections, this oyster was considered a 'true positive'. Due to the characteristic shape and size of the intracellular ciliate, the presence of a single ciliate in the cytoplasm of a digestive cell was confirmation of a positive diagnosis.

5.2.3 Results

1. Oysters with inflammation and negative for ciliate on original section (Group A)
The original histological section and five serial sections were analysed for the presence of inflammation and ciliates in the digestive gland (Table 5.2.1). This table displays the results of the analysis of the original section and five serial sections for

each of the ten oysters. The presence of ciliates and inflammation were recorded as a POS for positive and a NEG for negative. Once all the serial sections had been analysed, the oyster was then given a TRUE Status as a POS if one or more sections were found to have the ciliate (later referred to as 'true positive') and a NEG if none of the sections contained ciliates (later referred to as 'true negative').

The sensitivity of the histological analysis was 50%, with a Negative Predictive Value (NPV) of 66.7% (Table 5.2.2). Due to the nature of the parameters set out above, the specificity and Positive Predictive Value (PPV) was 100%. Of the ten oysters chosen for analysis, 50% were subsequently deemed 'true positive' on serial sections, due to the presence of at least one ciliate in the digestive cells. Within the first serial section being analysed, three out of the five oysters deemed 'true positives' were already exhibiting a positive result. One of the truly diseased oysters were found to be positive on the third serial section and another on the fifth serial section. Subsequently, if the oyster was still negative by the second serial section, there was a 71% chance it was a 'true negative'. Of the 'true negative' oysters, two of the five were free of inflammation on all 5 serial sections.

2. Oysters without inflammation or ciliates on original section (Group B)
Once the original and five serial sections of the seven chosen oysters were analysed, four remained 'true negatives' (Table 5.2.3). The sensitivity of the histological analysis on inflammation-free oysters was calculated at 38.9%, with an NPV of 68.6% (Table 5.2.4). Of the oysters discovered to have infections, two out of the three were found to have ciliates on the first serial section, and the remaining oyster was found to have ciliates on the second serial section. Subsequently, if an oyster was still negative for the presence of the ciliate by the first serial section, it is four times more likely to remain ciliate-free and be deemed 'true negative' after five serial sections are analysed. All oysters selected for their inflammation free status on their original sections remained negative for inflammation, despite some being positive for the parasite.

5.2.4 Discussion

Histology is a widely used screening tool for the general health of aquatic animals (Elston 1996), including the silver lipped pearl oyster. It enables the industry and government bodies to maintain a close watch on the disease status of the aquaculture industry, and discover outbreaks of disease early so effective management procedures can limit the spread of such diseases. As part of this routine health monitoring, health certificates must be obtained before some movements of pearl oysters can occur along the north western coast of Australia. The consequences in the past regarding the inadvertent translocation of pathogens for diseases such as withering syndrome in abalone (Friedman and Finley 2003), bonamiosis in the flat oyster, (Elston 1996), and infectious pancreatic necrosis in rainbow trout (Yoshimizu 1996) have solidified the importance of ruling out disease prior to transport.

Table 5.2.1. The histological analysis of the original sections and 5 serial sections of individual oysters negative for the ciliate and positive for inflammation on the original section.

Section	0 (original)		1		2		3		4		5		TRUE
Oyster	Inflam	Ciliate	Inflam	Ciliate	Inflam	Ciliate	Inflam	Ciliate	Inflam	Ciliate	Inflam	Ciliate	Status
1	POS	NEG	POS	POS	POS	NEG	POS	NEG	POS	POS	POS	POS	POS
2	POS	NEG	POS	NEG	POS	NEG	POS	POS	POS	POS	POS	POS	POS
3	POS	NEG	POS	NEG	NEG	NEG	POS	NEG	POS	NEG	POS	NEG	NEG
4	POS	NEG	POS	POS	POS	NEG	POS	NEG	POS	POS	POS	POS	POS
5	POS	NEG	NEG	NEG	NEG	NEG	NEG	NEG	NEG	NEG	NEG	NEG	NEG
6	POS	NEG	NEG	NEG	NEG	NEG	NEG	NEG	NEG	NEG	NEG	NEG	NEG
7	POS	NEG	POS	POS	POS	POS	POS	POS	POS	POS	POS	POS	POS
8	POS	NEG	POS	NEG	POS	NEG	POS	NEG	POS	NEG	POS	NEG	NEG
9	POS	NEG	POS	NEG	POS	NEG	POS	NEG	POS	NEG	POS	POS	POS
10	POS	NEG	POS	NEG	POS	NEG	POS	NEG	POS	NEG	POS	NEG	NEG

Table 5.2.2: The tabled data from the raw observations from Table 5.2.1 indicating the calculated sensitivity, specificity and the predictive values for the histology diagnosis of a ciliate infection in inflamed oysters within an at-risk population.

	TRUE POSITIVE	TRUE NEGATIVE	Totals	Sensitivity (%)	Specificity (%)	PPV (%)	NPV (%)
Section POSITIVE	15	0	15	50	100	100	66.67
Section NEGATIVE	15	30	45				
Totals	30	30	60				

Table 5.2.3. The histological analysis of the original sections and 5 serial sections of individual oysters negative for the ciliate and inflammation on the original section.

Section	0 (original)		1		2		3		4		5		TRUE
Oyster	Inflam	Ciliate	Inflam	Ciliate	Inflam	Ciliate	Inflam	Ciliate	Inflam	Ciliate	Inflam	Ciliate	Status
1	NEG	NEG	NEG	NEG	NEG	NEG	NEG	NEG	NEG	NEG	NEG	NEG	NEG
2	NEG	NEG	NEG	POS	NEG	POS	NEG	NEG	NEG	POS	NEG	NEG	POS
3	NEG	NEG	NEG	NEG	NEG	NEG	NEG	NEG	NEG	NEG	NEG	NEG	NEG
4	NEG	NEG	NEG	NEG	NEG	NEG	NEG	NEG	NEG	NEG	NEG	NEG	NEG
5	NEG	NEG	NEG	NEG	NEG	NEG	NEG	NEG	NEG	NEG	NEG	NEG	NEG
6	NEG	NEG	NEG	NEG	NEG	POS	NEG	POS	NEG	NEG	NEG	NEG	POS
7	NEG	NEG	NEG	POS	NEG	POS	NEG	NEG	NEG	NEG	NEG	NEG	POS

Table 5.2.4: The tabled data from the raw observations from Table 5.2.3 indicating the calculated sensitivity, specificity and the predictive values for the histology diagnosis of a ciliate infection in inflammation-free oysters within an at-risk population.

	TRUE POSITIVE	TRUE NEGATIVE	Totals	Sensitivity (%)	Specificity (%)	PPV (%)	NPV (%)
Section POSITIVE	7	0	7	38.89	100	100	68.57
Section NEGATIVE	11	24	35				
Totals	18	24	42				

Despite other diagnostic techniques being more sensitive, (Diggles, Cochennec-Laureau et al. 2003; Balseiroa, Conchasb et al. 2006) the use of histology has other advantages over modern molecular techniques. Several diseases and conditions can be diagnosed at once, in addition to useful information regarding the general health of the animal, its feeding history and other lesions (Diggles, Cochennec-Laureau et al. 2003). For this reason, histology will remain the standard test for routine health surveillance in the aquaculture industry.

It was necessary to make a major assumption during this study. We assumed oysters that did not display the presence of ciliates in their digestive glands within the original section and 5 serial sections were truly free of the ciliate. Due to the clustering of parasites in the digestive gland, supported by their negative binomial distribution (data not shown), it is entirely possible that some infected oysters were deemed true negatives in this study.

The results suggest the sensitivity of histology as a diagnostic tool in oysters in an at-risk population is low (38%) to moderate (50%). The incidence of disease in Group A and B was considered zero per cent using the original sections as a guide, however on examination of subsequent sections, the incidence of disease was 50% and 43%, respectively. This is of major concern considering histology is the primary diagnostic test used in the allocation of translocation permits. It highlights a requirement for the development of more sensitive molecular-based tests to target particular diseases. In the meantime, the examination of serial sections of oysters from at-risk populations should be included to rule out disease. The results indicate the analysis of just one serial section increases the detection of disease considerably, in both oysters that exhibit inflammation and those that do not.

5.3 FHU preparation for a cross infection study if ciliate infected oysters were found

5.3.1 Introduction

The aim of this protocol was to prepare for and design a cross infection trial to put in place when a source of ciliate infected bivalves became available for experimentation. The aim of the study was to co-inhabit oysters from an affected region with naïve oysters and look for infection in the naïve population. Naïve oysters will also have been inoculated with ciliates harvested from infected donor oysters. A modified version of this trial design was used for the cross infection experiment for the emerging disease, Oyster Oedema Disease (OOD) in December 2006.

5.3.2 Materials and Methods:

Live affected oysters or other bivalves sourced from an area with an active outbreak and a high prevalence of disease would be flown to aquarium facilities at Murdoch University's Fish Health Unit. Tanks measuring 12 x 24 x 18 inches were kept with internal recirculating filtration and aeration for the duration of the project (2005-2007).

The following tanks were set up to provide varying conditions for cross infection. Tank 1 will have been a negative control tank, containing sentinel oysters that had not had any exposure to the pathogen. Tank 2 will have been the positive control tank, containing only affected shell at 23^{o}C. Tank 3 will have been the first cross infection tank, with affected and unaffected oysters cohabiting in 23^{o}C. Tank 4 will have been a tank with unaffected oysters at 23^{o}C, filled with water from the tank holding the affected oysters. Tank 5 was the second cross infection tank, with the same conditions as Tank 3 but with a higher temperature of 28^{o}C. Tank 6 would contain only naïve shell that have been inoculated with ciliates sourced from infected oysters. This is summarised in Table 5.3.1.

Table 5.3.1: Four Aquariums 18" x 12" x 2' with internal filtration will be used in the experiment.

Tank	1	2	3	4	5	6
Affected oysters	0	5	7	0	7	8 innoculated spat
Unaffected oysters	25	0	25	25	25	25
Temperature	23^{o}C	23^{o}C	23^{o}C	23^{o}C	28^{o}C	23^{o}C
Water	Aged water + aquarium salt	Aged water + aquarium salt	Aged water + aquarium salt	Water from tank holding affected oysters	Aged water + aquarium salt	Aged water + aquarium salt

Oysters from the tanks were to be sampled every 24 hours from day 1 for the length of the experiment. Any mortalities would be recorded, also the temperatures and water quality values, such as pH, Ammonia and Nitrate, maintained in the tanks throughout the trial period. Oysters selected for sampling would be removed each day, halved sagittally with a scalpel blade and tissue samples fixed in 10% sea-water buffered formalin and half in 100% ethanol.

Oysters would be maintained on daily feeds of nutritional algae, Tahitian *Isochrysis galbana*, *Pavlova lutheri,* and C*haetoceros muelleri*. This also served as a partial daily water change for each of the tanks.

5.3.3 Discussion

Due to the relative youth of the aquaculture industry, new diseases continue to emerge. During an initial outbreak of a disease, it is essential to have plans in place for the immediate initiation of experiments such as a transmission trial to determine whether an infectious agent is responsible. The fish health unit at Murdoch University is the ideal place for such studies, since the recirculating system and its isolation from the coast removes the quarantine risks associated with flow-through systems that source their water directly from the ocean. With this design, sea water is made artificially and therefore limits the possibility that water borne micro-organisms could adversely affect the trial results. This design also has advantages over field trials, as variables such as weather, salinity, temperature and food sources are removed, and the oysters are contained in a completely controlled (and measurable) environment over the duration of the study. This trial plan could be put in place to further investigate this organism if an outbreak of the intracellular ciliate is detected in the future.

5.4 Health survey of other bivalve species for the detection of a reservoir host for the intracellular ciliate

5.4.1 Introduction

The intracellular ciliate had not been seen prior to 2001, despite regular histological screening of pearl oysters from the area for the previous seven years. The origin of the ciliate therefore needed to be investigated. As previously noted, the intracellular ciliate of pearl oysters displayed alarmingly similar morphological features to the ciliate that infects mussels in Canada. This raised questions as to whether the ciliate has been introduced to the area, or whether it is an endemic parasite of another bivalve species in the area. A comprehensive survey of the area of previous infections was performed to discover whether the intracellular ciliate has a reservoir of infection in another bivalve species.

5.4.2 Materials and Methods

A total of 345 bivalves were sampled and processed for histology as part of this survey. The sampling was performed during field trips to the areas of previous ciliate outbreaks, and whenever the opportunity arose, with the logistical support of the pearl companies involved.

Sampling trip to the Montebello Islands, July 2005

A total of 78 individual bivalves were sampled at various locations in the Montebello Islands in July, 2005. These locations included Crocus Island, (20°25'18"S, 115°31'35"E), West Bay (of Alpha Island, 20°24'31"S, 115°31'43"E) and Rose Channel, and the long lines at Bluebell Island, Horseshoe Lagoon and Burgundy Bay. The bivalve species sampled included Rock oysters *Saccostrea cucullata* (Born 1778), Razorbacks *Pinna deltodes* (Menke, 1843), Thick round shelled bivalves *Chama limbula* (Lamarck,1819), Small white shell *Lima lima* (Linnaeus,1758), Penguin shell *Pteria peasei* (Dunker, 1872), Red shells *Crenatula viridis* (Lamarck, 1819), Wild adult silverlip pearl oysters *Pinctada maxima* (Jameson, 1901), and bastard shells *Pinctada albina* (Lamarck, 1819) (juvenile), *Pinctada margaritifera* (Linnaeus, 1758) (juveniles), and *Pinctada margaritifera* (Linnaeus, 1758) (juveniles).

Sampling trip to Exmouth Gulf, September 2006
A total of 65 bivalves were sampled from Gales Bay, Exmouth Gulf in September 2006. Rock oysters (*Saccostrea cucullata*) were sampled (n=29) from the shoreline at Gales Bay, and 30 bastard shell (*Pinctada sp*.) were sampled from the A frame in Gales Bay.

Samples obtained during an outbreak of the intracellular ciliate and Oyster Oedema Disease in Exmouth Gulf, October 2006
A total of 98 bivalves were provided for examination during the October 2006 mortality event, later recognized as being due to Oyster Oedema Disease. The intracellular ciliate was observed during initial diagnostic testing of pearl shell, so farm staff were asked to fix bivalves from the area of the infection, using 10% sea water buffered formalin solution. Bivalves from Giralia Bay were sampled (n=23), including bastard shell (other *Pinctada sp.),* red shells *(Crenatula viridis),* and penguin shell *(Pteria peasei).* Bivalves were collected from Gales Bay (n=23), including mussels *Mytilus sp.* and *Brachidontes subramosus* (Hanley, 1844) and bastard shells, and 23 were fixed form the A frame in Gales Bay, including bastard shells and Penguin shell.

Sampling trip to Exmouth Gulf, May 2007
Bivalves were collected during a sampling trip to Giralia Bay, Exmouth Gulf in May 2007 (n=104). These bivalves included 96 bastard shell, seven mussels and one unidentifiable shell.

Identification, fixation and processing for histology
All bivalves were shucked on site, measured for size and fixed in sea water buffered 10% formalin solution, then processed at Murdoch University for histology according to usual procedures. These were stained with Hematoxylin and Eosin and viewed using an Olympus BH-2 microscope (Olympus Optical Co. Ltd.). Individual shells were labelled and identified back in Perth with the assistance of Mrs Shirley Slack-Smith at the Western Australian Museum.

5.4.3 Results of bivalve study in search of origin of ciliate

For the purpose of the bivalve study, the individuals examined were grouped into like species, and analysed for health and parasite burden. A tabulated summary of the results are presented in Table 5.4.1. Two photos of the collection methods used while sampling for this survey are included in Figure 5.4.1.

Results of bastard shell, Pinctada sp.

A total of 210 bastard shell, *Pinctada sp.* were collected during the sampling. Eleven were sampled from the Montebello Islands during July 2005, 30 from Gales Bay September 2006, 53 from Gales Bay October 2006, 21 from Giralia Bay October 2006, and 95 from Giralia Bay May 2007. Sixteen females were identified, 151 males and 43 were of unknown sex. One oyster from Gales Bay, sampled in October 2006, contained the intracellular ciliate in its digestive gland. Metazoan parasites were the most common foreign organism found in these bivalves, sighted in 53 individuals, or 25% of all *Pinctada sp.* sectioned. Twenty-two of the parasites were located in the digestive gland, 18 in the digestive tubules, 5 in the gills, 3 in the connective tissue lining the gut and 7 in the gut lumen. Twenty-five of these parasites were associated with granuloma formation. Figure 5.4.2 A is a photomicrograph of a metazoan parasite inhabiting the digestive gland of an oyster. A well organised granuloma is walling off the parasite.

The second most common finding were Rickettsial bodies, found in 17 individuals or 8.1% of all *Pinctada sp.* sampled. The majority were located in the gills (15/17), however a couple were located in the epithelial cells of the digestive gland. None of these were associated with a host response, such as a local haemocytic infiltrate. Figure 5.4.3 A is a photomicrograph of a Rickettsial infection within the gills of a bastard shell. Figure 5.4.3 B is of an infection within the digestive gland, located within the epithelial cells. Five individuals were infected with gregarine bodies, one of these oysters was from the Montebello Islands, and the remainder were from Giralia Bay in 2007. Four individuals contained Ancistrocomid ciliates, and one oyster contained viral inclusion bodies. Figure 5.4.2 B is photomicrograph of a heavy Ancistrocomid infection within the lumen of the stomach of an oyster. Two oysters contained bacteria within the section, a large rod approximately 4-5µm in length, sometimes associated with a local haemocytic aggregation. The section of two oysters also contained sections of their resident pea crab.

Table 5.4.1: A table of a summary of the bivalve survey results, with results grouped according to species of bivalve, location or origin and date collected.

	Montebello Is Jul-05		Gales Bay Sep-06		Gales Bay Oct-06		Giralia Bay Oct-06		Giralia Bay May-07		Total	
Pinctada sp. (excl. P.maxima)	11	100	30	100	53	100	21	100	95	100	210	100
metazoan parasites	0	0	11	37	16	30	2	9.5	23	24	52	25
rickettsial bodies	0	0	2	6.7	5	9.4	0	0	10	11	17	8.1
gregarine bodies	1	9.1	0	0	0	0	0	0	4	4.2	5	2.4
ancistrocomids	0	0	0	0	0	0	1	4.8	3	3.2	4	1.9
viral inclusion bodies	0	0	0	0	0	0	0	0	1	1.1	1	0.5
invasive bacteria	0	0	0	0	2	3.8	0	0	0	0	2	1
intracellular ciliates	0	0	0	0	1	1.9	0	0	0	0	1	0.5
Pteria peasei	15	100	0	100	20	100	1	100	1	100	37	100
metazoan parasites	1	6.7	0	0	3	15	0	0	0	0	4	11
rickettsial bodies	0	0	0	0	2	10	0	0	0	0	2	5.4
gregarine bodies	3	20	0	0	0	0	0	0	0	0	3	8.1
viral inclusion bodies	1	6.7	0	0	0	0	0	0	0	0	1	2.7
Pinna deltodes	2	100	0	100	0	100	0	100	0	100	2	100
metazoan parasites	1	50	0	0	0	0	0	0	0	0	1	50
Pinctada maxima (wild)	5	100	0	100	0	100	0	100	0	100	5	100
metazoan parasites	1	20	0	0	0	0	0	0	0	0	1	20
viral inclusion bodies	1	20	0	0	0	0	0	0	0	0	1	20
Mytilus and Brachidontes sp.	1	100	8	100	0	100	0	100	7	100	16	100
protozoal bodies	1	100	0	0	0	0	0	0	0	0	1	6.3
metazoan parasites	0	0	6	75	0	0	0	0	2	29	8	50
Saccostrea cucullata	23	100	29	100	0	100	0	100	0	100	52	100
metazoan parasites	0	0	14	48	0	0	0	0	0	0	14	48
Haplosporidian parasites	12	52	4	14	0	0	0	0	0	0	16	55
ancistrocomids	0	0	1	3.4	0	0	0	0	0	0	1	3.4

Note: No parasites were found in specimens from the following species of bivalve: *Lima lima, Crenatula viridis* and *Chama limbula*

Figure 5.4.1: A: Photo of the collection bag at a coastal sampling site in the Montebello Islands, rock oysters (S. cuccullata) are visible on the rocks in the photo **B:** A Hookah breathing system (courtesy of D. Bearham and Morgan &Co.) was required for sampling the adult Pinctada maxima and other deep water bivalves in the Montebello Islands.

A

B

Figure 5.4.2: A: Metazoan parasite within a granuloma in the digestive gland of a pearl oyster, Scale bar: 80 µm. **B:** Heavy Ancistrocomid infection within the lumen of the stomach of a bastard shell, Scale bar: 80 µm.

A

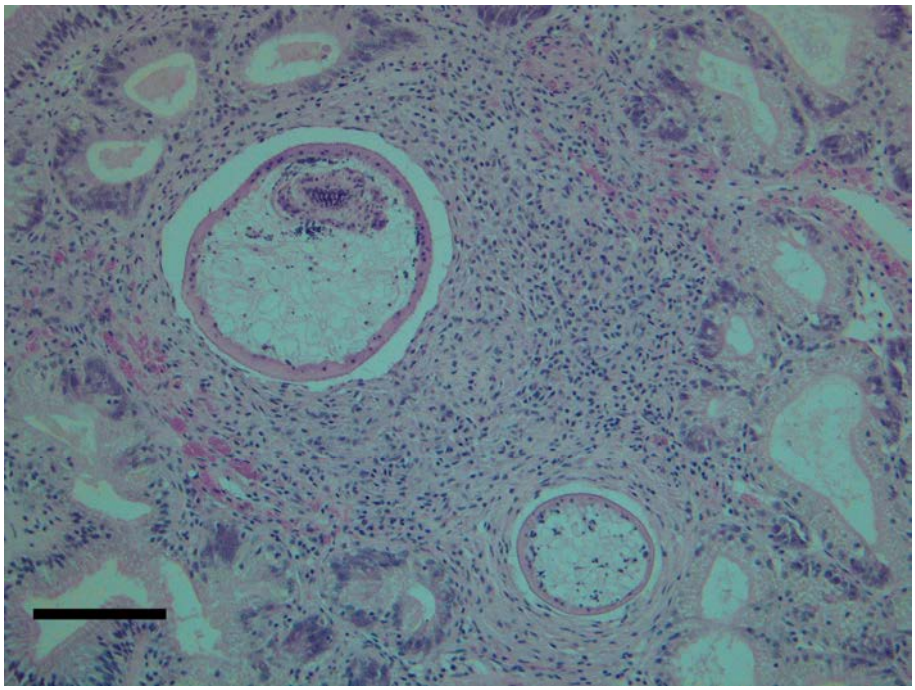

B

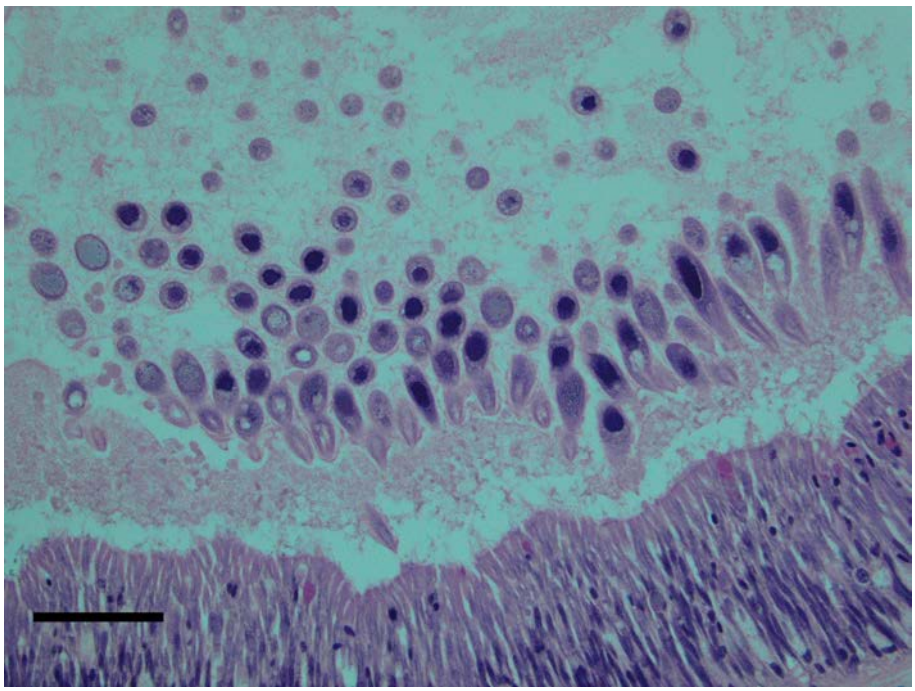

Figure 5.4.3 A: A photomicrograph of a Rickettsial infection within the gills of a bastard shell. Scale bar: 80 µm. B: A Rickettsial body within the digestive gland, located within the epithelial cells. Scale bar: 20 µm. Note the differences in the scale bars to indicate the size variation of the bodies.

A

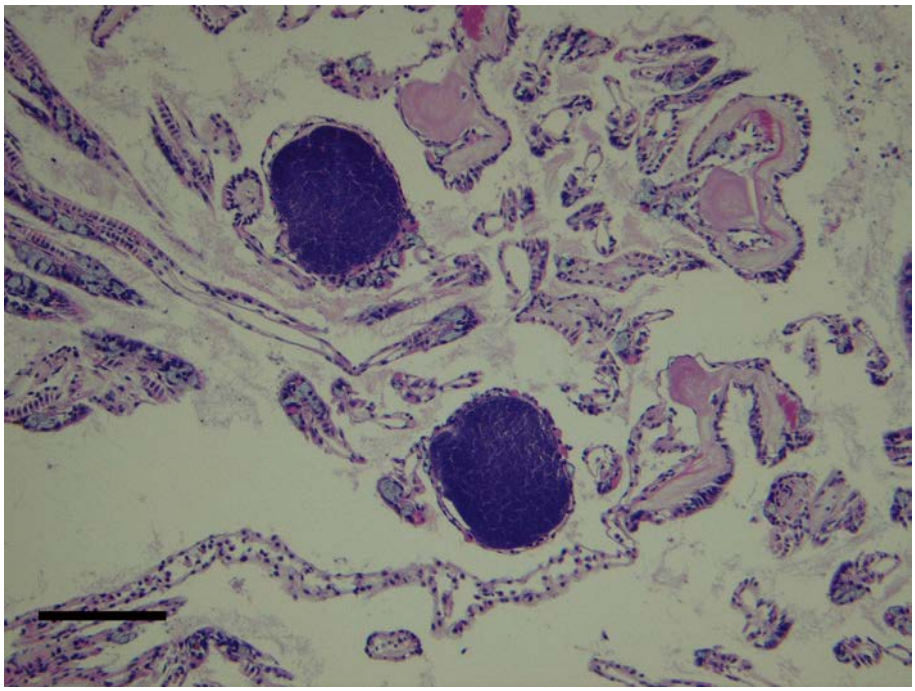

B

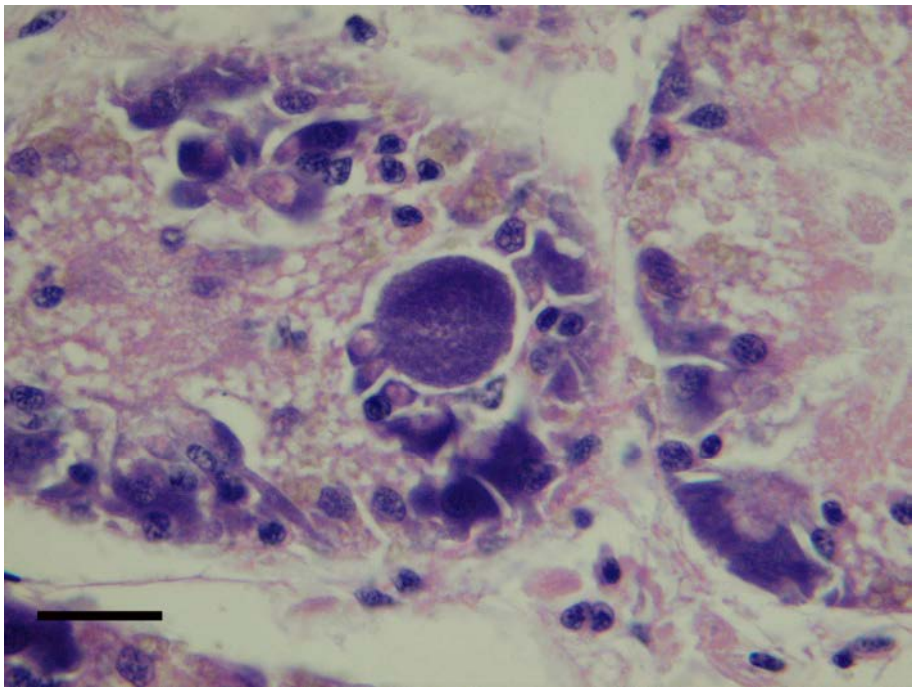

A large number of oysters sampled (76/210) displayed inflammation in their tissues. Twenty-seven individuals had granuloma formation. The most common site of haemocytic aggregations was the digestive gland, seen in 37 oysters. This was closely followed by the connective tissue lining the gut, which occurred in 25 oysters. Seven bastard shell contained aggregation in their mantle or palps, one in the gonad, three in the heart, one in the kidney and four in the gills. Twenty-six or 34% were present with no aetiological agent visible in section. Twenty-seven oysters had areas of degenerative necrosis within the section. Twenty-one of these changes were located in the digestive gland, four in the gonad and six in the gut or stomach.

Results of Penguin shell Pteria peasei

A total of 37 penguin shell, *Pteria peasei*, were sampled during the survey. Fifteen were collected from the Montebello Islands in July 2005, 20 were from Gales Bay in 2006, 1 from Giralia Bay in 2006 and 1 from Giralia Bay in 2007. Twenty-two females were identified, 2 males and 13 were of unknown sex. Once again, the most common parasite encountered was of the metazoan variety, infecting 4 of the 37 oysters, or 11%. The second most prevalent parasites were gregarine bodies, found in three of the 37 penguin shell. One of these was in an atypical location within the interstitium of the digestive gland (Figure 5.4.4). The third most common parasite were Rickettsial bodies. Two individuals from Gales Bay 2006 were infected with these parasites, one infection located in the gills and one in the digestive gland. One individual contained a severe focally extensive haemocytic infiltrate centred on a digestive tubule. Within this foci was multiple ovoid eosinophilic amorphous bodies approximately 6-8µm in size, possibly viral inclusion bodies (Figure 5.4.5).

Eleven penguin shell (nearly 30%) contained inflammation. One oyster had mild multifocal haemocytic aggregations in the heart, 5 had inflammation in the connective tissue lining the gut, two had diffuse inflammation in the digestive gland, and 3 had formed granulomas. One penguin shell had a degenerative necrotic change in its digestive gland. Figure 5.4.6 is a photomicrograph of this oysters digestive gland, displaying an intense haemocytic infiltrate, effacing the normal architecture and ulceration of the gut epithelial lining.

Results of Razorbacks Pinna deltodes

Two razorbacks were sampled from the Montebello Islands in July 2005. Both were larger than 200mm in size. One of these had metazoan parasites in their digestive gland, and the same individual also had a large metazoan parasite in the mantle, associated with mild local inflammation.

Figure 5.4.4: A: An atypical gregarine infection in penguin shell, located within the interstitium of the digestive gland, Scale bar 20 µm, **B:** A photomicrograph of a typical location for gregarine bodies, within the epithelium of the digestive glands, Scale bar 40 µm

A

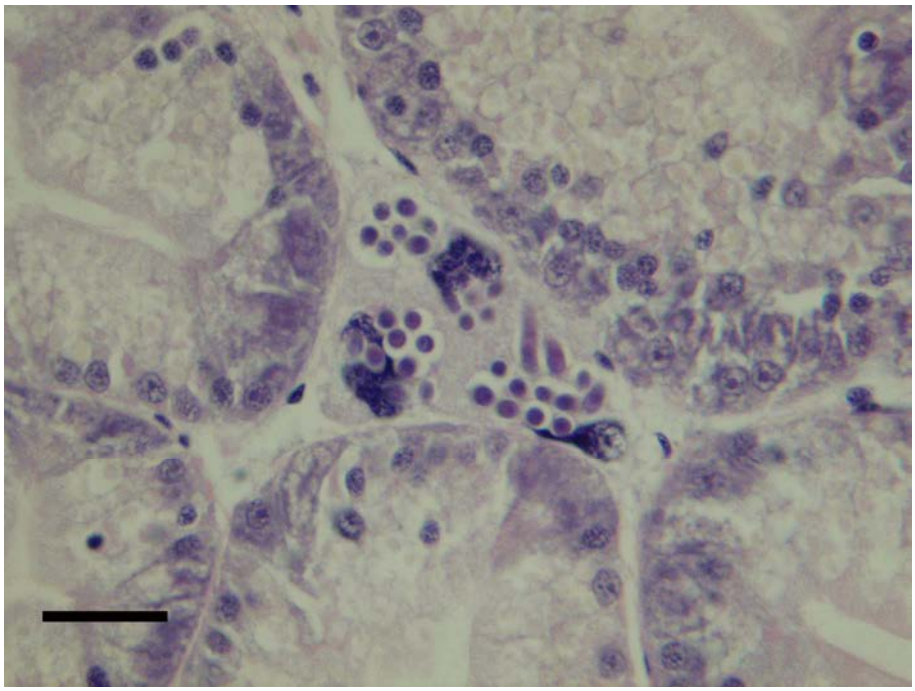

B

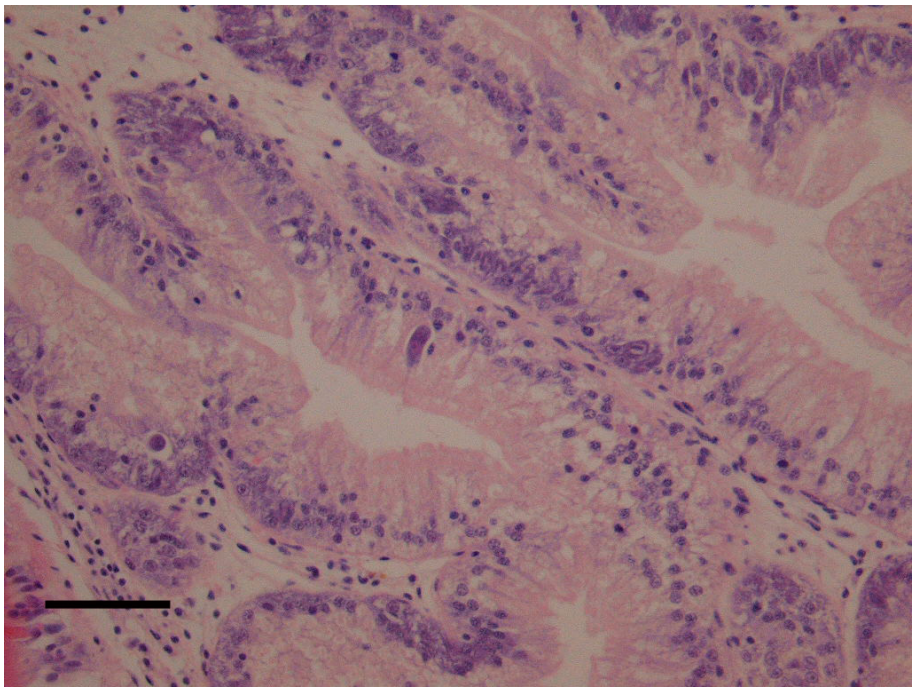

Figure 5.4.5: A photomicrograph of the digestive gland of a *P.peasei* individual containing a severe focally extensive haemocytic infiltrate centred on a digestive tubule. Within this foci was multiple ovoid eosinophilic amorphous bodies approximately 6-8µm in size, possibly viral inclusion bodies, Scale: 80 µm, B: The eosinophilic bodies at a higher magnification, Scale: 20 µm

A

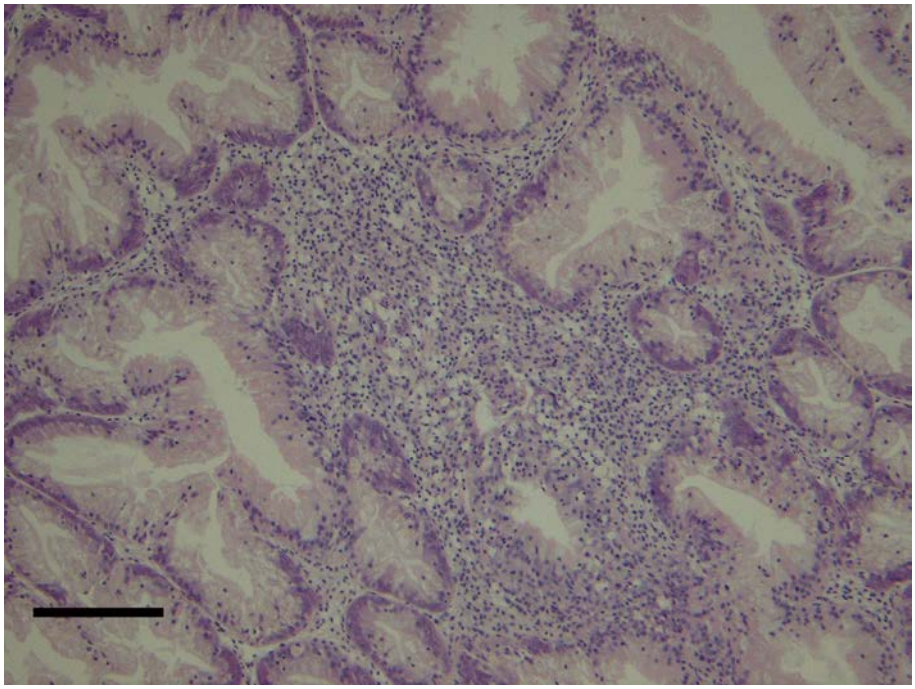

B

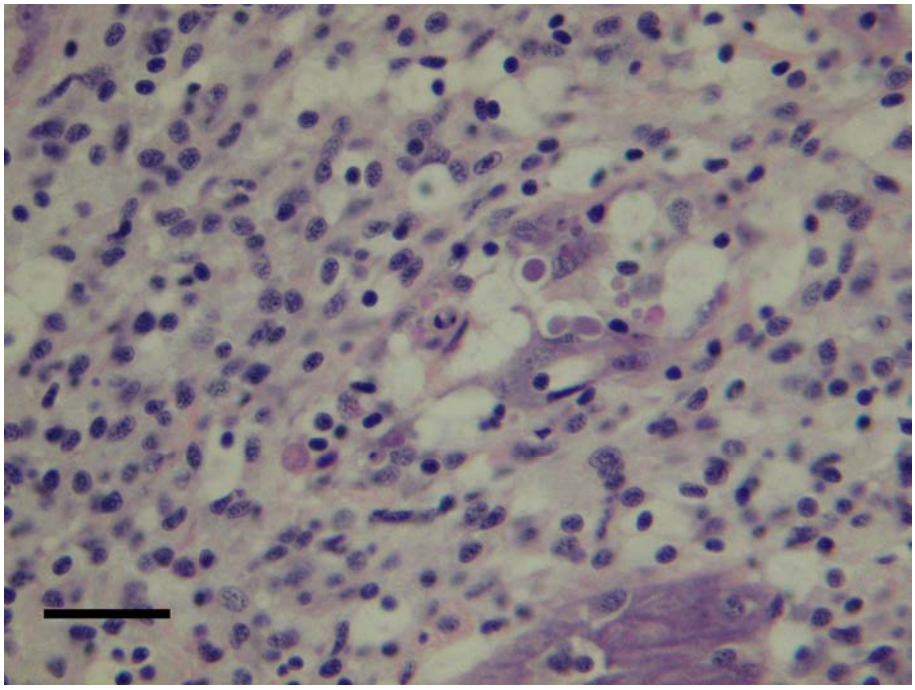

Figure 5.4.6: A: A photomicrograph of this oysters digestive gland, displaying an intense haemocytic infiltrate, effacing the normal architecture and ulceration of the gut epithelial lining, Scale 80 µm. **B:** Protozoal parasite within the digestive gland of a mussel, Scale bar: 20 µm.

A

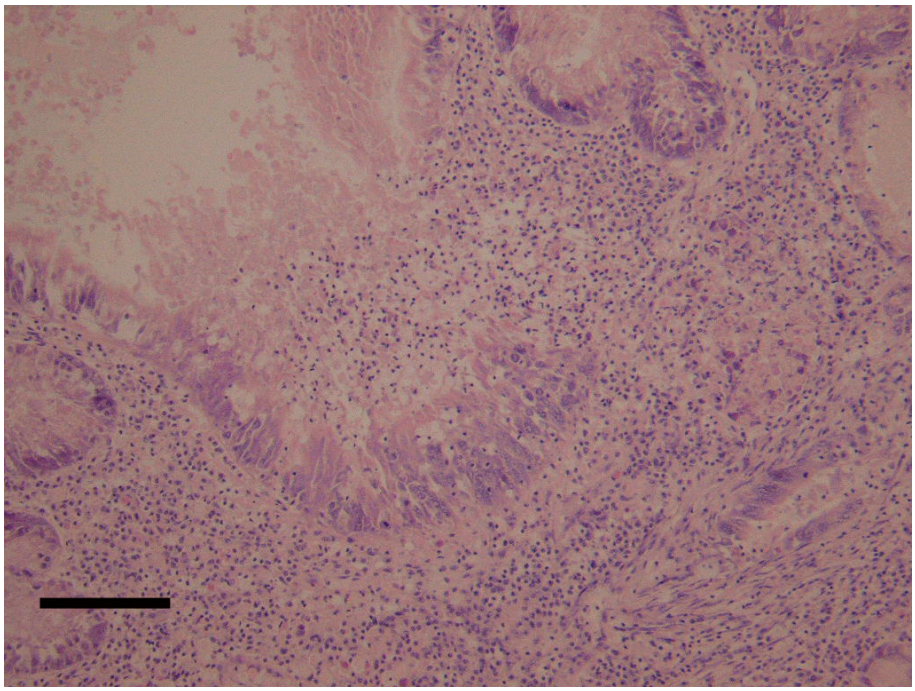

B

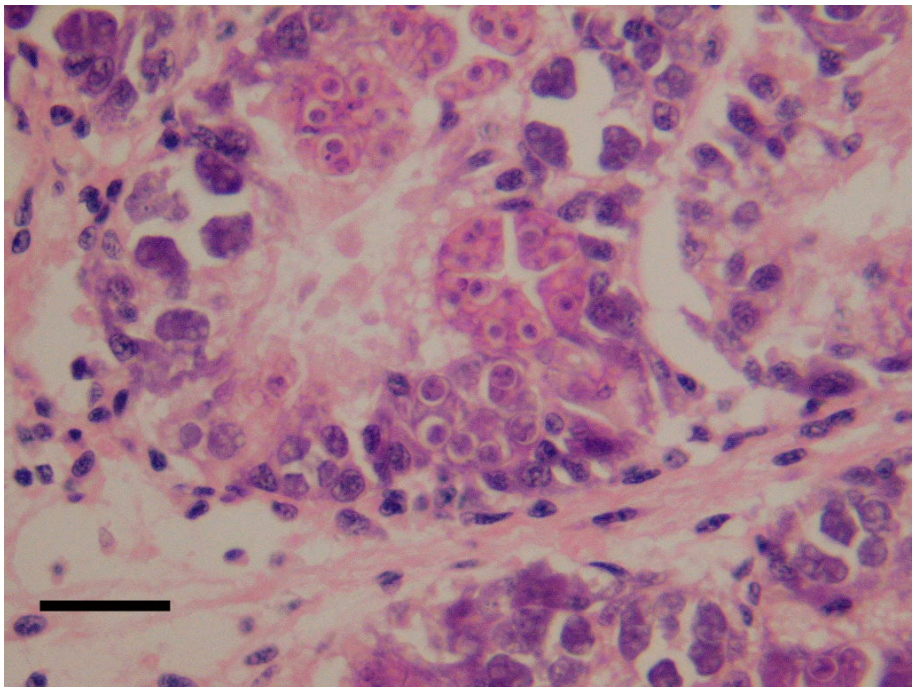

Results of Pinctada maxima (wild)

Five adult silverlip pearl oysters were collected using the Hookah breathing system in the Montebello Islands, July 2005. One of these oysters contained viral inclusion bodies, and the same individual contained metazoan parasites in its digestive gland. Two oysters had mild to moderate diffuse inflammation of their digestive glands.

Results of Mussels Mytilus sp. and Brachidontes subramosus

A total of 16 mussels were sampled during the bivalve survey. Six of these were females, 8 were males and 2 were of unknown sex. One mussel was collected from the Montebello Islands in July 2005, 8 were from Gales Bay in 2006 and 7 were from Giralia Bay in 2007. They were between 11 and 32mm in size. Once again, the most common abnormality were metazoan parasites, with 50% of the mussels affected. Eight of the metazoan infections were located in the digestive gland, one within the gonad, 2 within the connective tissue of the palps and one in the mantle. Eight were associated with granuloma formation. One mussel had a severe infection of an unnamed protozoal parasite with sporoblasts within its digestive gland (Figure 5.4.6 B). This parasite had previously been seen and described in pearl oysters by Jones and Creeper 2006, however has not previously been described in mussels.

Results of Rock oysters, Saccostrea cucullata

A total of 52 rock oysters were sampled during this bivalve survey. Twenty-three oysters were collected from the Montebello Islands in 2005 and 29 were collected from Gales Bay in 2006. Eleven were males, 7 were females and the remainder of unspecified sex. Fourteen (48%) of the rock oysters were infected with metazoan parasites, 10 within a granuloma. Sixteen (55%) were infected with a Haplosporidian parasite, *Minchinia sp*., which was confirmed by PCR (Bearham, Spiers et al. 2007). One oyster contained Ancistrocomid ciliates. Five rock oysters had degenerative necrotic changes evident in their gut epithelium or digestive gland.

Results of white shell, Lima lima

One individual of white shell was collected and examined as part of this bivalve survey. It was of unspecified sex and 15 mm in size. No abnormalities or parasites were detected on section.

Results of red shells, Crenatula viridis

A total of 12 red shells were collected during the bivalve survey. Eleven were from Rose Channel in the Montebello Islands, collected in July 2005 and one was from Giralia Bay, sampled in October 2006. They ranged between 11 and 26 mm in size. Eight individuals sectioned were male, 2 were female and 2 were of undetermined sex. Two of these individuals contained a mild diffuse haemocytic infiltrate of the digestive tract and one had a vacuolar change in its digestive gland. No parasites were detected in any of the sections.

Results of thick round shells, Chama limbula

A total of 9 *C. limbula* shells were sampled during the field trip to the Montebello Islands in July 2005. Four were from West Bay, 4 were collected from Crocus Island, and 1 was collected from Rose Channel. They were all between 45-55 mm in size. Two females and 5 males were identified, with the remaining 2 of unspecified sex. No abnormalities or parasites were detected in any of the sections.

5.4.4 Discussion

With a total of 345 bivalves sampled commencing 2005 to 2007, from 8 geographical locations and over 11 species of bivalve included, one oyster contained the intracellular ciliate. This oyster was a 20mm male bastard shell (*Pinctada sp*.) from Gales Bay, sampled in October 2006. It was sampled during a mortality event, later diagnosed as being due to Oyster Oedema Disease (OOD). On initial examination into the mortality event, pathologists at the WA Department of Fisheries discovered the ciliate on histology. Unfortunately, due to the high mortality sustained due to OOD, no pearl oysters were available for sampling, processing or to provide a ciliate infected population for a transmission trial from this event. The surviving bivalves that cohabitate with the pearl oyster on the long lines were included in this study, sampled within days of the mortality event, and evidently provided the only ciliate infected bivalve during the course of sampling for this project.

The discovery of the intracellular ciliate infecting a *Pinctada sp.* other than *P. maxima* raises concerns over the origin of the parasite. Bastard shells are a common fouling organism of pearl farm long lines, so are often in close proximity to the farmed pearl oysters. If these closely related oysters are acting as a reservoir for parasitic disease, it would be a particularly difficult management issue to control the spread. To address this issue, perhaps bastard shell should be included on routine health checks to act as sentinel animals for the diseases of pearl oysters. However, at an intracellular ciliate prevalence of 0.5% in bastard shell, this may not be a viable option.

The northern hemisphere intracellular ciliate of mussels infects three *Mytilus* sp.; *Mytilus edulis, Mytilus trossulus* and *Mytilus galloprovincialis*, which may indicate either there are different species of ciliate that are host specific, or there is a small range of closely related hosts suitable for this ciliate. Given this, perhaps other *Pinctada* sp. will be susceptible to the pearl oyster intracellular ciliate. Cross infection trials with infected pearl oysters cohabitating with bastard shells in a controlled environment may shed some light on this issue. The bastard shell found to be infected during the course of this bivalve survey may be an incidental host, rather than the source of the disease outbreak.

An interesting outcome from this survey was observing the differences in parasitic populations between species of bivalve and between geographical locations. Metazoan parasites featured strongly in all bivalve populations, with the exception of *L. lima, C. viridis* and *C. limbula*. Rickettsial bodies were only seen in *Pinctada sp*.

and *P. peasei*, as were gregarine bodies. Viral inclusion bodies were observed in wild *P. maxima, Pinctada sp*. and *P. peasei*. *S. cuccullata* were the only bivalve with a Haplosporidian burden. The discovery of the protozoal parasite with sporoblasts infecting the entire digestive gland of a mussel was a surprise, given a very similar parasite has been recorded in pearl oysters by Jones and Creeper 2006 but has not been reported inhabiting any other bivalve species. With further investigation, this could be either another parasite 'jumping' host, or in fact different but closely related parasites infecting two bivalve species.

5.5 Historical distribution of ciliate in Western Australia

5.5.1 Introduction

In order to understand the outbreak dynamics of the intracellular ciliate, the historical distribution of the ciliate was investigated using archival information from the WA Department of Fisheries. Records pertaining to ciliate infections and related health surveillance were made available between October 2001, when the ciliate was first discovered, and 2007. As with all retrospective studies, the only information available was from records and personal observations from members of the industry. Only the infections confirmed using histopathology were included in the study.

5.5.2 Findings of a retrospective study into the ciliates distribution

The intracellular ciliate was first observed during routine health surveillance of pearl oysters in 2001. The first known cases were in October 2001, from leases belonging to two pearling companies (PC1 and PC2) in Exmouth Gulf and the Montebello Islands. The initial batches of oysters had a ciliate infection prevalence of between 4 – 30%. In December of the same year, a third pearl company (PC5) had a batch of oysters from Wapet Shoal (Exmouth Gulf) tested, and these were negative for the ciliate. The intracellular ciliate has not been found in Wapet Shoal since. Also in December 2001, a batch from Burgundy Bay (Montebello Islands) belonging to PC2 was found to have the ciliate in 52% of its spat. In February 2002 a fourth pearl company (PC6) submitted spat from Claret Bay, Haynes Peninsula and Gales Bay. The smaller spat were found to be 100% infected with the ciliate, however the larger spat from Haynes Peninsula in the Montebello Islands and Gales Bay in Exmouth Gulf were recorded as having a very low incidence. PC3 were confirmed to still have the ciliate at a prevalence of up to 23% in June and up to 85% in November of the same year. In February 2003, the ciliate was found for the first time on Lowendale Island, in spat from a fifth pearl company, PC4. All spat smaller than 60mm were infected. The ciliate was not detected again until September 2005, when it was recorded in 10% of a batch of spat from Gales Bay, Exmouth Gulf. This same area was the site of the last known occurrence in October 2006 where 48% of the batch of spat were infected. This information is summarised in Table 5.5.1. Figure 5.5.1 is a satellite image including Exmouth Gulf (E.G.), Montebello Islands (M.I.) and Lowendale Island (L.I.) indicating the years when the intracellular ciliate was

recorded from 2001-2006. Figure 5.5.2 is a diagrammatical representation of the sites where the ciliate was diagnosed and the maximum prevalences recorded. A graphic representation of the Montebello Islands (Figure 5.5.2 A), Lowendale Island (Figure 5.5.2 B), and the Exmouth Gulf area (Figure 5.5.2 C) were included.

Figure 5.5.3 is a bar graph depicting the maximum prevalence of ciliate infections within at-risk populations of pearl oysters between 2001 and 2006, and the months of the year they occurred. The results of the different years are superimposed. The highest prevalences occurred during February, where they reached 100%. November was the second highest prevalence recorded at 85%, followed by December and October. The lowest months, excluding the months where no data was available, were September and July. The graph shows a curve, indicating the summer months had the highest prevalences and the lowest were during the middle of the year.

Figure 5.5.1: A satellite image including Exmouth Gulf (E.G.), Montebello Islands (M.I.) and Lowendale Island (L.I.) indicating the years when the intracellular ciliate was recorded from 2001-2006. Image: Google Earth

Table 5.5.1: A table of the occurrences of intracellular ciliate infections in Zone 1 from 2001 to 2007, showing prevalence of infection and origin of spat. The pearling companies are coded. Some information is not obtainable due to incomplete records available.

Date	Co.	Origin of spat	Lease	Size of spat	Prevalence
Oct-01	PC1	Exmouth Gulf	Not specified	Not specified	4%
	PC1	Montebello Islands	Not specified	Not specified	4%
	PC1	Montebello Islands	Not specified	>50mm	0%
	PC2	Montebello Islands	Not specified	>50mm	0%
	PC2	Montebello Islands	Not specified	20mm	30%
	PC2	Montebello Islands	Not specified	50mm	1%
Dec-01	PC5	Exmouth Gulf	Wapet Shoal	Not specified	0%
Dec-01	PC2	Montebello Islands	Burgundy Bay	Not specified	52%
Feb-02	PC6	Montebello Islands	Haynes Peninsula	Small	100%
		Montebello Islands	Claret Bay	Small	100%
		Montebello Islands	Haynes Peninsula	New spat	100%
		Montebello Islands	Haynes Peninsula	Medium	Rare
		Exmouth Gulf	Gales Bay	Large spat	Rare
Jun-02	PC3	Not specified	Not specified	20-25mm	15%
				30mm	10%
				35mm	23%
				40-50mm	7%
Nov-02	PC3	Not specified	Not specified	20mm	85%
				30mm	15%
				40mm	6%
				60mm	0%
				70mm	0%
				80mm	0%
				100mm	0%
Feb-03	PC4	Montebello Islands	Lowendale Island	Shell >60mm	0%
				Shell <60mm	100%
Sep-05	PC2	Exmouth Gulf	Gales Bay	30-60mm	10%
Oct-06	PC2	Exmouth Gulf	Gales Bay	<70mm	48%

Figure 5.5.2: A: Montebello Islands with years when ciliate were found and maximum prevalences recorded. **B:** Lowendale Island (including the key indicating the size of red dot associated with the maximum prevalence of intracellular ciliate infected oysters recorded in the area). **C:** Exmouth Gulf area

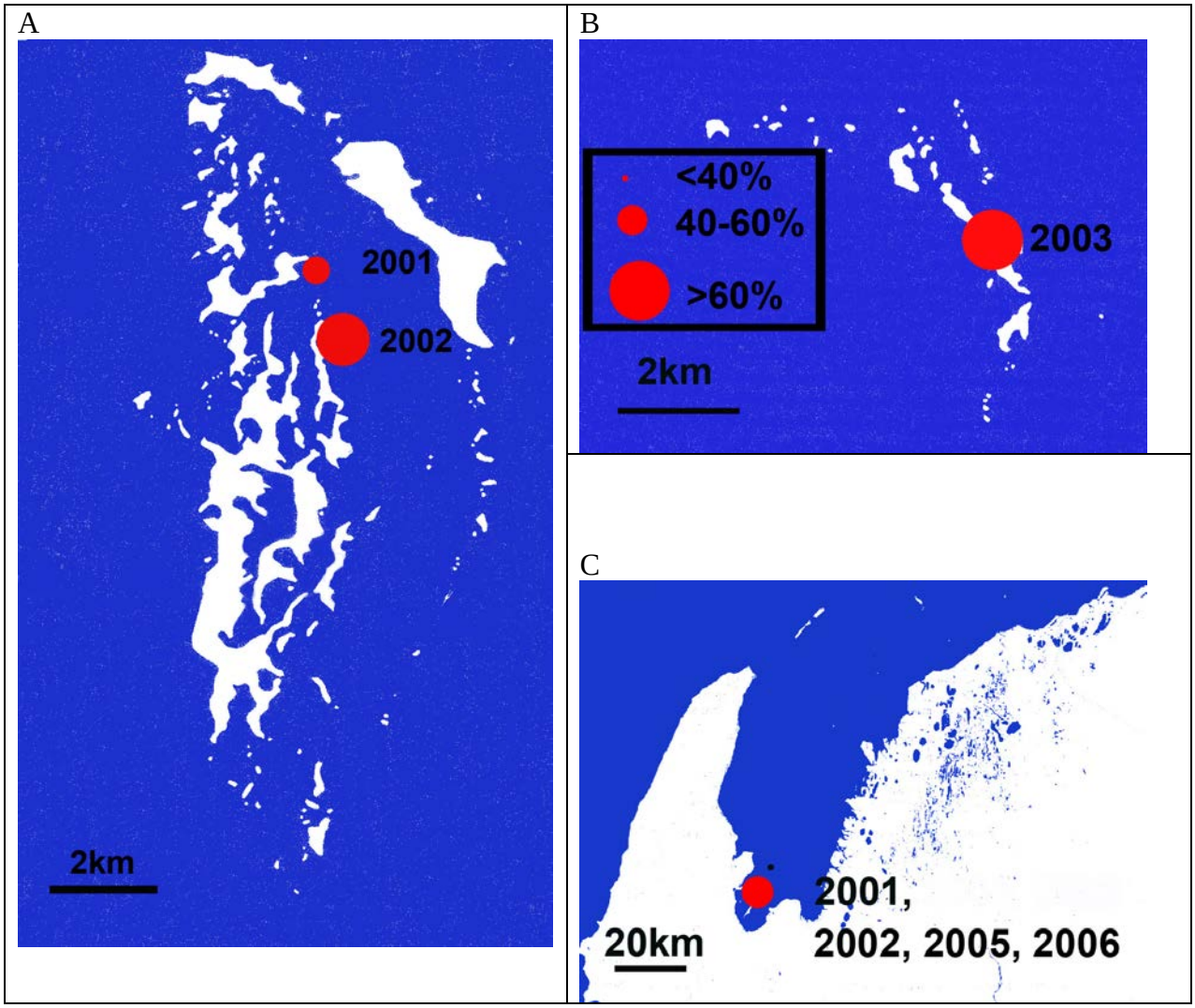

Figure 5.5.3: A bar graph depicting the maximum prevalence of ciliate infections within at-risk populations of pearl oysters between 2001 and 2006, and the months of the year they occurred.

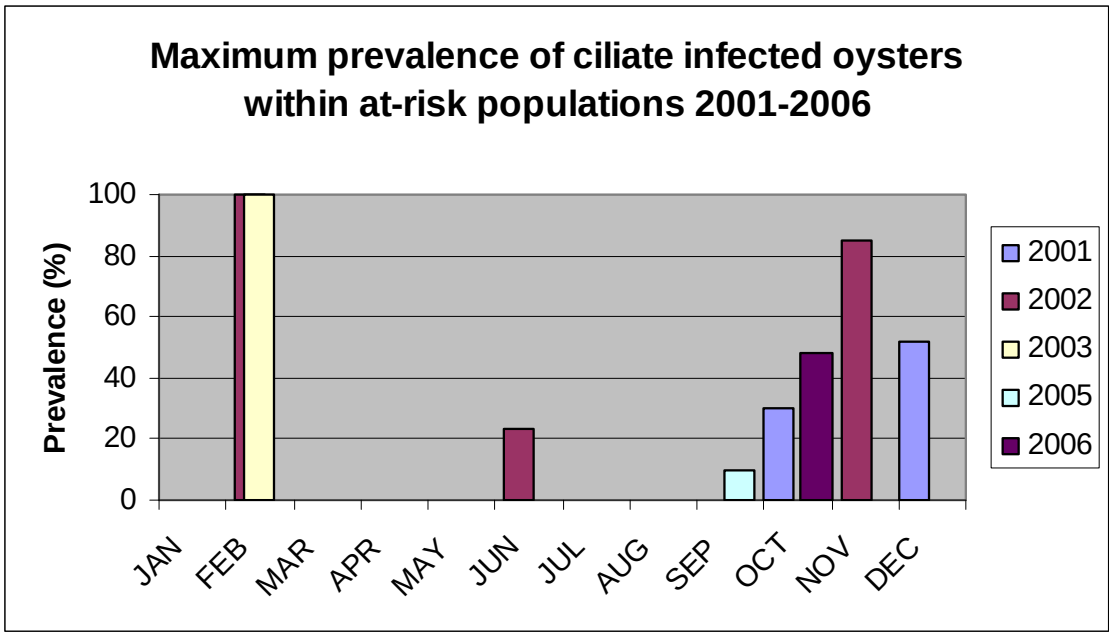

5.5.3 Discussion

There were a number of limitations to this study. The main one being a comprehensive study into the distribution of the ciliate was not carried out at the time of the original outbreak. Within the same month (i.e. October 2001), the ciliate was observed in pearl oyster spat belonging to two different pearl companies on leases in both Exmouth Gulf and the Montebello Islands. Due to movement of shell from the Montebello Islands to Exmouth Gulf and vice versa, the region the ciliate originated from cannot be determined, as was the length of time the ciliate had been present in the shell before they were tested as part of a translocation permit. It is also unfortunate that over time some details of the oysters have become unavailable, such as the size of the spat tested, and their lease of origin. These results therefore probably do not perfectly reflect the correct historical distribution of the ciliate.

The surveys carried out as part of this project reflect an extremely low prevalence of ciliate infections, with 284 pearl oyster spat examined without finding a single ciliate, and 345 bivalves examined, providing one positive individual. If, at any time in the past the prevalence of this ciliate was significant in the pearl oysters of the region, it does not seem to be the case now. The infections continue to be diagnosed sporadically. Since the main outbreak in 2001-2002, one batch of oysters has been found to have the ciliate in 2003, none in 2004, one batch with a low prevalence of 10% in 2005, and a 48% infection rate in one batch of spat in 2006. When compared

against the hundreds of oysters that are examined histologically each year by pathologist in the Department of Fisheries, this reveals a very low incidence rate.

5.6 Weather and seawater temperature implications in outbreaks of ciliate infections

5.6.1 Introduction

The occurrence of a disease is often a combination of several factors. It is a commonly held theory that in order for a disease to arise, there has been an interaction of host factors, environmental factors, and factors influencing the aetiological agent. In this section, the environment was considered as an influence in the occurrence of the ciliate outbreaks. As reviewed in section 4.1.1, haemocyte function, and therefore an oysters' ability to fight disease, can be influenced by environmental factors such as temperature and salinity.

Secondly, environmental factors can also influence the aetiological agent. Infectious Hypodermal and Haematopoietic Necrosis Virus (IHHNV) is a serious disease of cultured penaeid shrimp, in particular the Pacific white shrimp, *Litopenaeus vannamei*. A study performed by Montgomery-Brock, Tacon *et al* in 2007 investigating the virus replication in shrimp tissues under different environmental conditions found temperature had a profound effect. Viral replication was much lower in shrimp held at elevated temperatures compared with those in the cooler water.

Dermo disease, caused by *Perkinsus marinus*, in Pacific oysters, *Crassostrea virginica*, is widely recognized as a warm weather disease (Fisher 1988). This has implications for the distribution of disease, particularly with the recent trend of increasing water temperatures in response to climate change. A retrospective study found a close correlation between the northern expansion of the disease and the increase in winter sea surface temperatures in the area (Cook, Folli *et al* 1998).

Due to the sporadic nature of the outbreaks of the intracellular ciliate, the environment may be an important factor in its occurrence. A retrospective study into the weather and sea surface temperatures associated with the ciliate infections could be used to highlight patterns of occurrence, which could help predict when outbreaks are more likely to arise.

5.6.2 A study into the weather conditions associated with the ciliate outbreaks

The Bureau of Meteorology has a weather station located at Learmonth Airport ($22^{o}14'26"S$, $114^{o}05'48"E$) recording data since January 1945. Learmonth is the

airport that services the town of Exmouth. Unfortunately, there is no specific data for the Montebello Islands or Exmouth Gulf, so the Learmonth recordings were used in this study to give a general indication of weather in the area.

The mean maximum temperatures for the months of the year from 1945 to current were available from the Bureau of Meteorology. At Learmonth, the weather is at its warmest during the months of December to March, and coolest during the middle of the year between May and September. The mean maximum daily temperatures for each month was graphed in Figure 5.6.1, and superimposed over this data was the combined maximum prevalence of ciliate infections within at-risk populations from 2001-2006 with respect to the months of the year they occurred. Anecdotally, the ciliate infections were observed mostly during the warmer months, and this graph supports this observation. The ambient temperature appears to emulate the pattern of the ciliates prevalence within oyster populations.

The ambient temperature is not the only weather variable that may influence parasite burden. The fresh water run-off from heavy rainfall has the ability to reduce the salinity of the coastal seawater. Variations in salinity can influence disease, in the example of *Haplosporidium nelsoni*, or MSX disease, which occurs when there are high salinity conditions (Fisher 1988). The total monthly precipitate at Learmonth Airport for the years 2001-2006 inclusive is depicted in graph (Figure 5.6.2). The mean monthly precipitation is included as a dark blue line. The majority of rain falls between April and July, with very little rain recorded for the months October to December. This data was from the Learmonth Airport weather station was supplied by the Bureau of Meteorology. It could be surmised that due to the very low rainfall during the summer months, the salinity in Exmouth Gulf and surrounding waters could be at its highest during that time. Further investigation into the pathogenesis of the intracellular ciliate infections could determine whether there is a correlation between infectivity and ocean salinity.

Figure 5.6.1: Graph of combined maximum prevalence of ciliate infections within at-risk populations from 2001-2006 with respect to the months of the year they occurred, with the mean maximum temperature for those months from the Learmonth Airport weather station.

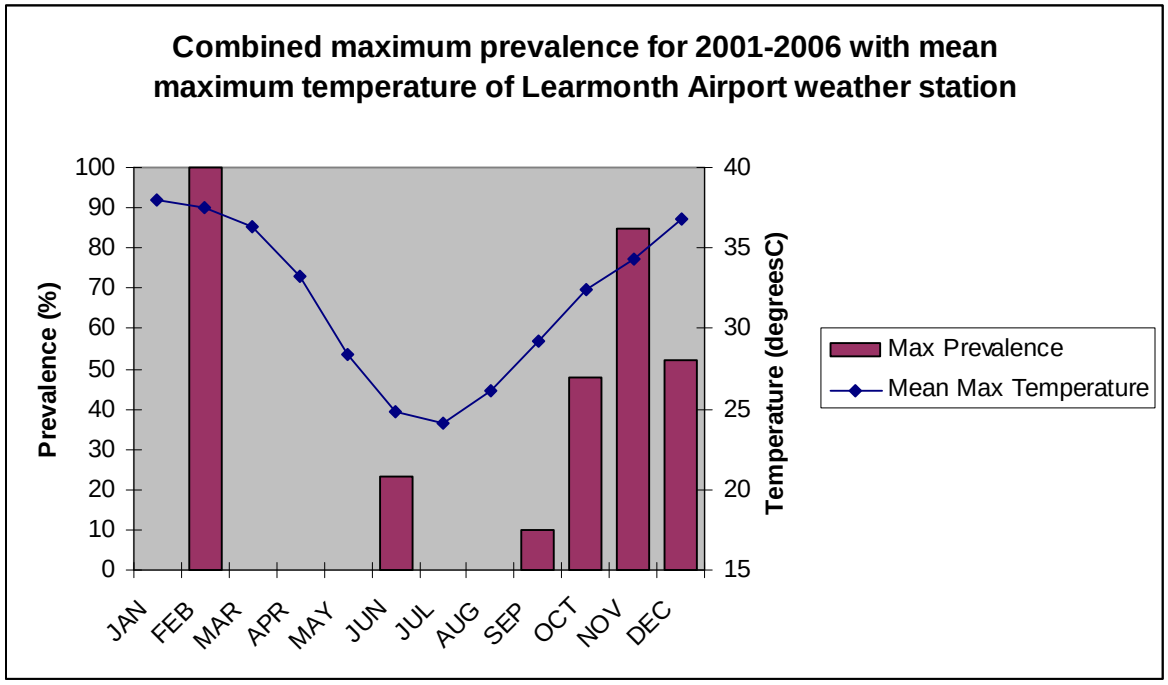

5.6.3 A study into the sea surface conditions associated with the ciliate outbreaks

During the course of this project, a Tinytag Explorer 4.2 (Gemini Data Logger UK Ltd.) was attached to a large piece of farming equipment in Gales Bay, Exmouth Gulf at a site of a previous ciliate infection. This was to record the water temperature in the area so in the event of the ciliate occurring, the water temperature preceding and during the outbreak could be analyzed. Unfortunately, towards the end of the project it was discovered that the equipment had been moved accidently inland and the data recorded was of no use. Luckily, however, the CSIRO Marine Research have data recorders in the area of Exmouth Gulf, Barrow Island (near Montebello Island), and other sites along the Western Australian coast that record the seawater temperature.

The mean monthly ocean temperatures were plotted on Figure 5.6.3. The CSIRO's data from Barrow Island (near Montebello Islands) and Exmouth Gulf was included on the graph. The sea surface temperatures, although almost 10^{o}C cooler, reflect the curve of the air temperature of the region, as depicted in Figure 5.6.1. The warmest temperatures occurred during January to April, and the cooler months were June to September. This was graphically represented in Figures 5.6.4 and 5.6.5, where the February and July sea surface temperatures display a large range in water temperature over the year. Figure 5.6.4 is from February, when historically, the highest prevalence of ciliate infections have occurred in at-risk oysters, up to 100%.

Water temperatures in the regions of interest reach almost 30^{o}C. In contrast, the graphic from July in the same year depicts a much lower temperature of around 20^{o}C for the Montebello Islands and Exmouth Gulf.

5.6.4 Discussion

This study has highlighted two environmental variables that may affect the prevalence of the infections of the intracellular ciliate. The temperature of both the air and the water follow the pattern of prevalence. This may not be a coincidence. It has been recorded how diseases may be affected by environmental temperature, either by its effect of the oysters ability to fight disease, or the physiology of the aetiological agent. Further research into the ciliate may give answers to the ideal conditions for growth and replication of this organism. In the mean time, however, it could be predicted that the sporadic outbreaks of the intracellular ciliate will be more severe during the warmer months of December to March. It is therefore wise to restrict any further surveillance sampling for the ciliate to these months, on the assumption it will be more likely to be detected if present. Despite routine health surveillance in the pearling leases north of the Montebello Islands, the intracellular ciliate has not yet been detected. This could be attributed to the Department of Fisheries restriction of infected shells movement from Zone 1. If temperature was the only limiting factor in this organisms survival, it could be hypothesized that other regions on the Western Australian coastline are in danger of infection, should the ciliate spread. The mean monthly temperature from Roebuck Bay, near Broome on the northern part of the Western Australian coast was included on Figure 5.6.3. From the graph, it is clear the water temperatures in the north are only a few degrees warmer over the year than those around Exmouth. If infected shell were permitted to be moved out of Zone 1, chances are the conditions are favourable for the survival of the intracellular ciliate in other Zones.

The second environmental condition that may be affecting the survival and proliferation of the intracellular ciliate is salinity. As discussed in section 5.6.2, the lower rainfall and therefore presumably higher salinity of the summer months may have been a contributing factor. More detailed monitoring of water salinity on the farms or aquarium trials need to be performed in future to assess this possibility.

The seasonal distribution of the ciliate may not be due to weather at all. It is possible the increase in prevalence could be more to do with management factors instead. Pearl oysters spawn towards the latter part of the year, when the water warms, and therefore the young spat are released from the hatcheries early the following year. The introduction of naïve spat into the ocean environment may contribute to the increased infection rates during this period. This is another possibility that may be determined through more controlled experimentation.

Figure 5.6.2: A graph depicting the total monthly precipitate at Learmonth Airport for the years 2001-2006 inclusive. The mean monthly precipitation is included as a dark blue line. The majority of rain falls between April and July, with very little rain recorded for the months October to December. Data supplied by the Bureau of Meteorology at the Learmonth Airport weather station.

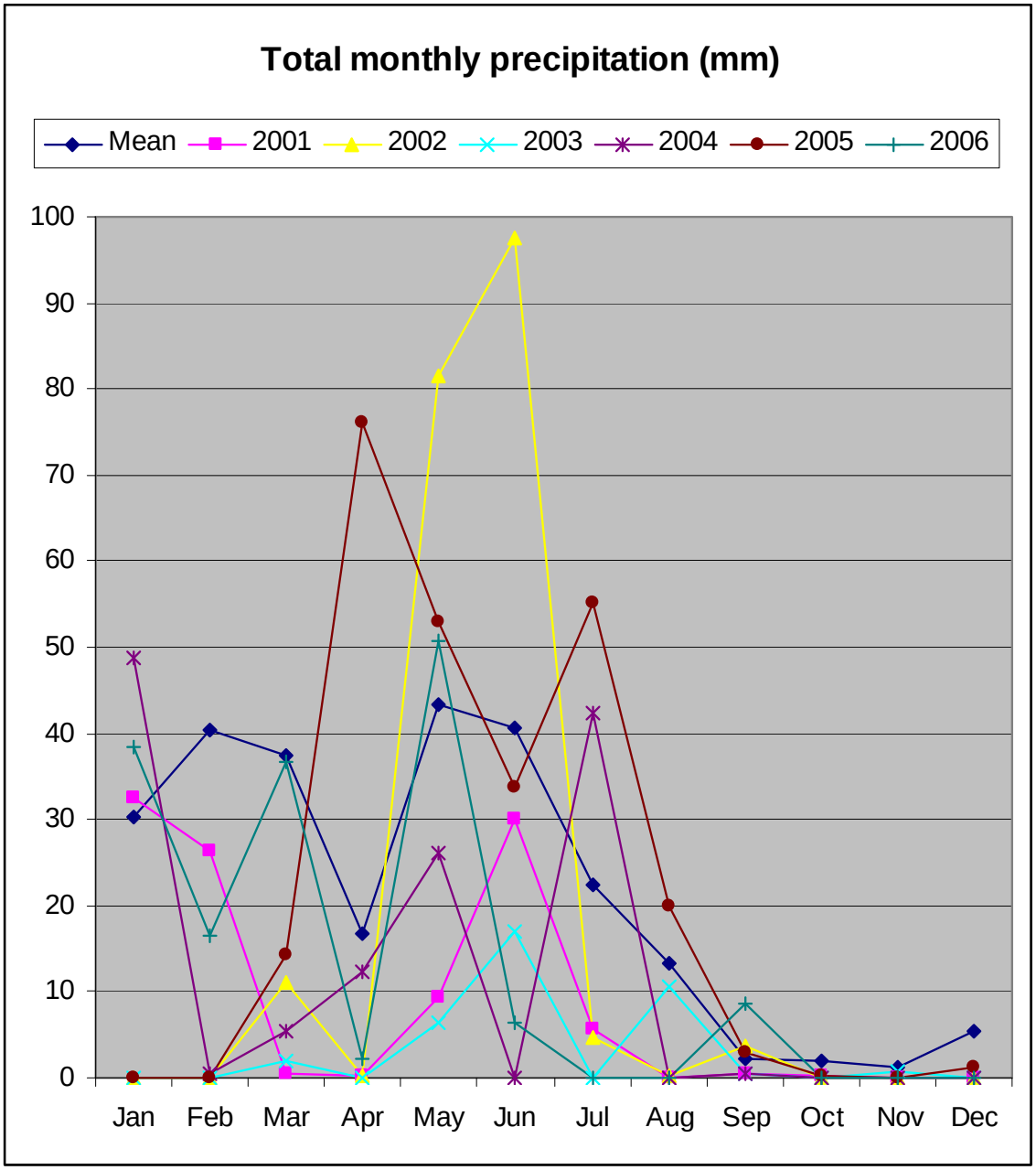

Figure 5.6.3: A graph depicting the mean monthly ocean temperatures for Barrow Island, Exmouth Gulf and Roebuck Bay.

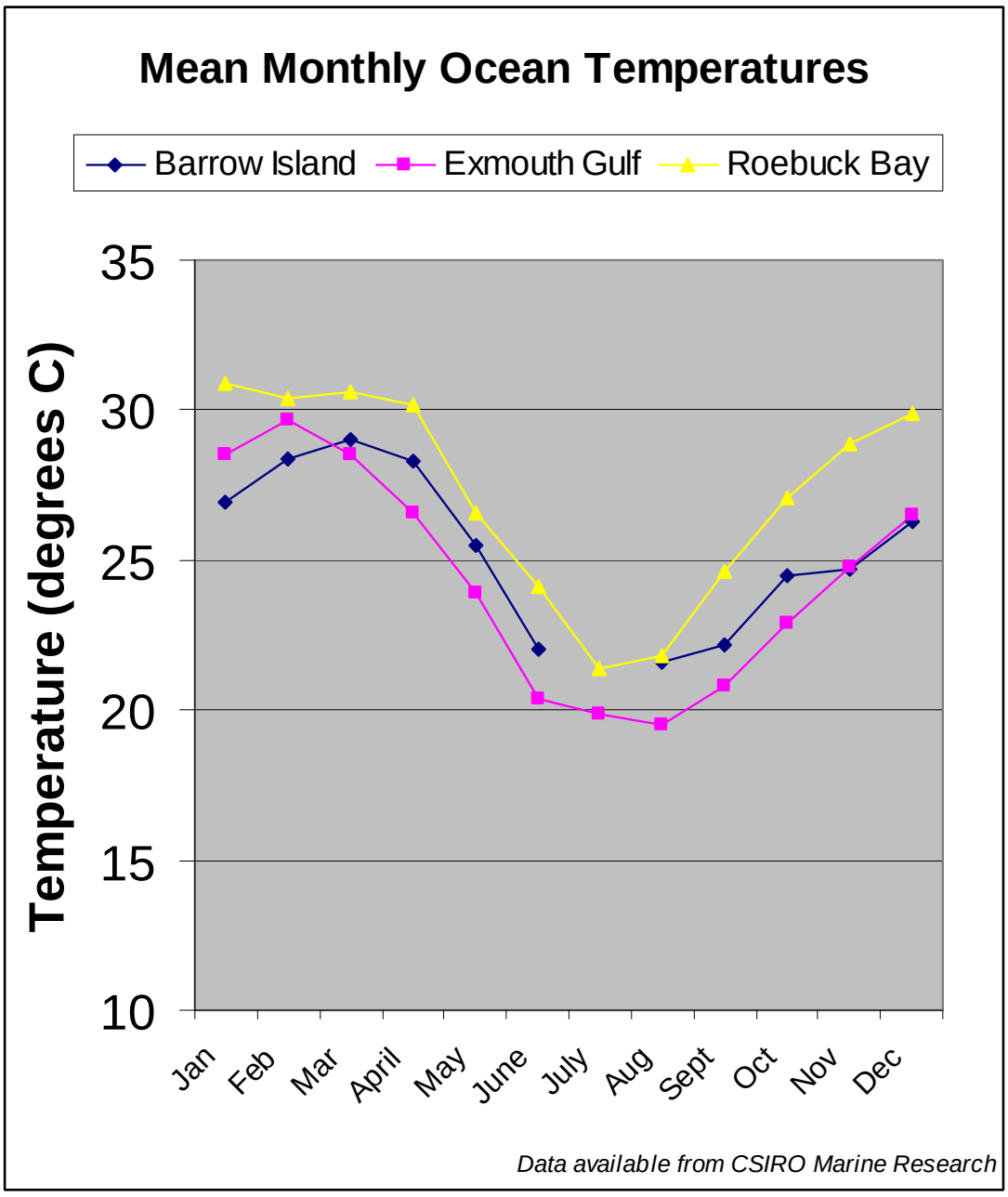

Figure 5.6.4: The sea surface temperatures for the region of Shark Bay to Montebello Islands in February, 2006, displaying the temperatures reaching up to 30°C. Data sourced from CSIRO.

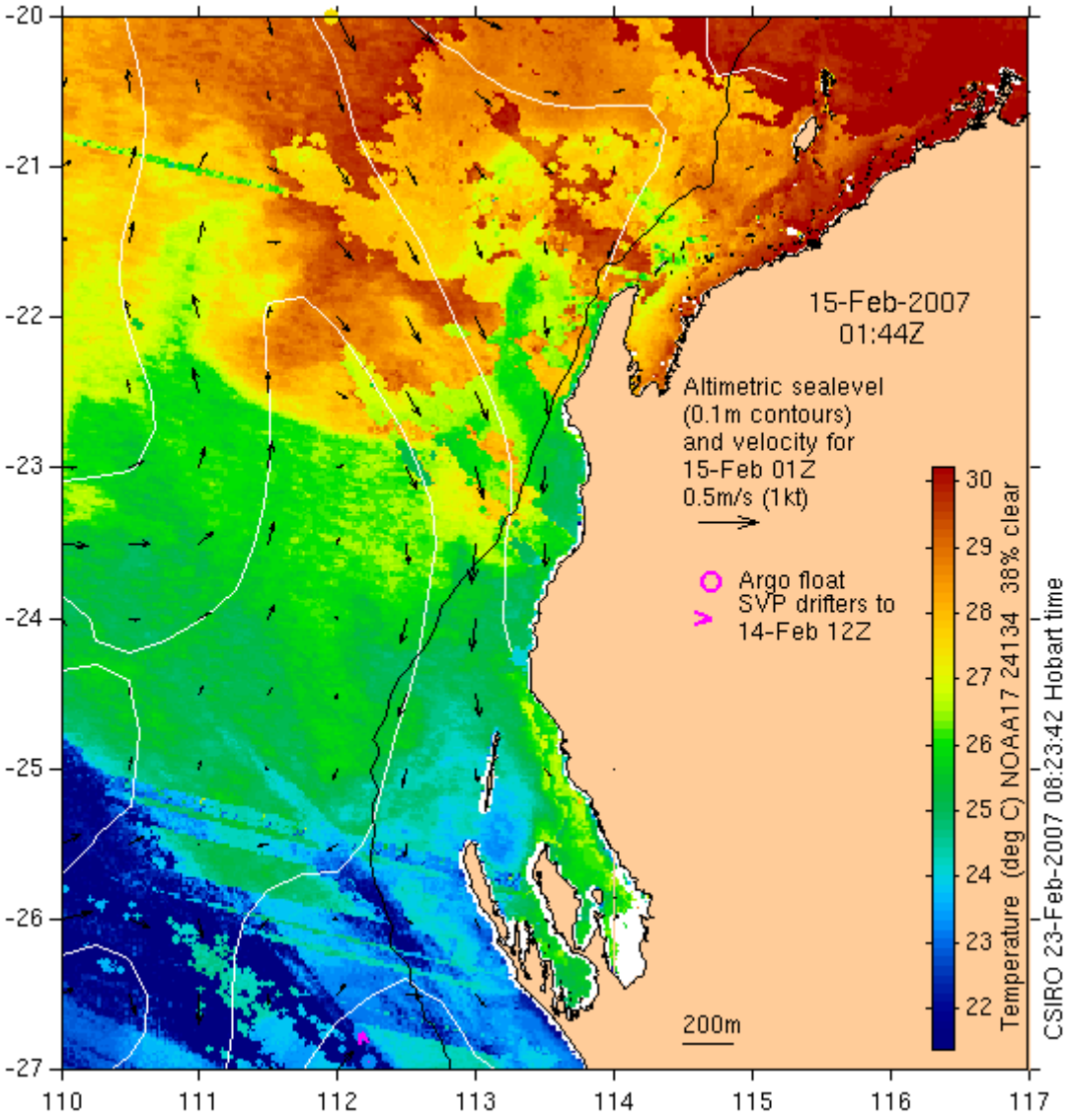

Figure 5.6.5: The sea surface temperatures for the region of Shark Bay to Montebello Islands in July, 2006, displaying the temperatures reaching as low as 20°C. Data sourced from CSIRO.

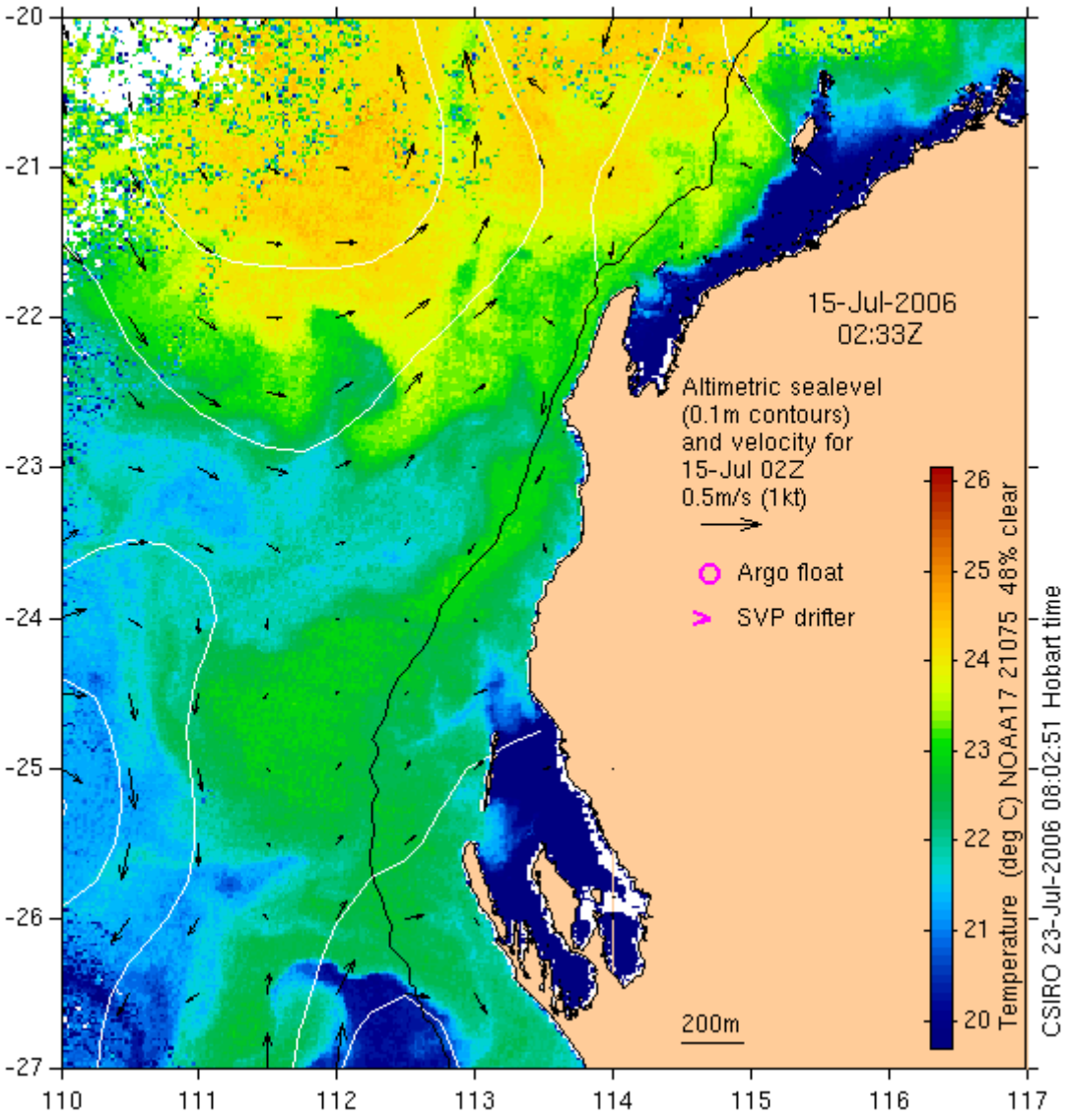

Chapter 6: Molecular Investigations into the intracellular ciliate

Photo: Doug Bearham and Morgan & Co. staff loading processing gear and specimens onto the Morgan &Co. seaplane at the end of a field trip in the Montebello Is., 2005

This Chapter is the findings of studies into the molecular characterisation of the intracellular ciliate. The first part is an investigation into PCR test development, with a view to sequencing the 16s ssu gene of the ciliate. Oyster DNA from formalin fixed, paraffin embedded sections were successfully extracted, amplified and sequenced. The second part of the Chapter was an in-situ hybridisation investigation using a probe designed from the 16s ssu gene of Phyllopharyngea ciliates, with some success.

6.1 PCR Test development

6.1.1 Introduction: Molecular tools for diagnosis and characterization

The use of molecular tools to diagnose and characterise disease-causing organisms is an expanding area of research. Polymerase Chain Reaction (PCR), when used correctly, is a very sensitive, specific tool in the detection of genetic material from an individual species. It is also a means to compare like species and determine their phylogenetics.

Many researchers to analyse relationships between members of the Phylum Ciliophora have used small sub-unit ribosomal DNA and RNA (ssu rDNA and rRNA). Phylogenetic relationships between the Classes, and individual species within the Classes, Phyllopharyngea (Snoeyenbos-West, Cole et al 2004), Spirotrichea (Shang, Chen et al 2002), Prostomatea, Colpodea, Nassophorea, Litostomatea (Stechmann, Schlegel et al 1998), Armophorea, Oligohymenophorea, Plagiopylea, Heterotrichea and Karyorelictea (Lynn, 2003) have been performed. Within the Class Phyllopharyngea, individuals representing all subclasses except Rhynchodia have been investigated (Snoeyenbos-West, Cole et al 2004), highlighting the difficulties in determining molecular information from this subclass of organisms.

Molecular techniques such as PCR are now recognised as sensitive and specific diagnostic tools for diseases in aquaculture. PCR tests have been developed for many pathogens of oysters including *Perkinsus* sp. (Goggin and Lester, 1995), *Haplosporidium* sp. (Burrenson and Reece, 2006) and *Minchinia* sp. (Bearham, Spiers et al 2007). Primers for PCR can be developed to be species or genera specific, and their relative low cost compared with traditional histological techniques mean surveillance of many individual oysters quickly and reliably is possible.

6.1.2 Materials and Methods

Extraction of DNA from samples

The samples used and the DNA extraction methods were described in detail in section 2.3. These included extraction from formalin fixed, paraffin embedded samples and fresh tissue.

Polymerase Chain Reaction

Each PCR was performed using reaction mixtures that had a total volume of 50ul and contained reaction buffer (67mM Tris-HCl, 16.6 mM (NH4)2SO4, 0.45% Triton X-100, 0.2 mg/mL gelatin, and 0.2 mM dNTPs), 2 mM of $MgCl_2$, 40 pmol of each primer, and 0.55 U of Taq polymerase and template DNA. Each of the reaction mixtures was subjected to: (1) an initial denaturation phase of 5 minutes at 94^{o}C, (ii) 35 amplication cycles, each cycle consisting of 30 seconds denaturation phase at

94^{o}C, 30 seconds of annealing at 48^{o}C, 4 min extension at 68^{o}C and (iii) a final 7 minutes extension at 68^{o}C. The success of each PCR was determined by loading a 10ul aliquot of the PCR products on a 2% agarose gel and electrophoresing it for 20 minutes at 46mA. Detection of the PCR products was performed using ethidium bromide staining. A P*hi*/*Hae*III Marker (Promega, Sydney) was used as a DNA standard and viewed using UV light supplied by a Gel DocTM (Bio Rad, Sydney). Digital images were viewed and saved by using the Quality One TM computer program (Bio Rad, Sydney).

Primers used during the study(5'–3')
Conserved regions were identified using GeneTool-Lite v1.0 program of the following ciliate sequences; *Glauconema trihymene* ssu rRNA gene, *Cardiostomatella vermeforme* 16s rRNA gene, *Dexitrichides pangi* 16s ssu rRNA gene, *Kiitricha marina* 16s rRNA gene, *Mesanophrys carcini* 16s ssu rRNA gene, *Paranophrys magna* 16s ssu rRNA gene, *Parauronema longum* 16s ssu rRNA gene and *Pseudokeronopsis flava* 16s rRNA gene.

F Cili 1	GGCCGTTCTTAGTTGGTGGAGTGAT
R Cili 1	CGCGTGCGGCCCASGACATMTA

Conserved regions were identified from numerous ciliates, based on the 16s ssu gene from *Loxodes striatus*, using GeneTool-Lite v1.0.

F Cili 2	GGCAGCAGGCGCGYAAATTACCC
F Cili 3	CYGGGGGGAGTATGGTCGCAAGRCTGAAAC
R Cili 2	GCGGCTGCTGGCACCA

Figure 6.1.1 displays the relative positions of the ciliate primers F Cili 1, F Cili 2, F Cili 3, R Cili 1 and R Cili 2 on the Ciliophora 16s ssu gene (not to scale).

Figure 6.1.1: The relative positions of the ciliate primers on the Ciliophora 16s ssu gene (not to scale).

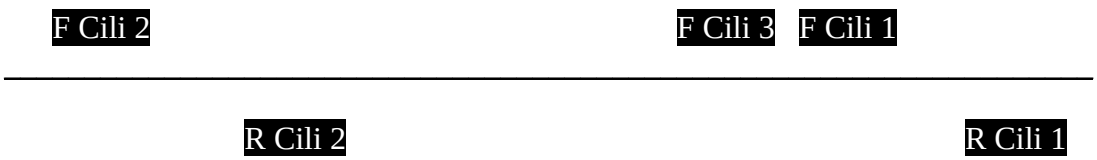

Conserved regions of multiple Ciliophora were multi-aligned using GeneTool-Lite v1.0 to produce the following primers.

ZOE B F1	CACCGCCCGTCGCTCCTACCG
ZOE B R1	TCACCTACGGAAACCTTGT
ZOE B F2	ACACCGCCCGTCGCTCCTA

Conserved regions of the 16s ssu gene from members of Phyllopharyngea were compared using GeneTool-Lite v1.0 to identify conserved regions, and the following primers were created. The product estimated to be around 242 base pairs.

F PHYLLO 1	CGGGAAAACTTACCAGGG
R PHYLLO 1	ACGCGTGCGGCCCAGAACTTC

Other primers used within the study were as follows.
To amplify bivalve DNA, to test extractions (Biotechniques 1998)

16 R3	GCTGTTATCCCTRNRGTA	Biotechniques 1998
Proto16F	AWRWGACRAGAAGAC	Biotechniques 1998

To amplify protozoal DNA in the preference to metazoan DNA (Bower, Carnegie et al 2004)

18S-EUK581-F	GTGCCAGCAGCCGCG
18S-EUK1134-R	TTTAAGTTTCAGCCTTGCG

To amplify Opalinid DNA, to rule out the ciliate being an opalinid (Kostka, Hampl 2004)

BA	CCATGGCAGTAAGGGGTAACGAA
PK	CACACCAGATATGGGTTATGC

DNA Sequencing
PCR products where purified for sequencing using a QIAquick PCR purification kit (QIAGEN) according to manufacturer's instructions. The cycle sequencing was then completed using Big Dye 3.1 sequencing chemistry.

The PCR products were run on polyacrylamide gels in an ABI 377 XL Automated Sequencer (Applied Biosystems), with reaction mixtures as follows (per tube); *ca* 350 ng template (*ca* 4 µL PCR product), 4 µL dye terminator mix, 1.0 µL ddH_20, 1.6 picomoles (1.6 µL at working solution) of either forward or reverse primer. To limit cost, each cycle sequencing reaction was performed at half the volume of the manufacturers' recommendations (Applied Biosystems). Each reaction was denatured at 96 ^oC for 2 minutes, run at 25 cycles, with 10 seconds denaturation at 96^oC, five seconds of annealing at 50^oC, 4 minutes of extension at 60^oC and finally cooling and holding at 8^oC (Figure 6.1.2).

The following ethanol precipitation procedure cleaned the sequencing products of unincorporated dye terminators. 1μL of 3M sodium acetate (pH 5.2), 1 μL of 125 mM EDTA (disodium salt) and 25μL of 100 % ethanol was added to each product, mixed, and placed on ice for 20 minutes. The tubes were then placed in a centrifuge for 30 minutes at 13000 rpm. The supernatant was discarded and the remaining pellet washed with 125μL of 80% ethanol and then centrifuged at room temperature for five minutes at 13000 rpm. The supernatant was again discarded, with the final pellet dried in a vacuum manifold for 15 minutes.

Figure 6.1.2: Polymerase Chain Reaction thermal cycler settings, repeated for 35 cycles unless otherwise stated, with an annealing temperature of 50°C, unless otherwise stated.

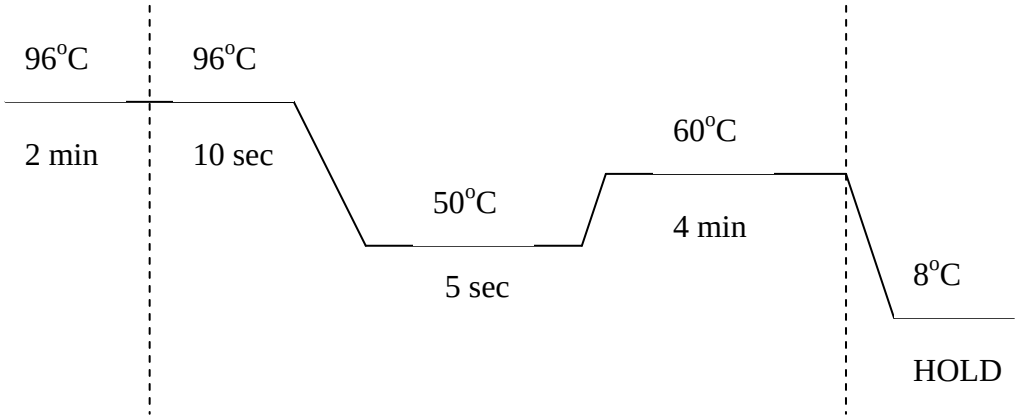

Before automated sequencing, the PCR products were mixed with a loading buffer consisting of 5:1 deionised formamide, 25 mM EDTA (pH 8.0) and 50 mg/mL blue dextran (Applied Biosystems). These were then denatured at 95°C for five minutes and stored on ice until loading. Approximately 0.8μL of each sample was loaded into wells on a 48cm well-to-read LongRanger™ polyacrylamide gel and run for about 11 hours according to the manufacturers protocol (Applied Biosystems).

Laser Dissection Microscopy

A formalin fixed, paraffin embedded oyster with a high burden of intracellular ciliate was chosen for Laser Dissection Microscopy. This was processed according to procedures outlined by the University of Western Australia Biomedical Imaging and Analysis Facility. Selected blocks were sectioned at 4-5um thin sections with no cover-slip. The slides were deparaffinised in xylene and air dried. The ciliates were identified on section and were catapulted into an eppendorf tube lid for further processing. These cells were extracted using Epicentre Cell Extraction protocol.

6.1.3 Results

Many primer sets were used during the course of this investigation. Of these sets, the following were the ones that produced some meaningful outcomes. The results obtained with the Laser Dissection Microscopy were also included.

The results associated with the F/R Cili 1 primer set
Formalin fixed, paraffin embedded pearl oyster samples with a heavy burden of ciliates were processed using the Freeze-Boil extraction method. These extractions were placed in a PCR reaction as described previously. At first, the thermal cycler reaction was repeated for 35 cycles with an annealing temperature of 48^{o}C. There were bright bands in the sample lanes, however there was also a band in the negative control lane (with no DNA). The annealing temperature was increased to 55^{o}C to attempt to increase the specificity of the annealing. There was still a bright band in the negative control lane. The annealing temperature was again increased, this time to 62^{o}C for 35 cycles. This reaction produced a difference between the negative control and the sample lanes. There was still an indistinct line in the gel <230 base pairs in length within the negative control lane, however in the sample lanes, there was a bright, distinct line at the range of 230-270 base pairs. These bright products were cut from the gel and sequenced according to the procedure described above. This sequence was identified using a BLAST search as *Pinctada maxima* 18s gene.

The results associated with the ZOE B F1/R1 primer set
Formalin fixed, paraffin embedded pearl oyster samples with a heavy burden of ciliates were processed using the Freeze-Boil extraction method. These extractions were placed in a PCR reaction as described previously. The thermal cycler reaction was repeated for 35 cycles with an annealing temperature of 44^{o}C. The negative control reaction contained no DNA. The positive control contained an extraction of *Paramecium caudatum* culture, and another negative control reaction contained an extraction of uninfected pearl oyster tissue. With this relatively low annealing temperature, all lanes of the ethidium bromide gel contained traces of DNA product. However, the lanes containing the *Paramecium* and the ciliate extractions were brighter and more distinct compared with the other lanes. The base pair length of the product appeared to be within the range expected (<300). The PCR product from this reaction was sequenced according to the procedure described above. This sequence was identified using a BLAST search as *Pinctada maxima* 18s gene.

The results associated with the ZOE B F2/R1 primer set
Formalin fixed, paraffin embedded pearl oyster samples with a heavy burden of ciliates were processed using the Freeze-Boil extraction method. These extractions were placed in a PCR reaction as described previously. The thermal cycler reaction was repeated for 35 cycles with an annealing temperature of 44^{o}C. The negative control reaction contained no DNA. The positive control contained an extraction of *Paramecium caudatum* culture, and another negative control reaction contained an

extraction of uninfected pearl oyster tissue. With this relatively low annealing temperature, all lanes of the ethidium bromide gel contained traces of DNA product. However, the lanes containing the *Paramecium* and the ciliate extractions were brighter and more distinct compared with the other lanes. The base pair length of the product appeared to be within the range expected (<300). The PCR product from this reaction was sequenced according to the procedure described above. This sequence was identified using a BLAST search as *Pinctada maxima* 18s gene.

The results associated with the 18S-EUK-581 F/18s-EUK-1134 R (Bower, Carnegie et al 2004) primer set

Formalin fixed, paraffin embedded pearl oyster samples with a heavy burden of ciliates were processed using the Freeze-Boil extraction method. These extractions were placed in a PCR reaction as described previously. The thermal cycler reaction was repeated for 35 cycles with an annealing temperature of 55^{o}C. The negative control reaction contained no DNA. The positive control contained an extraction of *Paramecium caudatum* culture, and another negative control reaction contained an extraction of uninfected pearl oyster tissue. This primer set successfully amplified *Paramecium* DNA, however was not able to amplify formalin fixed paraffin embedded tissue as effectively. These primers were then paired with various other ciliate primers to shorten the expected PCR product to be within suitable limits for formalin fixed material, however no other success was obtained.

The results associated with the PHYLLO R1/F1 primer set

Formalin fixed, paraffin embedded pearl oyster samples with a heavy burden of ciliates were processed using the Freeze-Boil extraction method. These extractions were placed in a PCR reaction as described previously. The thermal cycler reaction was repeated for 30 cycles with an annealing temperature of 55^{o}C. The negative control reaction contained no DNA. The positive control contained an extraction of *Paramecium caudatum* culture, and another negative control reaction contained an extraction of uninfected pearl oyster tissue. With this annealing temperature, all lanes of the ethidium bromide gel remained empty except the one containing the *Paramecium* sample. The reaction was then repeated with a higher $MgCl_2$ of 3.3mM, using the thermal cycler set at 50 cycles and an annealing temperature of 50^{o}C. This again produced no product except for the *Paramecium*. Finally, another PCR was performed with the $MgCl_2$ at 5mM, 50 cycles and an annealing temperature of 50^{o}C. This reaction contained an additional sample of the ciliate extraction mixed with the *Paramecium* sample, to discover whether an inhibitory substance in the ciliate sample may have been obscuring the results. A faint band appeared in all lanes of the gel, except the Paramecium and the Paramecium + ciliate lanes that contained a bright, distinct line. The PCR of the ciliate sample with this primer set was repeated and the product was sequenced. The sequence results were difficult to interpret since they were multilayered, suggesting the primers were not as specific as required.

The results associated with the use of Laser Dissection Microscopy

The extractions obtained using the Laser Dissection Microscope were placed in a PCR reaction as described previously. The thermal cycler reaction was repeated for 35 cycles with an annealing temperature of 44^{o}C. The negative control reaction contained no DNA. The positive control contained an extraction of *Paramecium caudatum* culture, and another negative control reaction contained an extraction of uninfected pearl oyster tissue. Several primer sets were used in this PCR. The sets that produced positive results were F/R Cili 1 to amplify ciliate DNA and 16R3/Proto16F to detect oyster DNA. These reactions were repeated with an annealing temperature of 48^{o}C, and the PCR product was sequenced. Unfortunately, the sequence results suggested mixed DNA sequences, indicating the primers were not as specific as required for these samples.

6.1.4 Discussion

Unfortunately, the investigation into the molecular aspects of the intracellular ciliate failed to produce a sequence of use in its phylogenetic characterization. However, formalin fixed, paraffin embedded oyster DNA was successfully extracted, amplified and sequenced, indicating the process is adequate for this type of material.

DNA extraction and amplification of intracellular organisms provides a unique set of obstacles for the molecular biologist. One major complication is the unavoidable risk of host DNA overwhelming the parasite DNA and thereby producing a stronger product than the parasite. This is particularly so when first designing primers, when the sequence of the primers are not perfectly complementary to the target gene. In order to test this theory, in-situ hybridization was performed to identify whether the primers were in fact binding to the parasite, discussed in section 6.2.

Another complication was due to the only available samples being formalin fixed and embedded in paraffin. Formalin fixation produces DNA-protein cross-linkages and can cause fragmentation, thereby resulting in decreased length and quality of extracted DNA (Gilbert, Haselkorn, et al. 2007). Popular universal primers, such as those designed by Medlin, Elwood et al 1988 and Bower and Carnegie et al 2004, are of limited use in this case due to their long PCR product of approximately 1800 and 544 base pairs, respectively.

Inhibitory substances can hinder some PCR reactions, such as by inhibiting the activity of *Taq* polymerase enzyme (Moreno, Botella et al 2004). They can be from varying substances such as Immunoglobulin G (Al-Soud, Jonsson et al 2000), leukocyte DNA and heme compounds (Morata, Queipo-Ortuno et al 1998), to name a few. To test whether this was occurring with the ciliate samples, the extractions from formalin-fixed, paraffin embedded ciliates were mixed with *Paramecium* sp. extractions and processed by PCR. This produced a clear PCR product on gel, indicating there was no inhibitory substances limiting the efficiency of the PCR reaction in the ciliate samples. To be sure, in-situ hybridization was also performed

using these samples, as this technique is less prone to inhibitory substances (Moreno, Botella et al 2003).

Due to the numerous set backs during this study, an appropriate extraction protocol was identified, and successful sequencing reactions were performed. There is a rarity of information on intracellular ciliates, and this is probably due to the technical difficulties associated with this sort of investigation. However, a good start was made which can only be expanded upon for future investigators.

6.2 In situ hybridisation

6.2.1 Introduction

In-situ hybridization is a molecular technique used to visualize probe attachment to DNA while still in the tissue of origin. It offers the advantages of histology, by providing visual identification of the structures involved, and also the specificity and sensitivity of molecular techniques.

6.2.2 Materials and Methods

Probes were labelled with digoxigenin at the 5' end using DIG Oligonucleotide Tailing Kit (Roche Diagnostics) according to manufacturers protocol. Probes were developed using the following sequences:

R PHYLLO 1	5'ACG CGT GCG GCC CAG AAC TTC 3'
18S EUK 1134R	5' TTT AAG TTT CAG CCT TGC G 3'
SSR 69	5' AGCCCAAAACCAACAAAACGTCCACATGCG 3'

A 166 base pair probe based on the PCR product obtained with the primer set:

MinchF1B	5' CTCGCGGGCTCAGCTT 3'
MinchR2B	5' GGCGCTTTGCAGATTCCCCA 3'

Formalin fixed, paraffin embedded pearl oyster tissues were selected for this study based on whether they contained large numbers of intracellular ciliate, or Ancistrocomid ciliates for the positive control. Unstained sections of these blocks 6µm thick were placed on aminoalkylsilane-coated slides. These were then deparaffinised using xylene, re-hydrated in an ethanol series, rinsed and then immersed in pure water. The sections were then digested in a Proteinase K solution (Proteinase K 0.5g/mL, o.5mM Tris-HCl, pH 7.6) for 45 minutes, then immersed in pure water at 4^{o}C for 10 minutes. The pure water was replaced for another 10 minutes at 4^{o}C.

The post-fixing stage used 0.4% paraformaldehyde in x1 PBS pre-cooled to 4^{o}C for 20 minutes. The sections were then washed in pure water and incubated in a pre-hybridisation solution at 42^{o}C for 1 hour. The pre-hybridisation solution contained 1mM Tris-HCl pH 7.4, 20 mM standard saline citrate (SSC), 0.1mM EDTA, 5% (w/v) dextran sulfate and 50% (v/v) formamide.

The slides were then covered in 50µl of hybridisation solution and denatured for 15 minutes in a 95^{o}C oven. The hybridisation solution consisted of 1µg labelled probe with 1mM Tris-HCl pH 7.4, SSC 20mM, 0.1mM EDTA, 5% (w/v) dextran sulfate and 50% (v/v) formamide. After denaturation, the slides were transferred to a 42^{o}C oven and incubated overnight. The hybridisation solution was then drained off the slides and they were rinsed and immersed in 40mM SSC for 20 minutes. This rinse and immersion for 20 minutes was then repeated once. The slides were then incubated for 30 minutes at 42^{o}C in a solution of 0.1% SSC, 2mM $MgCl_2$ and 0.1% Triton X-100, and then covered in Tris-buffered saline containing 3% bovine serum albumin and 0.1% Triton X-100 (TBSBT) for 5 minutes. The sections were then incubated in anti-digoxigenin alkaline-phosphatase conjugate prediluted 1:600 in TBSBT for 30 minutes to detect hybridization of the probes. The sections were then washed in Tris-buffered saline and alkaline phosphatase substrate buffer for 5 minutes each. The slides were then stained with BM purple (Roche Applied Science) overnight and counterstained with Brazilian hematoxylin. Negative controls included uninfected sections and incubation with an identical hybridisation mix but without labelled probe.

6.2.3 Results

The results associated with the R PHYLLO 1 probe

Formalin fixed paraffin blocks treated with the PHYLLO probe produced a positive staining for the intracellular ciliate and the Ancistrocomid ciliates, with minimal background staining. Figure 6.2.1 are photomicrographs of the in-situ hybridisation of ciliate infected oysters using the R PHYLLO 1 probe. Figure 6.2.1 A is a photo of the digestive gland of a pearl oyster, inhabited by numerous intracellular ciliates, highlighted by dark blue staining. Figure 6.2.1 B is a photo of the digestive gland of a pearl oyster at higher magnification, displaying the dark blue stained nuclei of the intracellular ciliates. Figure 6.2.2 is also a photomicrograph of the in-situ hybridisation of oysters using the R PHYLLO 1 probe. This photo is of the Ancistrocomid positive control slide, indicating a dark blue staining associated with the Ancistrocomid nuclei. This probe positively stained both the intracellular ciliate and the Ancistrocomid ciliates, without staining the underlying oyster tissues, indicating the probe is closer to the sequence of the ciliate compared to the oyster.

Results associated with the 18S EUK 1134R probe

Formalin fixed paraffin blocks treated with the EUK probe failed to produced a positive staining for the intracellular ciliate or the Ancistrocomid ciliates. Figure 6.2.3 is a photo micrograph of the in-situ hybridisation of ciliate infected oysters

using the 18S EUK 1134R probe. Figure 6.2.3 A is a photo of the digestive gland of a pearl oyster, inhabited by numerous intracellular ciliates, none of which are staining positive using this probe. Figure 6.2.3 B is a photo of the Ancistrocomid positive control slide, indicating minimal positive staining for the ciliates using this probe.

Results associated with the oligonucleotide SSR 69 probe and the polynucleotide probe based on the PCR product obtained with the primer set MinchF1B and MinchR2B

These probes were developed based on the ssu rDNA gene of aligned haplosporidian parasites. The SSR 69 oligonucleotide probe was commercially synthesized (Geneworks, Sydney). During a study into the specificity of these probes, the polynucleotide probe produced strong positive signals for all Haplosporidian parasites tested, including individuals representing *Minchinia* sp., *Bonamia* sp. and *Haplosporidium* sp. The oligonucleotide was specific to members of *Minchinia* sp. (Bearham, Spiers et al 2007). Both probes failed to give a positive result for the intracellular ciliate. These results indicated that the intracellular ciliate was not closely related to the Haplosporidian parasites.

6.2.4 Discussion

In-situ hybridization was successfully performed on formalin fixed, paraffin embedded oyster tissues during this study. The probe that produced the most promising results, and the one that could be used in future research into this area, was the R PHYLLO 1 probe, designed by identifying conserved regions of the 16s ssu gene from members of Phyllopharyngea using GeneTool-Lite v1.0. It produced a positive staining on slides containing Ancistrocomid ciliates, and the intracellular ciliate, without staining the surrounding oyster tissue. This probe sequence was used as a reverse PCR primer in section 6.1, using a similarly designed forward primer F PHYLLO 1. Unfortunately a successful sequence could not be produced using this primer set, and based on these in-situ hybridisation results using the reverse probe, the problem may be linked to the unspecificity of the forward primer. Future study into an appropriate forward primer to pair with R PHYLLO 1 is needed.

Figure 6.2.1: The in-situ hybridisation of ciliate infected oysters using the R PHYLLO 1 probe. **A:** The digestive gland of a pearl oyster, inhabited by numerous intracellular ciliates, highlighted by dark blue staining, Scale bar: 80 µm. **B:** The digestive gland of a pearl oyster at higher magnification, displaying the dark blue stained nuclei of the intracellular ciliates, Scale: 20 µm.

A

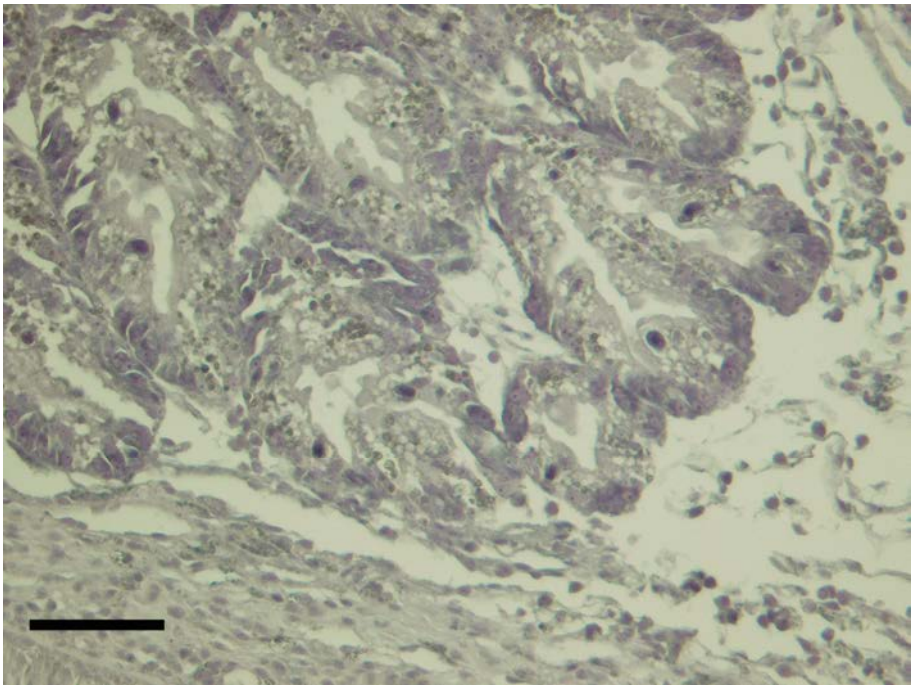

B

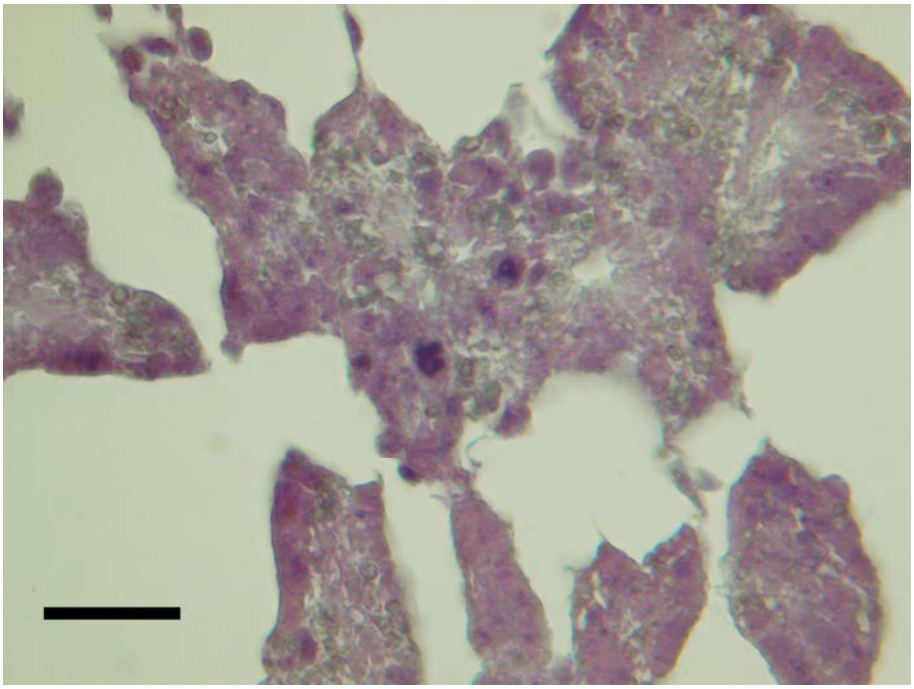

Figure 6.2.2: The in-situ hybridisation of oysters using the R PHYLLO 1 probe. This photo is of the Ancistrocomid positive control slide, indicating a dark blue staining associated with the Ancistrocomid nuclei. Scale bar: 80 µm.

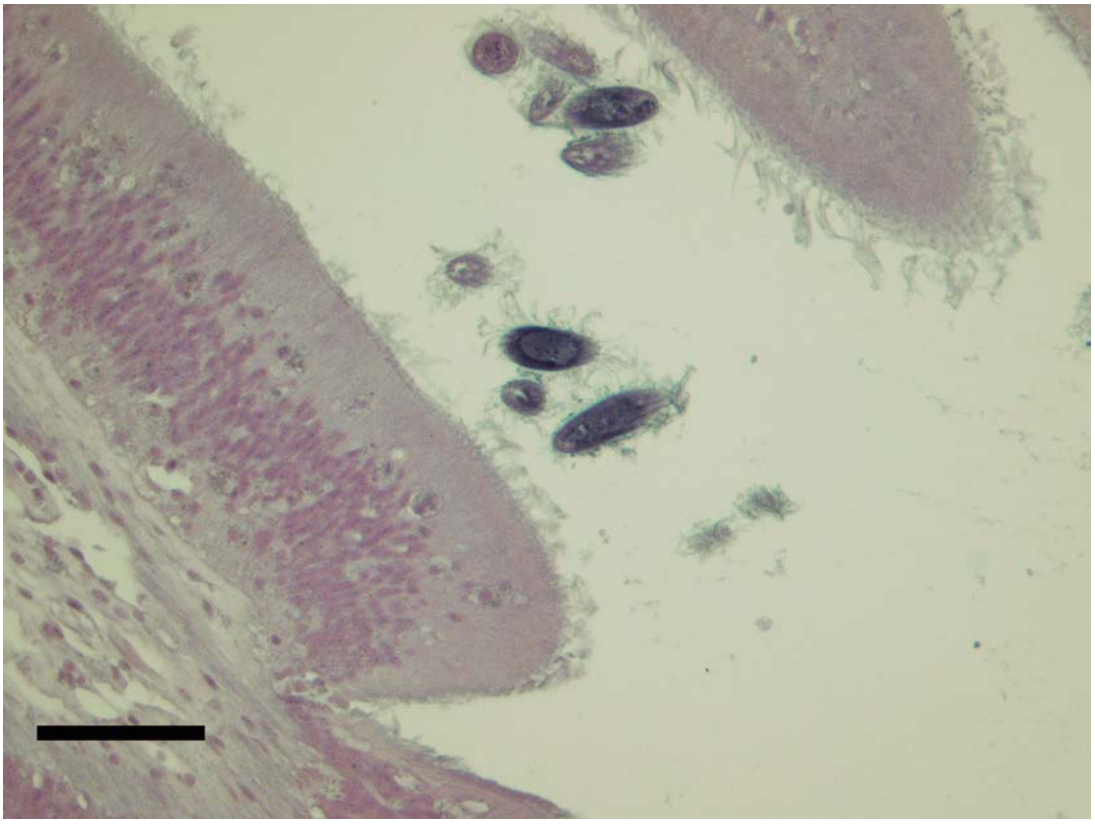

Figure 6.2.3: The in-situ hybridisation of ciliate infected oysters using the 18S EUK 1134R probe. **A:** The digestive gland of a pearl oyster, inhabited by numerous intracellular ciliates, none of which are staining positive using this probe, Scale bar: 80 µm. **B:** The Ancistrocomid positive control slide, indicating minimal positive staining for the ciliates using this probe, Scale: 80 µm.

A

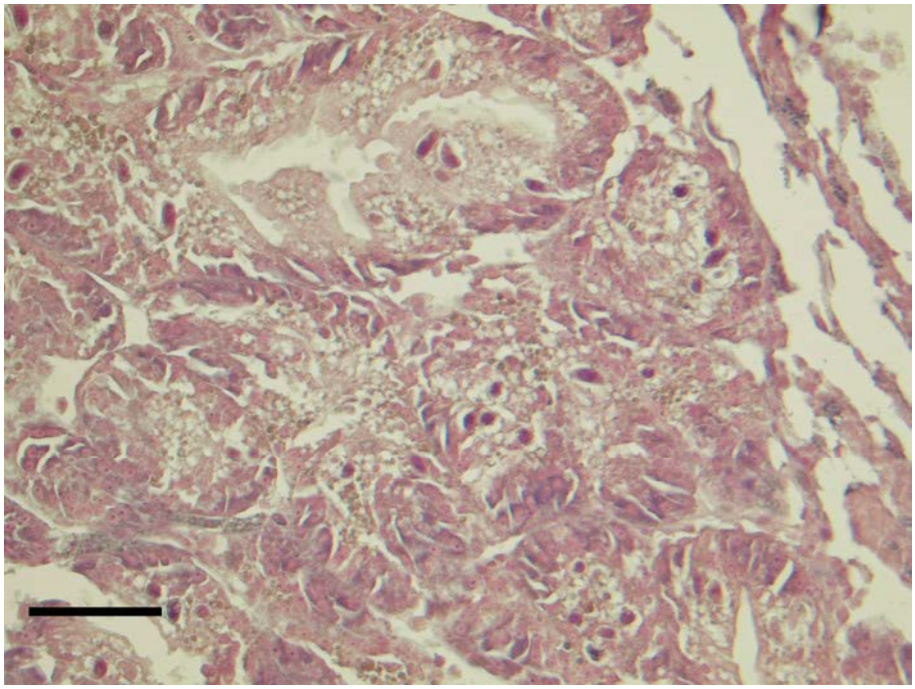

B

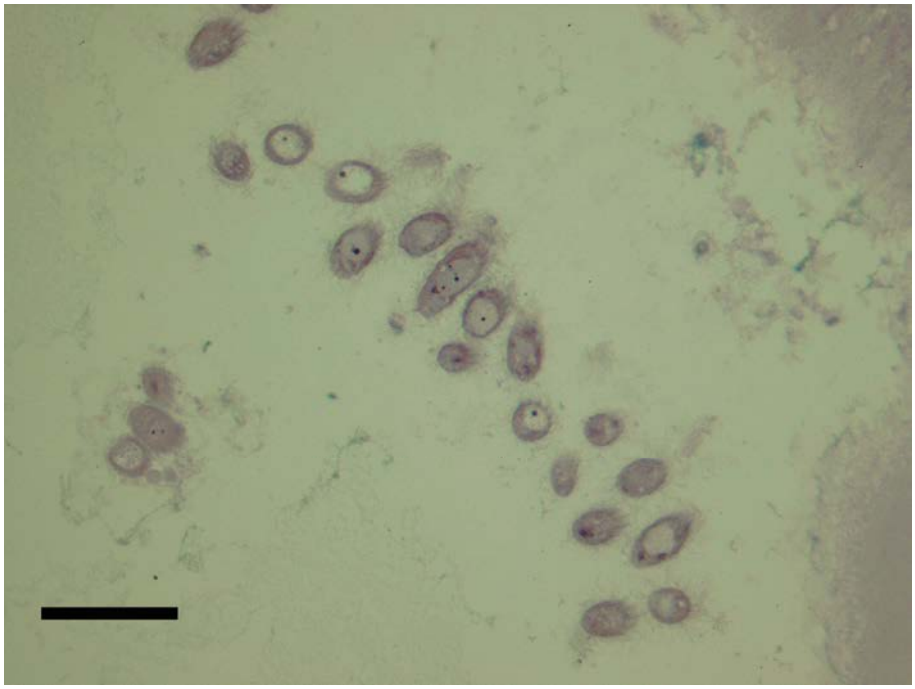

Chapter 7: Discussion

A new parasitic intracellular ciliate affecting Western Australian pearl oysters was investigated, in particular its morphological characteristics, pathological effects and distribution. A morphology study revealed a ciliated protozoan with features suggestive of a classification within the Rhynchodid ciliates of the Ciliophora class Phyllopharyngea; however, definitive classification was not achieved. This was due to the only available samples being formalin fixed, paraffin embedded tissues, which are undesirable for detailed morphological visualisation. The limitations of these processed tissues also restricted molecular investigations into the parasite, whereby prohibiting the phylogenetic classification of the organism.

A study was carried out on another intracellular ciliate that infects the digestive gland of commercially important mussels in Canada, and the similarities between the morphological characteristics of the two species were alarming. Given this new information, questions were raised as to the origin of the Western Australian parasite, and whether it was an exotic invader from the Northern Hemisphere. Another hypothesis was if the ciliate was an endemic parasite of another bivalve species in Western Australian waters, and has jumped host to occur in pearl oysters.

In order to address these concerns, a comprehensive survey was performed to assess the health and parasite status of other species of bivalves in areas close to affected farms. During this investigation, one male bastard oyster (*Pinctada* sp.) was found be infected with the intracellular ciliate. A debate of whether bastard oysters were the original host occurred, highlighting the Canadian intracellular ciliate's predilection for closely related *Mytilus* sp. If bastard oysters were identified as a reservoir for parasitic diseases of pearl oysters, this would present several serious management dilemmas in limiting the spread, as these oysters are common hitchhikers on pearl farm infrastructure.

Field trials were performed throughout the course of the project, placing naïve pearl oyster spat in areas of previous ciliate infections. These were designed as surveillance for ciliate infections on pearl farms and to give insight into the infectivity of the organism. Unfortunately, no intracellular ciliates were found during this study. Cyclonic activity in the area prohibited regular sampling of trial oysters. The oysters sampled were examined histologically and a comprehensive health survey was completed.

Meanwhile, in optimistic preparation for live ciliate-infected pearl oysters becoming available, cells from several organs of the pearl oyster were cultured in vitro. This was considered necessary if the growth of this assumed-obligate intracellular ciliate was to be achieved in the laboratory for complete morphological examination. Since the culture of bivalve cell lines is a much needed and poorly understood science, the

culture of mantle tissue derived cells, digestive gland derived cells and adductor muscle derived cells of silverlip pearl oysters during the course of this study was an important achievement. The commercial implications for this research in both the pearling industry and worldwide aquaculture should not be underestimated. Currently, donor oysters are required during the pearl seeding process to provide the nacre-producing mantle cells to transplant into the oysters. Bivalve aquaculture would profit greatly with the advent of a reliable bivalve cell line, particularly in the research of several economically important diseases.

In order to document the potential effect of the intracellular ciliate on the pearling industry, a study into the pathology associated with ciliate infections was completed. The ciliate was found to inhabit the apical cytoplasm of the oysters digestive cells within the digestive gland, causing pathological changes to the cells. A host reaction to the presence of the ciliate, a haemocytic infiltrate, was demonstrated using a histopathology survey. In light of this information, it would seem the ban on translocation of infected oysters out of Zone 1 was justified. This parasite adversely affects the nutrient absorbing organ of pearl oysters, and therefore could potentially affect the productivity of this commercially important bivalve.

To understand the epidemiology of this disease, archival records from the Western Australian Department of Fisheries were analysed. The geographic distribution of the parasite, its prevalence during outbreaks and the implications of environmental conditions in these cases were investigated. The disease was found to have the highest prevalence during the summer months of warmer ambient temperature, warmer seawater temperatures and reduced rainfall, and presumably higher salinity. Whether this was due to environmental conditions or to management practices remains to be proven.

7.1 Further development

The complete characterisation and identification of this parasite was severely hampered during the course of this project by the lack of live ciliate-infected pearl oysters available. Complete taxonomic characterisation of an organism requires a range of visualisation techniques, including histology, TEM, SEM, live observations and special stains. Molecular techniques can also give insight into its taxonomic affiliations, however this also requires correctly preserved specimens and specific primer design.

Long-term field trials involving ciliate-infected pearl oysters are required to understand the pathogenicity of the parasite and the precise effect that this organism has on the growth and productivity of the pearl oyster. As with any production animal, any threat to the health of a pearl oyster in the farm environment must be taken seriously, as it could have a significant financial impact in the long term. Aquarium cross infection trials could reveal important epidemiological factors of this disease, such as temperature, salinity and species specificity.

The Western Australian pearl industry has had few serious disease problems in the past. This being said, with an increase in the industry's dependability on hatchery reared oysters, and the resultant intensification of industry practices, the potential for new disease causing organisms to be discovered has never been more apparent. As a result, it is absolutely necessary to have a clear protocol for sample collection in the event of any new disease outbreak.

As an essential outcome of this project, a complete sample collection protocol was created, outlining the samples required for an initial characterisation of an organism (Appendix 8.7). These include the identification of individual oysters, to be sagittally sectioned with one half processed for histology in order to identify disease-infected individuals, and the other half fixed correctly for either molecular investigation or ultrastructural viewing using SEM or TEM. Due to the sporadic nature of some diseases, it cannot be assumed infected pearl oysters will become available during the course of a project. The need for immediate quarantine and the destruction of infected oysters is understandable, however it is also important to correctly identify the aetiological agent so tailored management measures can be put in place to limit the spread.

As transcontinental travel becomes commonplace in the world today, the transmission of diseases which have a potentially devastating impact on aquacultural species will continue to be a threat. Strict controls imposed by Government bodies to limit the translocation of disease-infected stock go a long way to limit local spread of known diseases. International collaboration with specialists in aquatic animal health will help to identify diseases originating from further a field, and should be encouraged. Successful identification, management and containment of diseases affecting bivalves in other countries will limit the possibility of spread to Australian shores, thereby helping to ensure the productivity and profitability of our aquaculture industry for years to come.

7.2 Planned outcomes

A planned outcome of the project was the postgraduate training of a veterinary scientist in aquatic animal health pathology, specifically in molluscan pathology. This has been achieved through using the proect as a postgraduate research training degree for Dr Zoe Spiers who has continued to pursue higher training in the field of Veterinary Pathology. There is an international shortage of Veterinary Pathologists and only a very small percentage of these have expertise in molluscan pathology.

By describing the host parasite interaction and host response that oysters mount against the infection it has been possible to discover significant new knowledge of this potentially serious disease. This information will provide evidence that can

significantly influence the revision and development of regulations that govern the movement and management of stock particularly for the benefit of Zone 1 pearling industry stakeholders.

7.3 Conclusions

A new intracellular ciliate infection of pearl oysters was described and found to be very similar in morphology to a ciliate found in Canadian mussels. The possibility that these two infections are caused by the same or very closely related organisms cannot be dismissed.

No intracellular ciliates were detected in naïve *P maxima* spat held in controlled field trials to detect the natural host of the organism. The locations were deliberately chosen from farm leases that had previous outbreaks of ciliate infection in order to detect if a reservoir of infection persisted in such environments. With a total of 345 bivalves surveyed during 2005 to 2007, from 8 geographical locations and over 11 species of bivalve included, only one bastard shell (*Pinctada* sp.) oyster contained the intracellular parasite and only one protozoal parasite was identified in a novel host bivalve species.

A positive correlation between the presence of the ciliate and an inflammatory response of the digestive gland was demonstrated using statistical techniques. Pathological changes to the infected cells were demonstrated using histopathology and electronmicroscopy but the sensitivity of histology to detect ciliates in at risk populations was low (38%) to moderate (50%).

These findings indicate that the infection does have the potential to significantly reduce the health of infected oysters. However, there is little evidence that under current extensive field conditions that this infection alone is causing high enough mortality or morbidity in susceptible stock to significantly interrupt commercial operations. Nevertheless, the infection may have the potential to significantly affect the viability of artificially reared stock under hatchery conditions should it become established under such conditions.

Methods were developed to culture adductor muscle, mantle tissue and digestive gland derived cells from pearl oysters and cells could be maintained *in vitro* for up to 75 days, using a number of varying cell culture media. This information will greatly improve the future diagnosis of parasitic, bacterial and viral intracellular infections that require the use of such *in vitro* culturing techniques. An experimental design for a cross infection trial using oysters held under strict biosecure conditions at Murdoch University, should the ciliate or any other potential pathogen become available, was completed.

7.4 Benefits and adoption

The knowledge generated by this project will be a significant benefit to any future revision of the policy and procedures governing the regulation of stock movement between pearling zones of Western Australia. The results of this study indicate that there is little evidence that this ciliate infection is currently causing any significant impact on production.

Building on work of Hine and Thorne (1998) this project included an extensive survey of shellfish associated with pearl oystes. The epidemiological data, and the results of the study determining the limits of detection and sensitivity of histopathological examination for the detection of the ciliate in tissues, will significantly improve the confidence of surveillance sampling regimes designed to certify stock free from disease. A revision of the samples that need to be collected and preserved in the event of a new disease outbreak as well as the logistical issues associated with transporting perisherable samples long distances will be of great benefit to future disease investigations.

This study has shown the potential to culture *P maxima* tissues in the laboratory and the new knowledge generated concerning the *in vitro* culture of oyster cells will be of great benefit to anyone requiring the use of this technique. Such information is necessary to culture viral and intracellular bacterial infections and may provide other hitherto unrecognised benefits to the industry.

There is a significant national benefit in the postgraduate training of a veterinary pathologist in molluscan pathology. Dr Spiers is highly likely to be retained in this professional capacity for the long term and her continuing education, expertise and leadership potential should be recognised and supported.

Appendices

8.1 Composition of fixatives and algae culture media

8.1.1 10% Sea water buffered formalin solution

To make 1L of fixative solution:
Stabilform Formaldehyde 37/7 (30-60% Formaldehyde, 1-<10% Methanol) 100 mL
Sea water 900 mL

This solution can be made up on site using clean sea water. Care must be taken when handling Stabilform Formaldehyde and appropriate clothing should be worn. Small oysters should have their shells opened to allow the formalin solution to penetrate the tissues quickly, and for larger oysters, tissues should be sliced into 1cm this sections before fixation. At least 24 hours should be allowed for full fixation. After which tissues may be removed from formalin, washed in tap water, wrapped in damp gauze for transportation.

8.1.2 Guillard's F2 Medium for algae culture (Jeffrey and LeRoi 1997)

Major Nutrients
The following was dissolved in 100mL of distilled water; Sodium Nitrate ($NaNO_3$), 7.5 g and Sodium dihydrogen orthophosphate (NaH_2PO_4), 0.5 g.

Trace Metals
Stock Solutions
Separate stock solutions were prepared by dissolving each of the following in 100mL of distilled water; Cupric pentahydrate ($CuSO_4.5H_2O$), 0.98 g; Zinc Sulphate heptahydrate ($ZnSO_4.7H_2O$) , 2.2 g; Cobalt chloride hexahydrate ($CoCl_2.6H_2O$), 1.0 g; Manganese chloride tetrahydrate ($MnCl_2.4H_2O$), 18.0 g; Sodium Molybdate dihydrate ($Na_2MoO_4.2H_2O$), 0.63 g.
Working Solution
The following was dissolved in 1 L of distilled water, with the aid of a heater/stirrer; Citric acid ($C_6H_8O_7.H_2O$), 16.8 g; Ferric Citrate ($FeC_6H_5O_7.H_2O$), 3.0 g; 1 mL of each metal stock solution.

Vitamins
Stock solution
10mg of biotin was weighed out and brought to 96 mL with distilled water, then 27.75 mg of B12 was also weighed out and brought to 25 mL with distilled water. Into small vials was added 2 mL of the biotin solution and 0.2 mL of the B12 solution. Vials were frozen until a working solution was prepared.
Working solution
Stock solution vial was thawed and added to 100 mL of distilled water. 40 mg of thiamine was added and brought to 200 mL with distilled water. It was mixed thoroughly and kept refrigerated. The major nutrients and trace metals were added to the algal cultures at 1 mL/L and the vitamins at 0.5 mL/L.

8.2 Composition of media used in bivalve cell culture

8.2.1 Composition of L-15 Medium Leibovitz

Leibovitz with L-glutamine, (Sigma-Aldrich) Components (g/L)

Calcium Chloride (anhydrous) - 0.1396
Magnesium Chloride (anhydrous) – 0.09366
Magnesium Sulphate (anhydrous) – 0.09767
Potassium Chloride – 0.4
Potassium Phosphate Monobasic (anhydrous) – 0.06
Sodium Chloride – 8.0
Sodium Phosphate Dibasic (anhydrous) – 0.19
L-Alanine – 0.225
L-Alanine (free base) – 0.5
L-Aspargine (anhydrous) – 0.25
L-Cysteine (free base) – 0.12
L-Glutamine – 0.3
L-Glycine – 0.2
L-Histidine – 0.25
L-Isoleucine – 0.125
L-Leucine – 0.125
L-Lysine Monohydrochloride – 0.0937
L-Methionine – 0.075
L-Phenylalanine – 0.125
L-Serine – 0.2
L-Threonine – 0.3
L-Tryptophan – 0.02
L-Tyrosine (free base) – 0.3
L-Valine – 0.1
Choline Chloride – 0.001
Flavin Mononucleotide-Na – 0.0001
Folic Acid – 0.001
Myo-Inositol – 0.002
Niacinamide – 0.001
DL-Pantothenic Acid (hemicalcium) – 0.001
Pyridoxine-HCl – 0.001
D-Galactose – 0.9
Phenol Red-Na – 0.011
Pyruvic Acid-Na – 0.55

8.3 Pearl oyster field trial survey results

July 2005 Montebellos Field Trip

Bivalve #	Slide #	Origin	Date	Species	Sex	Size (mm)	Comments
1	HO5-0638 G	Turtle Bay	Jul-05	P.maxima	U	42	metazoan parasite in mantle
2	HO5-0626 J	Turtle Bay	Jul-05	P.maxima	M		segmental parasite in perifery of DG
3	HO5-0626 L	Turtle Bay	Jul-05	P.maxima	U		NAD
4	HO5-0638 U	Turtle Bay	Jul-05	P.maxima	U	19	NAD
5	HO5-0639 B	Blue Bell	Jul-05	P.maxima	U		gregarine bodies in DG
6	HO5-0638 F	Blue Bell	Jul-05	P.maxima	U	38	no DG sectioned, NAD
7	HO5-0639 G	Blue Bell	Jul-05	P.maxima	U		gregarine bodies in DG, mild diffuse inflammation in DG
8	HO5-0638 I	Blue Bell	Jul-05	P.maxima	U	21	NAD
9	HO5-0638 X	Horseshoe	Jul-05	P.maxima	U		NAD
10	HO5-0638 E	Horseshoe	Jul-05	P.maxima	U		NAD
11	HO5-0638 O	Horseshoe	Jul-05	P.maxima	U		Ancistrocomid ciliate in gut, gregarine bodies in DG
12	HO5-0626 K	Horseshoe	Jul-05	P.maxima	U	32	NAD
13	HO5-0638 W	Burgundy	Jul-05	P.maxima	U		NAD
14	HO5-0638 D	Burgundy	Jul-05	P.maxima	U		NAD
15	HO5-0626 I	Burgundy	Jul-05	P.maxima	U		NAD
16	HO5-0638 V	Burgundy	Jul-05	P.maxima	U		NAD

September 2006 Exmouth Field Trip

Bivalve #	Slide #	Origin	Date	Species	Sex	Size (mm)	Comments
17	H06-0970K	Giralia Bay A	Sep-06	P.maxima	U	50	Diapedesis of cells into lumen of tubules, eosinophillic starburst
18	H06-0972J	Giralia Bay A	Sep-06	P.maxima	U	48	mf to coal mod infl DG, lrg metazoan in lumen of Dig tubules, sc organism
19	H06-969M	Giralia Bay A	Sep-06	P.maxima	U	47	Gregarine in DG
20	H06-0970D	Giralia Bay A	Sep-06	P.maxima	U	39	Greg,foc necr. DG
21	H06-0972S	Giralia Bay A	Sep-06	P.maxima	U	45	NAD
22	H06-968S	Giralia Bay A	Sep-06	P.maxima	U	40	NAD
23	H06-0973J	Giralia Bay A	Sep-06	P.maxima	U	47	sloughed epithelial cells
24	H06-0974J	Giralia Bay A	Sep-06	P.maxima	U	48	NAD
25	H06-0974T	Giralia Bay A	Sep-06	P.maxima	U	42	Greg, vacuolated eptih in DG - pink spherical inclusions inside cells
26	H06-969G	Giralia Bay A	Sep-06	P.maxima	U	48	Anc, Greg, metaz in DG and stomach
27	H06-969T	Giralia Bay A	Sep-06	P.maxima	U	43	Infiltrate of cells into lumen of DG, diapedesis
28	H06-0970B	Giralia Bay A	Sep-06	P.maxima	U	52	metaz in gut lumen
29	H06-0973S	Giralia Bay A	Sep-06	P.maxima	U	48	Anc in gut lumen, mf infl DG
30	H06-0973H	Giralia Bay A	Sep-06	P.maxima	U	42	focal necr of DG epith
31	H06-0971M	Giralia Bay A	Sep-06	P.maxima	U	50	Greg
32	H06-0975E	Giralia Bay A	Sep-06	P.maxima	U	44	Greg
33	H06-0974G	Giralia Bay A	Sep-06	P.maxima	U	44	mild diff infl DG
34	H06-0972F	Giralia Bay A	Sep-06	P.maxima	U	35	heavy Anc in gut, DG tubules, mod diff infl of DG and interstitium of gut
35	H06-0973E	Giralia Bay A	Sep-06	P.maxima	U	30	DG necr
36	H06-0975A	Giralia Bay A	Sep-06	P.maxima	U	42	DG gut necr
37	H06-968N	Giralia Bay A	Sep-06	P.maxima	U	54	gut necr
38	H06-0970E	Giralia Bay A	Sep-06	P.maxima	U	49	gut necr
39	H06-0971H	Giralia Bay A	Sep-06	P.maxima	U	63	focal necr of DG epith
40	H06-968T	Giralia Bay A	Sep-06	P.maxima	U	47	NAD
41	H06-0974H	Giralia Bay A	Sep-06	P.maxima	U	46	Greg, Anc in DG, diff mod infl DG, mod mf infl in palps and gut CT, sc organism
42	H06-0973D	Giralia Bay A	Sep-06	P.maxima	Male	22	Heavy Anc in stomach n oesoph n DG, diff mod infl DG, metaz in

Bivalve #	Slide #	Origin	Date	Species	Sex	Size (mm)	Comments
							stomach
43	H06-0971K	Giralia Bay A	Sep-06	P.maxima	U	48	NAD
44	H06-0974M	Giralia Bay A	Sep-06	P.maxima	U	43	Greg
45	H06-0972I	Giralia Bay A	Sep-06	P.maxima	U	36	Metaz in oesoph
46	H06-0971J	Giralia Bay A	Sep-06	P.maxima	U	46	NAD
47	H06-0971L	Giralia Bay A	Sep-06	P.maxima	U	42	Heavy Anc in gut, focally extensive severe infl in DG
48	H06-0970R	Giralia Bay A	Sep-06	P.maxima	U	46	NAD
49	H06-0974I	Giralia Bay A	Sep-06	P.maxima	U	46	NAD
50	H06-0972H	Giralia Bay A	Sep-06	P.maxima	U	53	NAD
51	H06-0970I	Giralia Bay A	Sep-06	P.maxima	U	56	NAD
52	H06-0974B	Giralia Bay A	Sep-06	P.maxima	U	39	mild diff infl DG
53	H06-0970A	Giralia Bay A	Sep-06	P.maxima	U	47	focal necr of DG epith
54	H06-0971I	Giralia Bay A	Sep-06	P.maxima	U	41	mf mod infl in interstitium of gill, mild infl DG, oedema of CT
55	H06-0974F	Giralia Bay A	Sep-06	P.maxima	U	41	Anc mod in gut, Greg, diff mild infl DG and interstitium of gut
56	H06-0970M	Giralia Bay A	Sep-06	P.maxima	U	44	diff infl of interst of gut
57	H06-0972N	Giralia Bay A	Sep-06	P.maxima	U	34	Greg
58	H06-0975G	Giralia Bay A	Sep-06	P.maxima	U	48	NAD
59	H06-0972G	Giralia Bay A	Sep-06	P.maxima	U	30	Mild diff infl interst of gut
60	H06-0972M	Giralia Bay A	Sep-06	P.maxima	U	51	Heavy Anc in gut, DG tubules, mild diff infl DG
61	H06-0970H	Giralia Bay A	Sep-06	P.maxima	U	52	Anc in DG tubules
62	H06-0975O	Giralia Bay A	Sep-06	P.maxima	U	48	focal deg necr of DG epith – chronic metaz infection
63	H06-0973C	Giralia Bay A	Sep-06	P.maxima	U	59	NAD
64	H06-0971G	Giralia Bay A	Sep-06	P.maxima	U	43	Granuloma in CT near DG
65	H06-0970O	Giralia Bay A	Sep-06	P.maxima	U	46	NAD
66	H06-0972Q	Giralia Bay A	Sep-06	P.maxima	U	40	Greg
67	H06-0970C	Giralia Bay A	Sep-06	P.maxima	U	50	Greg
68	H06-0975D	Giralia Bay A	Sep-06	P.maxima	U	38	Greg, granuloma in CT of mantle
69	H06-0971F	Giralia Bay A	Sep-06	P.maxima	U	37	Anc, focal deg necr DG (chronic parasite)
70	H06-0979S	Giralia Bay A	Sep-06	P.maxima	U	30	Anc, Greg
71	H06-0973M	Giralia Bay A	Sep-06	P.maxima	U	50	ciliates OR sloughed epith cells in DG lumen
72	H06-0971C	Giralia Bay A	Sep-06	P.maxima	U	44	Heavy Anc in gut, diff mild infl DG
73	H06-969D	Giralia Bay A	Sep-06	P.maxima	U	36	NAD
74	H06-0971B	Giralia Bay A	Sep-06	P.maxima	U	33	NAD
75	H06-969K	Giralia Bay A	Sep-06	P.maxima	U	34	NAD
76	H06-0975N	Giralia Bay A	Sep-06	P.maxima	U	35	NAD
77	H06-0975T	Giralia Bay A	Sep-06	P.maxima	U	43	Greg
78	H06-0974P	Giralia Bay A	Sep-06	P.maxima	U	40	Anc, Greg, granuloma in CT palps
79	H06-0973R	Giralia Bay A	Sep-06	P.maxima	U	32	NAD
80	H06-969A	Giralia Bay A	Sep-06	P.maxima	U	40	Greg, mf to coal deg necr DG
81	H06-969P	Giralia Bay A	Sep-06	P.maxima	U	34	Heavy Anc gut and DG
82	H06-0974A	Giralia Bay A	Sep-06	P.maxima	U	40	focal necr DG, focally extensive h/c infiltrate efacing DG (50%) w necr
83	H06-0973K	Giralia Bay A	Sep-06	P.maxima	U	35	NAD
84	H06-0973B	Giralia Bay A	Sep-06	P.maxima	U	32	Greg
85	H06-0974K	Giralia Bay A	Sep-06	P.maxima	U	34	Greg
86	H06-0972L	Giralia Bay A	Sep-06	P.maxima	U	34	NAD
87	H06-969B	Giralia Bay A	Sep-06	P.maxima	U	32	Anc, massive diff necr deg DG, gut, Greg in lumen gut, bacteria epth CT of palps
88	H06-0972P	Giralia Bay A	Sep-06	P.maxima	U	39	Greg, necr deg DG. Palps
89	H06-0973P	Giralia Bay A	Sep-06	P.maxima	M	29	NAD
90	H06-968C	Giralia Bay A	Sep-06	P.maxima	M	25	NAD
91	H06-968J	Giralia Bay A	Sep-06	P.maxima	U	29	Greg, mild diff infl DG
92	H06-968P	Giralia Bay A	Sep-06	P.maxima	U	44	Greg
93	H06-0978R	Giralia Bay A	Sep-06	P.maxima	U	31	Anc, metazoan in gut
94	H06-969J	Giralia Bay A	Sep-06	P.maxima	U	40	Greg
95	H06-0970Q	Giralia Bay A	Sep-06	P.maxima	U	41	NAD
96	H06-969F	Giralia Bay A	Sep-06	P.maxima	U	39	mild diff infl DG
97	H06-0975X	Giralia Bay A	Sep-06	P.maxima	U	33	Heavy Anc, diff mild infl DG
98	H06-0973Q	Giralia Bay A	Sep-06	P.maxima	U	30	NAD
99	H06-0975C	Giralia Bay A	Sep-06	P.maxima	U	35	NAD
100	H06-0975S	Giralia Bay A	Sep-06	P.maxima	U	36	Greg, mod diff infl DG and CT og

Bivalve #	Slide #	Origin	Date	Species	Sex	Size (mm)	Comments
							gut
101	H06-968A	Giralia Bay A	Sep-06	P.maxima	U	40	diff, mod infl DG, foc necr deg, sloughing, metazoan in lumen of gut
102	H06-0974O	Giralia Bay A	Sep-06	P.maxima	M	44	NAD
103	H06-0971Q	Giralia Bay A	Sep-06	P.maxima	U	35	foc deg, necr DG with intralesional metazoan
104	H06-0975R	Giralia Bay A	Sep-06	P.maxima	U	44	Greg, diff mild infl DG
105	H06-0975H	Giralia Bay A	Sep-06	P.maxima	U	36	Anc
106	H06-968O	Giralia Bay A	Sep-06	P.maxima	U	36	Heavy Anc, metazoan in lumen
107	H06-0975Y	Giralia Bay A	Sep-06	P.maxima	U	45	Anc
108	H06-0971P	Giralia Bay A	Sep-06	P.maxima	U	39	Heavy Anc, Greg, mod diff infl DG
109	H06-969C	Giralia Bay A	Sep-06	P.maxima	U	42	foc deg, necr DG with intralesional metazoan
110	H06-0974L	Giralia Bay A	Sep-06	P.maxima	U	44	Greg, mf infl CT of gut
111	H06-968E	Giralia Bay A	Sep-06	P.maxima	U	31	NAD
112	H06-0975J	Giralia Bay A	Sep-06	P.maxima	M	36	necr deg DG focal
113	H06-0973G	Giralia Bay A	Sep-06	P.maxima	U	38	Oedema of CT
114	H06-0979H	Giralia Bay A	Sep-06	P.maxima	U	35	diff infl DG mild
115	H06-0975B	Giralia Bay A	Sep-06	P.maxima	U	37	NAD
116	H06-0970T	Giralia Bay A	Sep-06	P.maxima	U	45	Anc
117	H06-0970P	Giralia Bay A	Sep-06	P.maxima	U	42	mild infl mf CT gut
118	H06-968H	Giralia Bay A	Sep-06	P.maxima	U	38	Greg
119	H06-968K	Giralia Bay A	Sep-06	P.maxima	U	40	Greg
120	H06-0979R	Giralia Bay A	Sep-06	P.maxima	U	20	Greg
121	H06-968Q	Giralia Bay A	Sep-06	P.maxima	U	31	infl in CT of gut
122	H06-0975V	Giralia Bay A	Sep-06	P.maxima	U	50	Greg, mf infl CT of gut and mantle
123	H06-0972C	Giralia Bay A	Sep-06	P.maxima	U	40	mod diff infl DG
124	H06-969O	Giralia Bay A	Sep-06	P.maxima	U	36	Anc
125	H06-968B	Giralia Bay A	Sep-06	P.maxima	M	23	metazoan in lumen of gut
126	H06-968I	Giralia Bay A	Sep-06	P.maxima	U	37	NAD
127	H06-0974Q	Giralia Bay A	Sep-06	P.maxima	M	40	mf to coal mod infl with some necr assoc
128	H06-0973L	Giralia Bay A	Sep-06	P.maxima	U	40	foc deg necr DG. Diff mild infl DG
129	H06-0973T	Giralia Bay A	Sep-06	P.maxima	U	30	Heavy Anc
130	H06-0975P	Giralia Bay A	Sep-06	P.maxima	U	15	Anc, necr deg palp epith with intrales bacteria
131	H06-0972E	Giralia Bay A	Sep-06	P.maxima	U	43	deg necr intrales bacteria in DG, palps, epith, CT
132	H06-0972T	Giralia Bay A	Sep-06	P.maxima	U	31	NAD
133	H06-969Q	Giralia Bay A	Sep-06	P.maxima	U	35	necr deg gut epth, DG, intrales bacteria
134	H06-0972B	Giralia Bay A	Sep-06	P.maxima	U	45	mf infl mod DG with assoc necr deg of DG tubules
135	H06-0974E	Giralia Bay A	Sep-06	P.maxima	M	33	foc mecr with intralestional metazoan
136	H06-0970L	Giralia Bay A	Sep-06	P.maxima	U	40	foc necr deg DG
137	H06-0971A	Giralia Bay A	Sep-06	P.maxima	U	38	deg necr foc gut epith w intrales bacteria in CT
138	H06-0971N	Giralia Bay A	Sep-06	P.maxima	U	42	foc deg necr DG, foc mod infl heart
139	H06-0971D	Giralia Bay A	Sep-06	P.maxima	U	42	Greg, mild diff infl DG
140	H06-0975M	Giralia Bay A	Sep-06	P.maxima	U	38	diff mild infl foc necr DG
141	H06-0975K	Giralia Bay A	Sep-06	P.maxima	U	30	NAD
142	H06-0973F	Giralia Bay A	Sep-06	P.maxima	U	34	Greg
143	H06-0975Q	Giralia Bay A	Sep-06	P.maxima	M	34	NAD
144	H06-0974N	Giralia Bay A	Sep-06	P.maxima	U	38	deg necr DG and gut epth w intrales bacteria
145	H06-968G	Giralia Bay A	Sep-06	P.maxima	U	49	NAD
146	H06-969L	Giralia Bay A	Sep-06	P.maxima	U	47	Greg
147	H06-0971T	Giralia Bay A	Sep-06	P.maxima	U	40	Anc
148	H06-0975U	Giralia Bay A	Sep-06	P.maxima	U	42	foc deg necr DG
149	H06-969E	Giralia Bay A	Sep-06	P.maxima	M	19	deg necr DG sloughing
150	H06-0971S	Giralia Bay A	Sep-06	P.maxima	U	14	NAD
151	H06-0974D	Giralia Bay A	Sep-06	P.maxima	U	41	NAD
152	H06-968M	Giralia Bay A	Sep-06	P.maxima	U	39	metazoan in DG tubule
153	H06-0971O	Giralia Bay A	Sep-06	P.maxima	U	45	Anc, foc necr deg DG, gut epth w intrales bacteria
154	H06-0975W	Giralia Bay A	Sep-06	P.maxima	U	39	Anc, mf infl CT of gut
155	H06-0971E	Giralia Bay A	Sep-06	P.maxima	U	47	Anc, Greg

Bivalve #	Slide #	Origin	Date	Species	Sex	Size (mm)	Comments
156	H06-0970J	Giralia Bay A	Sep-06	P.maxima	U	46	mf necr deg w mild infl DG
157	H06-968L	Giralia Bay A	Sep-06	P.maxima	M	34	NAD
158	H06-0975L	Giralia Bay A	Sep-06	P.maxima	U	38	Anc in gut
159	H06-0973N	Giralia Bay A	Sep-06	P.maxima	U	39	NAD
160	H06-0973A	Giralia Bay A	Sep-06	P.maxima	U	53	NAD
161	H06-968F	Giralia Bay A	Sep-06	P.maxima	U	43	deg necr mantle epith w bacteria
162	H06-0974R	Giralia Bay A	Sep-06	P.maxima	U	50	diff mild infl DG
163	H06-0970F	Giralia Bay A	Sep-06	P.maxima	U	25	metazoan in DG tubule
164	H06-969N	Giralia Bay A	Sep-06	P.maxima	U	44	Greg
165	H06-0971R	Giralia Bay A	Sep-06	P.maxima	U	46	necr deg mantle epith, DG w intrales bacteria
166	H06-0972D	Giralia Bay A	Sep-06	P.maxima	U	50	deg necr palp epth w bacteria
167	H06-0972R	Giralia Bay A	Sep-06	P.maxima	U	43	granuloma in DG
168	H06-0970S	Giralia Bay A	Sep-06	P.maxima	U	45	NAD
169	H06-0972O	Giralia Bay A	Sep-06	P.maxima	U	35	granuloma in DG
170	H06-0970N	Giralia Bay A	Sep-06	P.maxima	U	37	granuloma in CT near muscle
171	H06-0975I	Giralia Bay A	Sep-06	P.maxima	U	47	Anc, necr deg palp epth, DG, gut epth w bacteria foc infl
172	H06-0972K	Giralia Bay A	Sep-06	P.maxima	U	44	NAD
173	H06-0972A	Giralia Bay A	Sep-06	P.maxima	U	41	Anc in DG tubules
174	H06-969I	Giralia Bay A	Sep-06	P.maxima	U	43	NAD
175	H06-0973O	Giralia Bay A	Sep-06	P.maxima	U	53	Anc, mf infl in CT of gut
176	H06-0974C	Giralia Bay A	Sep-06	P.maxima	U	47	Anc, mod diff infl DG
177	H06-0974S	Giralia Bay A	Sep-06	P.maxima	U	48	Anc
178	H06-0975F	Giralia Bay A	Sep-06	P.maxima	U	43	Greg
179	H06-0970G	Giralia Bay A	Sep-06	P.maxima	U	42	foc necr deg infl gut epith, DG w bacteria
180	H06-0973I	Giralia Bay A	Sep-06	P.maxima	U	32	diff mild DG infl
181	H06-968D	Giralia Bay A	Sep-06	P.maxima	U	40	Greg

May 2007 Exmouth Field Trip

L1 = Line 1 transferred from Giralia one week previously

B1 = Bottom line transferred from Giralia 6 months previously

Bivalve	Slide #	Origin	Date	Species	Sex	Size (mm)	Comments
182	H07-0515A	L1 GalesBayB	May-07	P.maxima	U	29	Moderate diffuse inflammation of DG, pink filled vacuoles 5-10um in dig cells, loss of epith on palps
183	H07-0515B	L1 GalesBayB	May-07	P.maxima	U	34	mild - moderate inflammation in DG
184	H07-0515C	L1 GalesBayB	May-07	P.maxima	U	34	NAD
185	H07-0515D	L1 GalesBayB	May-07	P.maxima	U	30	moderate inflammation of DG, Rikketsial-like bodies in DG epithelium
186	H07-0515E	L1 GalesBayB	May-07	P.maxima	U	25	metaz in interstit of DG with focal infl
187	H07-0515F	L1 GalesBayB	May-07	P.maxima	U	35	NAD
188	H07-0515G	L1 GalesBayB	May-07	P.maxima	U	25	NAD
189	H07-0515H	L1 GalesBayB	May-07	P.maxima	U	38	mild - moderate inflammation in DG
190	H07-0515I	L1 GalesBayB	May-07	P.maxima	U	31	diff infl of gut interst, focal necr DG (cells swollen, piknotic nucl, structure remains)
191	H07-0515J	L1 GalesBayB	May-07	P.maxima	U	30	NAD
192	H07-0515K	L1 GalesBayB	May-07	P.maxima	U	30	NAD
193	H07-0515L	L1 GalesBayB	May-07	P.maxima	U	25	NAD
194	H07-0515M	L1 GalesBayB	May-07	P.maxima	U	35	diff necr/deg DG
195	H07-0515N	L1 GalesBayB	May-07	P.maxima	U	21	Rikketsial bodies in cytopl of DG - mod infn but no infl
196	H07-0515O	L1 GalesBayB	May-07	P.maxima	U	21	NAD
197	H07-0515P	L1 GalesBayB	May-07	P.maxima	U	20	NAD
198	H07-0515Q	L1 GalesBayB	May-07	P.maxima	U	12	NAD
199	H07-0515R	L1 GalesBayB	May-07	P.maxima	U	24	NAD
200	H07-0515S	L1 GalesBayB	May-07	P.maxima	U	25	focal sloughing of DG epith, piknotic nucl
201	H07-0515T	L1 GalesBayB	May-07	P.maxima	U	24	mod infl of DG, thinning loss of epith around add muscle
202	H07-0515U	B1 GalesBB	May-07	P.maxima	U	80	Loss of epith mantle, oed, foc necr

Bivalve	Slide #	Origin	Date	Species	Sex	Size (mm)	Comments
							DG, mf infl DG, Greg
203	H07-0515V	B1 GalesBB	May-07	P.maxima	M	75	expanded h/lymph vessels, loss of epith mantle
204	H07-0515W	B1 GalesBB	May-07	P.maxima	U	90	mild infl DG, epith loss
205	H07-0515X	B1 GalesBB	May-07	P.maxima	M	100	epth loss
206	H07-0515Y	B1 GalesBB	May-07	P.maxima	U	90	epth loss
207	H07-0516A	B1 GalesBB	May-07	P.maxima	U	60	Greg, mod infl DG
208	H07-0516B	B1 GalesBB	May-07	P.maxima	U	70	NAD
209	H07-0516C	B1 GalesBB	May-07	P.maxima	M	80	Anc in tubules
210	H07-0516D	B1 GalesBB	May-07	P.maxima	U	60	Granulomas with metaz in mantle CT, oed of epth mantle
211	H07-0516E	B1 GalesBB	May-07	P.maxima	U	80	some loss of epith
212	H07-0516F	B1 GalesBB	May-07	P.maxima	M	90	focal areas of DG necr
213	H07-0516G	B1 GalesBB	May-07	P.maxima	M	80	metaz in lumen of oesoph
214	H07-0516H	B1 GalesBB	May-07	P.maxima	M	90	focal areas of DG necr and epth sloughing, pik nucl, vacuol cytopl
215	H07-0516I	B1 GalesBB	May-07	P.maxima	U	80	Anc in tubules
216	H07-0516J	B1 GalesBB	May-07	P.maxima	U	90	Anc in tubules
217	H07-0516K	B1 GalesBB	May-07	P.maxima	M	80	Focal infl DG
218	H07-0516L	B1 GalesBB	May-07	P.maxima	M	100	Focal necr DG and oesoph, sloughing, Anc
219	H07-0516M	B1 GalesBB	May-07	P.maxima	M	80	NAD
220	H07-0516N	B1 GalesBB	May-07	P.maxima	M	80	Greg, focal sloughing of DG
221	H07-0516O	B1 GalesBB	May-07	P.maxima	M	80	NAD
222	H07-0516P	B1 GalesBB	May-07	P.maxima	U	60	mf infl CT mantle
223	H07-0516Q	B1 GalesBB	May-07	P.maxima	U	90	NAD
224	H07-0516R	B1 GalesBB	May-07	P.maxima	M	80	loss of gastric epith, Anc in lumen
225	H07-0516S	B1 GalesBB	May-07	P.maxima	M	60	Focal necr DG
226	H07-0516T	B1 GalesBB	May-07	P.maxima	M	80	mf infl DG and mantle CT, Anc in stomach
227	H07-0516U	B1 GalesBB	May-07	P.maxima	M	50	focal necr DG
228	H07-0516V	B1 GalesBB	May-07	P.maxima	M	80	mf areas infl DG
229	H07-0516W	B1 GalesBB	May-07	P.maxima	M	70	NAD
230	H07-0516X	B1 GalesBB	May-07	P.maxima	U	70	Granuloma in CT near DG, Diff mild infl DG, Anc in dig tubules
231	H07-0516Y	B1 GalesBB	May-07	P.maxima	U	70	Heavy Anc in stomach, diff mod infl DG mantle CT, organism in stomach

September 2006 Hatchery pearl oyster spat from Whalebone Island

Oyster	Slide	Origin	Date	Species	Sex	Size	Comment
232	H06-883K	Whalebone Is	Sep-06	P.maxima	U	25	NAD
233	H06-883K	Whalebone Is	Sep-06	P.maxima	U	20	Anc in tubules
234	H06-883K	Whalebone Is	Sep-06	P.maxima	U	20	foc deg necr DG
235	H06-883K	Whalebone Is	Sep-06	P.maxima	U	23	Anc
236	H06-883L	Whalebone Is	Sep-06	P.maxima	U	25	Anc
237	H06-883L	Whalebone Is	Sep-06	P.maxima	U	22	Anc in tubules
238	H06-883L	Whalebone Is	Sep-06	P.maxima	U	20	foc deg necr DG
239	H06-883L	Whalebone Is	Sep-06	P.maxima	U	24	Anc in tubules
240	H06-884A	Whalebone Is	Sep-06	P.maxima	U	20	mod diff infl DG
241	H06-884A	Whalebone Is	Sep-06	P.maxima	U	23	Anc in tubules
242	H06-884A	Whalebone Is	Sep-06	P.maxima	U	22	mf haemocytic aggregates in heart
243	H06-884A	Whalebone Is	Sep-06	P.maxima	U	20	Anc, mod mf infl DG with necrosis
244	H06-884A	Whalebone Is	Sep-06	P.maxima	U	22	foc ext deg necr DG
245	H06-884B	Whalebone Is	Sep-06	P.maxima	U	27	Anc, mod diff infl DG, mf mod infl gut
246	H06-884B	Whalebone Is	Sep-06	P.maxima	U	22	NAD
247	H06-884B	Whalebone Is	Sep-06	P.maxima	U	20	Anc, foc mild infl DG
248	H06-884B	Whalebone Is	Sep-06	P.maxima	U	21	Anc, mild mf infl DG
249	H06-884C	Whalebone Is	Sep-06	P.maxima	U	25	NAD
250	H06-884C	Whalebone Is	Sep-06	P.maxima	U	21	Anc, mild diff infl CT gut
251	H06-884C	Whalebone Is	Sep-06	P.maxima	U	20	Anc
252	H06-884C	Whalebone Is	Sep-06	P.maxima	U	24	Anc in tubules
252	H06-884C	Whalebone Is	Sep-06	P.maxima	U	24	Anc in tubules
253	H06-884D	Whalebone Is	Sep-06	P.maxima	U	22	mild foc infl DG
254	H06-884D	Whalebone Is	Sep-06	P.maxima	U	20	Anc, foc mild infl DG
255	H06-884D	Whalebone Is	Sep-06	P.maxima	U	21	Anc
256	H06-884D	Whalebone Is	Sep-06	P.maxima	U	22	deg necr epith stomach
257	H06-884E	Whalebone Is	Sep-06	P.maxima	U	23	Anc
258	H06-884E	Whalebone Is	Sep-06	P.maxima	U	21	Pea crab in mantle cavity
259	H06-884E	Whalebone Is	Sep-06	P.maxima	U	21	Anc
260	H06-884E	Whalebone Is	Sep-06	P.maxima	U	25	Anc
261	H06-884F	Whalebone Is	Sep-06	P.maxima	U	26	mild diff infl CT gut
262	H06-884F	Whalebone Is	Sep-06	P.maxima	U	20	NAD
263	H06-884F	Whalebone Is	Sep-06	P.maxima	U	21	metazoan in gut lumen, mf infl DG
264	H06-884F	Whalebone Is	Sep-06	P.maxima	U	25	NAD
265	H06-884G	Whalebone Is	Sep-06	P.maxima	U	23	Anc
266	H06-884G	Whalebone Is	Sep-06	P.maxima	U	28	NAD
267	H06-884G	Whalebone Is	Sep-06	P.maxima	U	20	Anc
268	H06-884G	Whalebone Is	Sep-06	P.maxima	U	24	NAD
269	H06-884H	Whalebone Is	Sep-06	P.maxima	U	19	NAD
270	H06-884H	Whalebone Is	Sep-06	P.maxima	U	22	Anc, mf necr deg DG
271	H06-884H	Whalebone Is	Sep-06	P.maxima	U	22	mf mild infl CT gut
272	H06-884H	Whalebone Is	Sep-06	P.maxima	U	29	NAD
273	H06-884H	Whalebone Is	Sep-06	P.maxima	U	21	NAD
274	H06-884J	Whalebone Is	Sep-06	P.maxima	U	17	Anc
275	H06-884J	Whalebone Is	Sep-06	P.maxima	U	21	Anc, mild diff infl DG
276	H06-884J	Whalebone Is	Sep-06	P.maxima	U	17	Anc in tubules
277	H06-884J	Whalebone Is	Sep-06	P.maxima	U	19	Anc
278	H06-884J	Whalebone Is	Sep-06	P.maxima	U	21	Anc, foc ext deg necr DG
279	H06-884K	Whalebone Is	Sep-06	P.maxima	U	22	Anc
280	H06-884K	Whalebone Is	Sep-06	P.maxima	U	23	Anc
281	H06-884K	Whalebone Is	Sep-06	P.maxima	U	22	Anc, oedema in CT
282	H06-884K	Whalebone Is	Sep-06	P.maxima	U	26	Anc, mild diff infl CT gut
283	H06-884L	Whalebone Is	Sep-06	P.maxima	U	23	oedema of CT gut
284	H06-884L	Whalebone Is	Sep-06	P.maxima	U	29	NAD

8.5 Protocol for haemolymph collection: sent to pearl farms

Materials:

- 20 x 100mL bottles of Citrate (supplied by Murdoch University)
- Syringes (supplied by Murdoch University)
- Esky with ice packs and packing foam

Methods:

1. Open adult pearl shell, round side down
2. Use syringe to obtain liquid haemolymph (clear fluid) from the oyster – should be able to obtain approximately 20-30mLs from each adult shell
3. Fill each Citrate bottle with haemolymph to 100mLs
4. Screw lid firmLy on each , mix gently until powder is dissolved
5. Place bottles in cool esky with ice and packing foam
6. Transport bottles of haemolymph to Murdoch University as soon as possible

Address to send esky:

Attn: Z. Spiers (ext. 2479)
Loading Bay 5
School of Veterinary and Biomedical Sciences
Murdoch University
South Street
Murdoch WA 6150

Thankyou!

8.6 Composition of solutions in molecular study

8.6.1 2% Agarose gel for screening DNA extractions

To make 200mL of 2% Agarose:

Agarose	4 gm
10 X TBE buffer	20 mL
ddH_2O	180 mL

Method:

Boil in microwave until agarose is completely dissolved, and solution is clear. Stir occasionally. Take caution when stirring as solution super heats and may reboil.

Storage:

Store at room temperature and reheat before each gel.

8.6.2 0.5µg/mL Ethidium Bromide working solution

Dilution required:

Stock solution is 1mg/mL, so a dilution of 1/2000 is required to achieve the working solution of 0.5µg/mL.

Method:

Mix 0.25mL of stock solution into 500mL H_2O.

Storage:

Store at 4^oC, label correctly, as it is a carcinogen, and wear protective clothing.

8.6.3 10 X TBE (Tris-borate) Buffer

To make 10 X TBE solution::

Tris	450mM
Boric Acid	450 mM
EDTA	10 mM (pH 8.0)

Method

Combine ingredients and adjust pH to 8.3

Storage:

Store at room temperature

8.6.4 Lambda DNA

To make 900µl of 5ug/mL working solution:

Lambda DNA (Promega)	10µl
Sterile H_2O	890µl

Storage:

Dispense into 100µl aliquots, store at -20^oC, only remove and defrost immediately before use.

8.6.5 Composition of gel for checking PCR

PCR samples:

In each lane, include 2µl dye and 10µl PCR product

Using Phi174/Hae III standard:
In the first lane, include 2µl dye and 10µl Phi (10µg/mL solution)
Fragment sizes (bp) in descending order are: 1353, 1078, 878, 603, 310, 281, 271, 234, 194, 118 and 72.

8.6.6 Composition of gel for checking DNA extractions

DNA samples:
In each lane, include 2µl dye, 6µl H_2O and 2µl DNA. These volumes may be altered.
Using Lambda standard:
In the first lane, include 2µl dye, 3µl H_2O and 5µl of 5µg/mL solution of Lambda.

8.7 Protocol for new disease investigation

The following list is the minimum sample requirements for the investigation of a new disease. As many individual oysters should be included as possible, particularly if a relatively low prevalence of disease is suspected.

1. Histopathology

10% seawater buffered formalin solution

Samples prepared for histopathology provide a range of information on the overall health of the oyster, the impact the disease has on various oyster tissues, the oysters' response to the disease, and can allow pathologists to identify basic morphological features of the organism, providing clues as to its taxonomic classification. Shucked oysters should be placed in 10% seawater buffered formalin solution, and immersed for a minimum time to allow for fixation, such as 12 hours, to preserve the quality for DNA for future in-situ hybridisation procedures.

2. Ultrastructural detail

Half in 5% seawater buffered glutaraldehyde solution Half in 10% seawater buffered formalin solution

Details of an organism are revealed using Transmission Electron Microscopy or Scanning Electron Microscopy. This allows the pathologist to identify ultrastructural features to identify the organism down to its species. It is important to identify individual oysters by labelling pots, section them sagittally and place half into a pot of 10% formalin for histology, and the other half in a pot of 5% glutaraldehyde. Number both pots with the same number, so the individual oyster can be identified. Histology will reveal the infected oysters, and its corresponding half can be used for ultrastructural studies.

3. Molecular studies

Half in 100% ethanol Half in 10% seawater buffered formalin solution

The preservation of DNA in ethanol will allow pathologists to extract phylogenetic information about the disease-causing organism. It is important to identify individual oysters by labelling pots, section them sagittally and place half into a pot of 10% formalin for histology, and the other half in a pot of 100% ethanol. Number both pots with the same number, so the individual oyster can be identified.

4. Culture

Half refrigerated at $4^{o}C$

Half in 10% seawater buffered formalin solution

Refrigerated tissues can allow for the culture of cells, bacteria and other organisms. It is important to identify individual oysters by labelling pots, section them sagittally and place half into a pot of 10% formalin for histology, and the other half in a pot and placed in the refrigerator. Number both pots with the same number, so the individual oyster can be identified.

5. Live oysters

Live individuals for transport to a quarantine facility

Live oysters should be transported by air to a quarantine facility to undergo cross infection trials with uninfected oysters and pathogenesis studies in a controlled environment. Oyster can be placed in eskys, cup side down, covered with moist newspaper and accompanied with ice packs. Travel time should be kept to a minium.

References

ACT Parliamentary Council (2005). Animal Diseases (Endemic Diseases) Declaration 2005 (No.1). J. Stanhope.

Al-Soud, W. A., L. J. Jonsson, et al. (2000). "Identification and characterisation of Immunoglobulin G in blood as a major inhibitor of diagnostic PCR." J. Clin. Microbiol. **38**(1): 345-350.

Atlas, R. M. Detecting Gene Sequences using the Polymerase Chain Reaction. Methods in Aquatic...? Kemp, Lewis Publishers.

Auffret, M. (1988). "Bivalve hemocyte morphology." American Fisheries Society Special Publication **18**: 169-177.

Australian Bureau of Agriculture and Resource Economics (ABARE) (2003). "Australian Fisheries Statistics 2002." http://abareonlineshop.com/product.asp?prodid=12527.

Balouet, G. and M. Poder (1985). Current Status of Parasitic and Neoplastic Diseases of Shellfish: a Review. Fish and Shellfish Pathology. A. E. Ellis. London, Academic Press**:** 371-385.

Balseiroa, P., R. F. Conchasb, et al. (2006). "Comparison of diagnosis techniques for the protozoan parasite *Bonamia ostreae* in flat oyster *Ostrea edulis*." Aquaculture **261**(4): 1135-1143.

Bancroft, J. D. and M. Gamble (2002). Theory and Practice of Histological Techniques, Fifth Edition, Churchill Livingstone.

Barber, B. J., R. Langan, et al. (1997). "*Haplosporidium nelsoni* (MSX) Epizootic in the Piscataqua River Estuary (Maine/New Hampshire, U.S.A.)." J. Parasitol. **83**(1): 148-150.

Barbosa-Solomieu, V., L. Miossec, et al. (2004). "Diagnosis of Osteid herpesvirus 1 in fixed paraffin-embedded archival samples using PCR and in situ hybridisation." Journal of Virological Methods **119**: 65-72.

Barker Jorgensen, C. (1996). "Bivalve filter feeding revisited." Marine Ecology Progress Series **142**: 287-302.

Bearham, D., Z. Spiers, et al. (2007). "Detection of *Minchinia* sp. in rock oysters *Saccostrea cucullata* (Born, 1778) using DNA probes." Journal of Invertebrate Pathology **In Press**.

Bick, H. (1972). Ciliated Protozoa. Geneva, World Health Organization.

Bishop, M. J., R. B. Carnegie, et al. (2006). "Complications of a non-native oyster introduction: facilitation of a local parasite." Mar. Ecol. Prog. Ser. **325**: 145-152.

Blood, D. C. and V. P. Studdert (1999). Saunders Comprehensive Veterinary Dictionary, Second Edition. London, W.B. Saunders.

Boulo, V., J.-P. Cadoret, et al. (2000). "Infection of cultured embryo cells of the pacific oyster, *Crassostrea gigas*, by pantropic retroviral vectors." In Vitro Cellular and Developmental Biology **36**: 395-399.

Boussaid, B., J. L. Grippari, et al. (1999). "*Trichodina* sp. Infestation of *Crassostrea gigas* Oyster Gills in Brittany, France." Journal of Invertebrate Pathology **73**: 339-342.

Bower, S. M., P. Carnegie, et al. (2004). "Preferential amplification of parasitic protistan SSU rDNA from metazoan tissues." Journal of Eukaryotic Microbiology **51**(3): 325-332.

Bower, S. M. and G. R. Meyer (1993). "*Stegotricha enterikos* gen. nov., sp. nov. (class Phyllopharyngea, order Rhynchodida), a parasitic ciliate in the digestive gland of Pacific oysters (*Crassostrea gigas*) and its distribution in British Columbia." Canadian Journal of Zoology **71**(10): 2005-2017.

Burleigh, B. A. and A. Woolsey (2002). "Cell signalling and *Trypanosoma cruzi* invasion." Cellular Microbiology **4**(11): 701-711.

Burreson, E. M. and K. S. Reece (2006). "Spore ornamentation of *Haplosporidium nelsoni* and *Haplosporidium costale* (Haplosporidia), and incongruence of molecular phylogeny and spore ornamentation in the Haplosporidia." J. Parasitol. **92**(6): 1295-1301.

Burreson, E. M. and N. A. Stokes (2000). "Increased virulence in an introduced Pathogen: *Haplosporidium nelsoni* (MSX) in the Eastern Oyster *Crassostrea virginica*." Journal of Aquatic Animal Health **12**: 1-8.

Chaitanawisuti, N., S. Kritsanapuntu, et al. (2004). "Research and development on commercial land-based aquaculture of spotted babylon, *Babylonia areolata* in Thailand: Pilot hatchery-based seedling operation." Aquaculture Asia **9**(3): 16-20.

Chase, M. R., R. J. Etter, et al. (1998). "Extraction and amplification of mitochondrial DNA from formalin-fixed deep-sea mollusks." BioTechniques **24**: 243-247.

Chen, S. N. and C. M. Wen (2000). "Establishment of cell lines derived from oyster, *Crassostrea gigas* Thunberg and hard clam, *Meretrix lusoria* Roding." Methods in Cell Science **21**: 183-192.

Chen, T.-T. and R. M. Stabler (1936). "Further Studies on the Endamoebae Parasitizing Opalinid Ciliates." Biological Bulletin **70**(1): 72-77.

Chen, Z., W. Song, et al. (2000). "Studies on Six *Euplotes* spp. (Ciliophora: Hypotrichida) Using RAPD Fingerprinting, Including a Comparison with Morphometric Analysis." Acta Protozoologica **39**: 209-216.

Chen, Z., W. Song, et al. (2003). "Species separation and identification of *Uronychia* spp. (Hypotrichia: Ciliophora) using RAPD Fingerprinting and ARDRA Riboprinting." Acta Protozoologica **42**: 83-90.

Cheng, T. C. (1988). "Strategies employed by parasites of marine bivalves to effect successful establishment in hosts." American Fisheries Society Special Publication **18**: 112-129.

Cheng, T. C. and E. Rifkin (1970). Cellular reactions in marine molluscs in response to helminth parasitism. Diseases of Fishes and Shellfishes**:** 443-496.

Cho, W. S. and C. Chae (2003). "PCR detection of *Actinobacillus pleuroneumoniae apx*IV gene in formalin-fixed, parafin embedded lung tissues and comparison

with *in situ* hybridization." Applied Microbiology **37**: 56-60.

Chu, F. E. (1988). "Humoral defence factors in marine bivalves." American Fisheries Society Special Publication **18**: 178-188.

Cockman, B. (1982). The cytoanatomy of the digestive structures of the silver-lipped oyster *Pinctada maxima*, Murdoch University.

Cook, T., M. Folli, et al. (1998). "The relationship between increasing sea-surface temperature and the northward spread of *Perkinsus marinus* (Dermo) disease epizootics in oysters." Estuarine, Coastal and Shelf Science **46**(4): 587-597.

Corliss, J. O. (1955). "The Opalinid Infusorians: Flagellates or Ciliates?" J. Protozool. **2**: 107-114.

Corliss, J. O. (1990). Phylum Zoomastigina Class Opalinata. Handbook of Protoctista**:** 239-245.

Corliss, J. O. and D. L. Lipscomb (1982). "Establishment of New Order in Kingdom Protista for *Stephanopogon*, Long-Known "Ciliate" Revealed Now as Flagellate." J. Protozool. **29**(2): 294.

Crosbie, P. (2005). Personal communication: Culturing Ciliates.

Culloty, S. C. and M. F. Mulcahy (1992). "An evaluation of anaesthetics for *Ostrea edulis*." Aquaculture **107**: 249-252.

da Silva, P. M., J. Fuentes, et al. (2005). "Growth, mortality and disease susceptibility of oyster *Ostrea edulis* families obtained from brood stocks of different geographical origins, through on-growing in the Ria de Arousa (Galicia, NW Spain)." Marine Biology **147**: 965-977.

Day, J. M., D. E. Franklin, et al. (2000). "Use of competitive PCR to detect and quantify *Haplosporidium nelsoni* infection (MSX disease) in the Eastern Oyster (*Crassostrea virginica*)." Marine Biotechnology **2**: 456-465.

Denkers, E. Y. and B. A. Butcher (2005). "Sabotage and exploitation in macrophages parasitized by intracellular protozoans." Trends in Parasitology **21**(1): 35-41.

Dept. Agriculture (2004). Western Australia's Agricultural, Food and Fisheries Industries 2002-2003, Dept of Agriculture**:** 56-58.

Dept. of Fisheries (2004). "The Health Status of Western Australian Aquaculture." http://www.fish.wa.gov.au/docs/aq/aq029/index.php?0308(Government of Western Australia).

Diggles, B. K., N. Cochennec-Laureau, et al. (2003). "Comparison of diagnostic techniques for *Bonamia exitiosus* from flat oysters *Ostrea chilensis* in New Zealand." Aquaculture **220**(1-4): 145-156.

Dupuy, C., S. Le Gall, et al. (1999). "Retention of ciliates and flagellates by the oyster *Crassostrea gigas* in French Atlantic coastal ponds: protists as a trophic link between bacterioplankton and benthic suspension-feeders." Marine Ecology Progress Series **177**: 165-175.

Dybdahl, R. and D. A. Pass (1985). An Investigation of mortality of the pearl oyster *Pinctada maxima*, in Western Australia. Perth, Fisheries Dept.

Elston, R. (1997). "Special Topic Review: Bivalve mollusc viruses." World Journal of Microbiology and Biotechnology **13**: 393-403.

Elston, R. A. (1980). "Functional Anatomy, histology and ultrastructure of the soft tissues of the larval American oyster, *Crassostrea virginica*." Proceedings of the National Shellfisheries Association **70**: 65-91.

Elston, R. A. (1996). "International trade in live molluscs: perspective from the Americas." Rev. sci. tech. Off. int. Epiz. **15**(2): 483-490.

Elston, R. A., D. Cheney, et al. (1999). "Invasive orchitophryid ciliate infections in juvenile Pacific and Kumomoto oysters, *Crassostrea gigas* and *Crassostrea sikamea*." Aquaculture **174**: 1-14.

Escalante-Ochoa, C., R. Ducatelle, et al. (1998). "The intracellular life of *Chlamydia psittaci*: How do bacteria interact with the host cell?" FEMS Microbiological Reviews **22**: 65-78.

Fasshauer, V., U. Gross, et al. (2005). "The parasitopherous vacuole membrane of *Encephalitozoon caniculi* lacks host cell membrane proteins immediately after invasion." Eukaryotic Cell **4**(1): 221-224.

Faucet, J., M. Maurice, et al. (2004). "Isolation and primary culture of gill and digestive gland cells from the common mussel *Mytilus edulis*." Methods in Cell Science **25**(3-4): 177-184.

Fayer, R., E. J. Lewis, et al. (2003). Cryptosporidium parvum in oysters from Commercial Harvesting Sites in the Chesapeake Bay. Emerging Infectious Diseases. **2003**.

Feng, S. Y. (1988). "Cellular defence mechanisms of oysters and mussels." American Fisheries Society Special Publication **18**: 153-168.

Figueras, A. J., C. F. Jardon, et al. (1991). "Diseases and parasites of mussels (*Mytilus edulis* Linneaus, 1758) from two sites on the east coast of the United States." Journal of Shellfish Research **10**(1): 89-94.

Fisher, W. S. (1988). "Environmental influence on bivalve hemocyte function." American Fisheries Society Special Publication **18**: 225-237.

Fisheries, D. o. (2005). "Introduced Marine Aquatic Invaders - A Field Guide: Black Striped Mussel." http://www.fish.wa.gov.au/sec/env/pests/index.php?0506(Government of Western Australia).

Fisheries Western Australia (2001). State of the Fisheries Report 2000/2001, Dept Agriculture WA.

Fisheries Western Australia (2004?). State of the Fisheries Report 2003/2004, Dept Agriculture WA.

Fisheries Western Australia (2005). State of the Fisheries Report 2004/2005, Dept Agriculture WA.

Flores, B. S., M. E. Siddal, et al. (1996). "Phylogeny of the Haplosporidia (Eukaryota: Alveolata) based on small subunit ribosomal RNA gene sequences." J. Parasitol. **82**(4): 616-623.

Foissner, W. (1991). "Basic Light and Scanning Electron Microscopic Methods for Taxonomic Studies of Ciliated Protozoa." European Journal of Protistology **27**: 313-330.

Ford, S. E., K. A. Ashton-Alcox, et al. (1993). "In vitro interactions between bivalve

hemocytes and the oyster pathogen *Haplosporidium nelsoni* (MSX)." J. Parasitol. **79**(2): 255-265.

Fried, J., W. Ludwig, et al. (2002). "Improvement of Ciliate Identification and Quantification: a New Protocol for Flourescence In Situ Hybridization (FISH) in Combination with Silver Stain Techniques." System. Appl. Microbiol. **25**: 555-571.

Friedman, C. S. and C. A. Finley (2003). "Anthropogenic introduction of the etiological agent of withering syndrome into northern California abalone populations via conservation efforts." Canadian Journal of Fisheries and Aquatic Sciences **60**(11): 1424.

Fromont, J., R. Craig, et al. (2005). "Excavating sponges that are destructive to farmed pearl oysters in Western and Northern Australia." Aquaculture Research **36**: 150-162.

Gilbert, M. T. P., T. Haselkorn, et al. (2007). "The isolation of nucleic acids from fixed, paraffin-embedded tissues - which methods are useful when?" PLoS ONE(6): 537 (1-12).

Goggin, C. L. and R. J. G. Lester (1995). "*Perkinsus*, a protistan parasite of abalone in Australia: A review." Mar. Freshwater Res. **46**: 639-646.

Government of WA (1994). "175th Anniversary of Western Australia." http://www.175anniversary.wa.gov.au/index.cfm?fuseaction=heritage_icons.june Accessed December, 2004.

Grizel, H. An Atlas of histology and cytology of marine bivalve molluscs.

Hancock, A. T. (1993). Reproduction in wild stocks of the silver-lipped pearl oyster *Pinctada maxima* (Jameson) (Mollusca:Pteriidae) in Western Australia, Murdoch University.

Herfort, A. (2004). Aquatic Animal Diseases Significant to Australia: Identification Field Guide. Canberra, Australian Government Department of Agriculture, Fisheries and Forestry.

Hervio, D., S. M. Bower, et al. (1996). "Detection, Isolation and Experimental Transmission of *Mikrocytos mackini*, a Microcell Parasite of Pacific Oysters, *Crassostrea gigas* (Thunberg)." Journal of Invertebrate Pathology **67**: 72-79.

Hine, P. M. and T. Thorne (1998). "*Haplosporidium* sp. (Haplosporidia) in Hatchery-Reared Pearl Oysters, *Pinctada maxima* (Jameson, 1901), in north Western Australia." Journal of Invertebrate Pathology **71**: 48-52.

Hine, P. M. and T. Thorne (2000). "A survey of some aquatic parasites and diseases of several species of bivalve mollusc in northern Western Australia." Diseases of Aquatic Organisms **40**: 67-78.

Humphrey, J. and J. Norton (2005). The Pearl Oyster *Pinctada maxima* (Jameson, 1901) An Atlas of Functional Anatomy, Pathology and Histopathology, Northern Territory Government Printing Office.

Jeffrey, S. W. and LeRoi, J.-M. (1997). Simple procedures for growing SCOR reference microalgal cultures. In: S.W. Jeffrey, R.F.C. Mantoura and S.W. Wright (Eds) Phytoplankton pigments in oceanography; Monographs on oceanographic methodology 10, UNESCO, France, pp 181-205

Jimenez, F. (2005). Detection and evaluation of temperature effects on cell proliferation in somatic tissues of the eastern oyster, *Crassostrea virginica*, by flow cytometry. Graduate Faculty, Louisiana State University and Agricultural and Mechanical College.

Jones, J. B. and J. Creeper (2006). "Diseases of pearl oysters and other molluscs: A Western Australian perspective." Journal of Shellfish Research **25**(1): 233-238.

Jones, T. C. (1981). "Interactions between murine macrophages and obligate intracellular protozoa." A. J. P. **102**(1): 127-132.

Jurand, A. and G. G. Selman (1969). The Anatomy of *Paramecium aurelia*. Great Britain, Macmillan and Co. Ltd.

Kidd, K. K. and G. Ruano Optimizing PCR.

Kleeman, S. N. (2002). "A "pop-off" technique for reprocessing histological sections of the paramyxean *Marteilia sydneyi* for electron microscopy." Parasitol Res **88**: 439-442.

Kleeman, S. N., F. Le Roux, et al. (2002). "Specificity of PCR and *in situ* hybridization assays designed for detection of *Marteilia sydneyi* and *M. refringens*." Parasitology **125**: 131-141.

Kostka, M., V. Hampl, et al. (2004). "Phylogenetic position of *Protoopalina intestinalis* based on SSU rRNA gene sequences." Molecular Genetics and Evolution **33**: 220-224.

Kudo, R. R. (1971). Protozoology. USA, Charles C Thomas Publisher.

Langdon, J. S., A. Masters, et al. (1995). "Bizarre organism from the skin of mahi mahi, *Coryphaena hippurus* L. (Teleostei: Coryphaenidae)." Journal of Fish Diseases **18**: 481-494.

Laruelle, F., D. P. Molloy, et al. (1999). "Histological analysis of mantle-cavity ciliates in Dreissena polymorpha: Their location, symbiotic relationship, and distinguishing morphological characteristics." Journal of Shellfish Research **18**(1): 251-257.

Le Deuff, R.-M., C. Lipart, et al. (1994). "Primary culture of Pacific oyster, *Crassostrea gigas*, heart cells." Methods in Cell Science **16**(1): 67-72.

Leibovitz, A. (1963). "The growth and maintenance of tissue-cell cultures in free gas exchange with the atmosphere." American Journal of Hygiene **78**(2): 173-180.

Leiriao, P., C. D. Rodrigues, et al. (2004). "Survival of protozoan intracellular parasites in host cells." European Molecular Biology Organisation (EMBO) Reports **5**(12): 1142-1147.

Lewis, T. E., C. D. Garland, et al. (1986). Manual of Hygiene for Shellfish Hatcheries. Hobart, University of Tasmania Printing Department.

Lin, X., J. Gong, et al. (2004). "Morphological studies on a new species of *Orthodonella*, with redescription of *O. gutta* (Cohn, 1866) Kahl, 1931 (Protozoa: Ciliophora: Synhymeniida) from coastal water off Qingdao, China." Journal of Natural History **38**: 2001-2011.

Lynn, D. H. (2003). "Morphology or molecules: How do we identify the major lineages of ciliates (Phylum Ciliophora)?" European Journal of Protistology **39**(4): 356-364.

Lynn, D. H. and E. B. Small (1990). Phylum Ciliophora. Handbook of Protoctista. L. Margulis, J. O. Corliss, M. Melkonian and D. Chapman. Boston, Jones and Bartlett Publishers**:** 498-523.

MacKinnon, D. L. and R. S. J. Hawes (1970). An Introduction to the Study of Protozoa. London, Oxford University Press.

Manwell, R. D. (1968). Introduction to Protozoology. New York, Dover Publications, Inc.

Margulis, L. (1996). "Archaeal-eubacterial mergers in the origin of Eukarya: Phylogenetic classification of life." Proc. Natl. Acad. Sci. USA **93**: 1071-1076.

McConville, M. J., D. de Souza, et al. (2007). "Living in a phagolysosome; metabolism of *Leishmania* amastigotes." Trends in Parasitology **23**(8): 368-375.

McGladdery, S. E. and S. M. Bower (2002). Synopsis of Infectious Diseases and Parasites of Commercially Exploited Shellfish: Intracellular Ciliates of Mussels.

McGladdery, S. E. and M. F. Stephenson (1991). "Parasites and diseases of suspension and bottom grown shellfish from eastern Canada." Bulletin Aquaculture Association of Canada **91**(3): 64-66.

Medlin, L., H. J. Elwood, et al. (1988). "The characterization of enzymatically amplified eukaryotic 16S-like rRNA-coding regions." Gene **71**: 491-499.

Metcalf, M. M. (1929). "The Opalinidae and their significance."? 448-452.

Miller, J., A. Jenny, et al. (1997). "Detection of *Mycobacterium bovis* in formalin-fixed, paraffin-embedded tissues of cattle and elk by PCR amplification of an IS6110 sequence specific for Mycobacterium tuberculosis complex organisms." J Vet Diag Lab Inv **9**: 244-249.

Montgomery-Brock, D., A. G. J. Tacon, et al. (2007). "Reduced replication of infectious hypodermal and hematopoietic necrosis virus (IHHNV) in *Litopenaeus vannamei* held in warm water." Aquaculture **265**(1-4): 41-48.

Morata, P., M. I. Queipo-Ortuno, et al. (1998). "Strategy for optimising DNA amplication in a periferal blood PCR assay used for diagnosis of human brucellosis." J. Clin. Microbiol. **36**(9): 2443-2446.

Moreno, Y., S. Botella, et al. (2003). "Specific detection of *Arcanobacteria* and *Campylobacter* strains in water and sewerage by PCR and flourescent in-situ hybridisation." Appl. Environ. Microbiol. **69**(2): 1181-1186.

Moret, K., K. Williams, et al. (1999). "Newfoundland cultured mussel (*Mylilus edulis*) industry 1997 health survey." Bulletin Aquaculture Association of Canada **99**(3): 35-37.

Morisaki, J. H., J. E. Heuser, et al. (1995). "Invasion of *Toxoplasma gondii* occurs by active penetration of the host cell." Journal of Cell Science **108**: 2457-2464.

Moulder, J. W. (1985). "Comparative biology of intracellular parasitism." Microbiological Reviews **49**(3): 298-337.

Mueller, U. G. and L. L. Wolfenbarger (1999). "AFLP genotyping and fingerprinting." Tree **14**(10): 389-394.

Murray, A. G. and E. J. Peeler (2005). "A framework for understanding the potential for emerging disease in aquaculture." Pre. Vet. Med. **67**(2-3): 223-235.

National Aquaculture Council (2006). "Australian Aquaculture Portal." http://www.australian-aquacultureportal.com/industrygroups/pearls.html Accessed 25.01.06.

Nishi, A., K.-i. Ishida, et al. (2005). "Reevaluation of the Evolutionary Position of Opalinids Based on 18S rRNA, and a- and b-Tubulin Gene Phylogenies." Journal of Molecular Evolution **60**: 695-705.

Norton, J., M. Shepherd, et al. (1993). "*Papovavirus-like* infection of the golden-lipped pearl oyster, *Pinctada maxima*, from the Torres Strait, Australia." Journal of Invertebrate Pathology **62**(2): 198-200.

OIE (2003). Manual of Diagnostic Tests for Aquatic Animals 2003. http://www.oie.int/eng/normes/fmanual/A_00002.htm, Updated 01/09/03, OIE.

OIE (2006). "Diseases Notifiable to the OIE." http://www.oie.int/eng/maladies/en_classification.htm(Updated 23/01/06): World Organisation for Animal Health.

Pal, S. G. (1971a). "The fine structure of the digestive tubules of *Mya arenaria* L. 1. Basiphil cell." Proc. malac. Soc. Lond. **39**: 303-309.

Pal, S. G. (1971b). "The fine structure of the digestive tubules of Mya arenaria L. 2. The digestive cell." Proc. malac. Soc. Lond. **40**: 161-170.

Patterson, D. J. (1986). "The fine structure of *Opalina ranarum* (family Opalinidae): Opalinid phylogeny and classification." Protistologica **21**: 413-428.

Pauley, G. B. (1966). "The acute inflammatory reaction in two different tissues of the pacific oyster, *Crassostrea gigas*." J. Fish. Res. Bd. Canada **23**(12): 1913-1921.

Pauley, G. B. and A. K. Sparks (1967). "Observations on Experimental Wound Repair in the Adductor Muscle and the Leydig Cells of the oyster *Crassostrea gigas*." Journal of Invertebrate Pathology **9**(3): 298-309.

Pitelka, D. R. (1963). Electron-Microscopic Structure of Protozoa. Great Britain, Pergamon Press Inc.

Reece, K. S., M. E. Siddal, et al. (2004). "Molecular phylogeny of the Haplosporidia based on two independent gene sequences." J. Parasitol. **90**(5): 1111-1122.

Renault, T., G. Flaujac, et al. (1995). "Isolation and culture of heart cells from the European flat oyster, *Ostrea edulis*." Methods in Cell Science **17**: 199-205.

Riley, J. L. and L. A. Katz (2001). "Widespread Distribution of Extensive Chromosomal Fragmentation in Ciliates." Mol. Biol. Evol. **18**(7): 1372-1377.

Roy, P., A. S. Dhillon, et al. (2004). "Detection of Avian Polymavirus Infection by Polymerase Chain Reaction Using Formalin-Fixed, Parafin-Embedded

Tissues." Avian Diseases **48**: 400-404.

Ruiz, G. M., P. M. Fofonoff, et al. (2000). "Invasion of coastal marine communities in North America: Apparent patterns, processes and biases." Annu. Rev. Ecol. Syst. **31**: 481-531.

Sambrook, J., E. F. Fritsch, et al. (1989). Molecular Cloning: A Laboratory Manual 2nd Edition. USA, Cold Spring Harbour Laboratory Press.

Sepp, R., I. Szabo, et al. (1994). "Rapid techniques for DNA extraction from routinely processed archival tissue for use in PCR." J. Clin. Pathol. **47**: 318-323.

Shang, H., Z. Chen, et al. (2002). "Species separation among seven *Euplotes* spp. (Protozoa: Ciliophora: Hypotrichida) using PCR/RFLP analysis of nuclear ribosomal DNA." J. Zool. Lond. **258**: 375-379.

Shang, H., W. Song, et al. (2003). "Phylogenetic Positions of two Ciliates, *Paranophrys magna* and *Mesanophrys carcini* (Ciliophora: Oligohymenophorea), within the Subclass Scuticociliatia Inferred from Complete Small Subunit rRNA gene sequences." Acta Protozoologica **42**: 171-181.

Shaw, M. K. (2003). "Cell invasion by *Theileria* sporozoites." Trends in Parasitology **19**(1): 2-6.

Shedlock, A. M., M. G. Haygood, et al. (1997). "Enhanced DNA extraction and PCR amplification of mitochondrial genes from formalin-fixed museum specimens." BioTechniques **22**: 394-400.

Shelley, C. C. (1994?). Pearl Oyster *(Pinctada maxima)* Aquaculture: Health Survey of Northern Territory, Western Australia adn Queensland Pearl Oyster Beds and Farms, Darwin Aquaculture Centre, 94/079**:** 1-93.

Snoeyenbos-West, O. L. O., J. Cole, et al. (2004). "Molecular Phylogeny of Phyllopharyngean Ciliates and their Group I Introns." J. Eukaryot. Microbiol. **5**(4): 441-450.

Snoeyenbos-West, O. L. O., T. Salcedo, et al. (2002). "Insights into the diversity of choreotrich and oligotrich ciliates (Class: Spirotrichea) based on geneological analyses of multiple loci." International Journal of Systematic and Evolutionary Microbiology **52**: 1901-1913.

Song, W. (2004). "Morphogenesis of *Cyrtohymena tetracirrata* (Ciliophora, Hypotrichia, Oxytrichidae) during binary fission." European Journal of Protistology **40**(3): 245-254.

Song, W. (2005). "Taxonomic description of two new marine oligotrichous ciliates (Protozoa, Ciliophora)." Journal of Natural History **39**(3): 241-252.

Sparks, A. K. (1985). Synopsis of Invertebrate Pathology Exclusive of Insects. Netherlands.

Sparks, A. K. and J. F. Morado (1988). "Inflammation and wound repair in bivalve molluscs." American Fisheries Society Special Publication **18**: 139-152.

Sparks, A. K. and G. B. Pauley (1964). "Studies of the Normal Postmortem Changes in the Oyster, *Crassostrea gigas* (Thunberg)." Journal of Insect Pathology **6**: 78-101.

Stauber, L. A. (1950). "The fate of india ink injected intracardially into the oyster, *Ostrea virginica* Gmelin." Biological Bulletin (Woods Hole)(98): 227-241.

Stechmann, A., M. Schlegel, et al. (1998). "Phylogenetic relationships between Prostome and Colpodean ciliates tested by small subunit rRNA sequences." Molecular Phylogenetics and Evolution(7): 48-54.

Stokes, N. A. and E. M. Burreson (1995). "A sensitive and specific DNA probe for the oyster pathogen *Haplosporidium nelsoni*." J. Eukaryot. Microbiol. **42**(4): 350-357.

Suss-Toby, E., J. Zimmerberg, et al. (1996). "*Toxoplasma* invasion: the parasitopherous vacuole is formed from host cell plasma membrane and pinches off via a fission pore." Proc. Natl. Acad. Sci. USA **93**: 8413-8418.

Tan, H. and N. W. Andrews (2002). "Don't bother to knock - the cell invasion strategy of *Trypanosoma cruzi*." Trends in Parasitology **18**(10): 427-428.

Taylor, J. J., P. C. Southgate, et al. (2004). "Effects of salinity on growth and survival of silver-lip pearl oyster *Pinctada maxima* spat." Journal of Shellfish Research **23**(2): 375-377.

WALIS (2002). Western Australian Land Information System Western Australian Atlas, http://www.atlas.wa.gov.au/, Government of Western Australia.

Wen, C. M., G. Kou, et al. (1993). "Cultivation of cells from the heart of a heart clam, *Meretrix lusoria* (Roding)." Journal of Tissue Culture Methods **15**: 123-130.

Wetzel, D., M., J. Schmidt, et al. (2005). "Gliding motility leads to active cellular invasion by *Cryptosporidium parvum* sporozoites." Infection and Immunity **73**(9): 5378-5387.

Wu, X. and J. Pan (1999). "Studies on Rickettsia-like Organism Disease of the Tropical Marine Pearl Oyster I: The Fine Structure and Morphogenesis of *Pinctada maxima* Pathogen Rickettsia-like Organism." Journal of Invertebrate Pathology **73**: 162-172.

Xin-Bai, S. and D. Ammermann (2004). "*Stylonychia harbinensis* sp. n., a new oxytrichid ciliate (Ciliophora, Hypotrichia) from the Heilongjiang Province, China." Protistology **3**(4): 219-222.

Xu, K., W. Song, et al. (1999). "Trichodinid ectoparasites (Ciliophora: Peritrichida) from the gills of mariculture molluscs in China, with the descriptions of four new species of *Trichodina* Ehrenberg, 1838." Systematic Parasitology **42**: 229-237.

Xu, K., W. Song, et al. (2000). "Observations on trichodinid ectoparasites (Ciliophora: Petricha) from the gills of maricultured molluscs in China, with descriptions of three new species of *Trichodina* Ehrenberg, 1838." Systematic Parasitology **45**: 17-24.

Xu, K., W. Song, et al. (2002). "Taxonomy of trichodinids from the gills of marine fishes in coastal regions of the Yellow Sea, with descriptions of two new species of *Trichodina* Ehrenberg, 1830 (Protozoa: Ciliophora: Peritrichia)." Systematic Parasitology **51**: 107-120.

Yonge, C. M. (1926). "Structure and Physiology of the Organs of Feeding and

Digestion in *Ostrea edulis*." J. Mar. Biol. Assoc. **14**: 295-386.

Yoshimizu, M. (1996). "Disease problems of salmonid fish in Japan caused by international trade." Rev. sci. tech. Off. int. Epiz. **15**(2): 533-549.

Yukihira, H., D. W. Klumpp, et al. (1998). "Comparative effects of microalgal species and food concentration on suspension feeding and energy budgets of the pearl oyster *Pinctada margaritifera* and *P.maxima* (Bivalvia:Pteriidae)." Marine Ecology Progress Series **171**: 71-84.

Yukihira, H., D. W. Klumpp, et al. (1998). "Effects of body size on suspension feeding and energy budgets of the pearl oysters *Pinctada margaritifera* and *P. maxima*." Marine Ecology Progress Series **170**: 119-130.

Yukihira, H., D. W. Klumpp, et al. (1999). "Feeding adaptions of the pearl oysters *Pinctada margaritifera* and *P.maxima* to variations in natural particulates." Marine Ecology Progress Series **182**: 161-173.

Yukihira, H., J. S. Lucas, et al. (2000). "Comparative effects of temperature on suspension feeding energy budgets of the pearl oysters *Pinctada margaritifera* and *P. maxima*." Marine Ecology Progress Series **195**: 179-188.